博士論文

^{13}C labeling-based approach towards unlocking of diterpenoid phytoalexins biosynthetic pathways in rice

(^{13}C 標識ジテルペン炭化水素の投与によるイネのファイトアレキシン生合成経路の解明)

東京大学大学院　農学生命科学研究科

応用生命工学専攻

平成２６年度入学　叶　忠峰

指導教官　野尻　秀昭

^{13}C labeling-based approach towards unlocking of diterpenoid phytoalexins biosynthetic pathways in rice

YE ZHONGFENG

A Dissertation

Presented for the

Doctor of Philosophy Degree

The University of Tokyo

TABLE OF CONTENTS

CHAPTER 3 ESTABLISHING FEEDING PLATFORMS OF THE LABELED SUBSTRATES INCORPORATED INTO DITERPENOID PHYTOALEXINS

CHAPTER 4 INVESTIGATION OF DITERPENE INTERMEDIATES IN THE BIOSYNTHETIC MUTANTS OF CYTOCHROME P450 MONOOXYGENASES FOR DITERPENOID PHYTOALEXINS

ABBRREVIATIONS

AIRC	phosphoribosylamidoimidazole-succinocarboxamide synthase
Ala	alanine
AMO-1618	2-isopropyl-4-dimethylamino-5-methylphenyl-1- piperidin ecarboxylatemethyl chloride
AsbAS1	*Arabidopsis thaliana* β-amyrin synthase
ATP	adenosine triphosphate
CCC	2-chloroethyl-trimethylammonium chloride
COSY NMR	correlation spectroscop y nuclear magnetic resonance
DIBOA	2,4-dihydroxy-1,4-benzoxazin-3-one
DMSO	Dimethyl sulfoxide
DTT	dithiothreitol
ent-CDP	*ent*-copalyl diphosphate
EDTA	ethylenediaminetetraacetic acid
GC-MS	gas chromatography mass spectrometry
GGDP	geranylgeranyl diphosphate
Glc	glucose
Gln	glutamine
GPAT	glutamine phosphoribosyl pyrophosphate amidotransferase
HpDTC1	*Hypnum plumaeforme* bifunctional diterpene cyclase
IPTG	isopropyl-β-D-thiogalactopyranoside
JA	jasmonic acid
Lac	lactose
LC-ESI-MS/MS	Liquid chromatography electrospray ionization tandem mass spectrometry
m/z	mass/charge number of ions
MEP	2*C*-methyl-D-erythritol 4-phosphate
MVA	mevalonate
NcIPI	*Neurospora crassa* isopentenyl diphosphate isomerase
NcMVK	*Neurospora crassa* mevalonate kinase
NcMVD	*Neurospora crassa* diphosphomevalonate decarboxylase
NcPMVD	*Neurospora crassa* phosphomevalonate kinase
NMR	nuclear magnetic resonance

ORF	open reading frame
OsCPS2	rice *ent*-copalyl diphosphate synthase 2
OsCPS4	rice *ent*-copalyl diphosphate synthase 4
OsKSL4	rice *ent*-kaurene-line synthase 4
OsKSL7	rice *ent*-kaurene-line synthase 7
OsKSL8	rice *ent*-kaurene-line synthase 8
OsKSL10	rice *ent*-kaurene-line synthase 10
P450	cytochrome P450 monooxygenase
PCR	polymerase chain reaction
SaGGPS	*Sulfolobus acidocaldalius* geranylgeranyl diphosphate synthase
SDS-PAGE	sodium dodecyl sulfate poly acrylamide gel electrophoresis
UV	ultraviolet

論文の内容の要旨

応用生命工学
平成２６年度博士課程入学
氏　名　　叶　忠峰
指導教員　　野尻　秀昭

論文題目

^{13}C labeling-based approach towards unlocking of diterpenoid phytoalexins biosynthetic pathways in rice

（^{13}C 標識ジテルペン炭化水素の投与によるイネのファイトアレキシン生合成経路の解明）

Introduction

In rice (*Oryza sativa*), 17 compounds have been identified as phytoalexins from leaves that were either infected with the *Magnaphorthe oryzae* or subjected to UV irradiation. Other elicitations, such as heavy metal treatment, also can induce phytoalexins production in rice. All these phytoalexins, except for the flavanone sakuranetin, are diterpenoid in nature, and can be classified into five groups based on their carbon frameworks: phytocassanes A-F, oryzalexins A-F, momilactone A and B, oryzalexin S, and casbane-type oxodepressin. Great efforts to disclose the whole biosynthetic pathway of the phytoalexins, momilactones and phytocassanes, have been made up to now. It is known that the majority of their biosynthetic genes are clustered in chromosomes 2 and 4. Genes encoding cytochrome P450 monooxygenases in the each cluster are shown to be involved in the oxidation step of *syn*-pimara-7,15-diene to *syn*-pimara-7,15-dienoic acid (*CYP99A2* and *A3*) in momilactones biosynthesis and the oxidation step of *ent*-cassa-12,15-diene to phytocassanes (*CYP71Z7*, *CYP76M7, M8*). Several lines of evidence from both *in vivo* and *in vitro* experiments have shown that many P450 genes are putatively responsible for the biosynthesis of diterpenoid phytoalexins in rice. However, there are still substrate-enzyme specificities among P450s that remain unclear and need to be explained in order to understand phytoalexins biosynthesis. A feeding approach with stable isotope (e.g., ^{13}C) will be an effective method to trace as-yet-unknown precursors or enzyme specific substrates derived

from known compounds such as *ent*-cassa-12,15-diene and *syn*-pimara-7,15-diene, the diterpene hydrocarbons for phytocassane (A-F) and momilactone (A and B), respectively. In this study, we synthesized ^{13}C-labeled diterpene compounds *in vitro* enzymatically, and performed feeding experiments for elucidating the possible diterpene biosynthetic pathways occurring *in planta*.

Chapter 2. Enzymatic production of ^{13}C-labeled diterpene hydrocarbons

Toward unlocking the biosynthetic pathway of rice diterpenoid phytoalexins, we first generated ^{13}C-labeled diterpene hydrocarbons used for feeding experiments in following chapters. The fully ^{13}C-labeled *ent*-cassa-12,15-diene and *syn*-pimara-7,15-diene, either of which is the precursor of phytocassanes or momilactones, were enzymatically synthesized from [U-$^{13}C_{20}$] geranylgeranyl diphosphate (GGDP). The synthesis of *ent*-cassa-12,15-diene from GGDP required two diterpene cyclases, OsCPS2 and OsKSL7 involving in *ent*-CDP synthesis from GGDP and *ent*-cassa-12,15-diene synthesis from *ent*-CDP, respectively. The synthesis of *syn*-pimara-7,15-diene from GGDP can be performed by using diterpene cyclase, HpDTC1. HpDTC1 has been identified from the moss, *H. plumaeforme*, and is involved in sequential two-step cyclizations from GGDP to *syn*-pimara-7,15-diene via *syn*-CDP. The yields of both labeled *ent*-cassa-12,15-diene and *syn*-pimara-7,15-diene from ^{13}C-mevalonate reached approximately 90% and 66%, respectively, indicating that both enzyme reactions are highly efficient for the synthesis of labeled substrates. GC-MS and ^{13}C-NMR spectra validated the production of the [U-$^{13}C_{20}$] *ent*-cassa-12,15-diene and [U-$^{13}C_{20}$] *syn*-pimara-7,15-diene from [U-$^{13}C_6$] mevalonate as fully labeled compounds. Thus, we were able to generate biosynthetic precursors of diterpenoid phytoalexins labeled with ^{13}C isotope, capable of chasing metabolites leading to diterpenoid phytoalexins.

Chapter 3. Establishing feeding platforms of the labeled substrates incorporated into diterpenoid phytoalexins

To investigate the bioconversion of the diterpene hydrocarbon precursor into phytoalexins *in planta*, both the labeled precursors were fed into leaf disks (6 mm diameter) or young leaves (30 mm in length) of wild-type rice plants (*O. sativa* 'Nipponbare'), and analyzed by LC-MS/MS, to confirm the presence of ^{13}C-labeled compounds. After the application of [U-$^{13}C_{20}$]

syn-pimara-7,15-diene, [U-$^{13}C_{20}$] momilactone A and [U-$^{13}C_{20}$] momilactone B were detected to be accumulated in the leaf disk. Successful [U-$^{13}C_{20}$] *ent*-cassa-12,15-diene feeding experiment on rice leaves also gave the direct evidence of biotransformation of ^{13}C-phytocassanes from [U-$^{13}C_{20}$] *ent*-cassa-12,15-diene. These results suggest the conversion of momilactones and phytocassanes from *syn*-pimara-7,15-diene and *ent*-cassa-12,15-diene, respectively, in rice plants. This implied that the biosynthetic pathways of diterpenoid phytoalexins from these diterpenes are definitely active in rice.

Chapter 4. Investigation of diterpene intermediates in the biosynthetic mutants of cytochrome P450 monooxygenases for diterpenoid phytoalexins

Characterization of *cyp71z7* T-DNA insertion mutant and *CYP76M7M8-RNAi* plants have previously shown that cytochrome P450 monooxygenase~~s~~ genes *CYP71Z6/Z7* and *CYP76M7/M8* in the phytocassane biosynthetic gene clusters are involved in oxidation steps of diterpenoid phytoalexins biosynthesis. Therefore, possible intermediates accumulated in these CYP-modified plants were further investigated by using our feeding system. The application of [U-$^{13}C_{20}$] *ent*-cassa-12,15-diene to *cyp71z7* mutant revealed that the accumulation of C2-oxygenated types of phytocassanes (^{13}C-phytocassane A, B and D) was obviously repressed whereas the accumulation of ^{13}C-labeled C2-non-oxygenated types of phytocassanes (^{13}C-phytocassane C, E) was enhanced compared with wild-type plants. Furthermore, GC-MS analysis confirmed two intermediates in *cyp71z7* mutant, 1-deoxyphytocassane C and 2-deoxyphytocassane A, both of which were proposed as the precursor of phytocassanes.

On the other hand, none of the ^{13}C labeled phytocassanes were found in *CYP76M7/M8-RNAi* lines fed with [U-$^{13}C_{20}$] *ent*-cassa-12,15-diene, implying that metabolic flow from *ent*-cassa-12,15-diene might stuck and intermediates would be accumulated in this RNAi line. GC-MS analysis showed that two distinctive peaks dominant in *CYP76M7/M8-RNAi* were detected and low level of ^{13}C isotopic signals were monitored on the mass fragmentation. Consequently, two intermediates, 3α-hydroxy-*ent*-cassadiene and 3α-hydroxy-*ent*-cassadien-2-one, were discovered by comparing with reference compounds *in vitro* assay.

Previous study has shown that CYP76M8 has enzymatic activity for hydroxylation at

C6-position of pimaradiene, a momilactone precursor. To investigate this point, [U-$^{13}C_{20}$] momilactone A accumulation level in *CYP76M7/M8-RNAi* lines and wild-type rice plants were examined by LC-MS/MS after feeding of [U-$^{13}C_{20}$] *syn*-pimara-7,15-diene. Accumulation level of both non-labeled ^{13}C-labeled momilactones apparently decreased in the *CYP76M7/M8-RNAi* line compared to that in wild-type plants, suggesting that CYP76M8 is most likely to be involved in both phytocassanes and momilactones biosynthetic pathways. Further GC-MS analysis revealed that fully ^{13}C-labeled compounds derived from [U-$^{13}C_{20}$] *syn*-pimara-7,15-diene with unknown mass spectrum decreased in the *CYP76M7/M8-RNAi* lines. Although the structural information of this unknown compound is still elusive, these results demonstrate that enzymatically synthesized [U-$^{13}C_{20}$] diterpene substrates are a powerful tool for chasing endogenous metabolites without suffering from unavoidable dilution with natural abundance.

Chapter 5. The application of ^{13}C-labeled diterpene hydrocarbons to other plants

It has recently been reported that some of the plants, other than rice can produce two distinct types of phytocassanes (phytocassane C and E) or momilactones. Further application of this feeding method, using [U-$^{13}C_{20}$] *syn*-pimara-7,15-diene and [U-$^{13}C_{20}$] *ent*-cassa-12,15-diene in newly found phytoalexins-producing non-model plants, the moss *Hypnum plumaeforme* and the nearest out-group of *Oryza* species *Leersia perrieri*, respectively, resulted in detection of bioconversion of these labeled substrates into phytoalexins in these plants. These results demonstrate that enzymatically synthesized [U-$^{13}C_{20}$] diterpene substrates are a powerful tool for chasing endogenous metabolites without dilution with naturally abundant unlabeled compounds.

Reference

Zhongfeng Ye, Kazuya Nakagawa, Masahiro Natsume, Hideaki Nojiri, Hiroshi Kawaide*, Kazunori Okada* Biochemical synthesis of uniformly ^{13}C-labeled diterpene hydrocarbons and their bioconversion to diterpenoid phytoalexins in planta. *Bioscience Biotechnology and Bioc hemistry*. 2017, Feb. 6: 1-9

CHAPTER 1

INTRODUCTION

1-1. Inductive production of phytoalexins in rice

Plants attacked by pathogenic microorganisms respond with a variety of defensive reactions, including the production of antimicrobial secondary metabolites known as phytoalexins. These compounds are transiently generated in response to signal molecules called elicitors, which are usually derived from pathogens, such as the rice blast fungus *Magnaporthe oryzae*. In rice (*Oryza sativa*), 17 compounds have been identified as phytoalexins from leaves that were either infected with the *M. oryzae* or subjected to UV irradiation. Other elicitations, such as heavy metal ions treatment, also can induce phytoalexin production in rice.[1-10] All these phytoalexins, except for the flavanone sakuranetin, are diterpenoids in nature, and can be classified into five groups based on their carbon frameworks: phytocassanes A-F,[6,7] oryzalexins A-F,[1-4] momilactone A and B,[10] oryzalexin S,[5] and casbane-type oxodepressin,[8] all of which are the active substances against pathogens growth (Fig.1-1).

1-2. Biosynthetic pathway of diterpenoid phytoalexins

All diterpenoid phytoalexins in plants are biosynthesized from geranylgeranyl diphosphate (GGDP) through 2*C*-methyl-D-erythritol 4-phosphate (MEP) pathway in plastids. The common precursor, GGDP, is postulated to be sequentially cyclized via *ent*-copalyl diphosphate (*ent*-CDP) to *ent*-cassa-12,15-diene and *ent*-sandaracopimaradiene, leading to phytocassane A to F and oryzalexins A to F. GGDP can be cyclized via *syn*-CDP to 9βH-pimara-7,15-diene and stemar-13-ene, leading to momilactones A and B and oryzalexin S (Fig.1-2). It has been demonstrated that all six diterpene cyclases are involved in the conversion of GGDP to the four diterpene hydrocarbon precursors via *ent*- or *syn*-CDP (Fig.1-2). So far, all of the diterpene-cyclase genes comprising the *OsCPS2*, *OsCPS4*, *OsKSL4*, *OsKSL7*, *OsKSL8*, and *OsKSL10* have been identified and characterized.[11] It has also been demonstrated that several genes of P450 monooxygenases and dehydrogenase are involved in the oxidation steps of diterpene hydrocarbon to the final products, phytoalexins. Furthermore, these diterpene-cyclase genes and P450 genes have been shown to be located on a narrow region of rice chromosomes as gene clusters; *OsCPS2*, *OsKSL7*, and six P450 genes (*CYP71Z6*, *Z7* and *CYP76M5-M8*) are clustered in chromosome 2, and *OsCPS4*, *OsKSL4*, and two P450 genes (*CYP99A2* and *CYP99A3*) are clustered in chromosome 4.[12,13] Line of evidences from both *in vivo* and *in vitro* experiments have shown that these P450 genes are most likely responsible for the biosynthesis of diterpenoid phytoalexins in rice.[14,24] However, there are still some uncharacterized enzymes, so that unidentified steps in the biosynthetic pathway remain to be clarified.

1-3. The origin of gene cluster

One of the interesting features of biosynthetic genes for diterpenoid phytoalexins in rice is gene clustering. However, it is still difficult to answer why rice plants possess such gene clusters consist of several genes encoding different types of enzyme with different functions. In order to understand the gene clustering, it would be important to follow history of gene clustering.

In 1961, *lac* operon was discovered in *E. coli*. Several related genes involved in an inducible and repressible enzyme systems first time gave the direct evidence for the regulation mechanism in lactose utilization of *E. coli*.[15-17] In prokaryotic organisms, related functional genes with a single promoter were assembled together and contained in classical operons, which also termed as clusters in secondary mechanism. In prokaryotic genomes, the organizations of genes within clusters were extremely essential for various complete biosynthetic pathways, which function on bacterial nutrient intake, substrates utilization and products synthesis. They share common regulatory factors and related functions.[18]

Gene clusters are found to be widely distributed in eukaryotic organisms as well, such as yeast, fungi, insects and plants. Unlike prokaryote, in eukaryotic genomes, genes order along chromosomes was assumed as random when it first appeared. In 2001, breakthrough in imprinted genes was made. These genes linked together in clusters and they are thought to reflect coordinated genes in chromosomal. Furthermore, imprinted genes encoded protein sequences are almost no common feature recognized, but functional relationship is existed between them. This finding provided strong evidence for non-random genes existence.[19] On the other hand, although clustered genes in eukaryotic were transcribed independently, they still share a common regulation mechanism on one biosynthetic pathway. Furthermore, it has been confirmed that clustered genes function on one synthetic pathway for various chemicals production through their own related function in mammalian. In 1994, Brayton *et al*. have confirmed both of human glutamine phosphoribosyl pyrophosphate amidotransferase (GPAT) and phosphoribosylamidoimidazole-succinocarboxamide synthase (AIRC) is required for *de novo* purine synthesis.[20] This two linked and closely non-homologous genes (GPAT and AIRC) are responsible for the initial step and later steps in purine biosynthesis, respectively.

In plants, the first gene cluster in maize, *Bx1* through *Bx5* on chromosome 4 for cyclic hydroxamic acids 2,4-dihydroxy-1,4-benzoxazin-3-one (DIBOA) biosynthesis were discovered in 1997.[21] Afterwards, Prof. Anne Osbourn in John Innes Centre group reported ß-amyrin synthase (AsbAS1) related gene cluster on avenacin biosynthetic pathway in diploid oat and clustered genes for marneral synthesis in *Arabidopsis thaliana*.[22,23] These gene clusters are all required for secondary metabolisms partly related to plant defense. In rice, two gene clusters on chromosome 2 and chromosome 4 responsible for phytocassanes and momilactones biosynthesis are found.[24] Very recently, these rice clusters have also been clarified in wild rice and closely related other wild species, other than cultivated rice.[25]

1-4. Evolutional diversity of the enzymes involved in diterpenoid phytoalexin biosynthesis

In cultivated rice, most of the biosynthetic genes responsible for down stream steps in further conversions of diterpene hydrocarbons to precursors of diterpenoids phytoalexins are tentatively determined so far.[24,26,27] Genes encoding P450 monooxygenases are involved in oxidation step of *syn*-pimara-7,15-diene to *syn*-pimara-7,15-dienoic acid (CYP99A2 and A3) on momilactones biosynthesis and that of *ent*-cassa-12,15-diene to phytocassanes (CYP71Z7, CYP76M7, M8). Several evidences from both *in vivo* and *in vitro* experiments have shown that many P450 genes are putatively responsible for the biosynthesis of diterpenoid phytoalexins in rice.[24] However, there has been still remaining steps to be identified, involved in P450 enzymes in later stage of the biosynthetic pathway. Recently, our group has reported that accumulation of phytocassanes and momilactones after stress treatment is confirmed in some of wild rice species harboring complete gene clusters.[25] Interestingly, wild rice incapable of producing either of diterpenoid phytoalexins did not maintain complete gene clusters, but possess some of homologous gene of P450 genes in the cluster of the phytoalexin-producing *Oryza* species. Closer comparative analysis of genome sequence between *O. sativa* and wild rice indicated that *CYP76M*, *CYP71Z*, *CYP99A* and *MAS* family genes control phytocassanes and momilactones biosynthetic route in rice plant besides *CPS* and *KSL* family genes. Correspondingly, in other wild species, *Leersia perrieri*, chromosomal map and LC-ESI-MS/MS results further confirmed that CYP76 and CYP71 family members are required for different phytocassanes biosynthesis or hydroxylation.[25] Hence, evolutionary ancestral wild rice has already possessed distinctive P450 genes, which seemed to be ancestor P450 genes evolved to the enzymes functioning in diterpenoid phytoalexin synthesis.

1-5. Elucidation of a nexus for a complexity of diterpenoid phytoalexins from discovery of CYP76 and CYP71 family

In th past 20 years, CYP76 and CYP71 family P450 monooxygenases have been well studied and elucidated. Mizutani *et al.* (1997) discovered a CYP76C1 play important role in hydroxylation of monoterpene geraniol in *A. thaliana*.[28] One year later, a CYP76B6 protein was confirmed as a enzyme, which is responsible for the hydroxylation of C-10 position on geraniol.[29] Afterwards, Lupien *et al*. (1999) clarified that limonene hydroxylases, has C3 or C6 hydroxylation activity on (-)-Limonene, belong to CYP71D subfamily.[30] In 2001, Ralston *et al*. gave the evidence that tobacco CYP71D20 expressed yeast microsomes had activities to catalyze C1 and C3 hydroxylation of 5-epi-aristolochene.[31] These early researches are extremely important as a pioneer work for the elucidation of phytoalexins biosynthetic route on diterpenes. From 2004, our group and Prof. Reuben Peters in

Iowa university group have started identifying and characterizing several CYP76M and CYP71Z7 family genes and proteins on the pathway to the diterpenoid phytoalexins.

Up to date, 10 members of CYP76M subfamily were systematically researched. On the pathway to phytocassanes, CYP76M7 was confirmed as a cytochrome P450 monooxygenase that catalyze the C11α-hydroxylation of *ent*-cassa-12,15-diene *in vitro*.[32] Furthermore, the products from CYP76M7, C11α-hydroxy-*ent*-cassadiene, was also found on methyl jasmonic acid induced rice leaves.[33] These findings suggested the conversion into C11α-hydroxy-*ent*-cassadiene from cassadiene actually occurred in rice plants. On the other hand, structure of the end product, phytocassanes, required a keto group bound to C11. C11-keto-*ent*-cassadiene was hardly detected in CYP76M7 *in vitro* assay, although native C11-keto-*ent*-cassadiene could be endogenously detected in rice plants.[32] Thus CYP76M7 may be responsible for a early step on the pathway to phytocassanes. Wang *et al*. (2012) reported a series of functional analysis of CYP76M subfamily members. Based on co-expression system, they clarified CYP76M(5-8) functions *in vitro*. CYP76M5 is found to hydroxylate *ent*-sandaracopimaradiene at C7β. CYP76M6 is able to hydroxylate *syn*-stemodene at C6β and *ent*-sandaracopimaradiene at C7β, respectively. And CYP76M8 is responsible for the hydroxylation of a wide range of diterpenes, *ent*-cassa-12,15-diene (C11α), *syn*-pimara-7,15-diene (C6β), *ent*-pimaradiene (C7β), *ent*-kaurene (C9α), *ent*-sandaracopimaradiene (C9α) and *ent*-isokaurene (C7α).[38] Such wide range substrates specificities presumably enable to compose a potential network with variety and complexity in diterpene derivation. The function of CYP76M(5-8) was partly confirmed *in vitro*, but their exact substrates and roles *in vivo* are still ambiguous.

Our genetic approach using *CYP76M7/M8* double knock-down lines indicated that accumulation of phytocassanes was strongly repressed relative to those of control.[38] Interestingly, *CYP76M7/M8* RNAi rice plants exhibited decrease in momilactones level in addition to phytocassanes depletion [unpublished data; Fig.4-2]. This result supports the idea that CYP76M7/M8 are responsible for both of phytocassanes and momilactones biosynthesis and they act on wide range of substrates consistent with the reports of *in vitro* enzyme assay.

In phytocassanes and momilactones biosynthesis, other CYPs families were also investigated *in vitro*. On the pathway to phytocassanes, CYP701A8 was also confirmed as a catalyst on *ent*-cassa-12,15-diene C3β-hydroxylation.[34] CYP71Z7 carries out C2-hydroxylation of *ent*-cassa-12,15-diene and may be responsible for conversion at a later step due to its poor recognition of *ent*-cassa-12,15-diene as an *in vitro* enzymatic substrates.[35] Based on such situation, C3α-hydroxy-C11-keto-*ent*-cassa-12,15-diene (1-deoxyphytocassane C) was assumed to be a hypothetical substrate for CYP71Z7 (Fig.1-3).[35] In our group, this assumption is verified by the analysis of *CYP71Z7* T-DNA mutant (*O. sativa* L. cv. Dongjin), indicating that significant accumulation of 1-deoxyphytocassane C in the mutant (Unpublished data; Fig.4-21; Fig.4-22). On the pathway to momilactones, it has been shown that CYP99A3 and CYP99A2 enable to oxidize C19 of *syn*-pimara-7,15-diene.[36, 37] Besides, it is proposed that CYP701A8 also acts as

C3β-hydroxylase of *syn*-pimara-7,15-diene, and C6β-hydroxylation of *syn*-pimara-7,15-diene is catalyzed by CYP76M8. As seen from above mentioned evidence, complexity of diterpenoid phytoalexin biosynthesis is thought to come from the diversity of catalytic variation of P450 enzymes represented by CYP71Z and CYP76M family together with CYP99A in rice.

1-6. Stable isotope tracing

Complexity in metabolic network has been shown in many reports. First, various reactions happened in plants or plant cells are regulated *in vivo* accurately. Second, the pathways of secondary metabolites are compartmentalized on different locations or organelles in plant cells, but they still share the common intermediates and reaction factors. Third, enzyme activity *in vitro* can not be simply used to evaluate their *in vivo* activity, because of variety of reactions responsible for their biosynthesis and degradation in plant cells.[39] Hence, methods of stable isotopic or radioactive isotopic labeling *in vivo* have been used for several decades and contributed to various secondary metabolic pathway elucidations.

Radioactive isotope (^{14}C, ^{3}H or ^{33}P) have been utilized for monitoring unknown intermediates for many years in different organisms. They produce radiated signal spontaneously without noise increase from natural compounds.[40] However, recent years, their limitation is becoming more and more obvious in application. Such as unstable, incompatible with mass spectrometry (MS), environmental contamination, biological perturbation and risks.[40,41] Gradually, radioactive isotopes are few applied to the metabolic flux analysis in plants and utilized for tracing research.[42] Recently, stable isotope is becoming main tool for tracing intermediates in plants.[42] Stable isotopes (^{13}C, ^{2}H, ^{18}O or ^{15}N) own 1 or 2 more neutrons than that of natural isotopes (^{12}C, ^{1}H, ^{16}O or ^{14}N). On MS, stable isotopic labeling compounds can be identified and distinguished from natural compounds by checking their precursor ion and product ion. So far, ^{13}C-labeling strategy has been widely used in metabolic flux analysis over four decades for carbon metabolism investigation in plants. ^{13}C-labeling experiment with MS and nuclear magnetic resonance (NMR) is one of the most simply and efficient method for analysis of metabolic intermediates or final products.

So far, in substrate feeding experiment, there are various feeding methods have been performed on plants. Pierre *et al*. (1980) has established the method for substrate feeding.[43] Excised maize root tips (sugar depletion) can be grown in cultured medium with sole carbon source, sucrose. They has confirmed that this root tips without sugar reserves or translocation can also absorb exogenous sugar supply directly under the decline of dioxygen uptake. Thereafter, various substrates feeding experiments were performed in different cultured medium through sole carbon source absorption. In 2006, jőrg Schwender *et al.* investigated metabolic fluxes on the network of sugars and amino acids in the developing of *Brassica napus* embryos.[44] Embryos were cultured seeds endosperm liquid with different labeling substrates.[45] They utilized exogenous labeling substrates, such as [1,2-$^{13}C_2$]glc, [U-$^{13}C_6$]glc, [U-$^{13}C_3$]Ala, [U-$^{13}C_5$]Gln and [^{15}N]Ala, to clarify metabolic fluxes through

mitochondrial metabolism.[44] Afterwards, from 2007 to 2013, some groups challenged the direct labeling experiment of $^{13}CO_2$ through photosynthesis on plants.[46-49] So far, more and more labeling experiments were performed in systematically. However, in secondary metabolism, a part of intermediates or substrates were hydrophobic and non-polarity. These types of compounds are difficult to be dissolved in liquid medium for plants absorption. New method has to be established for this feeding experiment in rice plants. In 1987, TJ Ingram and JB Reid have reported that 99.5% ethanol dissolved labeling substrates, such as *ent*-kaurene, *ent*-kaurenoic acid, were applied to peas fully expanded leaves (*Pisum sativum* L.) at three-leaf stage. Related labeled intermediates were detected and clarified on the route of gibberellins.[50] Applicably, in rice plants, we also try to utilize 99.5% ethanol dissolved labeling substrates for secondary metabolites investigation on the pathway to phytoalexins.

1-7. The purpose of this study

Great efforts to disclose the whole biosynthetic pathway of phytoalexins, momilactones and phytocassanes, have been made up to now, but there still be unidentified catalytic steps to reach the final products. Thus, we need to investigate more the intermediates of the diterpene phytoalexins in their biosynthetic pathway. A feeding approach with stable isotope (e.g., ^{13}C) will be an effective method to trace as-yet-unknown precursors derived from known compound such as *ent*-cassa-12,15-diene and *syn*-pimara-7,15-diene, the diterpene hydrocarbons for phytocassane (A-F) and momilactone (A and B), respectively. Therefore, in this study, I will synthesize ^{13}C-labelled compounds such as ^{13}C-*ent*-cassa-12,15-diene and ^{13}C-*syn*-pimara-7,15-diene *in vitro* enzymatic reactions, and used for the feeding experiment to cultured rice plants.

1-8. Figures

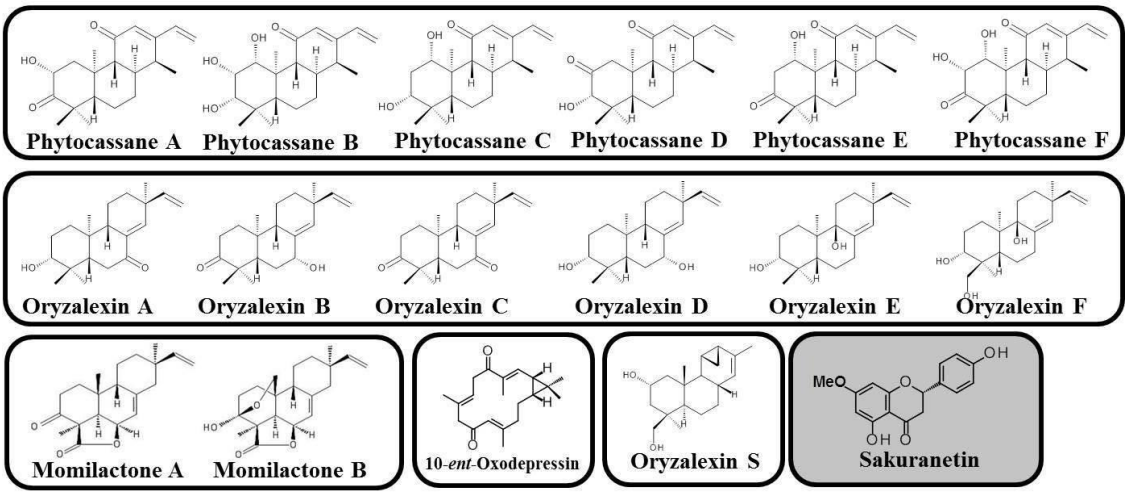

Figure 1-1. 16 diterpenoid phytoalexins and one flavanone sakuranetin

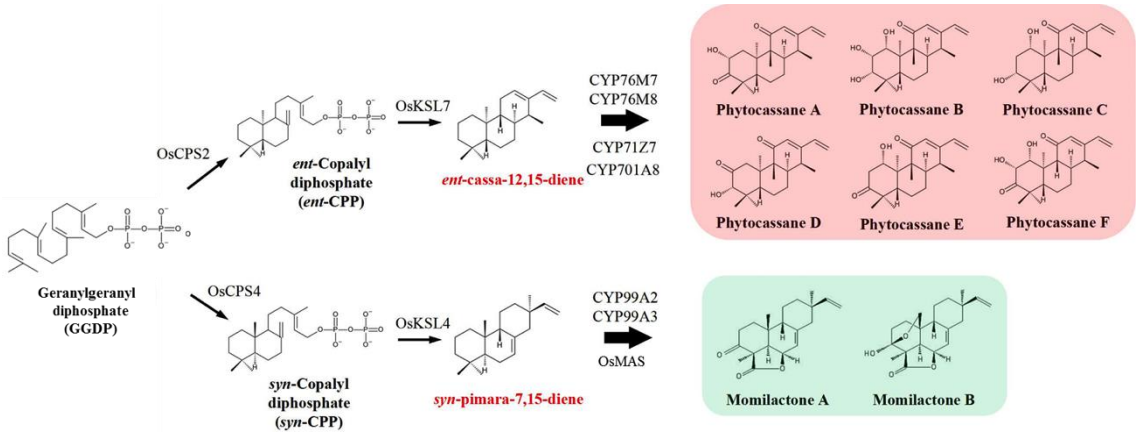

.Figure 1-2. Phytocassane (A-F) and momilactone (A and B) biosynthesis from GGDP *in vivo*

OsCPS2, rice *ent*-copalyl diphosphate synthase 2; **OsCPS4,** rice *syn*-copalyl diphosphate synthase 4; **OsKSL7,** rice *ent*-kaurene synthase-like 7; **OsKSL4**, rice *ent*-kaurene synthase-line 4;

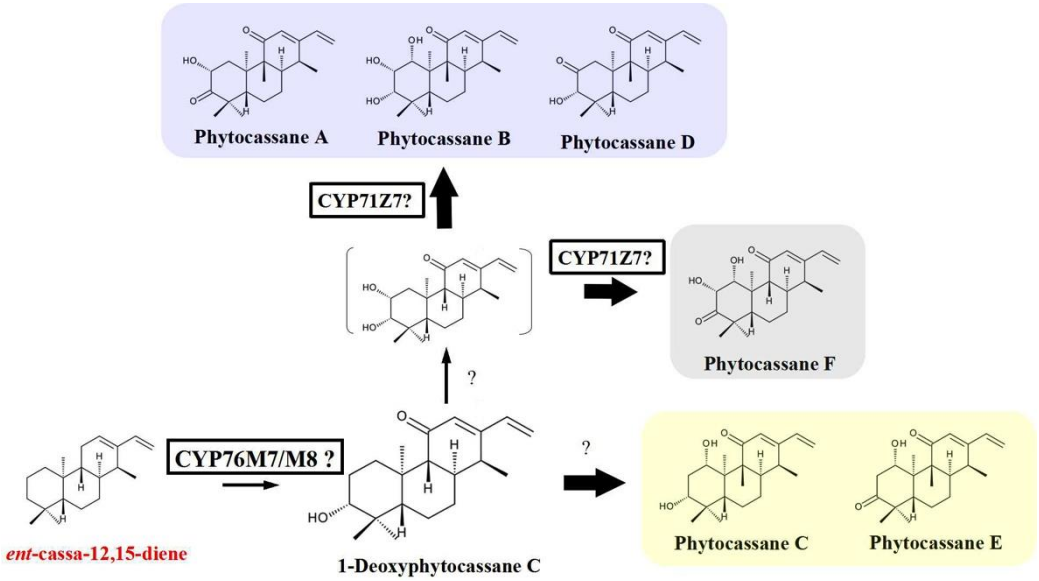

Figure 1-3. Hypothetical pathway from *ent*-cassa-12,15- diene to phytocassane (A-F)

Reference

[1] Akatsuka T, Kodama O, Sekido H, Kono Y, Takeuchi S. Novel phytoalexins (oryzalexins A, B and C) isolated from rice blast leaves infected with Pyricularia oryzae. Part I: isolation, characterization and biological activities of oryzalexins. *Agric. Biol. Chem.* 1985, 49, 1689-1694.

[2] Sekido H, Endo, T, Suga, R, Kodama O, Akatsuka T, Kono Y, Takeuchi S. Oryzalexin D 3,7-dihydroxy-(+)-sandaracopimaradiene), a new phytoalexin isolated from blast-infected rice leaves. *J. Pestic. Sci.* 1986, 11, 369-372.

[3] Kato H, Kodama O, Akatsuka T. Oryzalexin E, a diterpene phytoalexin from UV-irradiated rice leaves. *Phytochemistry.* 1993, 33, 79-81.

[4] Kato H, Kodama O, Akatsuka T. Oryzalexin F, a diterpene phytoalexin from UV-irradiated rice leaves. *Phytochemistry*. 1994, 36, 299-301.

[5] Kodama O, Li WX, Tamogami S, Akatsuka T. Oryzalexin S, a novel stemarane-type diterpene rice phytoalexin. *Biosci Biotechnol Biochem*. 1992, 56, 1002-1003.

[6] Koga J, Shimura M, Oshima K, Ogawa N, Yamauchi T, Ogasawara N. Phytocassanes A, B, C and D, novel diterpene phytoalexins from rice, *Oryza sativa L*. *Tetrahedron.* 1995, 51, 7907- 7918.

[7] Koga J, Ogawa N, Yamauchi T, Kikuchi M., Ogasawara N, Shimura M. Functional moiety for the antifungal activity of phytocassane E, a diterpene phytoalexin from rice. *Phytochemistry.* 1997, 44, 249-253.

[8] Inoue Y, Sakai M, Yao Q, Tanimoto Y, Toshima H, Hasegawa M. Identification of a novel casbane-type diterpene phytoalexin, *ent*-10-oxodepressin, from rice leaves. *Biosci Biotechnol Biochem*. 2013, 77, 760-765.

[9] Kodama O, Miyakawa J, Akatsuka T, Kiyosawa S. Sakuranetin, a flavanone phytoalexin from ultraviolet-irradiated rice leaves. *Phytochemistry.* 1992, 31, 3807-3809.

[10] Cartwright DW, Langcake P, Pryce RJ, Leworthy DP, Ride JP. Isolation and characterization of two phytoalexins from rice as momilactones A and B. *Phytochemistry.* 1981, 20: 535−537.

[11] Jwa NS, Agrawal GK, Tamogami S, Yonekura M, Han O, Iwahashi H, Rakwal R. Role of defense/stress-related marker genes, proteins and secondary metabolites in defining rice self-defense mechanisms. *Plant Physiol Biochem*. 2006, 44(5-6): 261-273.

[12] Otomo K, Kanno Y, Motegi A, Kenmoku H, Yamane H, Mitsuhashi W, Oikawa H, Toshima H, Itoh H, Matsuoka M, Sassa T, Toyomasu T. Diterpene cyclases responsible for the biosynthesis of phytoalexins, momilactones A, B, and oryzalexins A-F in rice. *Biosci Biotechnol Biochem*. 2004, 68(9): 2001-2006.

[13] Cho EM, Okada A, Kenmoku H, Otomo K, Toyomasu T, Mitsuhashi W, Sassa T, Yajima A, Yabuta G, Mori K, Oikawa H, Toshima H, Shibuya N, Nojiri H, Omori T, Nishiyama M and Yamane H. Molecular cloning and characterization of a cDNA encoding *en*t-cassa-12,15-diene synthase, a putative diterpenoid phytoalexin biosynthetic enzyme, from suspension-cultured rice cells treated with a chitin elicitor. *Plant Journal*. 2004, 37: 1-8

[14] Schmelz EA, Huffaker A, Sims JW, Christensen SA, Lu X, Okada K, Peters RJ. Biosynthesis, elicitation and roles of monocot terpenoid phytoalexins. *Plant J.* 2014, 79(4): 659-678

[15] Jacob F, Monod J. Genetic regulatory mechanisms in the synthesis of proteins. *J Mol Biol.* 1961, 3:318-356.

[16] Jacob F, Perrin D, Sánchez C, Monod J, Edelstein S. The operon: a group of genes with expression coordinated by an operator. *C R Biol.* 1960, 250: 1727-9.

[17] François Jacob and Jacques Monod. On the Regulation of Gene Activity. *Cold Spring Harb Symp Quant Biol.* 1961, 26: 193-211

[18] Boycheva S, Daviet L, Wolfender JL, Fitzpatrick TB. The rise of operon-like gene clusters in plants. *Trends Plant Sci.* 2014, 19(7): 447-459

[19] Reik W, Walter J. Genomic imprinting: parental influence on the genome. *Nat Rev Genet.* 2001, 2(1):21-32.

[20] Brayton KA1, Chen Z, Zhou G, Nagy PL, Gavalas A, Trent JM, Deaven LL, Dixon JE, Zalkin H. Two genes for de novo purine nucleotide synthesis on human chromosome 4 are closely linked and divergently transcribed. *J Biol Chem.* 1994, 269(7):5313-5321.

[21] Frey M, Chomet P, Glawischnig E, Stettner C, Grün S, Winklmair A, Eisenreich W, Bacher A, Meeley RB, Briggs SP, Simcox K, Gierl A. Analysis of a chemical plant defense mechanism in grasses. *Science.* 1997, 277(5326): 696-699.

[22] Qi X, Bakht S, Leggett M, Maxwell C, Melton R, Osbourn A. A gene cluster for secondary metabolism in oat: implications for the evolution of metabolic diversity in plants. *Proc Natl Acad Sci USA.* 2004, 101(21):8233-8238

[23] Field B, Fiston-Lavier AS, Kemen A, Geisler K, Quesneville H, Osbourn AE. Formation of plant metabolic gene clusters within dynamic chromosomal regions. *Proc Natl Acad Sci USA.* 2011, 108(38): 16116-16121

[24] Okada K. The biosynthesis of isoprenoids and the mechanisms regulating it in plants. *Biosci Biotechnol Biochem*. 2011, 75(7): 1219-1225

[25] Miyamoto K, Fujita M, Shenton MR, Akashi S, Sugawara C, Sakai A, Horie K, Hasegawa M, Kawaide H, Mitsuhashi W, Nojiri H, Yamane H, Kurata N, Okada K, Toyomasu T. Evolutionary trajectory of phytoalexin biosynthetic gene clusters in rice. *Plant J.* 2016, 87(3): 293-304.

[26] Zhong L, Wang K, Tan J, Li W, Li S. Putative cytochrome P450 genes in rice genome (*Oryza sativa L. ssp.* indica) and their EST evidence.*Sci China C Life Sci*. 2002, 45(5): 512-7.

[27] Toyomasu T. Recent advances regarding diterpene cyclase genes in higher plants and fungi. *Biosci Biotechnol Biochem.* 2008, 72(5): 1168-1175.

[28] Mizutani M, Ward E, Ohta D. Plant geraniol/nerol 10-hydroxylase and DNA coding therefor. *PCT International Patent Application.* 1997, 11184

[29] Collu G, Unver N, Peltenburg-Looman AM, van der Heijden R, Verpoorte R, Memelink J. Geraniol 10-hydroxylase, a cytochrome P450 enzyme involved in terpenoid indole alkaloid biosynthesis. *FEBS Lett*. 2001, 508(2):215-220.

[30] Lupien S, Karp F, Wildung M, Croteau R. Regiospecific cytochrome P450 limonene hydroxylases from mint (Mentha) species: cDNA isolation, characterization, and functional expression of (-)-4S-limonene-3-hydroxylase and (-)-4S-limonene-6-hydroxylase. *Arch Biochem Biophys.* 1999, 368(1):181-192.

[31] Ralston L, Kwon ST, Schoenbeck M, Ralston J, Schenk DJ, Coates RM, Chappell J. Cloning, heterologous expression, and functional characterization of 5-epi-aristolochene-1,3-dihydroxyl ase from tobacco (Nicotiana tabacum). *Arch Biochem Biophys.* 2001, 393(2):222-235.

[32] Swaminathan S, Morrone D, Wang Q, Fulton DB, Peters RJ. CYP76M7 is an *ent*-cassadiene C11alpha-hydroxylase defining a second multifunctional diterpenoid biosynthetic gene cluster in

rice. *Plant Cell*. 2009, 21(10):3315-3325.

[33] Peters RJ. Uncovering the complex metabolic network underlying diterpenoid phytoalexin biosynthesis in rice and other cereal crop plants. *Phytochemistry*. 2006, 67(21): 2307-2317.

[34] Wang Q, Hillwig ML, Wu Y, Peters RJ. CYP701A8: a rice ent-kaurene oxidase paralog diverted to more specialized diterpenoid metabolism. *Plant Physiol.* 2012, 158(3): 1418-1425.

[35] Yisheng Wu, Matthew L. Hillwig, Qiang Wang, Reuben J. Peters. Parsing a multifunctional biosynthetic gene cluster from rice: Biochemical characterization of CYP71Z6 & 7. *FEBS Lett.* 2011, 585(21): 3446-3451.

[36] Qiang Wang, Matthew L. Hillwig, Reuben J. Peters. CYP99A3: Functional identification of a diterpene oxidase from the momilactone biosynthetic gene cluster in rice. *Plant J.* 2011, 65(1): 87-95.

[37] Naoki Kitaoka, Yisheng Wu, Meimei Xu, Reuben J. Peters. Optimization of recombinant expression enables discovery of novel cytochrome P450 activity in rice diterpenoid biosynthesis. *Appl Microbiol Biotechnol*. 2015, 99(18): 7549-7558.

[38] Wang Q, Hillwig ML, Okada K, Yamazaki K, Wu Y, Swaminathan S, Yamane H, Peters RJ. Characterization of CYP76M5-8 indicates metabolic plasticity within a plant biosynthetic gene cluster. *J Biol Chem.* 2012 , 287(9): 6159-6168.

[39] Martine Dieuaide-Noubhani, Ana Paula Alonso. Plant Metabolic Flux Analysis. *Methods in Molecular Biology*. 2014.

[40] Freund DM, Hegeman AD. Recent advances in stable isotope-enabled mass spectrometry-based plant metabolomics. *Curr Opin Biotechnol.* 2016, 43:41-48.

[41] Hu VW, Heikka DS. Radiolabeling revisited: metabolic labeling with (35)S-methionine inhibits cell cycle progression, proliferation, and survival. *FASEB J.* 2000, 14(3):448-454.

[42] Batista Silva W, Daloso DM, Fernie AR, Nunes-Nesi A, Araújo WL. Can stable isotope mass spectrometry replace radiolabelled approaches in metabolic studies. *Plant Sci*. 2016, 249: 59-69

[43] Saglio PH, Pradet A. Soluble Sugars, Respiration, and Energy Charge during Aging of Excised Maize Root Tips. *Plant Physiol*. 1980, 66(3): 516-519

[44] Schwender J, Shachar-Hill Y, Ohlrogge JB. Mitochondrial metabolism in developing embryos of Brassica napus. *J Biol Chem*. 2006, 281(45): 34040-34047

[45] Schwender J, Ohlrogge JB. Probing *in vivo* metabolism by stable isotope labeling of storage lipids and proteins in developing Brassica napus embryos. *Plant Physiol*. 2002, 130(1):347-361.

[46] Römisch-Margl W, Schramek N, Radykewicz T, Ettenhuber C, Eylert E, Huber C, Römisch-Margl L, Schwarz C, Dobner M, Demmel N, Winzenhörlein B, Bacher A, Eisenreich W. $^{13}CO_2$ as a universal metabolic tracer in isotopologue perturbation experiments. *Phytochemistry.* 2007, 68(16-18): 2273-2289

[47] Huege J, Sulpice R, Gibon Y, Lisec J, Koehl K, Kopka J. GC-EI-TOF-MS analysis of *in vivo* carbon-partitioning into soluble metabolite pools of higher plants by monitoring isotope dilution after $^{13}CO_2$ labelling. *Phytochemistry*. 2007, 68(16-18): 2258-2272.

[48] Chen WP, Yang XY, Harms GL, Gray WM, Hegeman AD, Cohen JD. An automated growth enclosure for metabolic labeling of Arabidopsis thaliana with ^{13}C-carbon dioxide-an in vivo labeling system for proteomics and metabolomics research. *Proteome Sci*. 2011, 10;9(1): 9.

[49] Szecowka M, Heise R, Tohge T, Nunes-Nesi A, Vosloh D, Huege J, Feil R, Lunn J, Nikoloski Z, Stitt M, Fernie AR, Arrivault S. Metabolic fluxes in an illuminated Arabidopsis rosette. *Plant Cell*. 2013, 25(2): 694-714.

[50] Ingram TJ and Reid JB. Internode Length in Pisum: Gene na May Block Gibberellin Synthesis between *ent*-7alpha-Hydroxykaurenoic Acid and Gibberellin A_{12}-Aldehyde. *Plant Physiol*. 1987, 83(4): 1048-1053

CHAPTER 2

ENZYMATIC PRODUCTION OF ^{13}C-LABELED DITERPENE HYDROCARBONS

2-1. Introduction

Plants have self-defense response against pathogenic microorganisms and physical stress. One of the defense systems is a production of phytoalexins that are low molecular-weight secondary metabolites (specialized metabolites) induced by various stresses conditions. It has been well-studied as a model system that rice plant induces the production of diterpenoid phytoalexins family when rice blast fungus is infected and physical stresses such as heavy metal ions and UV irradiation are exposed to rice.[1,2] Diterpene phytoalexins, momilactones, phytocassanes and oryzalexins, are major compounds in rice having strong inhibitory activities microbial and plant growth inhibitions.

All diterpenoid phytoalexins are biosynthesized from geranylgeranyl diphosphate (GGDP) through 2*C*-methyl-D-erythritol 4-phosphate (MEP) pathway in plastid. In case of momilactone, for example, committed steps of the biosynthesis of momilactones A and B is cyclization reactions of GGDP to *syn*-pimara-7,15-diene via *syn*-copalyl diphosphate, conducted by two diterpene cyclases OsCPS4 and OsKSL4. [3] On the other hand, the biosynthesis of phytocassanes has committed steps from GGDP to *ent*-cassa-12,15-diene via *ent*-copalyl diphosphate, committed by two diterpene cyclases OsCPS2 and OsKSL7. [3,4] However, so far, few of evidence were provided to confirm *ent*-cassa-12,15-diene and *syn*-pimara-7-15-diene are the intermediate on the biosynthetic pathway of phytocassanes and momilactones directly. Few of compounds were directly confirmed as intermediates on the route of phytocassanes and momilactones in rice plants.

Therefore, a feeding approach with stable isotope (e.g., ^{13}C) will be an effective method to trace as-yet-unknown precursors derived from known compounds such as *ent*-cassa-12,15-diene and *syn*-pimara-7,15-diene. Previously Prof. Kawaide group in Tokyo Univ. of Agri. Tech. reported that enzymatically synthesized ^{13}C-mevalonate could be a starting point of the entire *in vitro* synthesis of diterpenoid phytohormone gibberellins. [5] It is also demonstrated that isotope labeled compounds (*ent*-[17-$^{3}H_2$] kaurenoic acid or [18-$^{2}H_1$] GA_{12}-aldehyde) was efficiently fed to peas (*Pisum sativum* L.) plants to trace the incorporation of *ent*-[17-$^{3}H_2$] kaurenoic acid or [18-$^{2}H_1$] GA_{12}-aldehyde into the precursors of gibberellins.[6] Applicably, a feeding approach with fully ^{13}C-labeled *ent*-cassa-12,15-diene or *syn*-pimara-7,15-diene should be one of the alternative way to disclose the pathway for diterpenoid biosynthesis. However, few of structural information were available from reported *ent*-cassa-12,15-diene or *syn*-pimara-7,15-diene. This is because it is difficult to obtain enough amount of products, which are enzymatically biosynthesized for nuclear magnetic resonance (NMR) analysis. Beside, milligram yields of ^{13}C labeled substrates were necessary for feeding experiment to investigate unknown intermediates in rice plants.

To achieve this goal, in this chapter, two hydrocarbons, *ent*-cassa-12,15-diene and *syn*-pimara-*7,15*-diene were enzymatically synthesized, and the all carbon atoms were substituted with ^{13}C-isotope. Generated [U-$^{13}C_{20}$] *ent*-cassa-12,15-diene and [U-$^{13}C_{20}$] *syn*-pimara-7,15-diene were fed to fully expanded leaves or leaf disks for intermediates detection in chapter 3 and 4.

2-2. Materials and Methods

2-2-1. Plasmids and Chemicals

Preparation: 100 mM ATP, 500 mM Tris-HCl pH7.43, 0.5 mM $MgCl_2$, 10xReaction Buffer A (20 mM DTT, 5 mM EDTA, 1/1000 Tablet protease inhibitor, 50 mM $MgCl_2$) (Tab. 2-1). Fully ^{13}C-labeled mevalonate, eight enzymes plasmids (*NcMVK*, *NcPMVK*, *NcMVD*, *NcIPI*, *SaGGPS*, *OsCPS2*, *OsKSL7 and HpDTC1*) were kindly gifted from Prof. Kawaide (Tokyo University of Agriculture and Technology).

Table 2-1. 10xEnzyme Reaction Buffer A (1 ml scale)

	Volume	Concentration in 10xReaction Buffer
100 mM DTT	200 μl	20 mM
500 mM EDTA	10 μl	5 mM
1 Tablet Protease Inhibitor dissolved in 2 ml	2 μl	1/1000 Tablet
100 mM $MgCl_2$	500 μl	50 mM
Milli Q Water	288 μl	
Total Volume	1 ml Stock	

2-2-2. Expression and purification of recombinant enzymes for *syn*-pimara-7,15-diene and *ent*-cassa-12,15-diene synthesis

Five enzymes for GGDP synthesis were expressed in *E.coli* (JM109), which was cultured in 2xYT medium (1% Yeast Extract, 1.6% Tryptone, 1% NaCl) containing ampicillin (100 μg/ml) at 37℃. For induction of target proteins expression, 1 mM isopropyl-β-D-thiogalactopyranoside (IPTG) was added when the bacteria OD_{600} value reached to 1.0. Similar to this 5 GGDP synthetic enzymes, HpDTC1 protein fused with His-tag were also induced with 1mM IPTG at 18℃. Following 16 h induction, the bacteria was harvested and then washed with Tris-HCl buffer (20 mM Tris-HCl at pH 7.43, 500 mM NaCl and 10% Glycerol). Washed bacteria was sonicated to obtain soluble protein under 10,500xg centrifugation for 30 min. 6 soluble fractions containing His-tag fusion proteins were mixed together and purified by a HiTrap Chelating HP column (GE Healthcare, Uppsala, Sweden) with elution buffer (20 mM Tris-HCl at pH7.43, 500 mM Imidazole, 500 mM NaCl and 10% Glycerol) according to manufacturer's instruction. All elution buffer in eluate was exchanged with 20 mM Tris-HCl on Nanosep 3k Omega Devices (Pall, Port Washington, New York, USA)

pGEX-4T-CPS2 and pGEX-4T-KSL7 transformants were precultured in LB medium (1% Bacto Tryptone, 0.5% yeast extract and 1% NaCl) containing carbenicillin (50 μg/ml) at 37℃. The preculture time of BL21(DE3): 13.5 h for CPS2 and 6 h for KSL7. A part of precultured bacteria was further cultured in flesh LB medium (1:100). When the optical density at 600 nm reached 1.5, 1 mM IPTG was used as inducing agent for recombinant GST-CPS2 and GST-KSL7 expression.

Following respective 4.5 h and 10.5 h shaking induction in 30℃, the bacteria was collected and washed with PBS buffer (140 mM NaCl, 2.7 mM KCl, 10 mM Na_2HPO_4 and 1.8 mM KH_2PO_4) for three times. Washed bacteria was sonicated to obtain soluble protein under 10,500xg centrifuge for 30 min. 2 soluble fractions were purified by Glutathione Sepharose™ 4B (GE Healthcare Inc., Sweden). 2 target proteins bound Glutathione Sepharose™ 4B were eluted with 30 mM Glutathione elution buffer under centrifugation. The elution buffer was exchanged with 25 mM Tris-HCl on Nanosep 3k Omega Devices (Pall, Port Washington, New York, USA). The concentration of CPS2 and KSL7 dissolved in 25 mM pH7.4 Tris-HCl was measured on SmartspecTM 3000 (Bio-Rad, California, USA), respectively.

Thereafter, all buffer exchanged enzymes were frozen in liquid nitrogen and stored in -80℃.

2-2-3. Enzymatic synthesis of [U-$^{13}C_{20}$] *ent*-cassa-12,15-diene and [U-$^{13}C_{20}$] *syn*-pimara-7, 15-diene from [U-$^{13}C_6$] MVA *in vitro*

For the synthesis of [U-$^{13}C_{20}$] *ent*-cassa-12,15-diene, two recombinant cyclases (0.8 mg of CPS2 and 1.0 mg of KSL7) were incubated with 2 mg of [U-$^{13}C_6$] mevalonate (MVA, hydrolyzed form) in a GGDP synthetic enzyme cocktail as described by Shimane *et al*. in 2014 (Tab. 2-2).[8] Following overnight incubation at 30°C, the reaction products were extracted four times with *n*-hexane and concentrated *in vacuo*. The amount of [U-$^{13}C_{20}$] *ent*-cassa-12,15-diene from each synthetic experiment was estimated using an internal standard of *ent*-kaurene by GC-MS analysis. The total yield was reached at 0.86 mg of [U-$^{13}C_{20}$] *ent*-cassa-12,15-diene.

Table 2-2. [U-$^{13}C_{20}$] *ent*-cassa-12,15-diene enzymatic synthesis

	10xBuffer*	500 mM Tris-HCl	500 mM MgCl2	100 mM ATP	5 GGDP synthetic enzymes mixture	OsCPS2	OsKSL7	[U-$^{13}C_{20}$]MVA
Conc.	1xBuffer	100 mM	15 mM	16 mM	4.1 mg	0.8 mg	1 mg	2 mg

*: 5 mM $MgCl_2$ come from 10xReaction Buffer

For the synthesis of *syn*-pimara-7,15-diene, the *HpDTC1* gene in the moss *H. plumaeforme*, inserted in a pCold I expression vector (TAKARA, Shiga, Japan), was used for the production of a His-tagged HpDTC1 recombinant protein.[9] The recombinant HpDTC1 protein (2.7 mg) was added into the GGDP synthetic enzyme cocktail as described above. [U-$^{13}C_6$] MVA (hydrolyzed form, 1.5 mg) was applied to the above reaction mixture, and [U-$^{13}C_{20}$] *syn*-pimara-7,15-diene was retrieved (0.47 mg).

A part of *n*-hexane extract was evaporated again and dissolved in 100% ethanol. The putative [U-$^{13}C_{20}$] *ent*-cassa-12,15-diene or [U-$^{13}C_{20}$] *syn*-pimara-7,15-diene dissolved in 99.5% ethanol (1 μg/μl) was prepared for subsequent feeding experiment on rice plants or leaf disk (in Chapter 3).

2-2-4. GC-MS analysis of [U-$^{13}C_{20}$] *ent*-cassa-12,15-diene and [U-$^{13}C_{20}$] *syn*-pimara-7,15-diene

Putative [U-$^{13}C_{20}$] *ent*-cassa-12,15-diene and [U-$^{13}C_{20}$] *syn*-pimara-7,15-diene were analyzed by Agilent 6890 N GC-5973 N MSD mass selective detector system (70 eV of ionization voltage) coupled with a capillary column Inert Cap 5MS/Sil (0.25 mm of diameter, 15 m of length, 0.25 μm of film thickness; GL Sciences Inc. Japan). The carrier helium flow rate was controlled at 1 ml/min. Each sample was auto injected into column at 70℃. After 1 min hold at 70℃, the oven temperature was increased by 10℃/min to 280℃ with 5 min hold.

2-2-5. Putative [U-$^{13}C_{20}$] *ent*-cassa-12,15-diene and [U-$^{13}C_{20}$] *syn*-pimara-7,15-diene structural validation on ^{13}C-^{13}C COSY NMR

NMR analysis was performed on JEOL JNM-A600 FT-NMR system at Tokyo University of Agriculture and Technology. The resulting products dissolved in cyclohexane-d_{12} were led into a NMR microtube (5 mm inner diameter, Shigemi, Tokyo, Japan). The solvent signals at 26.4 ppm were used as reference. NMR spectra for putative [U-$^{13}C_{20}$] *ent*-cassa-12,15-diene were collected using Bruker Avance III spectrometers. Following organic solvent exchange to C_6D_6(>99%), 468 μg of putative ^{13}C-*syn*-pimara-7-15-diene was also applied to NMR spectroscopy. The sample was assembled on a microsample tube (5 mm inner diameter, Shigemi, Tokyo, Japan) for NMR analysis. C_6D_6 signal at 128.0 ppm was used as reference.

2-3. Results

2-3-1. The expression and purification of *ent*-cassa-12,15-diene synthetic enzymes

For [U-$^{13}C_{20}$] *ent*-cassa-12.15-diene synthesis *in vitro*, 7 recombinant enzymes responsible for the conversion from MVA to *ent*-cassa-12,15-diene were prepared (Fig.2-1).[4,5] Initially, five plasmids each harboring the ORF, *NcMVK*, *NcPMVK*, *NcMVD*, *NcIPI* or *SaGGPS* in *pQE-30* vector was used for the experiment.[5] These five GGDP synthetic enzymes were produced in JM109 as His-tagged fusion proteins and were further purified together on HiTrap Chelating HP column (Fig. 2-2). Rice *ent*-copalyl diphosphate synthase 2 (OsCPS 2) and rice *ent*-cassa-12,15-diene synthase (OsKSL 7), both of which ORFs were introduced to *pGEX-4T* and expressed in *E.coli*, BL21(DE3), as GST-tagged fusion proteins, responsible for the conversion from GGDP to *ent*-cassa-12,15-diene (Fig. 2-1). Fig. 2-2 showed 5 GGDP synthetic enzymes mixture and 2 *ent*-cassa-7,15-diene cyclases were purified successfully .

2-3-2. The expression and purification of *syn*-pimara-7,15-diene synthetic enzymes

For *syn*-pimara-7,15-diene and [U-$^{13}C_{20}$] *syn*-pimara-7,15-diene synthesis, a series of enzymes were also expressed and purified (Fig. 2-8). 6 recombinant enzymes with His-tag, NcMVK, NcPMVK, NcMVD, NcIPI, SaGGPS and HpDTC1 responsible for the conversion assay from MVA to *syn*-pimara-7,15-diene were used (Fig. 2-7). soluble fraction of 6 enzymes were mixed and purified on HiTrap Chelating Column at a time. Quality of purified enzymes was confirmed by SDS-PAGE, and the result showed that 6 *syn*-pimara-7,15-diene synthetic enzymes mixture was obtained successfully (Fig. 2-8).

2-3-3. The GC-MS analysis of *ent*-cassa-12, 15-diene and *syn*-pimara-7,15-diene products from [U-$^{13}C_6$] MVA

The fully ^{13}C-labeled *ent*-cassa-12,15-diene and *syn*-pimara-7,15-diene, either of which is the precursor of phytocassanes or momilactones, were enzymatically synthesized from [U-$^{13}C_{20}$] GGDP according to the method we previously reported.[4,5] The synthesis of *ent*-cassa-12,15-diene from GGDP required two diterpene cyclases, OsCPS2 and OsKSL7 involving in *ent*-CDP synthesis from GGDP and *ent*-cassa-12,15-diene synthesis from *ent*-CDP, respectively.[4] Meanwhile, the synthesis of *syn*-pimara-7,15-diene from GGDP can be performed one diterpene cyclase, HpDTC1 identified from the moss *H. plumaeforme* involving in sequential two-step cyclizations from GGDP to *syn*-pimara-7,15-diene via *syn*-CDP.[7] The yields of both labeled *ent*-cassa-12,15-diene and *syn*-pimara-7,15-diene from [U-$^{13}C_6$] mevalonate reached at about 90% and 65%, respectively, indicating that both systems, in which two mono-functional cyclases involved for synthesis of *ent*-cassa-12,15-diene and one bi-functional cyclase HpDTC1 involved for synthesis of *syn*-pimara-7,15-diene, is highly efficient enzymatic synthesis method under the suitable reaction condition. The GC-MS spectra of natural abundant

ent-cassa-12,15-diene and synthesized [U-$^{13}C_{20}$] *ent*-cassa-12,15-diene indicated identical pattern each other even though each molecular ion peak and the fragment ion peaks is shifted by depending on numbers of ^{13}C stable isotope: natural *ent*-cassa-12,15-diene, *m/z* 272 (M^+, 33%), 257 (75%), 243 (7%), 119 (97%), 91 (75%), 79 (100%); [U-$^{13}C_{20}$] *ent*-cassa-12,15-diene, *m/z* 292 (M^+, 12%), 276 (47%), 261 (7%), 128 (100%), 98 (62%), 85 (93%) (Fig. 2-4A; Fig. 2-4B). These results indicated that all carbons in *ent*-cassa-12,15-diene were substituted by ^{13}C stable isotope (>99%). Additionally, the same retention time of products peak, 13.35 min (Fig. 2-3A and Fig. 2-3B) indicates that they share the similar structure and conformation. Total yield was reached at 860 μg of [U-$^{13}C_{20}$] *ent*-cassa-12,15-diene converted from 1.5 mg of [U- $^{13}C_6$] MVA, estimated as 90% conversion rate in this *in vitro* biosynthesis method.

Similarly, the GC-MS spectra of natural abundant *syn*-pimara-*7,15*-diene and [U-$^{13}C_{20}$] *syn*-pimara-*7,15*-diene were identical even though each molecular ion peak and the fragment ion peaks is shifted by depending on numbers of ^{13}C stable isotope: natural *syn*-pimara-*7,15*-diene, *m/z* 272 (M^+, 24%), 257 (60%), 243 (23%), 133 (42%), 119 (55%), 109 (100%) [U-$^{13}C_{20}$] *syn*-pimara-*7,15*-diene, *m/z* 292 (M+, 6%), 276 (34%), 261 (17%), 143 (49%), 128 (61%), 117 (100%) (Fig. 2-9). The mass spectrum and retention time of the peak 3 was identical with those of authentic *syn*-pimara-7,15-diene (peak 1) (Fig. 2-9A and Fig. 2-9B). No other cyclization products were identified in the extract. About 468 μg of product was converted from 1.5 mg of [U- $^{13}C_6$] MVA. Conversion efficiency reached to 65%. Taken together, GC-MS results confirmed both of [U-$^{13}C_{20}$] *ent*-cassa-12,15-diene and [U-$^{13}C_{20}$] *syn*-pimara-7,15-diene were enzymatically synthesized from [U- $^{13}C_6$] MVA successfully.

2-3-4. [U-$^{13}C_{20}$] *ent*-cassa-12,15-diene and [U-$^{13}C_{20}$] *syn*-pimara-7,15-diene structural validation on ^{13}C-^{13}C COSY NMR

The one-dimensional ^{13}C-NMR spectra could clearly obtain each 20 carbon signal derived from both [U-$^{13}C_{20}$] *ent*-cassa-12,15-diene and [U-$^{13}C_{20}$] *syn*-pimara-7,15-diene (Fig. 2-5A; Fig. 2-10A). The two-dimensional ^{13}C-NMR spectra of both labeled compounds clearly showed carbon-carbon connectivity, and all carbon signals from [U-$^{13}C_{20}$] compound could be traced and assigned (Fig. 2-5B; Fig. 2-9B; Fig. 2-6; Fig. 2-11; Tab.1; Tab.2). ^{13}C NMR of *ent*-cassa-12,15-diene (150MHz, $CDCl_2$) δ: 14.3 (d, C-20, $J_{10\text{-}20}$), 14.7 (d, C-17, $J_{14\text{-}17}$), 19.5 (dd, C-2, $J_{1\text{-}2,\ 2\text{-}3}$), 22.4 (dd, C-6, $J_{5\text{-}6,\ 6\text{-}7}$), 22.5 (d, C-18, $J_{4\text{-}18}$), 25.8 (dd, C-11, $J_{9\text{-}11,\ 11\text{-}12}$), 31.9 (dd, C-7, $J_{6\text{-}7,\ 7\text{-}8}$), 32.9 (ddd, C-14, $J_{8\text{-}14,\ 13\text{-}14,\ 14\text{-}17}$), 33.7 (dddd, C-4, $J_{3\text{-}4,\ 4\text{-}5,\ 4\text{-}18,\ 4\text{-}19}$), 33.9 (d, C-19, $J_{4\text{-}19}$), 36.1 (ddd, C-8, $J_{7\text{-}8,\ 8\text{-}9,\ 8\text{-}14}$), 37.7 (dddd, C-10, $J_{1\text{-}10,\ 5\text{-}10,\ 9\text{-}10,\ 10\text{-}20}$), 40.2 (dd, C-1, $J_{1\text{-}2,\ 2\text{-}10}$), 43.0 (dd, C-3, $J_{2\text{-}3,\ 3\text{-}4}$), 45.2 (ddd, $J_{8\text{-}9,\ 9\text{-}10,\ 9\text{-}11}$), 56.3 (ddd, C-5, $J_{4\text{-}5,\ 5\text{-}6,\ 5\text{-}10}$), 109.2 (d, C-16, $J_{15\text{-}16}$), 128.3 (dd, C-12, $J_{11\text{-}12,\ 12\text{-}13}$), 139.4 (dd, C-15, $J_{13\text{-}15,\ 15\text{-}16}$), 142.5 (ddd, C-13, $J_{12\text{-}13,\ 13\text{-}14,\ 13\text{-}15}$). According to the structure of *ent*-CPP and *syn*-CPP intermediates, the assignment from C1 to C10 has been fixed in previous reports. The cross-peak from C17 to C20 was shown in high fields (Fig. 2-6A), which were used for detecting the carbons with only single bonds. Furthermore, their coupling patterns

are doublet (d), which indicated the compound should consist of 4 methyl groups. However, the carbons connectivity from C12 to C16 cannot be detected in high fields. Those of olefinic quaternary carbons can only be traced on low fields (Fig. 2-6B), of which signals indicated the relevant carbons contained double bonds. Thus, the stereostructure of three rings junction was established by C10-C5 and C9-C8 ^{13}C-^{13}C COSY correlations. And all 20 carbons were assigned properly.

[U-$^{13}C_{20}$] *syn*-pimara-7,15-diene (150 MHz, C_6D_6). δc: 19.2 (dd, C-2, $J_{1\text{-}2,2\text{-}3}$), 22.0 (d, C-17, $J_{13\text{-}17}$), 22.2 (d, C-20, $J_{10\text{-}20}$), 22.9 (d, C-19, $J_{4\text{-}19}$), 24.1 (dd, C-6, $J_{5\text{-}6,6\text{-}7}$), 25.3 (ddd, C-5, $J_{4\text{-}5,5\text{-}6,5\text{-}10}$), 25.3 (dd, C-11, $J_{9\text{-}11,11\text{-}12}$), 32.9 (dddd, C-4, $J_{3\text{-}4,4\text{-}5,4\text{-}18,4\text{-}19}$), 33.7 (d, C-18, $J_{4\text{-}18}$), 35.3 (dddd, C-10, $J_{1\text{-}10,5\text{-}10,9\text{-}10,10\text{-}20}$), 37.1 (dd, C-1, $J_{1\text{-}2,1\text{-}10}$), 38.0 (dd, C-12, $J_{11\text{-}12,12\text{-}13}$), 39.0 (dddd, C-13, $J_{12\text{-}13,13\text{-}14,13\text{-}15,13\text{-}17}$), 43.3 (dd, C-3, $J_{2\text{-}3,3\text{-}4}$), 48.3 (dd, C-14, $J_{8\text{-}14,\ 13\text{-}14}$), 53.5 (ddd, C-9, $J_{8\text{-}9,9\text{-}10,9\text{-}11}$), 109.4 (d, C-16, $J_{15\text{-}16}$), 120.2 (dd, C-7, $J_{6\text{-}7,7\text{-}8}$), 137.0 (ddd, C-8, $J_{7\text{-}8,8\text{-}9,8\text{-}14}$), 150.5 (dd, C-15, $J_{13\text{-}15,15\text{-}16}$). Okada K *et al*. (2016) has confirmed that HpDTC1 catalyzes cyclization from GGDP via a putative reaction intermediate, *syn*-copalyl diphosphate (*syn*-CPP) to *syn*-pimaradiene.[7] C5, C9 and C10 formed junction on *syn*-CPP was retained to final products of HpDTC1. Furthermore, momilactones also kept this junction and a same A/B ring stereostructure, which was consisted of C1 to C10. ^{13}C-^{13}C COSY NMR 1D and 2D data also indicated A/B ring was consisted of 10 carbons and C5, C9 and C10 junctions jointed two rings (Fig. 10ABC). And coupling pattern (dd) between C8-C14 and C13-C14 suggested that 6 carbons were connected and cyclized from C8 to C14 (Tab. 2). This cyclization formed a C ring, which was established on A/B ring and made up of dovetail joint with B ring at C8 and C9. Additionally, C4, C10 and C13 were correlated with quaternary carbons nuclear, leading to the clarification of C15 to C20 structure (Tab. 2; Fig. 2-11). Afterwards, the chemical shift and coupling pattern of C7-C8 and C15-C16 suggested that C7 and C8 were bound together through an olefinic bond, as well as those of C15-C16 (Fig. 11B; Tab. 2). Taken together, carbon to carbon connectivity in ^{13}C-^{13}C COSY NMR elucidated [U-$^{13}C_{20}$] *syn*-pimara-7,15-diene stereostructure and confirmed [U-$^{13}C_{20}$] *syn*-pimara-7,15-diene was converted from [U-$^{13}C_6$] MVA successfully.

2-4. Discussion

To synthesize ^{13}C-diterpene hydrocarbon, we first obtained ^{13}C-MVA by using previously reported *in vitro* reaction system from ^{13}C-acetate.[5] Obtained ^{13}C-MVA was further converted into *ent*-cassadiene or *syn*-pimaradiene via geranylgeranyl diphosphate (GGDP) with the aid of a series of recombinant enzymes for the production of isopentenyl diphospate and dimethylallyl diphosphate (both building blocks of terpenoids), GGDP synthase, and diterpene cyclases involved in the production of *ent*-cassadiene (OsCPS2 and OsKSL7) and *syn*-pimaradiene (HpDTC1).

Successful *in vitro* synthesis of *ent*-cassa-12,15-diene from MVA has been achieved by 7 recombinant enzymes produced by *E. coli* system (Fig. 2-2) prior to synthesis of labeled compounds. Of 5 GGDP synthetic enzymes fused with His-tag were purified on a HiTrapChelating column together. This was the first trial performing 5 enzymes purification on one column at a time. The result suggests that mixture of these 5 enzymes and GST-OsCPS2 and GST-OsKSL7 well functions for producing a putative *ent*-cassa-12,15-diene from MVA. GC-MS results suggested the synthesized product from MVA is most likely to be *ent*-cassa-12,15-diene (Fig. 2-3). This data also indicated putative *ent*-cassa-12,15-diene conversion efficiency from MVA reached to 90% (Fig. 2-3; Fig. 2-4).

According to the condition fixed in the cold *ent*-cassa-12,15-diene synthesis, [U-$^{13}C_{20}$] *ent*-cassa-12,15-diene was also enzymatically synthesized from [U-$^{13}C_{20}$] MVA successfully. GC-MS and ^{13}C-^{13}C COSY NMR results confirmed the product from [U-$^{13}C_{20}$] MVA is [U-$^{13}C_{20}$] *ent*-cassa-12,15-diene, of which yield reached to 90% (Fig. 2-3; Fig. 2-4; Fig. 2-5). This data also indicated *ent*-cassa-12,15-diene is fully labeled with ^{13}C and its intermediates without ^{12}C dilution. Though no authentic *ent*-cassa-12,15-diene was available, the product from MVA and [U-$^{13}C_{20}$] MVA were still confirmed as *ent*-cassa-12,15-diene and [U-$^{13}C_{20}$] *ent*-cassa-12,15-diene, respectively (Fig. 2-5; Fig. 2-6), in comparison to the mass spectrum of *ent*-cassa-12,15-diene reported previously. ^{13}C-^{13}C COSY NMR results further gave chemical shifts to 20 carbons on [U-$^{13}C_{20}$] *ent*-cassa-12,15-diene. We speculate the carbons chemical shift of next intermediate on the pathway to phytocassanes will also be changed and distinguishable (Tab. 1). Based on the comparison, the changed chemical shift will provide information about binding groups enable to estimate possible structure of metabolites from *ent*-cassa-12,15-diene.

On the other hand, using the reconstituted *in vitro* MVA pathway, GGDP can also be converted to another intermediate, *syn*-pimara-7,15-diene, with HpDTC1 protein previously identified from the moss *H. plumaeforme*. According to this system, 6 recombinant proteins were successfully prepared from heterologous expression in *E.coli* (JM109 and BL21(DE3)) for *syn*-pimara-7,15-diene or [U-$^{13}C_{20}$] *syn*-pimara-7,15-diene synthesis. However, the conversion efficiency of the diterpene product from [U-$^{13}C_6$] MVA cannot reach to the extent relative to the reaction of *ent*-cassadiene synthesis (90%). It was speculated that bifunctional enzyme HpDTC1 is suitable for the *in vitro* conversion of GGDP to *syn*-pimaradiene, but it might be

better to use two enzymes for pimaradiene synthase such as OsCPS4 and OsKSL4 in rice to produce [U-$^{13}C_{20}$] *syn*-pimara-7,15-diene more efficiently.
Following the preparation of *syn*-pimara-7,15-diene synthetic enzymes, GC-MS results indicated putative [U-$^{13}C_{20}$] *syn*-pimara-7,15-diene was converted from [U-$^{13}C_6$] MVA by using prepared 6 enzymes (Fig.2-9). Mass spectrum of *syn*-pimara-7,15-diene has been reported previously with its structural characterization.[5] In comparison with the authentic mass spectrum, the product synthesized by the mixed 6 enzymes shared the same retention time with *syn*-pimara-7,15-diene. Furthermore, their ion molecular weight 292 and 272 suggested 20 carbons constitute the scaffold structure of the product, which should be a diterpenes (Fig. 2-9). So the product from [U-$^{13}C_6$] MVA was primary confirmed as [U-$^{13}C_{20}$] *syn*-pimara-7,15-diene, which was fully labeled with ^{13}C without ^{12}C dilution. Thereafter, NMR analysis further validated [U-$^{13}C_{20}$] *syn*-pimara-7,15-diene stereostructure through ^{13}C-^{13}C COSY method (Fig. 2-10; Table 2.; Fig. 2-11). ^{13}C-^{13}C COSY NMR data provided an evidence that product from [U-$^{13}C_6$] MVA can be used for final feeding experiment on rice plants (In chapter 3).

2-5. Brief Summary

In this chapter, we established a proper condition of enzymatic synthesis for [U-$^{13}C_{20}$] *ent*-cassa-12,15-diene and [U-$^{13}C_{20}$] *syn*-pimara-7,15-diene from [U-$^{13}C_6$] MVA. Furthermore, their structures were also clarified and validated. This synthesized [U-$^{13}C_{20}$] *ent*-cassa-12,15-diene and [U-$^{13}C_{20}$] *syn*-pimara-7,15-diene can be further used for feeding experiment on rice plants (In chapter 3).

2-6. Figures

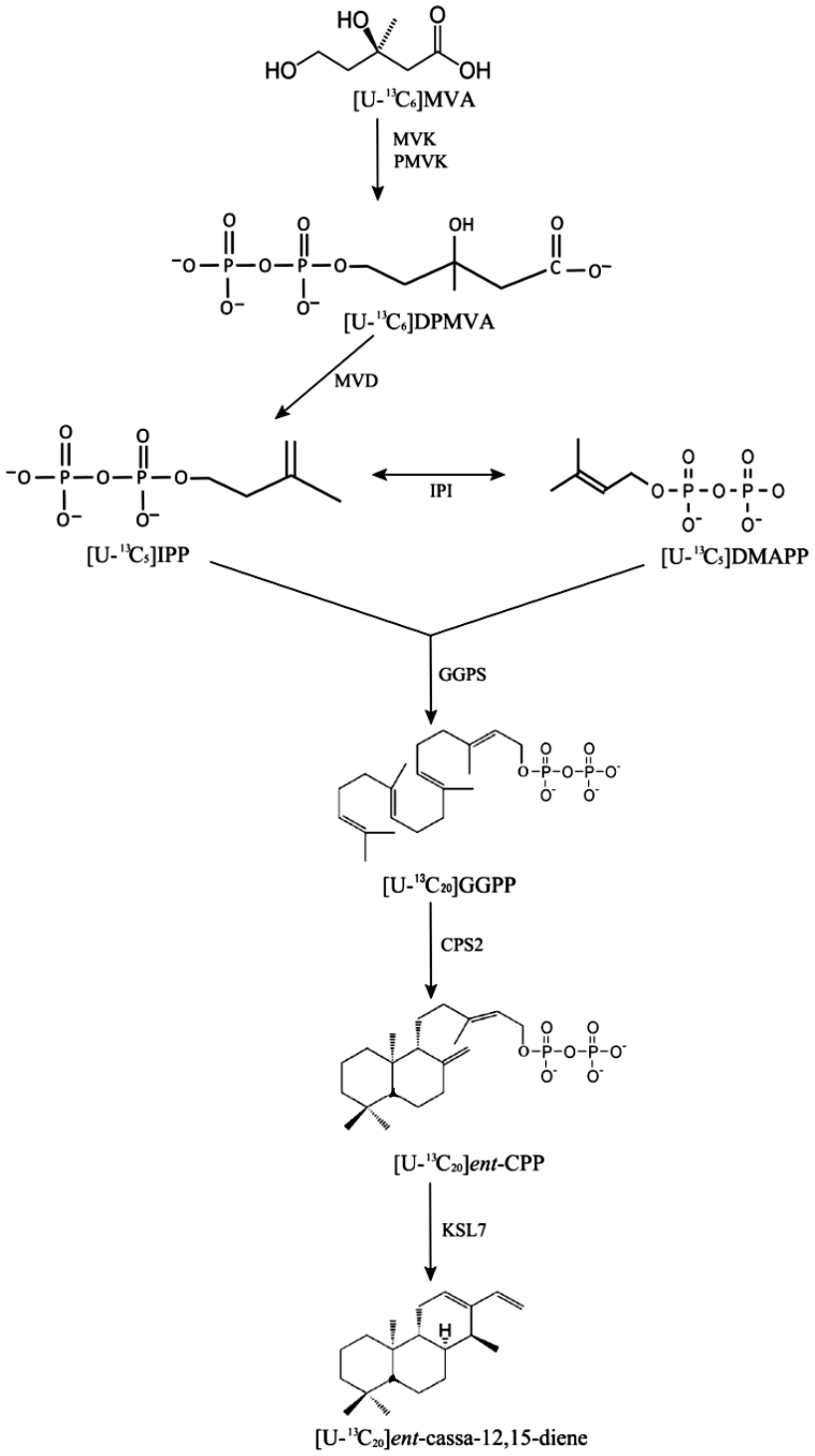

Figure 2-1. The putative synthetic route of [U-$^{13}C_{20}$] *ent*-cassa-12,15-diene dependent on MVA pathway *in vitro*.

MVK, mevalonate kinase; **PMVK,** phosphomevalonate kinase; **MVD,** diphosphomevalonate decarboxylase, **IPI,** isopentenyl diphosphate isomerase, **GGPS,** geranylgeranyl diphosphate synthase. **OsCPS2,** rice *ent*-copalyl diphosphate synthase 2; **OsKSL7,** rice *ent*-kaurene synthase-like 7

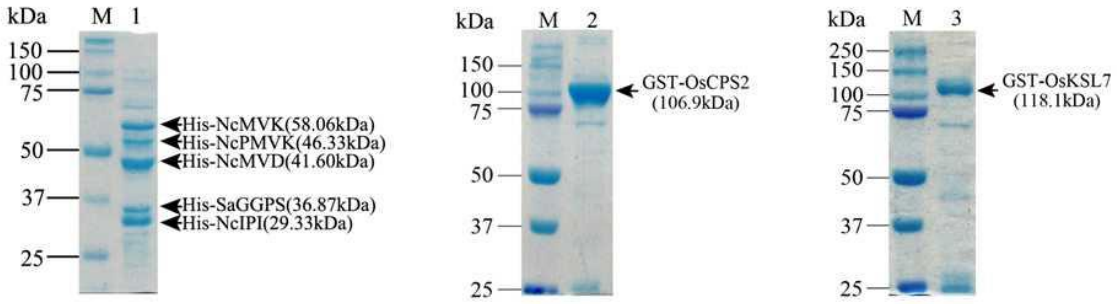

Figure 2-2. SDS-PAGE of purified 7 *ent*-cassa-12,15-diene synthetic enzymes from *E.coli* lysate.

M, Protein molecular mass marker; **Lane 1,** 5 purified His-tag fusion proteins for GGDP biosynthesis from MVA; **Lane 2 and lane 3,** two purified GST-tag fusion proteins for *ent*-cassa-12,15-diene synthesis from GGDP. 3 μg of purified proteins were applied to one lane.

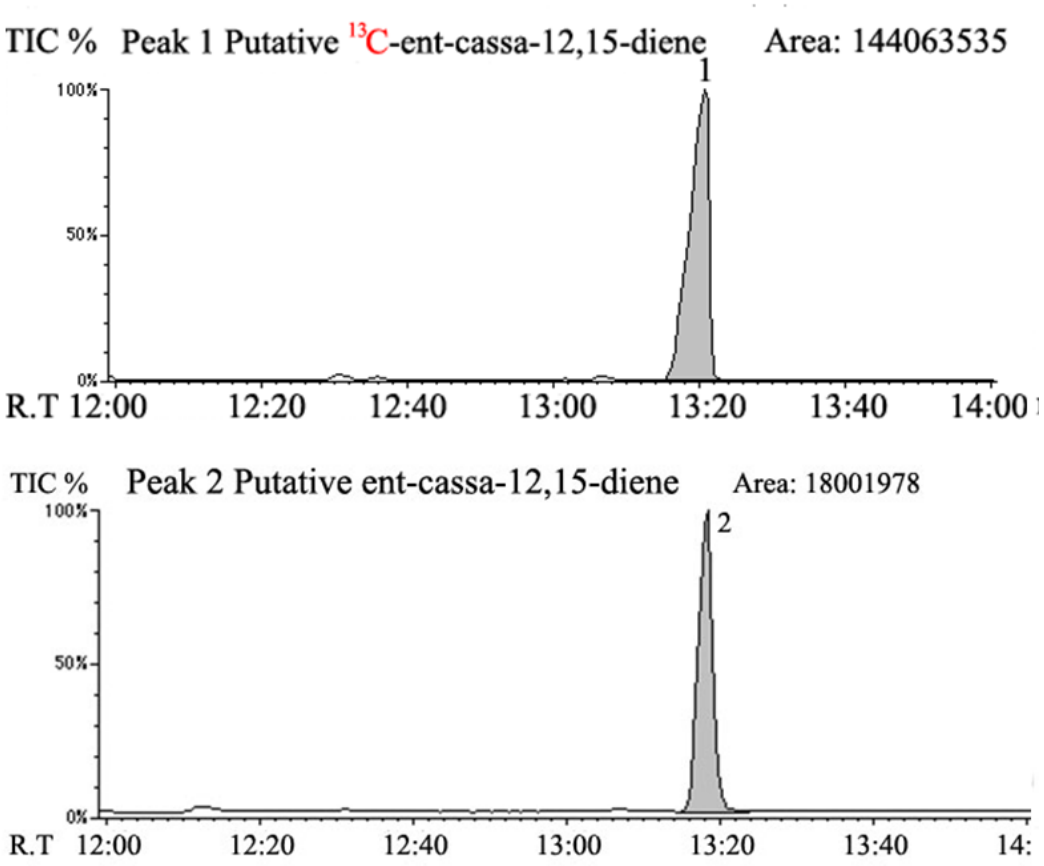

Figure 2-3. GC-MS analysis of 7 enzyme mixture products converted from the substrate, MVA and [U-$^{13}C_6$] MVA, respectively.

A, The reaction with the substrate, [U-$^{13}C_6$] MVA, accumulated a putative [U-$^{13}C_{20}$] *ent*-cassa-12,15-diene at 13.18 min of retention time.; **B,** 7 enzymes catalyzed MVA to *ent*-cassa-12,15-diene, of which retention time at 13.18 min on GC. . 1 μl of each extract was subjected to GC-MS.

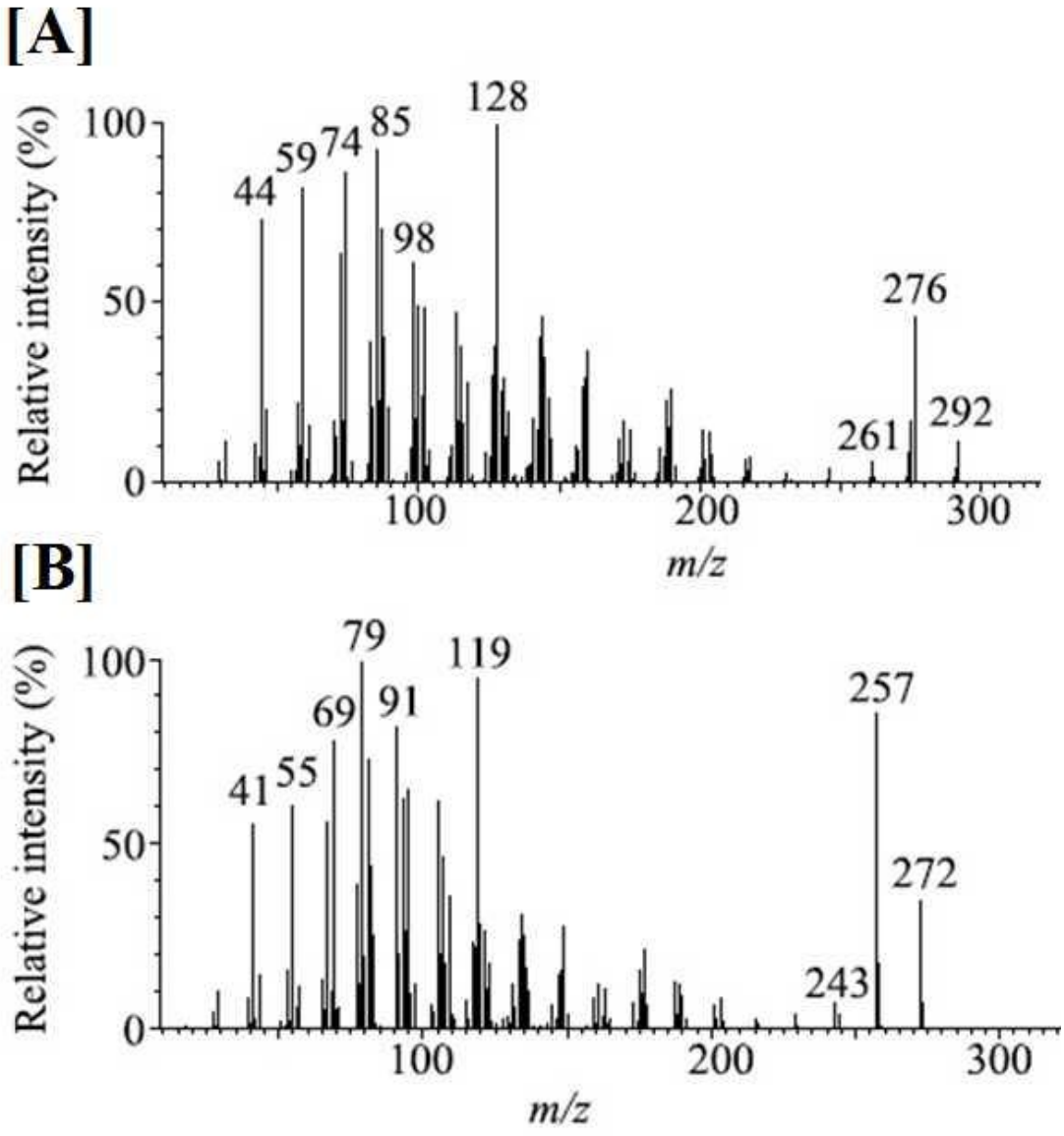

Figure 2-4. Mass spectra of putative [U-$^{13}C_{20}$] *ent*-cassa-12,15-diene and *ent*-cassa-12, 15- diene synthesized with 7 recombinant enzymes *in vitro*

A, Spectra of enzymatic synthesized [U-$^{13}C_{20}$] *ent*-cassa-12,15-diene; **B,** Spectra of enzymatic synthesized *ent*-cassa-12,15-diene

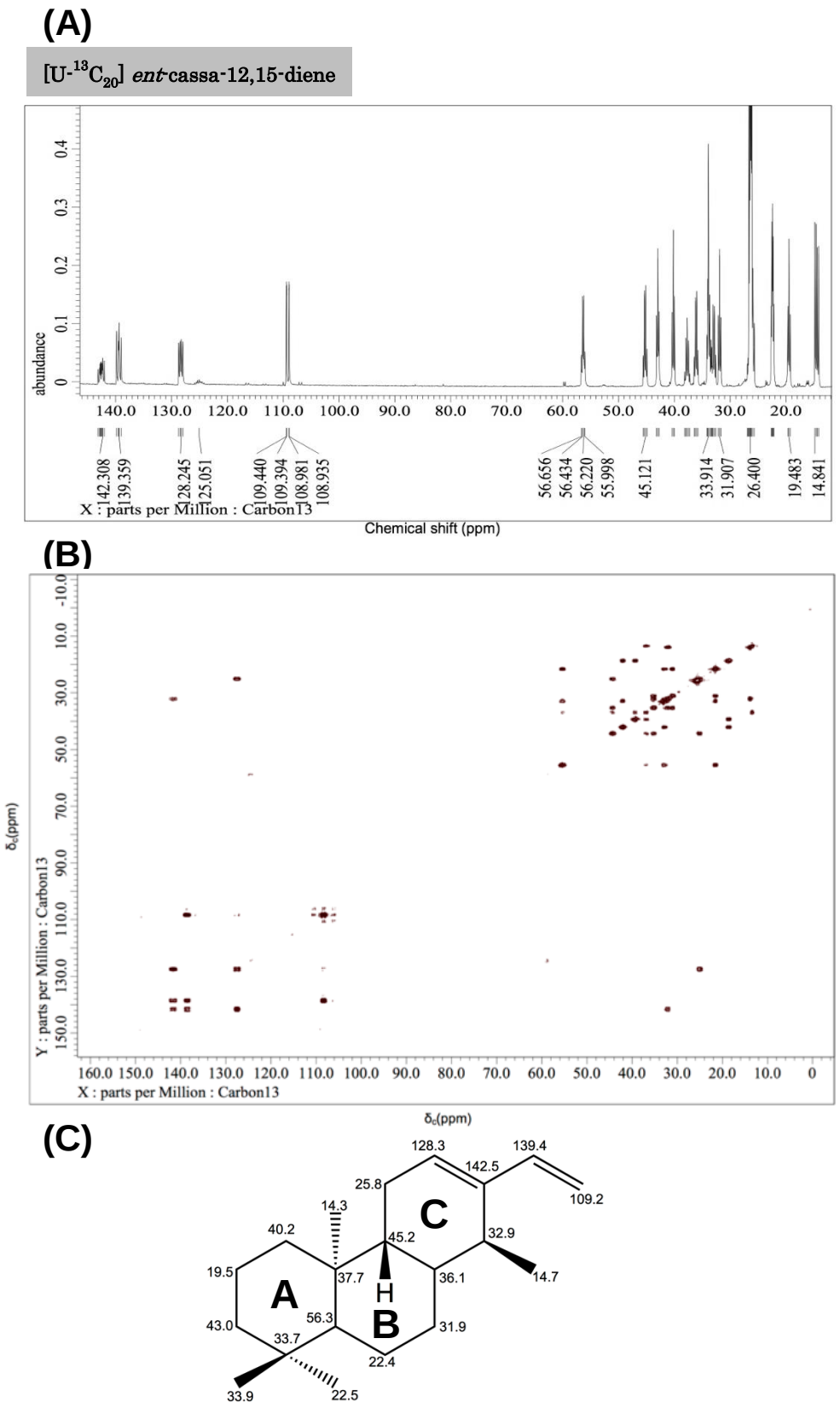

Figure 2-5. NMR spectra of [U-$^{13}C_{20}$] *ent*-cassa-12,15-diene.

(A) ^{13}C-NMR spectra and **(B)** two-dimensional ^{13}C-NMR spectra of [U-$^{13}C_{20}$] *ent*-cassa-12,15 -diene. Chemical shifts are represented on their structures of [U-$^{13}C_{20}$] *ent*-cassa-12,15-diene **(C)**

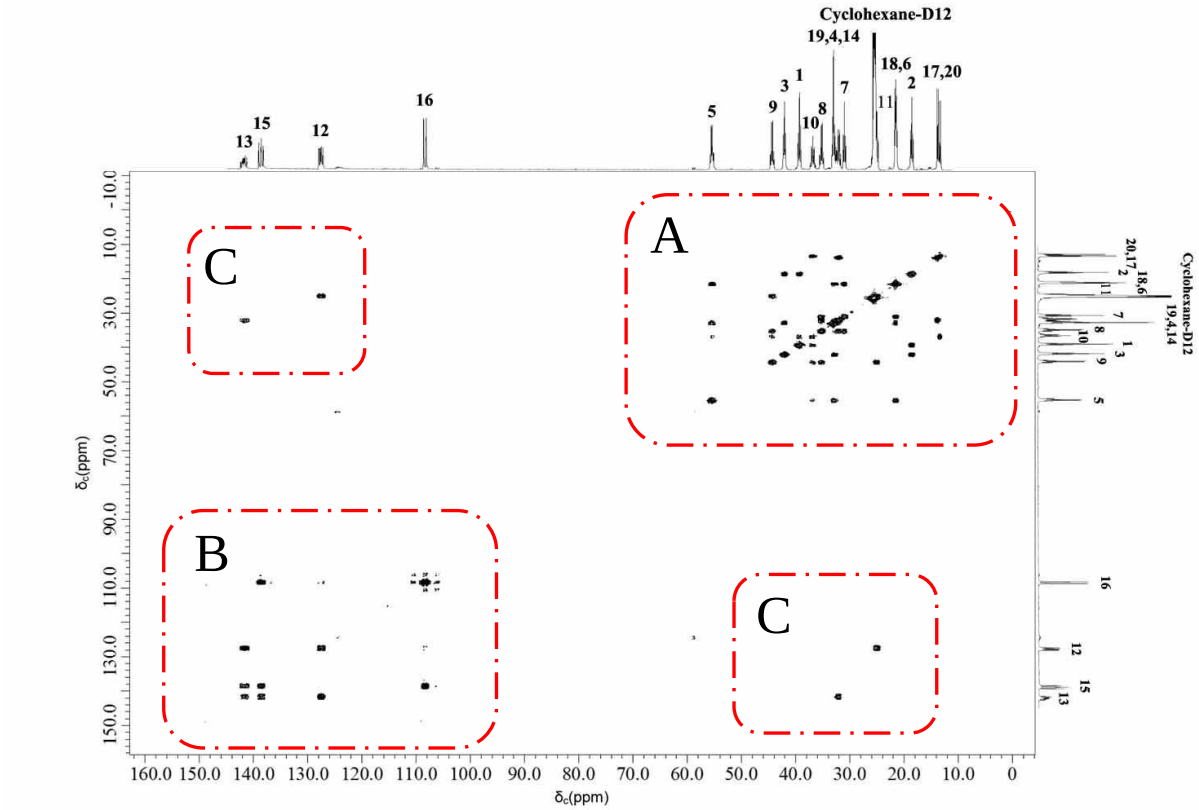

One-dimensional and Two-dimensional NMR spectrum of ^{13}C-*ent*-cassadiene

Figure 2-6. Combination of one-dimensional and two-dimensional ^{13}C-NMR spectra.

A, carbon-carbon connectivity in high field x high field region; **B,** carbon-carbon connectivity in low field x low field; **C,** carbon-carbon connectivity in high field x low field

TABLE 1.

^{13}C NMR data of full enzymatically synthesized [U-$^{13}C_{20}$] *ent*-cassadiene

Carbon Number	Chemical Shift (*ppm*)[α]	Coupling Pattern	^{13}C-^{13}C COSY Correlation
1	40.2	dd	2,10
2	19.5	dd	1,3
3	43.0	dd	2,4
4	33.7	dddd	3,5,18,19
5	56.3	ddd	4,6,10
6	22.4	dd	5,7
7	31.9	dd	6,8
8	36.1	ddd	7,9,14
9	45.2	ddd	8,10,11
10	37.7	dddd	1,5,9,20
11	25.8	dd	9,12
12	128.3	dd	11,13
13	142.5	ddd	12,14,15
14	32.9	ddd	8,13,17
15	139.4	dd	13,16
16	109.2	d	15
17	14.7	d	14
18	22.5	d	4
19	33.9	d	4
20	14.3	d	10

[α] Cyclohexane-D12 was used as reference (26.4 ppm)

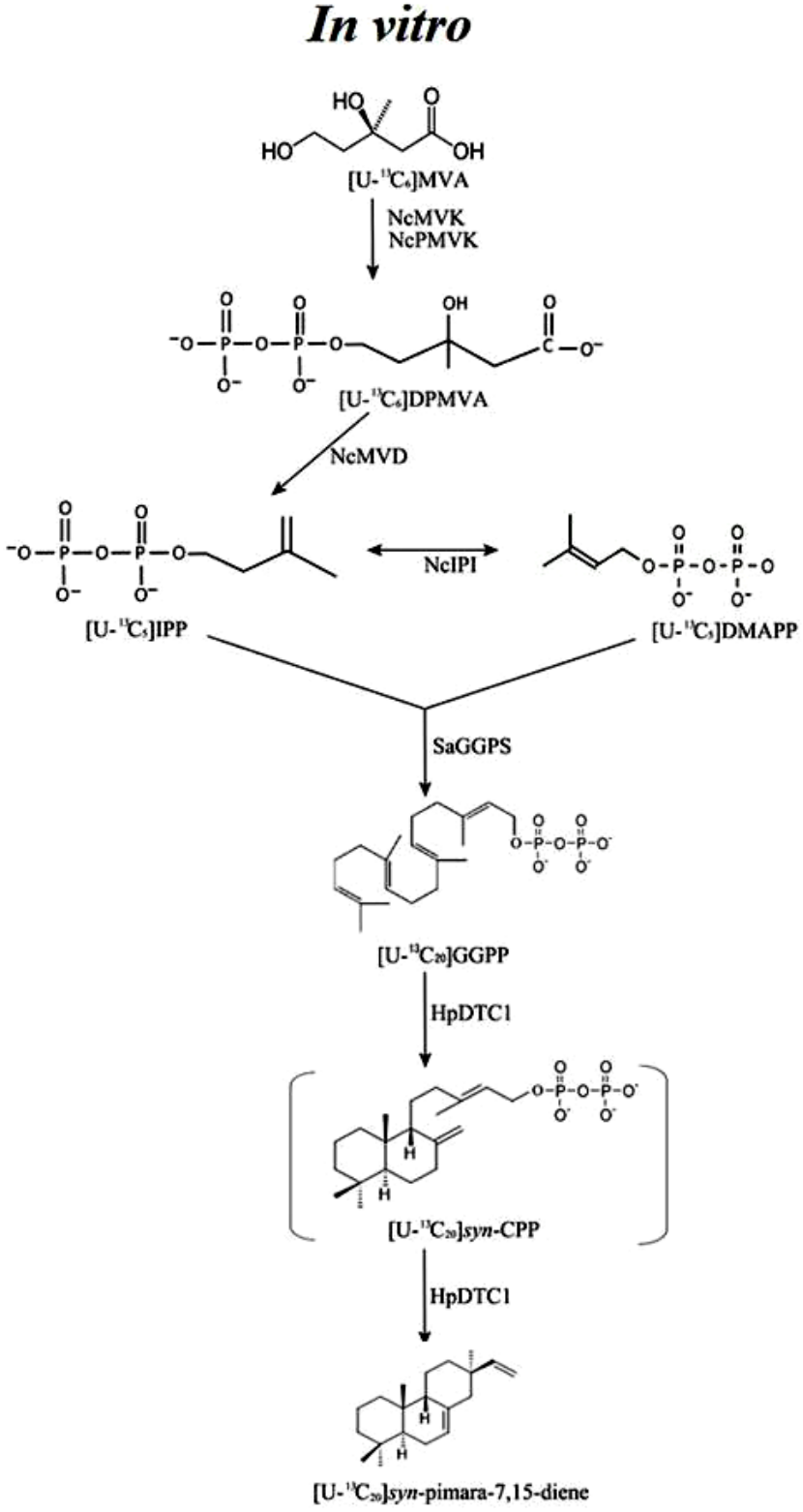

Figure 2-7. The putative synthetic route of [U-$^{13}C_{20}$] *syn*-pimara-7,15-diene dependent on MVA pathway *in vitro*.

MVK, mevalonate kinase; **PMVK,** phosphomevalonate kinase; **MVD,** diphosphomevalonate decarboxylase; **IPI,** isopentenyl diphosphate isomerase; **GGPS,** geranylgeranyl diphosphate synthase; **HpDTC 1,** *H. plumaeforme* diterpene cyclase 1

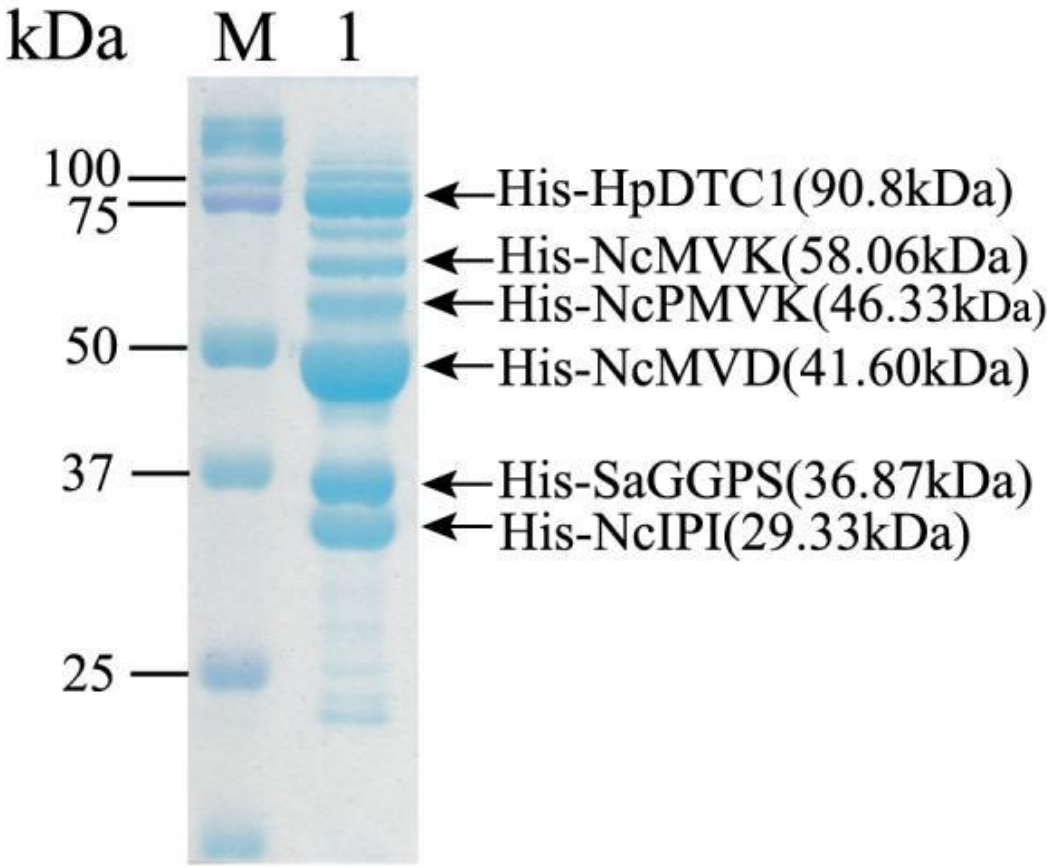

Figure 2-8. SDS-PAGE of purified 6 recombinant enzymes mixture from *E.coli* lysate.

M, Protein molecular mass marker; **Lane 1,** 6 purified His-tag fusion proteins for GGDP biosynthesis from MVA; 5 μg of purified proteins were applied to one lane.

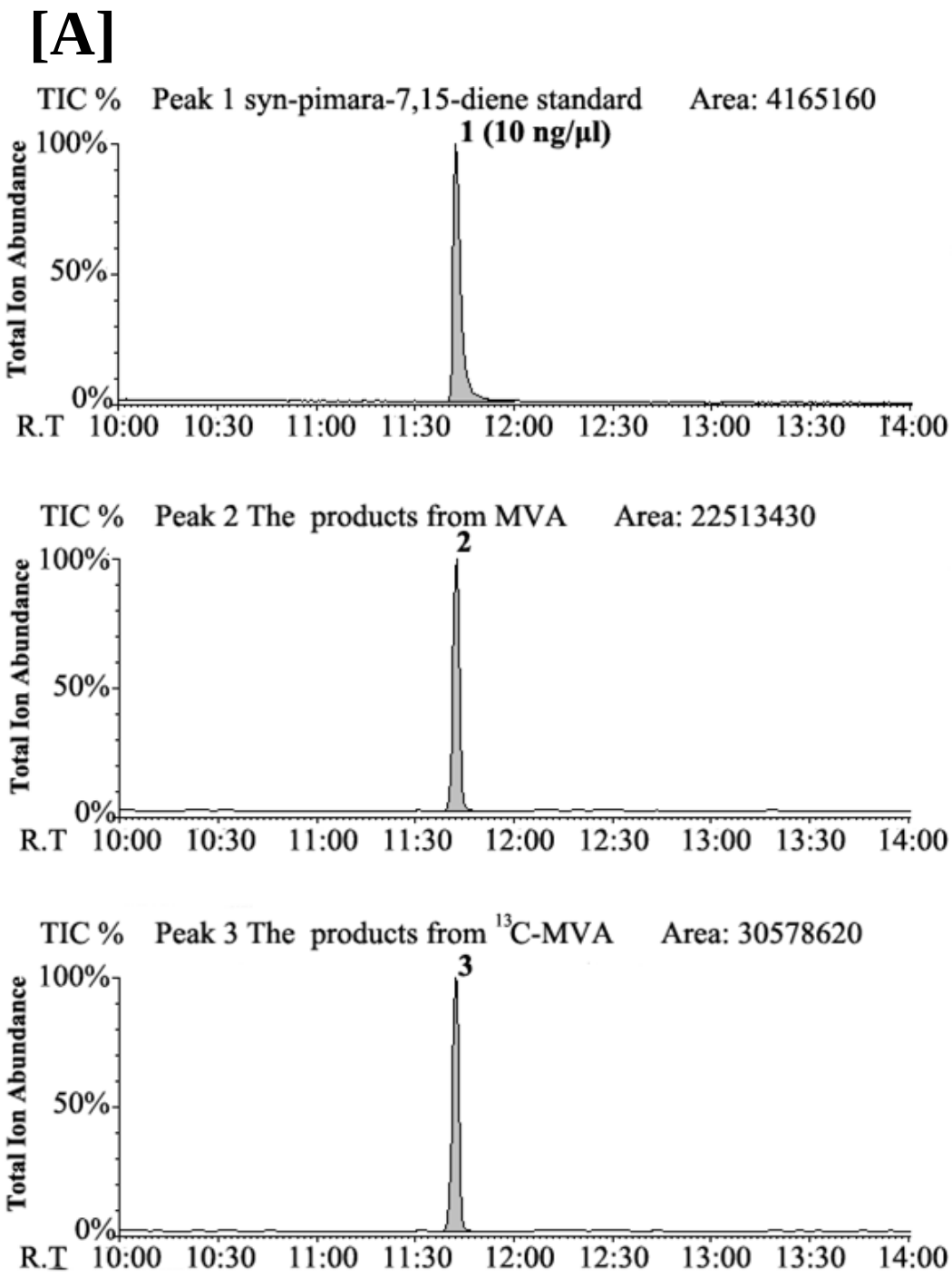

Figure 2-9. GC-MS chromatograms showing product of 6 enzymes cocktail from MVA and [U-$^{13}C_6$] MVA

A, The product of MVA and [U-$^{13}C_6$]MVA. Peak 1, authentic *syn*-pimara-7,15-diene; Peak 2, The products from MVA; Peak 3, the products from [U-$^{13}C_6$] MVA. ; **B,** Spectra of products from MVA and [U-$^{13}C_6$] MVA. 1 µl of each extract was subjected to GC-MS.

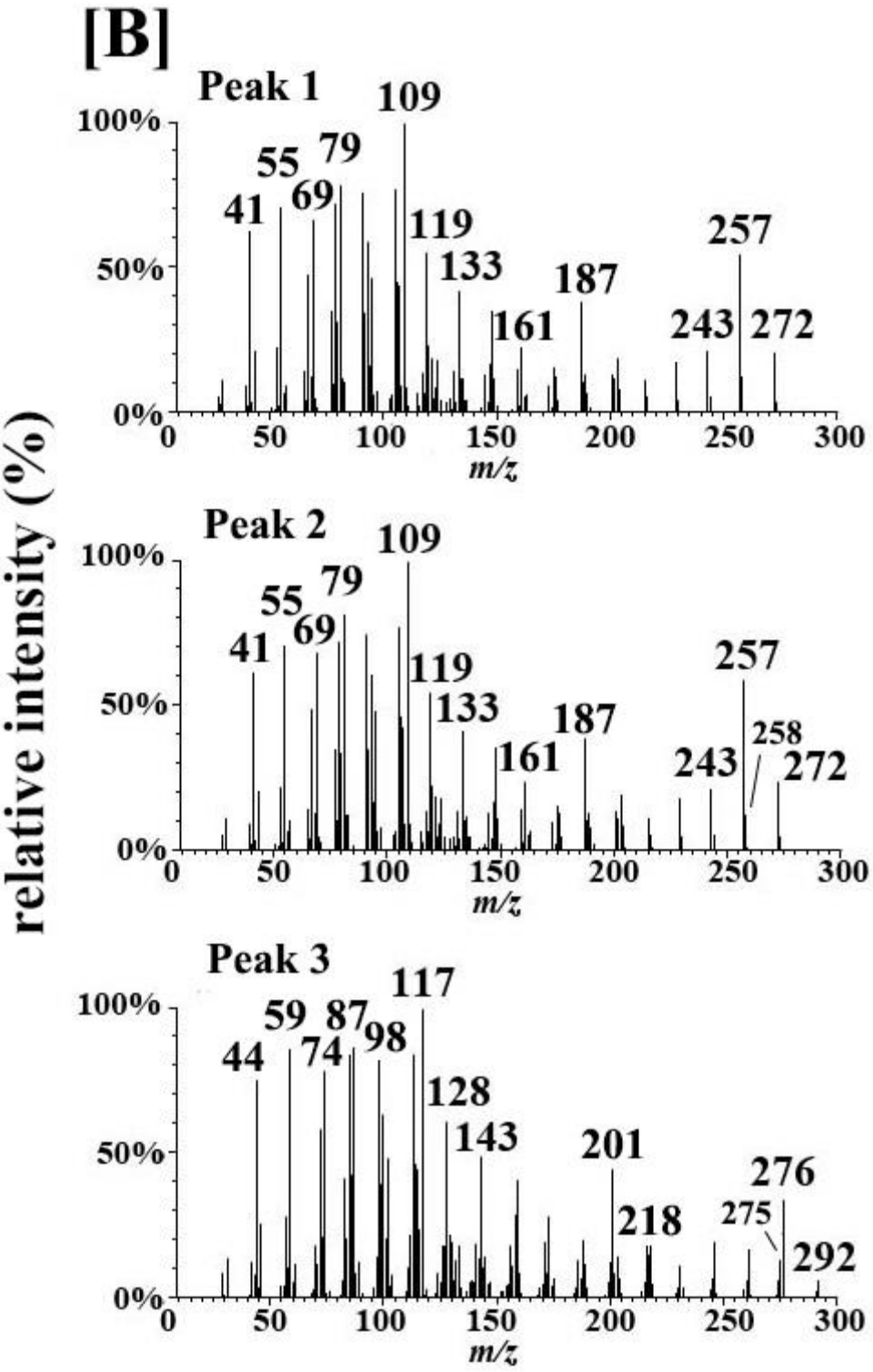

Figure 2-9. Continued

(A)

[U-$^{13}C_{20}$] *syn*-pimara-7,15-diene

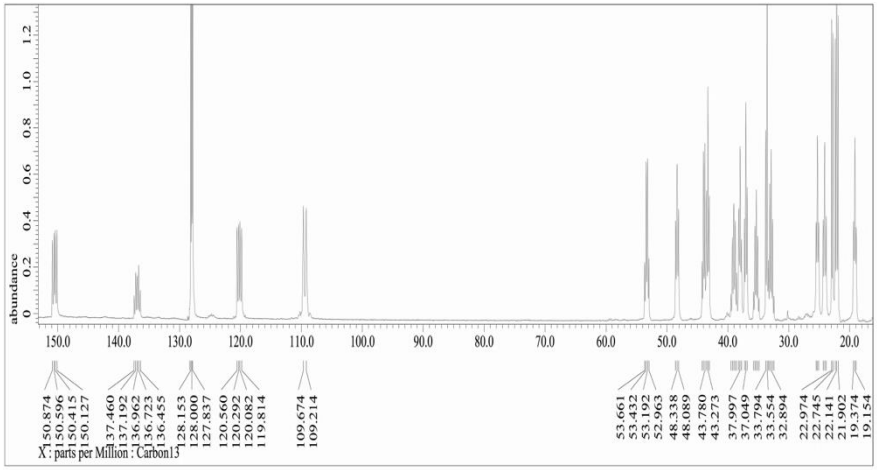

(B)

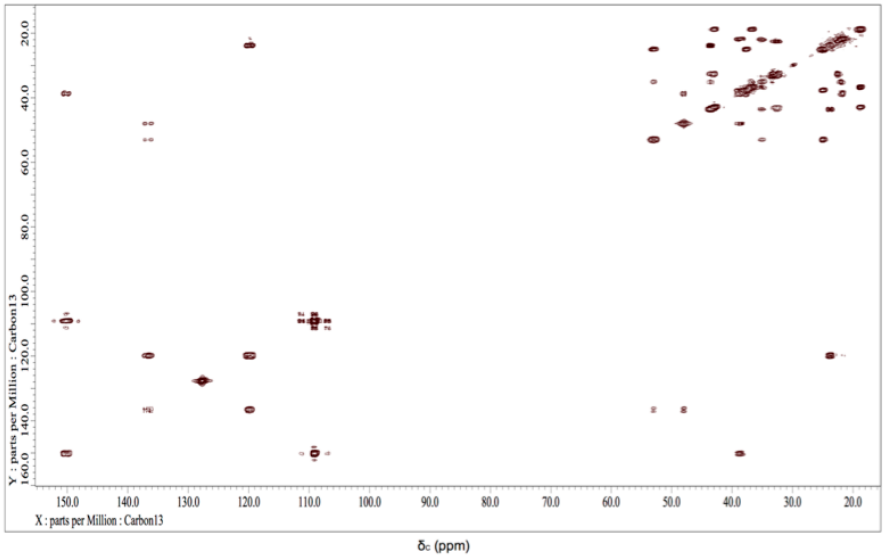

(C)

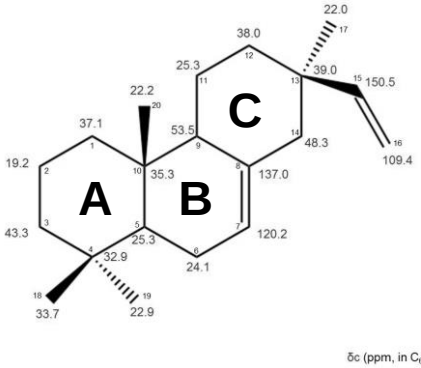

Figure 2-10. NMR spectra of [U-$^{13}C_{20}$] *syn*- pimara-7,15-diene

(A) ^{13}C-NMR spectra and **(B)** two-dimensional ^{13}C-NMR spectra of [U-$^{13}C_{20}$] *syn*-pimara-7,15 -diene. Chemical shifts are represented on their structures of [U-$^{13}C_{20}$] *syn*-pimara-7,15-diene **(C)**

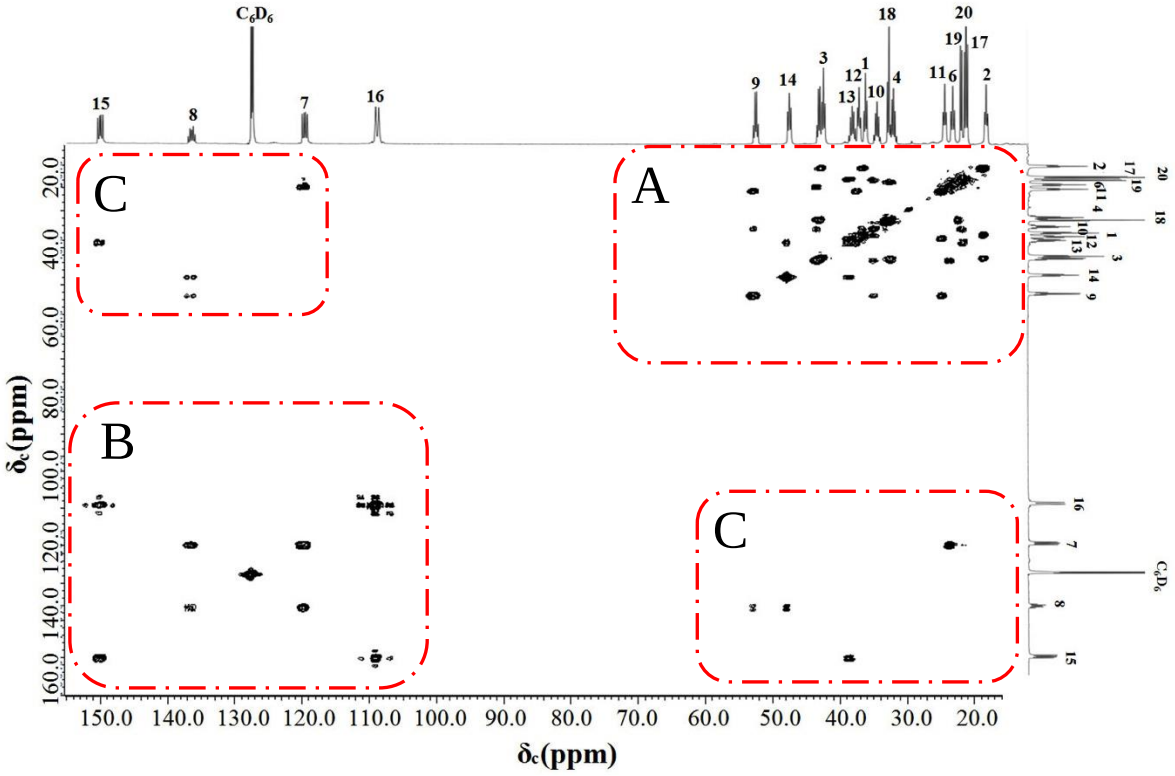

Figure 2-11. Combination of one-dimensional and two-dimensional [U-$^{13}C_{20}$] *syn*-pimara-7,15-diene ^{13}C-NMR spectra;.

A, carbon-carbon connectivity in high field x high field region;

B, carbon-carbon connectivity in low field x low field;

C, carbon-carbon connectivity in high field x low field

TABLE 2.

^{13}C-NMR data for 6 enzymes cocktail product

Carbon Number	Chemical shift δc (*ppm*)[α]	Coupling pattern	^{13}C-^{13}C COSY Connectivity
1	37.1	dd	2,10
2	19.2	dd	1,3
3	43.3	dd	2,4
4	32.9	dddd	3,5,19,18
5	25.3	ddd	4,6,10
6	24.1	dd	5,7
7	120.2	dd	6,8
8	137.0	ddd	7,9,14
9	53.5	ddd	8,10,11
10	35.3	dddd	1,5,9,20
11	25.3	dd	9,12
12	38.0	dd	11,13
13	39.0	dddd	12,14,15,17
14	48.3	dd	8,13
15	150.5	dd	13,16
16	109.4	d	15
17	22.0	d	13
18	33.7	d	4
19	22.9	d	4
20	22.2	d	10

[α] C_6D_6 was used as reference (128.0 ppm)

References

[1] VanEtten HD, Mansfield JW, Bailey JA and Farmer EE. Two classes of plant antibiotics: phytoalexins versus phytoanticipins. *Plant Cell*. 1994, 6: 1191-1192.

[2] Dixon RA. Natural products and plant disease resistance. *Nature*. 2011, 411: 843-847

[3] Otomo K, Kanno Y, Motegi A, Kenmoku H, Yamane H, Mitsuhashi W, Oikawa H, Toshima H, Itoh H, Matsuoka M, Sassa T, Toyomasu T. Diterpene cyclases responsible for the biosynthesis of phytoalexins, momilactones A, B, and oryzalexins A-F in rice. *Biosci Biotechnol Biochem*. 2004, 68(9):2001-2006.

[4] Cho EM, Okada A, Kenmoku H, Otomo K, Toyomasu T, Mitsuhashi W, Sassa T, Yajima A, Yabuta G, Mori K, Oikawa H, Toshima H, Shibuya N, Nojiri H, Omori T, Nishiyama M and Yamane H. Molecular cloning and characterization of a cDNA encoding *ent*-cassa-12,15-diene synthase, a putative diterpenoid phytoalexin biosynthetic enzyme, from suspension-cultured rice cells treated with a chitin elicitor. *Plant Journal.* 2004, 37: 1-8

[5] Sugai Y, Miyazaki S, Mukai S, Yumoto I, Natsume M and Kawaide H. Enzymatic total synthesis of gibberellin A_4 from acetate. *Biosci Biotechnol Biochem.* 2011a, 75(1): 128-135

[6] Ingram TJ and Reid JB. Internode Length in Pisum: Gene na May Block Gibberellin Synthesis between *ent*-7alpha-Hydroxykaurenoic Acid and Gibberellin A_{12}-Aldehyde. *Plant Physiol*. 1987, 83(4): 1048-1053

[7] Okada K. The biosynthesis of isoprenoids and the mechanisms regulating it in plants. *Biosci Biotechnol Biochem.* 2011, 75(7): 1219-1225

[8] Shimane M, Ueno Y, Morisaki K, Oogami S, Natsume M, Hayashi K, Nozaki H, Kawaide H. Molecular evolution of the substrate specificity of *ent*-kaurene synthases to adapt to gibberellin biosynthesis in land plants. *Biochem J*. 2014 462(3):539-546.

[9] Okada K, Kawaide H, Miyamoto K, Miyazaki S, Kainuma R, Kimura H, Fujiwara, K, Natsume M, Nojiri H, Nakajima M, Yamane H, Hatano Y, Nozaki H and Hayashi K. HpDTC1, a Stress-Inducible Bifunctional Diterpene Cyclase Involved in Momilactone Biosynthesis, Functions in Chemical Defence in the Moss *Hypnum plumaeforme*. *Sci Rep*. 2016, 6: 25316

CHAPTER 3

ESTABLISHING FEEDING PLATFORMS OF THE LABELED SUBSTRATES INCORPORATED INTO DITERPENOID PHYTOALEXINS

3-1. Introduction

Recently, stable isotope, is becoming main tool for tracing intermediates in plants.[1] Stable isotopes (^{13}C, ^{2}H, ^{18}O or ^{15}N) own 1 or 2 more neutrons than that of natural isotopes (^{12}C, ^{1}H, ^{16}O or ^{14}N). On mass spectrometry (MS), stable isotopic labeling compounds can be identified and distinguished from natural compounds by checking their precursor ion and product ion. So far, ^{13}C-labeling strategy has been widely used in metabolic flux analysis over four decades for carbon metabolism investigation in plants.

Feeding of labeled substrate to plant cells and chase of the metabolites after bioconversion *in planta* is one of the promising approaches to determine biosynthetic pathways of endogenous compounds. It is known that ^{13}C-labeled compound is quite useful to trace the signals in the metabolism detected by mass spectrometry analyses. In chapter 1, we described that enzymatically synthesized [U-$^{13}C_6$] mevalonate could be a starting point of the entire *in vitro* synthesis of diterpenoid phytohormone gibberellins.[2] It is also demonstrated that isotope labeled compounds (*ent*-[17-$^{3}H_2$] kaurenoic acid or [18-$^{2}H_1$] GA_{12}-aldehyde) was efficiently fed to peas (*Pisum sativum* L.) plants to trace the incorporation of *ent*-[17-$^{3}H_2$] kaurenoic acid or [18-$^{2}H_1$] GA_{12}-aldehyde into the precursors of gibberellins.[8] Thus, applicably, a feeding approach with ^{13}C-labeled diterpene hydrocarbons should be one of the alternative way to disclose the pathways for diterpenoid phytoalexins biosynthesis.

On the other hand, more efforts would be required to obtain high incorporation ratio into isotope labeled intermediates or products, and reduction of unlabeled compounds *in vivo* is quite important. Potential inhibitors to block the flow to native phytoalexins from ^{13}C-hydrocarbons may be chosen to improve the incorporation ratio. For example, 2-isopropyl-4-dimethylamino-5-methylphenyl-1-piperidin ecarboxylatemethyl chloride (AMO-1618), or 2-chloroethyl-trimethylammonium chloride (CCC), both of which are known as growth retardants on gibberellin biosynthesis, can be used to chemically block the metabolic pathway from GGDP to diterpene hydrocarbons.[3-5] Additionally, some genetically modified plants, *CPS4* mutant or *KSL4* mutant, also can be utilized to reduce unlabeled compounds on the pathway to momilactones.[14]

In this chapter, to trace incorporation of exogenously applied isotope labeled compound in plants, enzymatic synthesized [U-$^{13}C_{20}$] *ent*-cassa-12,15-diene or [U-$^{13}C_{20}$] *syn*-pimara-7,15-diene was fed to rice plants and moss, respectively. In order to obtain more ^{13}C-labeled end products, was further applied to rice plants with AMO-1618 treatment or *CPS4* Tos-17 mutant were integrated into feeding system with fully ^{13}C labeled diterpene substrates.

3-2. Materials and Methods

3-2-1. General materials

Rice *Oryza sativa* L. 'Nipponbare' was used as the plant material in this study. Rice seeds were sterilized with 70% ethanol for 2 min and 5% HClO solution for 15 min after the removal of husks. They were then washed with sterile water, planted in 0.5% agar and incubated in a greenhouse at 28°C. We also used the moss *Hypnum plumaeforme* grown for 1 month as described by Okada et al. in 2016,[13] and *Leersia perrieri*, closely related to *Oryza* species, maintained under vegetative growth. ^{13}C-labeled mevalonate used in this study was prepared with the support of ADEKA Co. Ltd..[2]

3-2-2. Condition for feeding experiment using intact plants

Incubation time for $CuCl_2$ treatment

For keeping a moisty environment and constant elicitation, all wild-type rice plants (*O. sativa* cv. Nipponbare) were incubated in 500 μM $CuCl_2$ solution soaked cheesecloths (Fig. S-1). The rice plants with cheesecloths were further kept in a glass tube. At different time point, 0 h, 24 h, 48 h, 72 h and 96 h, the phytocassanes from 3 rice plants (shoots and roots) were extracted with 100% methanol. Purified extract was detected on LC-ESI-MS/MS,

The amount and times for [U-$^{13}C_{20}$] ent-cassa-12,15-diene feeding

According to the feeding method in Table 3-1, 3 μg, 1 μg*3, 9 μg, 3 μg*3, 15 μg and 5 μg*3 of [U-$^{13}C_{20}$] *ent*-cassa-12,15-diene was applied to 6-day old wild-type rice leaf-1, respectively (Fig. S-2, Tab. 3-1). One rice plant was prepared for each feeding. The rice leaf-1 with 15 μl of 100% ethanol treatment was used as negative control (NC). All rice plants were incubated in 500 μM $CuCl_2$ solution soaked cheesecloths. After different treatment, leaf-1, leaf-2 and root were separated and extracted with 100% methanol at 72 h. After 48 h extraction, extracts were enriched, water removed, filtered and centrifuged. Purified samples were detected on LC-ESI-MS/MS.

Table 3-1. Amount and time course of ^{13}C-*ent*-cassa12,15-diene feeding to leaf-1

Amount of ^{13}C-*ent*-cassadiene	Time course			
	0 h	24 h	48 h	72 h
3 μg	3 μg	-	-	Sampling
1 μg *3	1 μg	1 μg	1 μg	Sampling
9 μg	9 μg	-	-	Sampling
3 μg *3	3 μg	3 μg	3 μg	Sampling
15 μg	15 μg	-	-	Sampling
5 μg *3	5 μg	5 μg	5 μg	Sampling

Incubation time for 9 μg of [U-$^{13}C_{20}$] ent-cassa-12,15-diene labeling

9 μg of [U-$^{13}C_{20}$] *ent*-cassa-12,15-diene was applied to rice leaves at 6-day old. As described in Table 3-2, this 9 μg of [U-$^{13}C_{20}$] *ent*-cassa-12,15-diene was applied to leaves at different time points with 500 μM $CuCl_2$ treatment (Fig. S-4). At each time point, 3 repetition were set. After 72 h incubation, the shoot and root were separated and extracted with 1 ml of 100% methanol. Following 48 h extraction, extracts were enriched, water removed, filtered and centrifuged. The remaining extract was detected on LC-ESI-MS/MS

Table 3-2. Time course for ^{13}C-*ent*-cassa-12,15-diene feeding after $CuCl_2$ treatment

	Feeding time point			
Time for $CuCl_2$ treatment	**0 h**	**24 h**	**48 h**	**72 h**
Amount of ^{13}C-*ent*-cassadiene	**9 μg**	**-**	**-**	**Sampling**
	-	**9 μg**	**-**	**Sampling**
	-	**-**	**9 μg**	**Sampling**

3-2-3. [U-$^{13}C_{20}$] *ent*-cassa-12,15-diene feeding experiment on wild-type rice plants (*O. sativa* L. cv. Nipponbare)

Rice plants (*Oryza sativa* L. cv. Nipponbare) leaves were treated with 500 μM $CuCl_2$ at 6th day after germination. Prior to use, [U-$^{13}C_{20}$] *ent*-cassa-12,.15-diene and [U-$^{13}C_{20}$] *syn*-pimara-7,15-diene purity and their structure have been checked by GC-MS and ^{13}C-^{13}C COSY NMR, respectively. Along with $CuCl_2$ treatment, 15 μg of [U-$^{13}C_{20}$] *ent*-cassadiene dissolved in 15 μl of 99.5% ethanol was also applied to fully expanded leaves (leaf-1) at two or three leaf stage of rice plants (Fig. 3-2). The rice plants in cheesecloths were incubated with [U-$^{13}C_{20}$] *ent*-cassadiene for 72 h. The leaf-1, other leaves and roots were separated and extracted with 500 μl of 100% methanol, respectively. The extracts were enriched, filtered and water was removed by dehydrated Na_2SO_4. The extract was centrifuged on 12,000g. Supernatant of methanol extract (60 μl) detected on LC-ESI-MS/MS.

3-2-4. [U-$^{13}C_{20}$] *syn*-pimara-7,15-diene feeding experiment on wild-type rice plants (*O. sativa* L.cv. Dongjin)

In multi well plate, the bottom of wells was filled with 0.5 mM $CuCl_2$ solution soaked cheesecloths, which were well-placed to leaf disc [U-$^{13}C_{20}$] *syn*-pimara-7,15-diene (1 μg/μl) dissolved in organic solvent (ethanol, methanol or *n*-hexane) was painted on the surface of leaf disk (Fig. S-5). Of most importance in this feeding experiment was making sure leaf disc can be exposed in air and fully treated with 0.5 mM $CuCl_2$ solution. Following 72 hours incubation, leaf disks were collected and extracted with 500 μl of 100% methanol for 48 h. Methanol extracts were concentrated to 150 μl in centrifugal vacuum. Afterwards, the extracts can be purified through 12,000g centrifugation or cheesecloths filtration. Purified extracts were detected on LC-ESI-MS/MS. The method on LC-ESI-MS/MS was same to those of previous.[7]

[U-$^{13}C_{20}$] *syn*-pimaradiene dissolved in 99.5% ethanol was further fed to wild-type rice plants (*Oryza sativa* L.cv. Nipponbare). Fresh leaf disks from 8 months old rice plants were used as material. 1 μg of [U-$^{13}C_{20}$] *syn*-pimaradiene was applied to each fresh leaf disk in multi well plate with 0.5 mM $CuCl_2$ solution soaked cheesecloths (Fig. 3-4). In no feeding group, 1 μl of 100% ethanol was painted on each leaf disk (Fig. 3-4). Following 72 h incubation, each group (24 leaf disks) was collected and extracted with 8 ml of 100% methanol for 48 h. The extracts were enriched, filtered and water removed. Purified extracts were analyzed on LC-ESI-MS/MS

3-2-5. Application of AMO-1618 on wild-type rice seeds or rice leaves (*O. sativa* L. cv. Nipponbare)

Sterile seeds were planted in each box with 0.5% agar solution. After planting, 100 μg of AMO-1618 (10 μl of aqueous solution) was applied to each seed. At 6th day after germination, all rice plants were treated with UV-irradiation, The condition as follows: time, 20 min; distance, 15 cm; wave length, 254 nm. Following UV-irradiation, the rice plants were incubated in water soaked cheesecloths for 72 h. The length of shoots and roots were measured with rules, respectively. Then shoots and roots were separated from each other and extracted with 1.5 ml of phytoalexins extraction solvent in 4℃, respectively (Fig. 3-7). After 12,000 rpm centrifugation, 5 μl of each extract was analyzed on LC-ESI-MS/MS

To investigate the direct effect of AMO-1618 on leaves, 500 μM Jasmonic acid (JA), 500 μM JA+100 μM AMO-1618 and 500 μM JA+200 μM AMO-1618 was applied to rice leaf disks, respectively (Fig. 3-11). Samples were collected at each time point after treatment. Each group was set 3 leaf disks. Each leaf disk was extracted with 0.5 ml of phytoalexins extraction solvent in 4℃ (Fig. 3-12). After 14,000 rpm centrifugation, 0.2 ml of extract was moved to a new tube and 5 μl was applied to LC-ESI-MSMS.

3-2-6. Application of [U-$^{13}C_{20}$] *syn*-pimara- 7,15-diene to AMO-1618 treated rice plants (*O. sativa* L. cv. Nipponbare)

Fresh leaf disks from 8-month old rice plants (*O. sativa* L. cv. Nipponbare) were used as the material. In feeding groups, 1 μg of [U-$^{13}C_{20}$] *syn*-pimara-7,15-diene (1 μg/μl in 100% *n*-hexane) was applied to each leaf disk. n=4. Different treatment was shown in Table 3-3 and Figure 3-14. After 72 h incubation, Each leaf disk was extracted with 500 μl of 100% methanol for 48 h. The extracts were enriched, water removed, filtered and centrifuged. Remaining extract was detected on LC-ESI-MS/MS.

Table 3-3. Different treatment on rice leaf disks

Group Name		The component in one well of cheesecloths	Different treatment on one leaf disk
1	A	150 µl (Water)	1 µl of *n*-hexane
2	B	150 µl (500 µM $CuCl_2$)	1 µl of *n*-hexane
3	C	150 µl (500 µM $CuCl_2$+200 µM AMO-1618)	1 µl of *n*-hexane
4	D	150 µl (500 µM $CuCl_2$)	1 µg of ^{13}C-*syn*-pimaradiene
5	E	150 µl (500 µM $CuCl_2$+200 µM AMO-1618)	1 µg of ^{13}C-*syn*-pimaradiene

3-2-7. Application of [U-$^{13}C_{20}$] *syn*-pimara- 7,15-diene to *CPS4* Tos-17 mutant leaf pieces (*O. sativa* L. cv. Nipponbare)

CPS4 Tos-17 mutant and wild-type leaf pieces from three weeks old rice plant (*O. sativa* L.cv. Nipponbare) were used as materials. In without feeding group, 1 µl of 100% ethanol was applied to one leaf piece (1 cm length). n=5 pieces*3. In feeding group, 1 µg of [U-$^{13}C_{20}$] *syn*-pimara-7,15-diene (1 µg/µl in 99.5% ethanol) was applied to each leaf piece (1 cm length). n=5 pieces*3. All leaf pieces were treated with 500 µM $CuCl_2$ soaked cheesecloths (Fig. 3-17). After 72 h incubation, one group, 15 leaf pieces, were divided into 3 parts. Each part, 5 leaf pieces, were collected and extracted with 4 ml of 100% methanol for 48 h. The extracts were enriched, water removed, filtered and centrifuged. Purified extracts were analyzed on LC-ESI-MS/MS.

3-2-8. Phytoalexins and [U-$^{13}C_{20}$] phytoalexins analysis on HPLC-ESI-MS/MS

The rice plants with [U-$^{13}C_{20}$] *ent*-cassa-12,15-diene or [U-$^{13}C_{20}$] *syn-pimara-7,15*-diene feeding were extracted with 100% methanol, of which extracts were filtered through cheesecloths inserted in a glass pipet (Asahi Glass Co., LTD, USA). The filtered methanol extracts were concentrated to about 100 µl *in vacuo*. Of 5 µl was subjected to PEGASIL ODS SP100 C18 Column (Length 150 mm, diameter 2.1 mm, Senshu Scientific Co., Ltd, Japan) on HPLC-ESI-MS/MS. Acetonitrile/H_2O/Acetic Acid (70/29.9/0.1) were used as flow phase for the quantification of phytocassanes and momilactones from standard and methanol extracts, which were bumped to ESI-MS/MS by HP1100 Series Binary Pump at 0.2 ml/min of flow rate and monitored by a tandem mass spectrometer (API3000, Applied Biosystems, Instrument, Forster City, USA). The condition of ESI-MS/MS was described as previously.[7]

3-3. Results

3-3-1. Condition for feeding experiment using intact plants

3-3-1-1. Determination of the condition in feeding experiment

Measurement of diterpenoids phytoalexin by LC-MS/MS in $CuCl_2$ treated rice plants revealed that accumulation of phytocassanes was reached to the peak at 72 h (Fig. S-1). Thus, total incubation time was set to 72 h for following ^{13}C labeling experiment. On the other hand, due to the [U-$^{13}C_{20}$] *ent*-cassa-12,15-diene or [U-$^{13}C_{20}$] *syn*-pimara-7,15-diene permeability and hydrophobicity, selection of the organic solvent for the feeding of hydrophobic compounds is extremely important. Timothy J. Ingram *et al.* (1987) have reported isotope labeled compounds (*ent*-[17-$^{3}H_2$] kaurenoic acid or [18-$^{2}H_1$] GA_{12}-aldehyde) dissolved in 99.5% ethanol was efficiently fed to peas (*Pisum sativum* L.) plants to trace the incorporation of *ent*-[17-$^{3}H_2$] kaurenoic acid or [18-$^{2}H_1$] GA_{12}-aldehyde into the precursors of gibberellins.[8] Consistently, our results from [U-$^{13}C_{20}$] *syn*-pimara-7,15-diene feeding experiment also suggested 99.5% ethanol is a suitable organic solvent for hydrophobic compounds feeding experiment (Fig. S-6). We further clarified a suitable feeding amount for better absorption on rice plant. It was confirmed that 9 μg of [U-$^{13}C_{20}$] *ent*-cassa-12,15-diene for one time feeding or 15 μg (5 μg x 3) for three times feeding is better for rice leaf absorption (Fig. S-3). Furthermore, the application of [U-$^{13}C_{20}$] *ent*-cassa-12,15-diene to rice leaves based on time course indicated that most of [U-$^{13}C_{20}$] phytocassanes accumulation level in extracts almost no difference at 0 h, 24 h and 48 h (Fig. S-4). Feeding at 0 h point was easy to be performed with $CuCl_2$ treatment. Thus we set the time to feed at 0 h for all feeding experiment in rice plants.

3-3-1-2. Establishment of HPLC-ESI-MS/MS methods for [U-$^{13}C_{20}$] phytocassanes and [U-$^{13}C_{20}$] momilactones detection

New method for LC-MS/MS has been established for ^{13}C labeled compounds detection (Tab. 3-4 and Tab. 3-5). These methods were mainly about [U-$^{13}C_{20}$] phytocassanes and [U-$^{13}C_{20}$] momilactones detection. According to the report by Shimizu *et al*. (2008), ESI-MS/MS can monitor a compound through its precursor ion and product ion.[7] Precursor ion was defined as ions of a particular mass-to-charge ratio, which can be used to distinguish protonated molecular ions from different compounds. Product ion also termed as fragment ions, which are created by collision-induced dissociation (Fig. 3-1). Momilactone A and momilactone B can be separated by their protonated molecular ions, *m/z* $[M+H]^+$, 315.175 and *m/z* $[M+H]^+$, 331.078, respectively and their fragment ions at *m/z* ($[MH-CO_2]^+$, 271.3) and ($[MH-H_2O-CO_2]^+$, 269.000), respectively. Thus the combinations of molecular ion and precursor ion of *m/z* (315.175/271.300) for momilactone A and *m/z* (331.078/269.000) for momilactone B, and *m/z* (316.98/299.10) for phytocassane A, D and E, *m/z* (335.071/317.100) for phytocassane B and *m/z* (319.114/301.200) for phytocassane C were used for the detection of non-labeled natural abundant

phytoalexins.

For the detection of [U-$^{13}C_{20}$] momilactone A and [U-$^{13}C_{20}$] momilactone B, molecular ion peak and the fragment ion peaks, which are shifted according to the numbers of ^{13}C stable isotope contained, were used: *m/z* (335.175/290.300) for [U-$^{13}C_{20}$] momilactone A and *m/z* (351.078/288.000) for [U-$^{13}C_{20}$] momilactone B.

Similar to those of [U-$^{13}C_{20}$]momilactones, combinations of molecular ion and precursor ion of [U-$^{13}C_{20}$] phytocassanes were set as follows: *m/z* (336.978/319.100) for [U-$^{13}C_{20}$] phytocassane A, D and E, *m/z* (355.071/337.100) for [U-$^{13}C_{20}$] phytocassane B and *m/z* (339.114/321.200) for [U-$^{13}C_{20}$] phytocassane C

3-3-2. [U-$^{13}C_{20}$] *ent*-cassa-12,15-diene and [U-$^{13}C_{20}$] *syn*-pimara-7,15-diene feeding experiment in rice plants (*O. sativa* L.cv. Nipponbare or Dongjin)

Following the method established on HPLC-ESI-MS/MS, 15 μg of [U-$^{13}C_{20}$] *ent*-cassa-12,15-diene with 15 μl of 99.5% ethanol was painted on the youngest fully expanded rice leaf-1 (Fig. 3-2).[8] LC-ESI-MS/MS results from each extract indicated wild-type rice plant (cv. Nipponbare) responds well to ethanol dissolved [U-$^{13}C_{20}$] *ent*-cassa-12,15-diene, of which unlabeled form has been proposed as the intermediate on the pathway to phytocassanes *in vitro*.[9] Correspond to previous report, our data confirmed [U-$^{13}C_{20}$] phytocassanes were accumulated when [U-$^{13}C_{20}$] *ent*-cassa-12,15-diene was fed to 6-day old rice plant under 500 μM $CuCl_2$ treatment (Fig 3-3B). The results from LC-ESI-MS/MS also showed the ratio of [U-$^{13}C_{20}$] phytocassanes in rice plants. 20.8% [U-$^{13}C_{20}$] phytocassane B (26.82 ng/g fresh weight leaf tissue), 46.4% [U-$^{13}C_{20}$] phytocassane C (59.74 ng/g fresh weight leaf tissue) and 32.7% [U-$^{13}C_{20}$] phytocassane E (42.09 ng/g fresh weight leaf tissue) can be converted from [U-$^{13}C_{20}$] *ent*-cassa-12,15-diene (15 μg) (Fig. 3-3C). The percentage and structure of phytocassane C and phytocassane E in extract indicated C3α-hydroxylation on *ent*-cassa-12,15-diene have a relative higher efficiency than those of C3α-oxidation (Fig. 3-3C). Together, this experiment demonstrated phytocassanes are definitely converted from *ent*-cassa-12,15-diene in rice plant and phytocassane C is the main product from *ent*-cassa-12,15-diene.

Following [U-$^{13}C_{20}$] *ent*-cassa-12,15-diene feeding experiment, incorporated [U-$^{13}C_{20}$] momilactone A and B ratio to unlabeled momilactone A and B were also investigated in leaf disks (Fig. 3-4). LC-MS/MS results from each extract showed both of [U-$^{13}C_{20}$] momilactone A (0.46 ng/leaf disk) and [U-$^{13}C_{20}$] momilactone B (0.11 ng/leaf disk) were converted from [U-$^{13}C_{20}$] *syn*-pimara-7,15-diene (1 μg/leaf disk) in leaf disks (Fig. 3-5B). Viewing from gained results, we further clarified both of [U-$^{13}C_{20}$] momilactone A and [U-$^{13}C_{20}$] momilactone B keep the same ratio, 15%, to unlabeled momilactone A and momilactone B (Fig. 3-5C). Together, *syn*-pimara-7,15-diene is the *in planta* intermediate of momilactone A and momilactone B definitely and momilactone A is the main product of *syn*-pimara-7,15-diene in wild-type rice leaves.

3-3-3. Effect of AMO-1618 on the growth of rice plants and phytoalexins accumulation (*O. sativa* L. cv. Nipponbare)

Timothy J. Ingram and James B. Reid have reported 100 μg of AMO-1618 per seed of peas (*Pisum sativum* L.) strongly reduced the internode length of peas plant.[9] This successful application promoted us to investigate the effect of AMO-1618 on rice seedling growth and phytoalexins biosynthesis in rice plants. Each of rice seeds was treated with 100 μg of AMO-1618 in advance (Fig. 3-7). The results in Figure 3-8 and Figure 3-9 suggested that rice seedlings growth in both of shoot and root were strongly inhibited by AMO-1618. It was speculated that AMO-1618 may repress most of CPSs activities and further block the gibberellin biosynthesis, which is of utmost importance for plants development. Subsequently, LC-MS/MS analysis indicated phytocassanes and momilactones accumulation level were drastically reduced by AMO-1618 treatment in shoots under UV elicitation, but in roots, their accumulation level was rather increased (Fig. 3-10; Fig. S-10). It seemed that AMO-1618 has unknown effect to enhance production of phytocassanes and momilactones in root under UV-irradiation (Fig. S-10).

On the other hand, jasmonic acid and AMO-1618 were also applied to wild-type rice leaf disks (*O. sativa* L. cv. Nipponbare) (Fig. 3-11). The results from the treatment with different concentration (100 μM and 200 μM) provided evidence that AMO-1618 can inhibit phytocassanes and momilactones biosynthesis in both concentrations. As expected, 200 μM showed higher inhibitory effect on phytoalexins accumulation (Fig. 3-13).

3-3-4. [U-$^{13}C_{20}$] *syn*-pimara-7,15-diene feeding experiment in AMO-1618 treated rice leaves (*O. sativa* L. cv. Nipponbare)

AMO-1618 has been confirmed as an inhibitor on phytocassanes and momilactones biosynthesis in either rice plant or rice cells (Fig. S-9; Fig. 3-10; Fig. 3-13). According to phytocassanes and momilactones biosynthetic pathway (Fig. 3-6; Fig. 3-16), unlabeled phytocassanes and momilactones accumulation are repressed in AMO-1618 treated rice plants, but [U-$^{13}C_{20}$] phytocassanes and [U-$^{13}C_{20}$] momilactones still can be biosynthesized in rice leaves with exogenous [U-$^{13}C_{20}$] *ent*-cassa-12,15-diene or [U-$^{13}C_{20}$] *syn*-pimara-7,15-diene feeding. In this feeding experiment, 200 μM AMO-1618 showed slight inhibition effect on momilactone A biosynthesis. However, [U-$^{13}C_{20}$] momilactone A biosynthesis was strongly repressed in rice leaves with [U-$^{13}C_{20}$] *syn*-pimara-7,15-diene feeding, though unlabeled momilactone A was only slightly inhibited (Fig. 3-15). It was speculated that AMO-1618 can inhibit CPSs activities, but it may arouse side effect on other enzymes activities on the pathway to momilactones in simultaneously. Therefore, [U-$^{13}C_{20}$] momilactones cannot be efficiently produced in AMO-1618 inhibited rice plants with [U-$^{13}C_{20}$] *syn*-pimara-7,15-diene labeling.

3-3-5. [U-$^{13}C_{20}$] *syn*-pimara-7,15-diene feeding experiment in Os*CPS4* Tos-17 mutant leaf pieces (*O. sativa* L. cv. Nipponbare)

The application of [U-$^{13}C_{20}$] *syn*-pimara-7,15-diene to *CPS4* Tos-17 mutant provides another way for [U-$^{13}C_{20}$] momilactones production without unlabeled momilactones dilution. The results from LC-ESI-MS/MS indicated unlabeled momilactone A and momilactone B were accumulated in wild type rice leaf pieces (*O. sativa* L.cv. Nipponbare), but was strongly reduced in *CPS4* Tos-17 mutant (Fig. 3-18A and B). This suggested used rice plant is exactly *CPS4* Tos-17 mutant. In this mutant, [U-$^{13}C_{20}$] *syn*-pimara-7,15-diene feeding results further showed [U-$^{13}C_{20}$] momilactones can be accumulated and their accumulation level was very close in both of wild-type and *CPS4* Tos-17 mutant (Fig. 3-18C). On the other hand, we also found unlabeled momilactones accumulation level in feeding group much higher than that in without feeding group (Fig. 3-18C). Taken together, [U-$^{13}C_{20}$] momilactone (A, B) can be obtained in *CPS4* Tos-17 mutant, though unlabeled momilactone (A, B) was strongly inhibited. We obtained more purified [U-$^{13}C_{20}$] momilactone (A, B) than that in wild type. This experiment also confirmed the inhibition effect of AMO-1618 is different from *CPS4* mutant.

3-4. Discussion

So far there was no direct evidence whether *ent*-cassa-12,15-diene is the intermediate on the pathway to phytocassanes or not. Successful and efficient synthesis of [U-$^{13}C_{20}$] *ent*-cassa-12,15-diene from [U-$^{13}C_6$] MVA makes the idea become available (Fig. 2-4; Fig. 2-5). Subsequently, successful [U-$^{13}C_{20}$] *ent*-cassa-12,15-diene feeding experiment on rice plant *Oryza sativa* gave the direct evidence to ^{13}C-phytocassanes biosynthetic route *in planta* (Fig. 3-3). Cotton gauze with 500 μM $CuCl_2$ solution treatment in an enclosed glass tube is good model for keeping moisture environment, constant elicitation, leaf respiration and constant ^{13}C labeled substrate absorption (Fig. S-2 and Fig. S-4). By using this model, 9 μg or 15 μg of [U-$^{13}C_{20}$] *ent*-cassa-12,15-diene was confirmed as a good condition for labeling. Furthermore, 72 h incubation should be a proper time point for efficient [U-$^{13}C_{20}$] phytocassanes biosynthesis (Fig. S-1B). The data obtained here confirmed *ent*-cassa-12,15-diene as an intermediate of phytocassanes in rice plant directly (Fig. 3-3; Fig. S-3; Fig. S-5). The application of [U-$^{13}C_{20}$] *syn*-pimara-7,15-diene to leaf disks was also achieved by using 99.5% ethanol or *n*-hexane in (Fig. 3-4; Fig. 3-5). In wild-type leaf disks, [U-$^{13}C_{20}$] *syn*-pimara-7,15-diene is shown to be converted to [U-$^{13}C_{20}$] momilactone (A and B) (Fig. 3-5B). In addition, [U-$^{13}C_{20}$] momilactone A and [U-$^{13}C_{20}$] momilactone B was found to be occupied same ratio (15%), to native momilactone (A and B) (Fig. 3-5C). Thus, *syn*-pimara-7,15-diene was validated as the intermediate on the pathway to momilactone (A and B) in wild type rice leaves.

Using the prepared ^{13}C-labeled diterpene hydrocarbons, it is clearly showed that ^{13}C labeling into end product of the pathway is nicely proceeded in the feeding experiment (Fig. 3-3 and Fig. 3-5). However, efficiency of the incorporation of ^{13}C-diterpene hydrocarbons into the diterpene phytoalexins was still limited to some extent (Fig. 3-3 and Fig. 3-5). Efforts were made in this chapter to enhance the

incorporation of ^{13}C-diterpene hydrocarbons by blocking of metabolic pathways leading to natural abundance of cassadiene and pimaradiene using AMO-1618, a potential chemical inhibitor for diterpene cyclase (Fig. 3-10; Fig. 3-13). It is found that AMO-1618 treatment to rice cells, rice plants or leaf disks obviously inhibited inductive production of diterpene phytoalexins under different elicitor's treatment (Fig. S-9; Fig. 3-10; Fig. 3-13). However, this treatment also affected incorporation of ^{13}C-diterpene hydrocarbons, consequently making ^{13}C signal of momilactones and phytocassanes weaker in AMO-1618 treated samples than non-treated one (Fig. 3-15). There might be unknown side effects for incorporation of ^{13}C-diterpene on AMO-1618 treatment. It would be an alternative way to enhance the ^{13}C incorporation in plants on using genetically modified plants, which are defective in the production of *syn*-pimaradiene or *ent*-cassadiene.

Given that the above results, *CPS4* Tos-17 mutant was utilized to enhance the incorporation of ^{13}C-diterpene hydrocarbons (Fig. 3-17). In this genetically modified mutant, accumulation level of [U-$^{13}C_{20}$] momilactone (A and B) revealed that the conversion efficiency of [U-$^{13}C_{20}$] momilactone (A and B) in *CPS4* Tos-17 mutant was similar to those of wild type (Fig. 3-18C). This result indicated *CPS4* Tos-17 mutant did not affect other related genes or enzymes activities on the pathway to momilactones. It further confirmed that AMO-1618 inhibition effect was more unspecific than that of genetically modification. Furthermore, accumulation level of [U-$^{13}C_{20}$] momilactone (A and B) occupied to be similar percentage (28% and 23%) to native momilactone A and momilactone B in wild type rice leaves (Fig. 3-18). In contrast, the ratio of [U-$^{13}C_{20}$] momilactone (A and B) in *CPS4* Tos-17 mutant occupied about 70% to native momilactone (A and B) and they become the main products in incorporation (Fig. 3-18). Therefore, in this feeding experiment, more concentrated [U-$^{13}C_{20}$] momilactone (A and B) signals can be observed from *CPS4* Tos-17 mutant without dilution of natural abundant native momilactone (A and B).

CYP99A2 and A3 or CYP71Z7 and CYP76M7, M8 are shown to be responsible for the either momilactones or phytocassanes production in rice, however, similar homologs with high homology was not found in RNA-seq data. Seeking of ^{13}C-labeled intermediates, which is converted from ^{13}C-pimaradiene, might be possible approach that will be able to find a biosynthetic pathway committed by as yet unknown P450 enzymes distinctive in the moss.

3-5. Brief Summary

In this chapter, feasible method for [U-$^{13}C_{20}$] *ent*-cassa-12,15-diene and [U-$^{13}C_{20}$] *syn*-pimara-12,15-diene labeling experiment in plants or leaves was established. By using this method, the hydrophobic or no polarity compounds can be converted to end products in rice leaves or other plants directly. Successful bioconversions of [U-$^{13}C_{20}$] phytocassane (A-E) and [U-$^{13}C_{20}$] momilactone (A and B) in plants made it possible to investigate unknown intermediates on the biosynthetic route of phytocassanes and momilactones in following chapter.

3-6. Figures and Tables

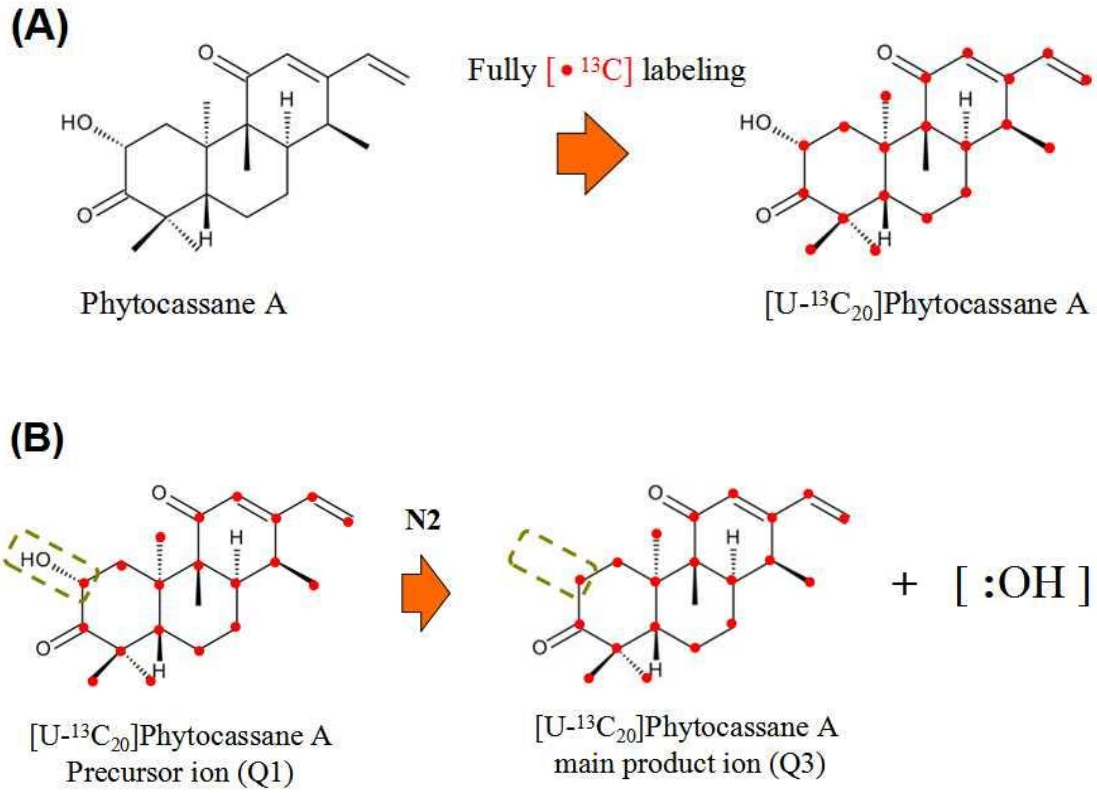

Figure 3-1. Hypothetical [U-$^{13}C_{20}$] phytocassanes deformation in Electrospray Ionization with Tandem Mass Spectrometry (ESI-MS/MS).

A, Biosynthesized phytocassane A or other phytocassanes will be fully labeled with ^{13}C in rice plant with [U-$^{13}C_{20}$] *syn*-pimara-7,15-diene feeding; **B,** Fully labeled ^{13}C-phytocassanes can be ionized and deformed in ESI-MS/MS. Ions were created by the addition of hydrogen cation. Precursor ion (Q1) or product ion (Q3): $[\mathbf{M}+H]^+$.

Table 3-4.

The method for Phytocassanes and [U-$^{13}C_{20}$]Phytocassanes detection on LC-MS/MS

	Q1 Mass (Da)	Q3 Mass (Da)	Time (msec)	DP (volts)	FP (volts)	CE (volts)	CXP (volts)
Phytocassane A	316.978	299.100	150.0	26.000	120.000	15.000	26.000
Phytocassane B	335.071	317.100	150.0	41.000	180.000	21.000	30.000
Phytocassane C	319.114	301.200	150.0	31.000	140.000	17.000	18.000
Phytocassane D	316.978	299.100	150.0	26.000	120.000	15.000	26.000
Phytocassane E	316.978	299.100	150.0	26.000	120.000	15.000	26.000
1-Deoxyphytocassane C	303.208	147.100	150.0	61.000	240.000	31.000	14.000
^{13}C-Phytocassane A	336.978	319.100	150.0	26.000	120.000	15.000	26.000
^{13}C-Phytocassane B	355.071	337.100	150.0	41.000	180.000	21.000	30.000
^{13}C-Phytocassane C	339.114	321.200	150.0	31.000	140.000	17.000	18.000
^{13}C-Phytocassane D	336.978	319.100	150.0	26.000	120.000	15.000	26.000
^{13}C-Phytocassane E	336.978	319.100	150.0	26.000	120.000	15.000	26.000
^{13}C-1-Deoxyphytocassane C	323.208	157.100	150.0	61.000	240.000	31.000	14.000

Table 3-5.

The method for momilactones and [U-$^{13}C_{20}$]momilactones detection on LC-MSMS

	Q1 mass (Da)	Q3 mass (Da)	Time (msec)	DP (volts)	FP (volts)	CE (volts)	CXP (volts)
Momilactone A	315.175	271.300	150.0	41.000	190.000	25.000	12.000
Momilactone B	331.078	269.000	150.0	51.000	230.000	25.000	20.000
^{13}C-Momilactone A	335.175	290.300	150.0	41.000	190.000	25.000	12.000
^{13}C-Momilactone B	351.078	288.000	150.0	51.000	230.000	25.000	20.000

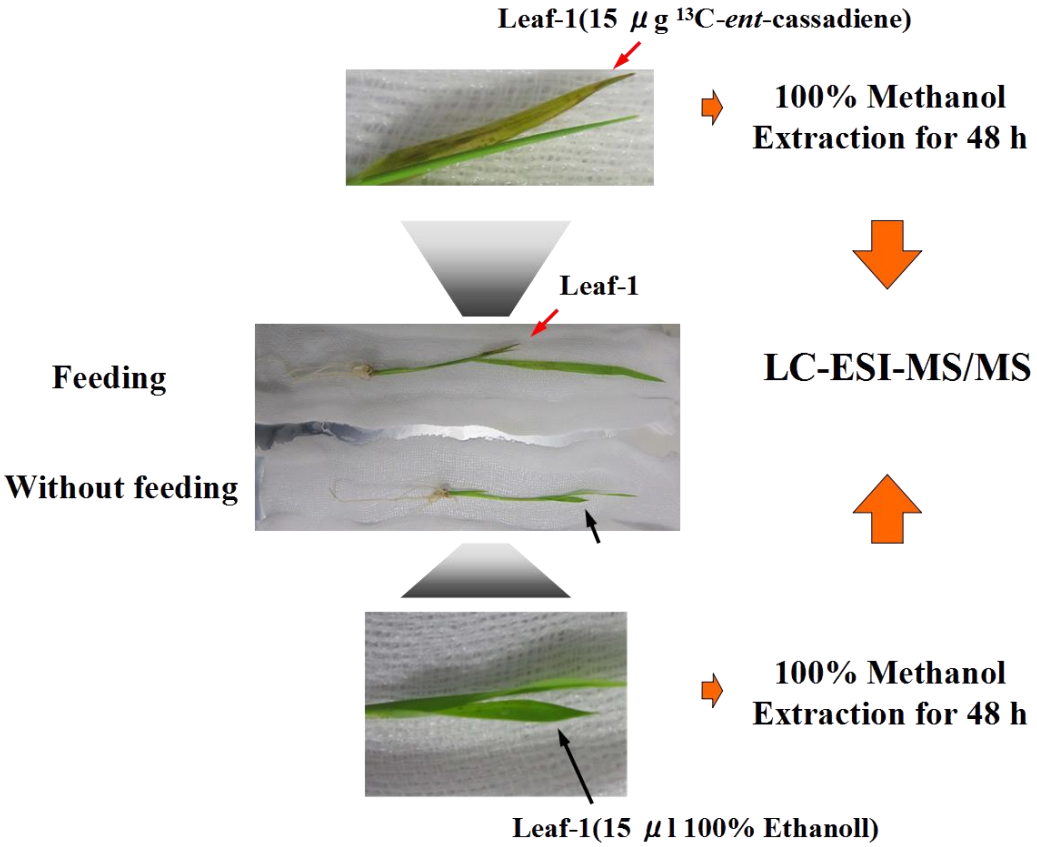

Figure 3-2. [U-$^{13}C_{20}$] *ent*-cassa-12,15-diene application on rice leaf-1 (*O. sativa* L. cv. Nipponbare) with 500 µM $CuCl_2$ treatment in cheesecloths.

Without feeding, first expanded leaf was treated with 15 µl of 100% Ethanol in 500 µM $CuCl_2$ soaked cheesecloths; **Feeding,** first expanded leaf was treated with 15 µg of [U-$^{13}C_{20}$] *ent*-cassadiene (1 µg/µl in 100% ethanol) in 500 µM $CuCl_2$ soaked cheesecloths. Rice plants were 6 day old seedling. Incubation time was 72 h.

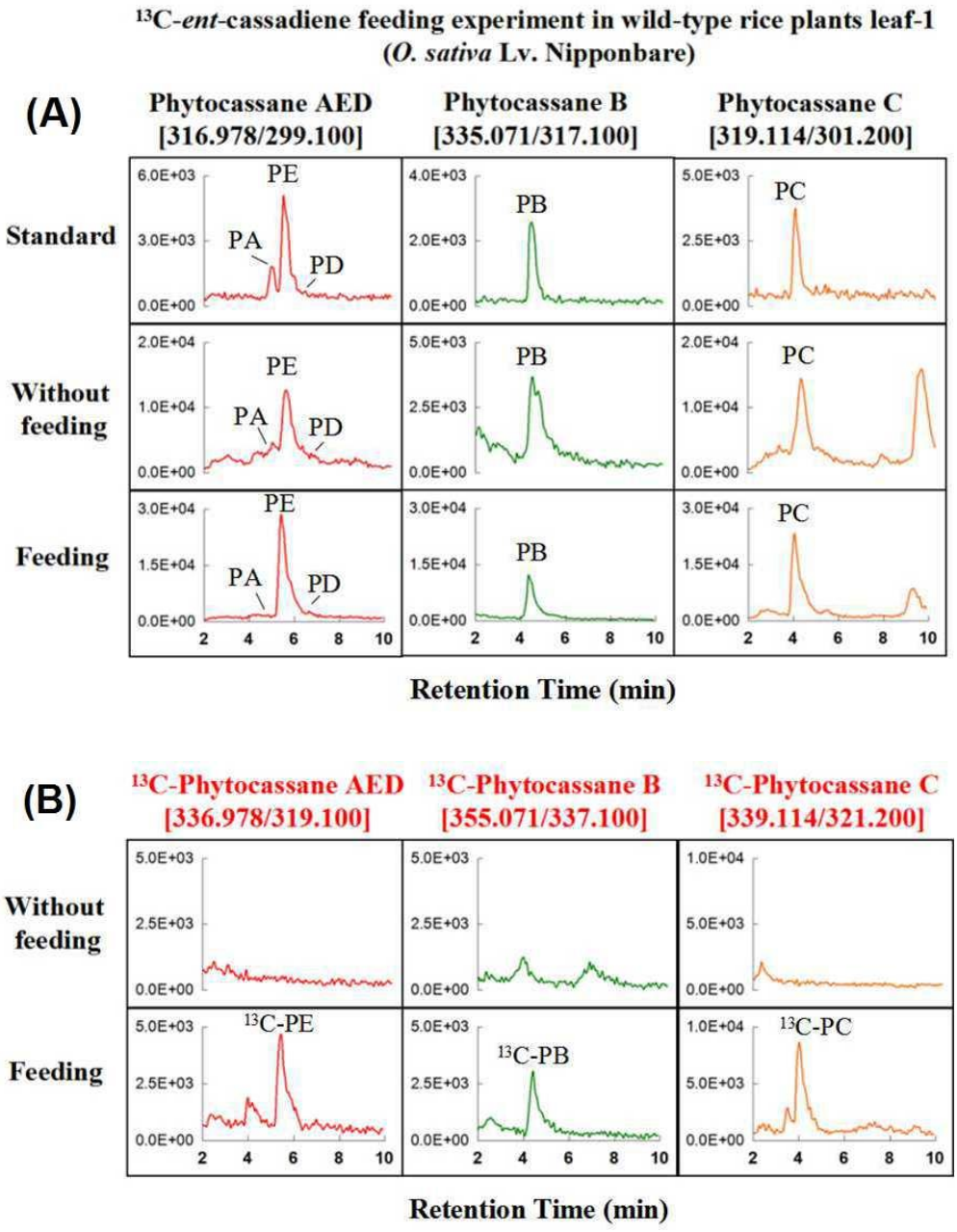

Figure 3-3. Phytocassanes and [U-$^{13}C_{20}$] phytocassanes accumulation level in 6-day old rice leaf-1 (*O. sativa* L. cv. Nipponbare) with 15 µg of [U-$^{13}C_{20}$] *ent*-cassa-12,15-diene feeding and 500 µM $CuCl_2$ elicitation in cheesecloths.

A, Unlabeled phytocassane (A-E) analysis on LC-ESI-MS/MS. **PA,** Phytocassane A; **PB,** Phytocassane B; **PC,** Phytocassane C; **PD,** Phytocassane D; **PE,** Phytocassane E. **B,** [U-$^{13}C_{20}$] phytocassane (A-E) analysis on LC-ESI-MS/MS. **^{13}C-PB**, [U-$^{13}C_{20}$] phytocassane B; **^{13}C-PC**, [U-$^{13}C_{20}$] phytocassane C, **^{13}C-PE,** [U-$^{13}C_{20}$] phytocassane E. **C,** Phytocassanes and [U-$^{13}C_{20}$] phytocassanes accumulation level in one gram rice tissue. The ratio of phytocassanes occupied in total phytocassanes. 5 µl of each extract was analyzed.

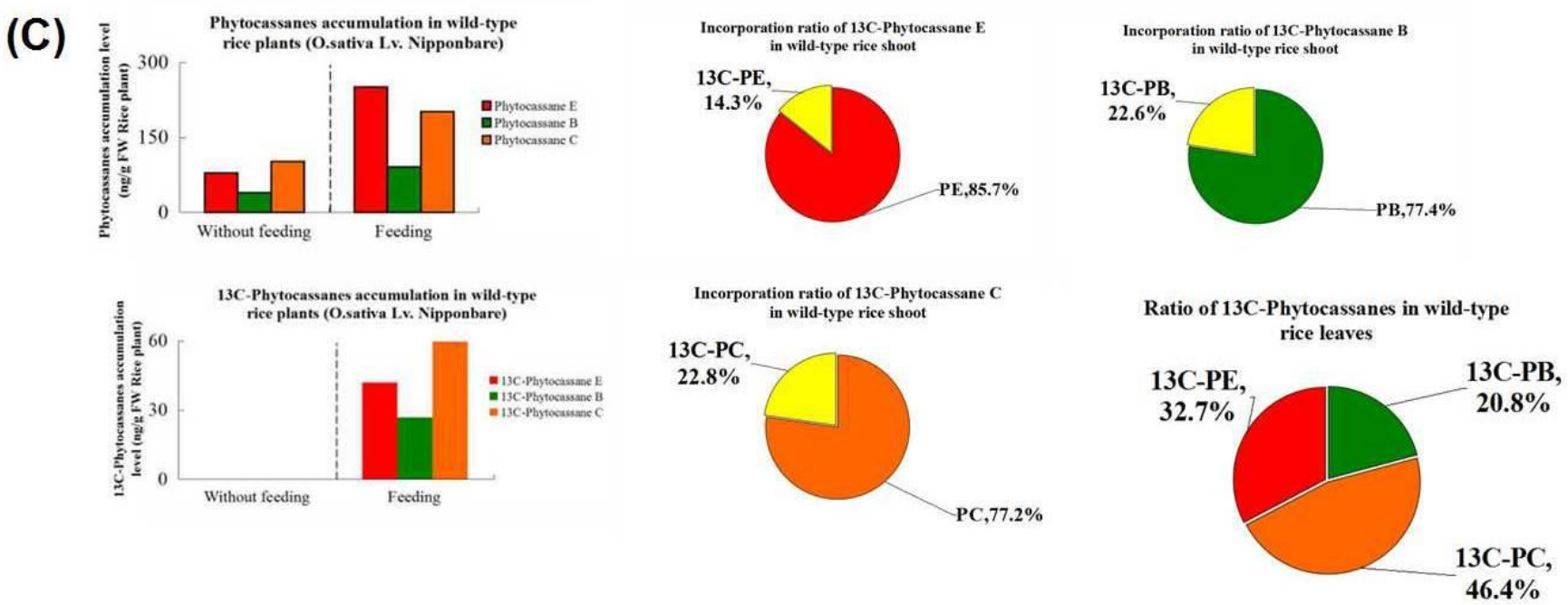

Figure 3-3. Continued

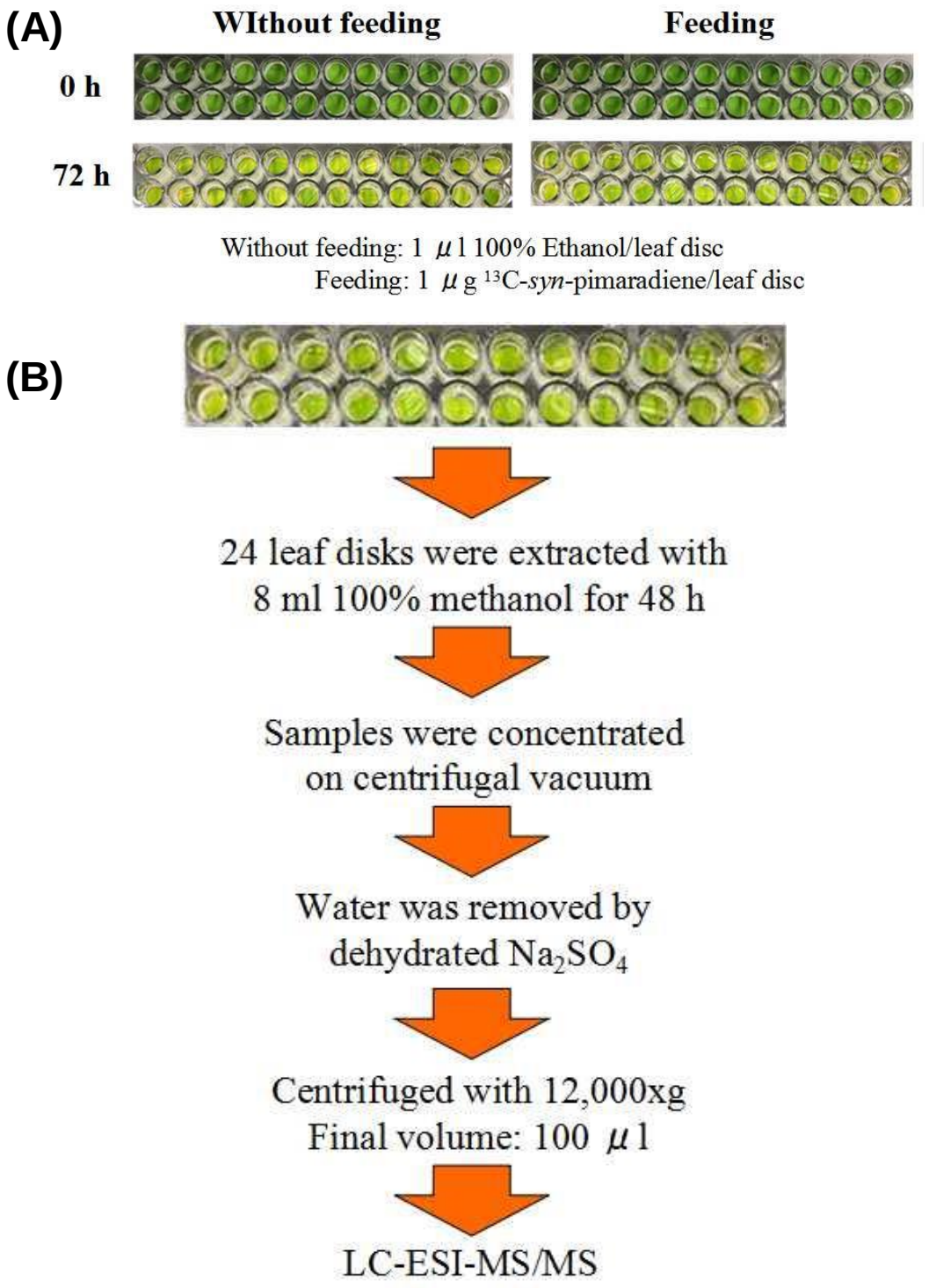

Figure 3-4. The application of [U-$^{13}C_{20}$] *syn*-pimaradiene to fresh wild-type leaf disks (*O. sativa* L.cv. Nipponbare).

A, Without feeding, 1 µl of 100% ethanol was applied to one well leaf disk in 500 µM $CuCl_2$ soaked cheesecloths; Feeding, 1 µg of [U-$^{13}C_{20}$] *syn*-pimaradiene was also applied to one well leaf disk in 500 µM $CuCl_2$ soaked cheesecloths; **B,** a schematic diagram for momilactones or [U-$^{13}C_{20}$] momilactones extraction from leaf disks. 24 wells leaf disks for one extract. N=1. 5 µl of each extract was subjected to HPLC-ESI-MS/MS.

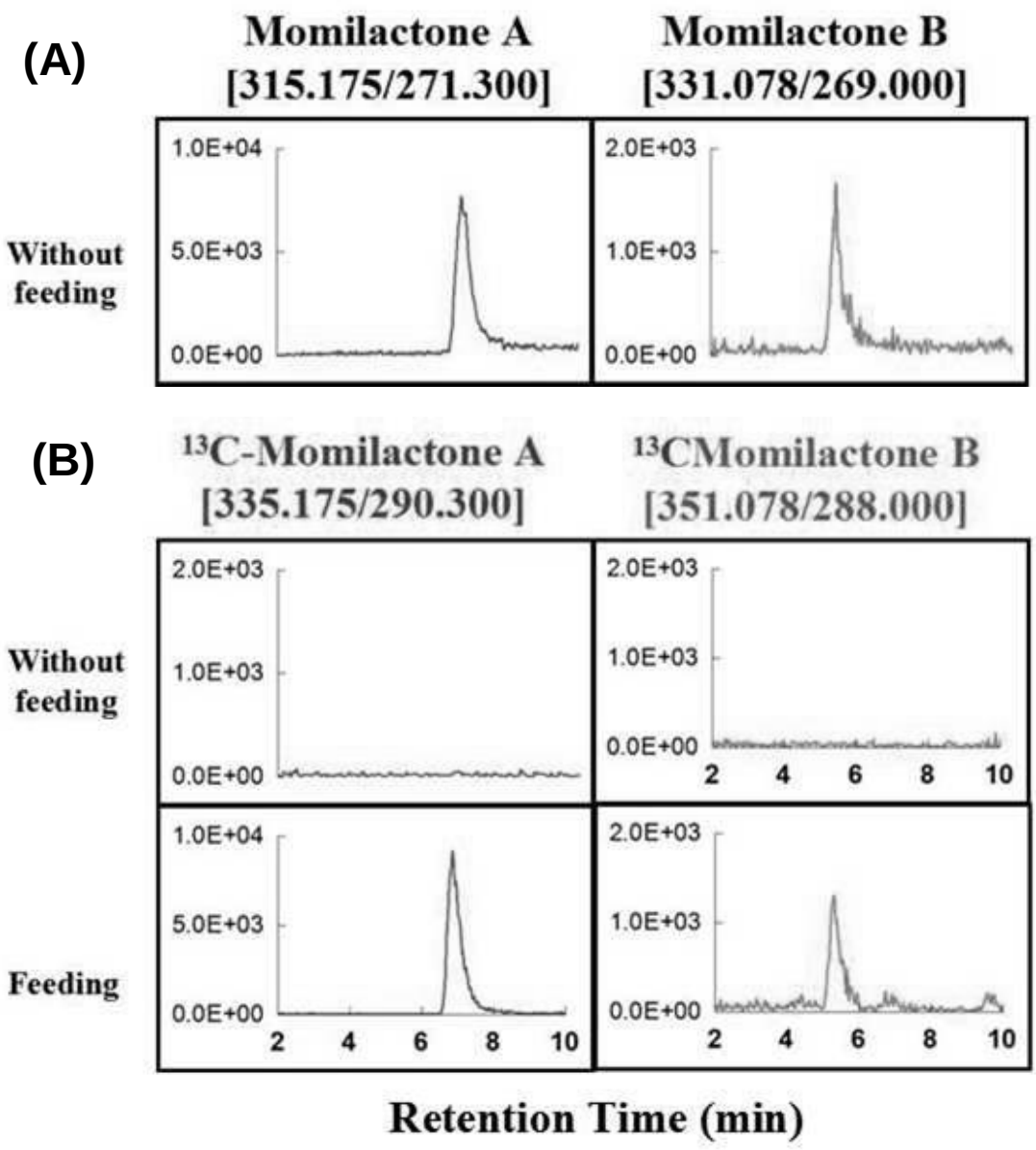

Figure 3-5. LC-ESI-MS/MS analysis of [U-$^{13}C_{20}$] momilactones in wild-type leaf disks (*O. sativa* L.cv. Nipponbare).

A, Native momilactones accumulation level analysis in without feeding leaf disks. **B,** Biosynthesis of [U-$^{13}C_{20}$] momilactone (A, B) in leaf disks from without feeding or feeding group. **C,** the incorporation ratio of [U-$^{13}C_{20}$] momilactones in unlabeled momilactones. 1 μg of [U-$^{13}C_{20}$] *syn*-pimara-7,15-diene was applied to each leaf disk. Extract from 24 leaf disks. 5 μl of each extract was subjected to LC-ESI-MS/MS. **MA,** momilactone A; **MB,** momilactone B; **^{13}C-MA**, [U-$^{13}C_{20}$] momilactone A; **^{13}C-MB**, [U-$^{13}C_{20}$] momilactone B.

(C)

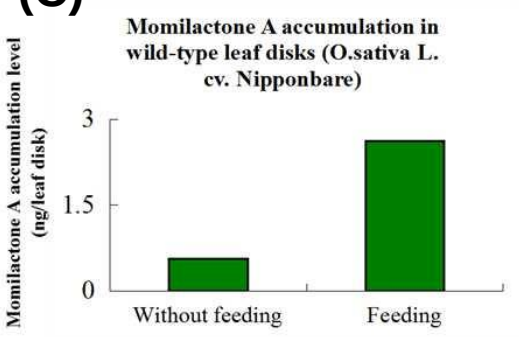

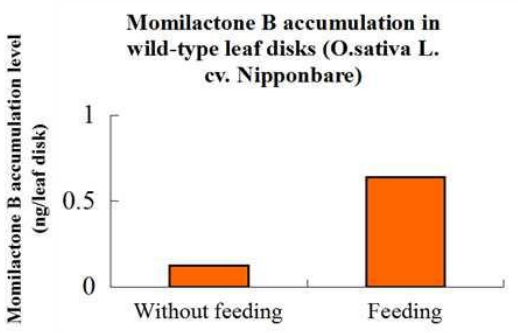

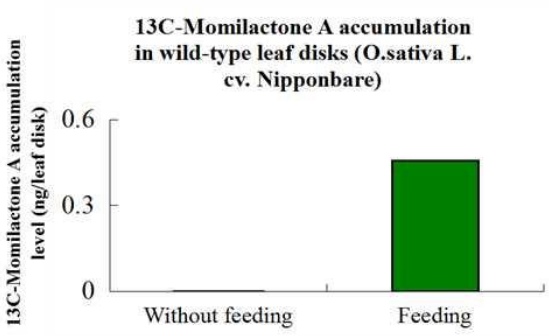

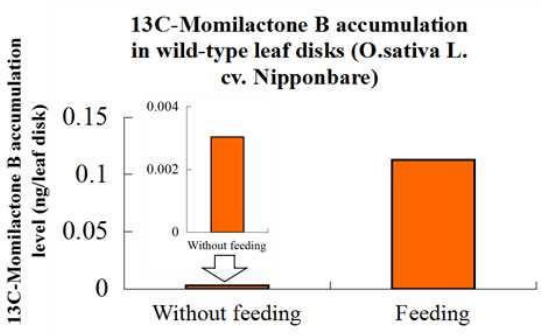

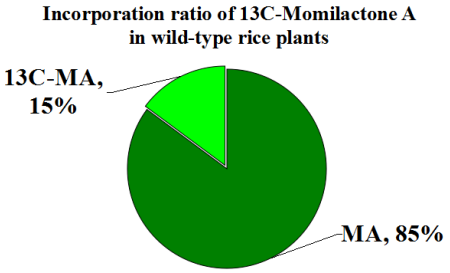

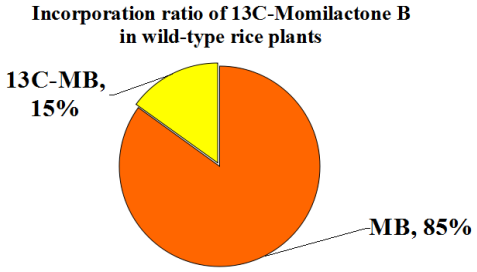

Figure 3-5. Continued

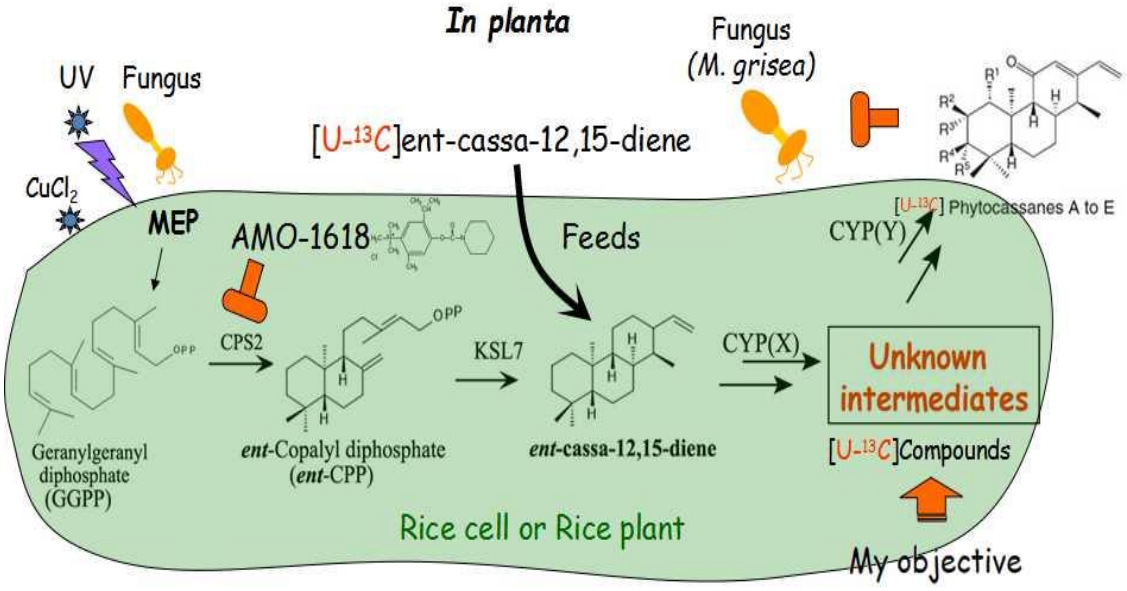

Figure 3-6. A schematic diagram of [U-$^{13}C_{20}$] *ent*-cassa-12,15-diene feeding in AMO-1618 effected rice plants or rice cells.

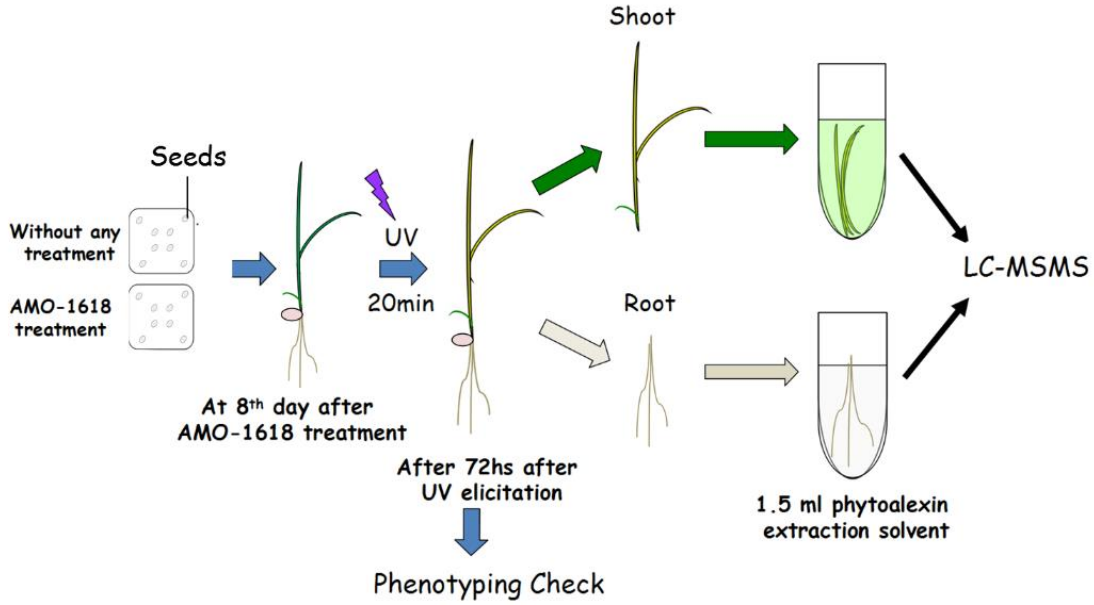

Figure 3-7. A schematic diagram for AMO-1618 treatment on rice plants (*O. sativa* L.cv. Nipponbare) under UV-irradiation.

Without any treatment: Planted seeds were not treated with any chemicals; **AMO-1618 treatment,** 100 μg of AMO-1618 dissolved in 10 μl of sterile water was applied to one rice seed. All rice plants were treated with UV-irradiation at 8 days old. 5 μl of each extract was applied to LC-ESI-MS/MS.

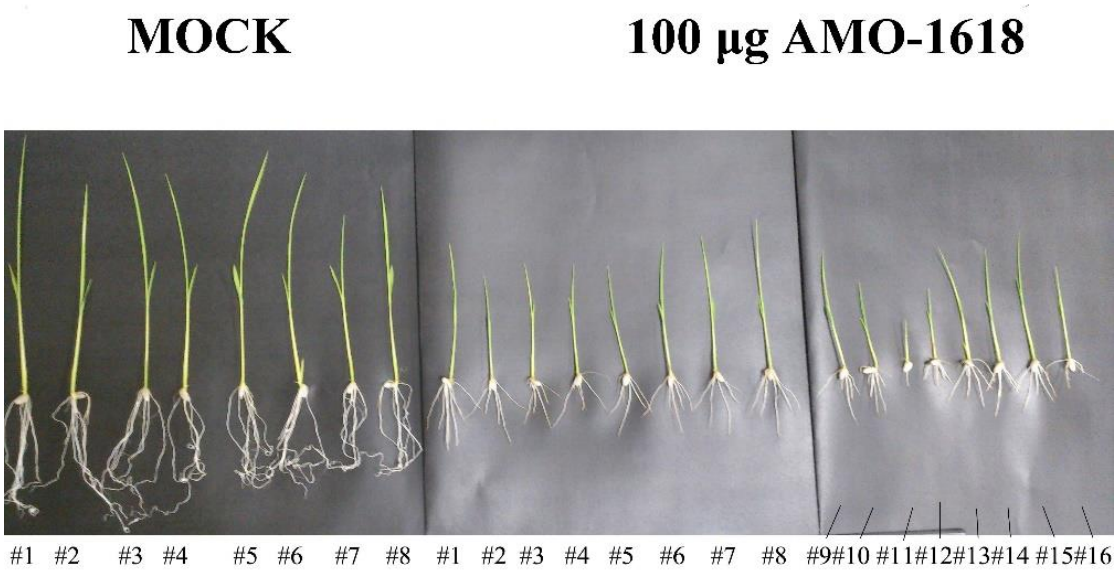

Figure 3-8. The phenotype of rice plants without or with 100 μg of AMO-1618 treatment.

MOCK, without any treatment; **100 μg of AMO-1618,** each rice seed were treated with 100 μg of AMO-1618. The length of shoots and roots were measured with rule. n(MOCK)=8; n(AMO-1618)=16

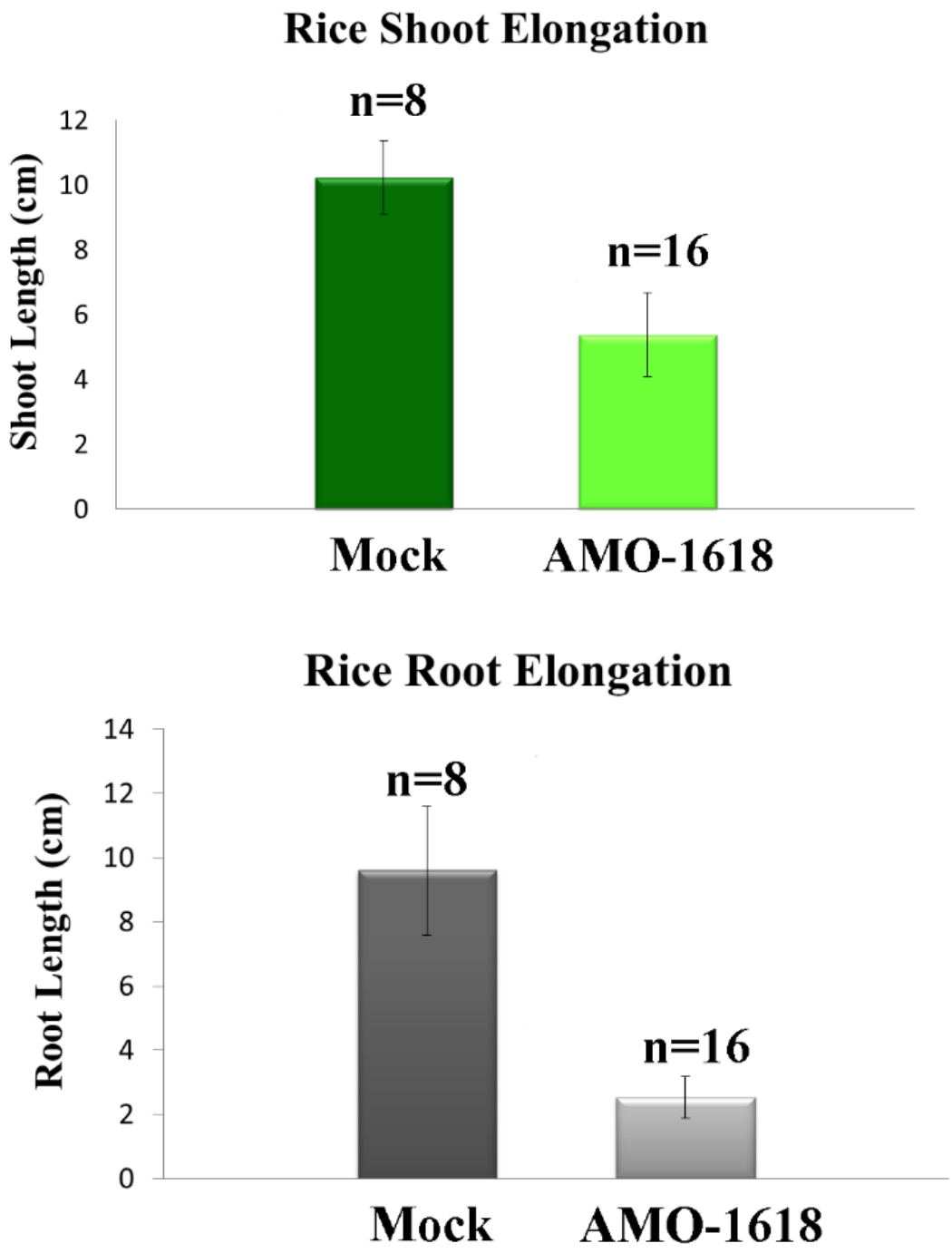

Figure 3-9. The effect of AMO-1618 on shoots and roots elongation. **Mock,** n=8; **AMO-1618,** n=16;

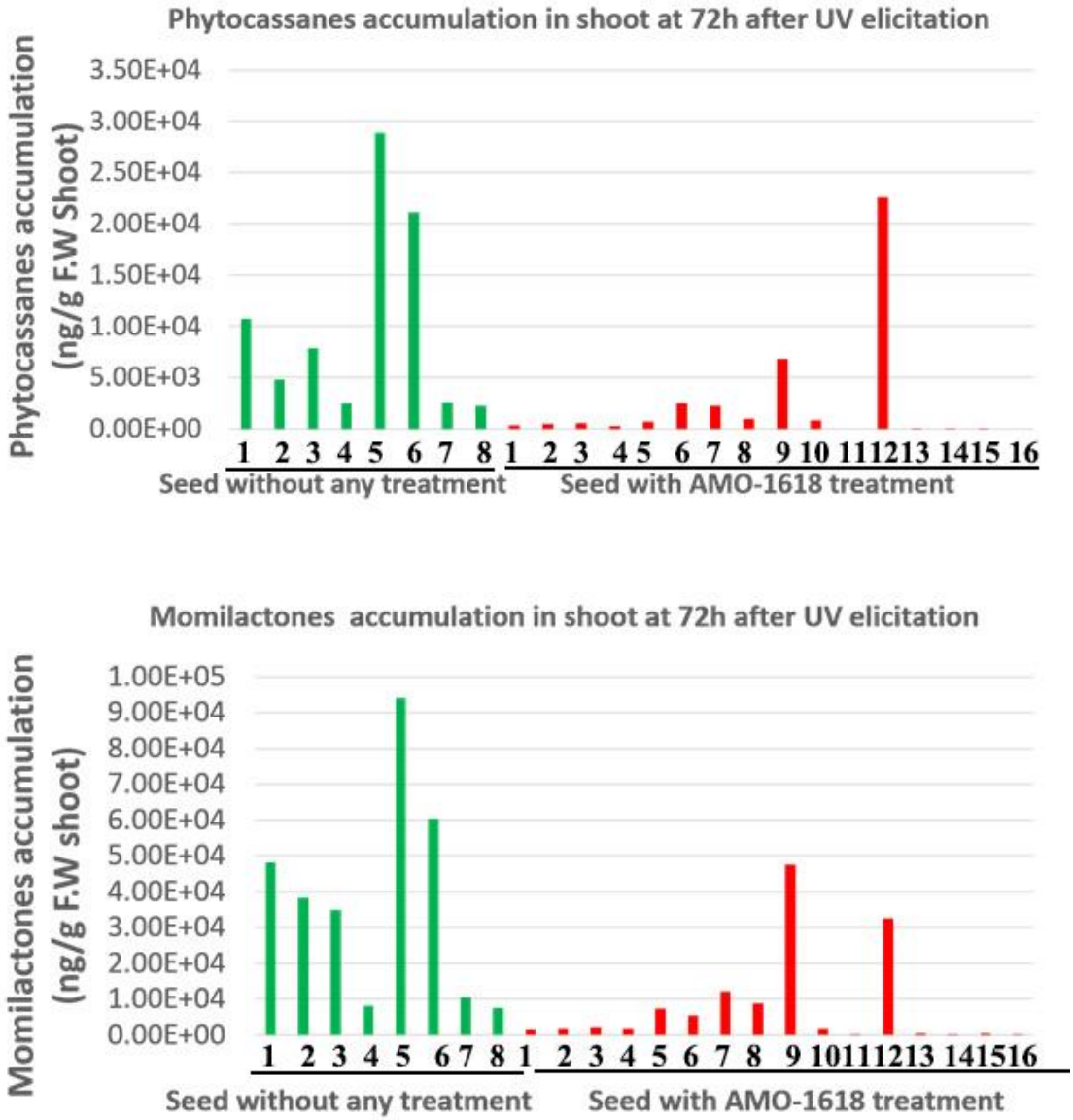

Figure 3-10. The effect of AMO-1618 on phytocassanes and momilactones accumulation level in rice shoots.

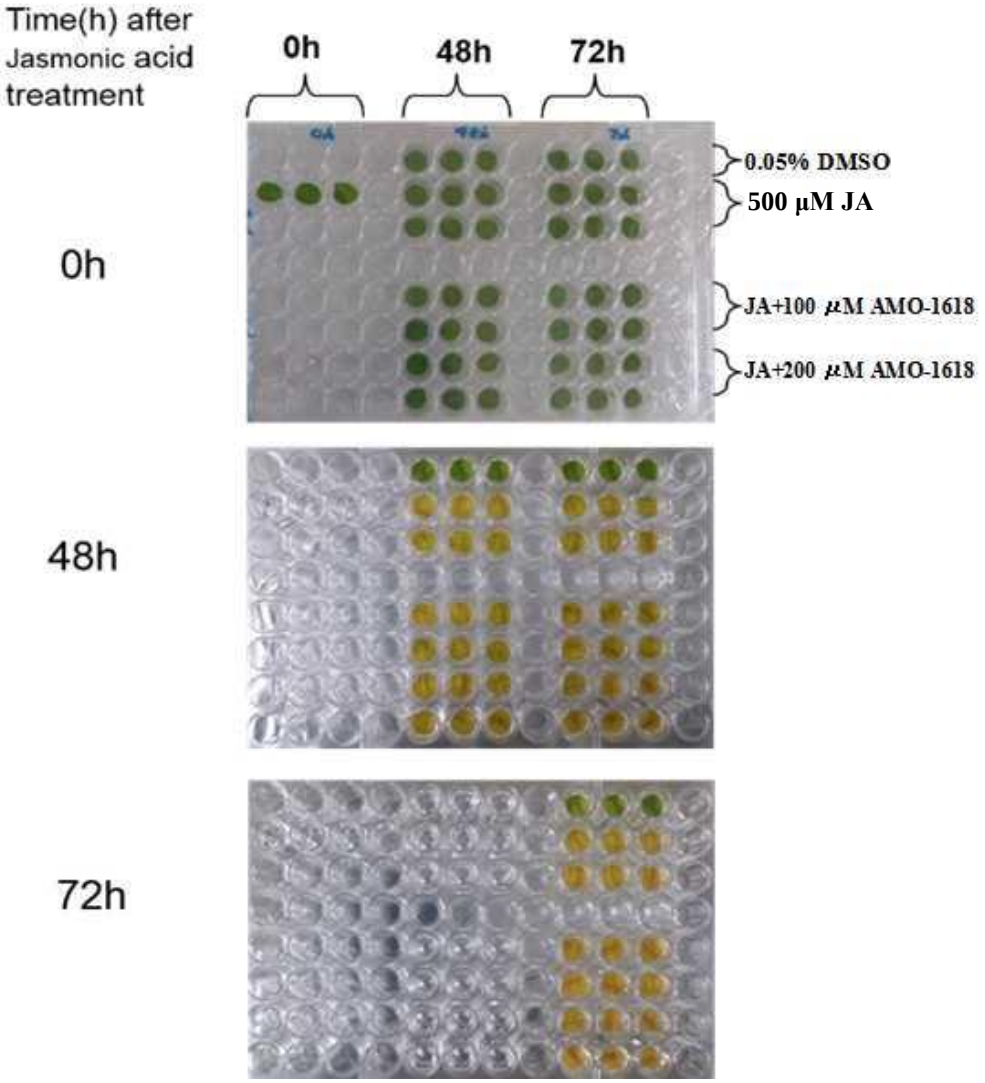

Figure 3-11. The effect of jasmonic acid (JA) and AMO-1618 on 6 weeks old leaf disks.

0 h, leaf disks without any treatment were collected at 0 h, n=3; **48 h,** leaf disks with different treatment (0.05% DMSO, 500 µM JA, 500 µM JA+100 µM AMO-1618 and 500 µM JA+200 µM AMO-1618) were collected at 48 h, respectively. n=6; **72 h,** leaf disks with different treatment (0.05% DMSO, 500 µM JA, 500 µM JA+100 µM AMO-1618 and 500 µM JA+200 µM AMO-1618) were collected at 72 h. n=6;

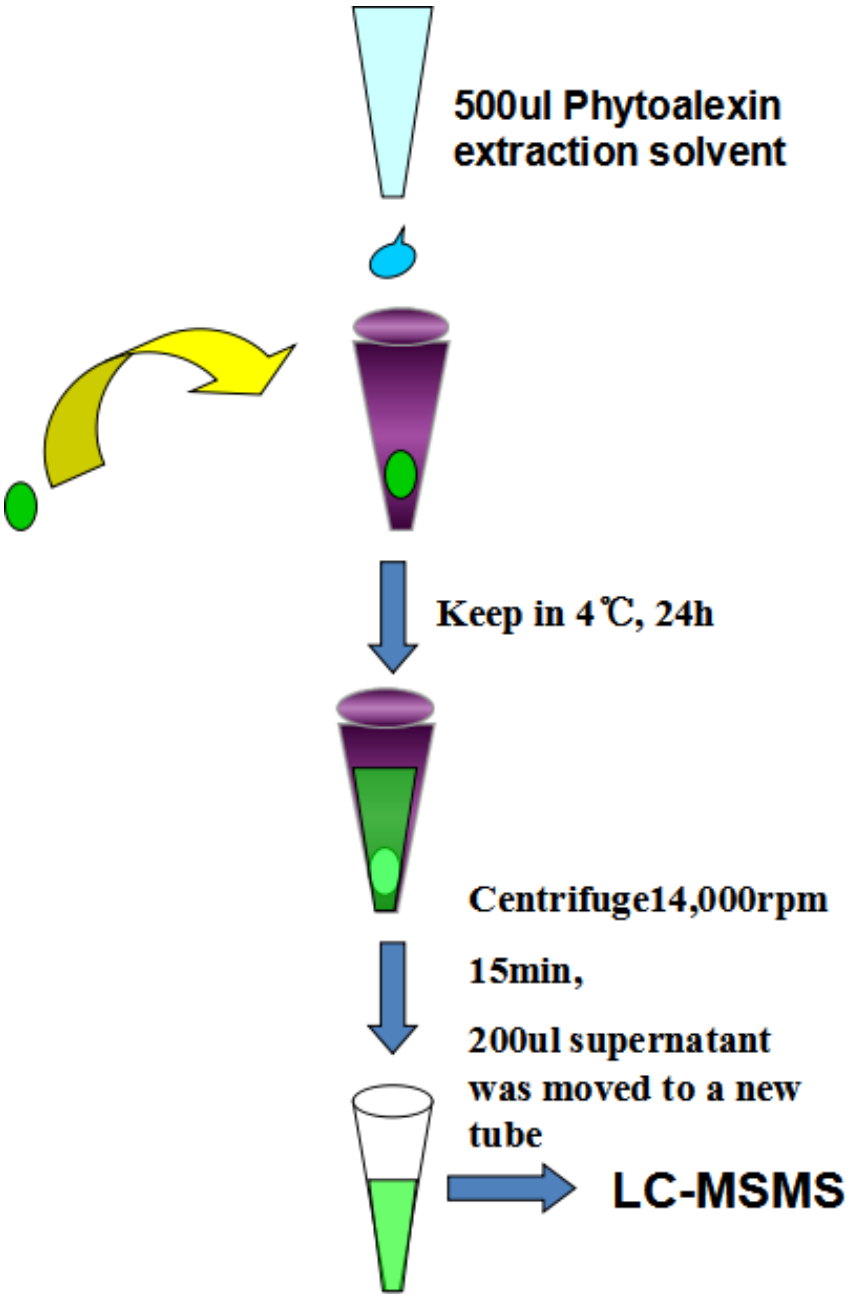

Figure 3-12. The method for phytoalexins extraction from leaf disks.

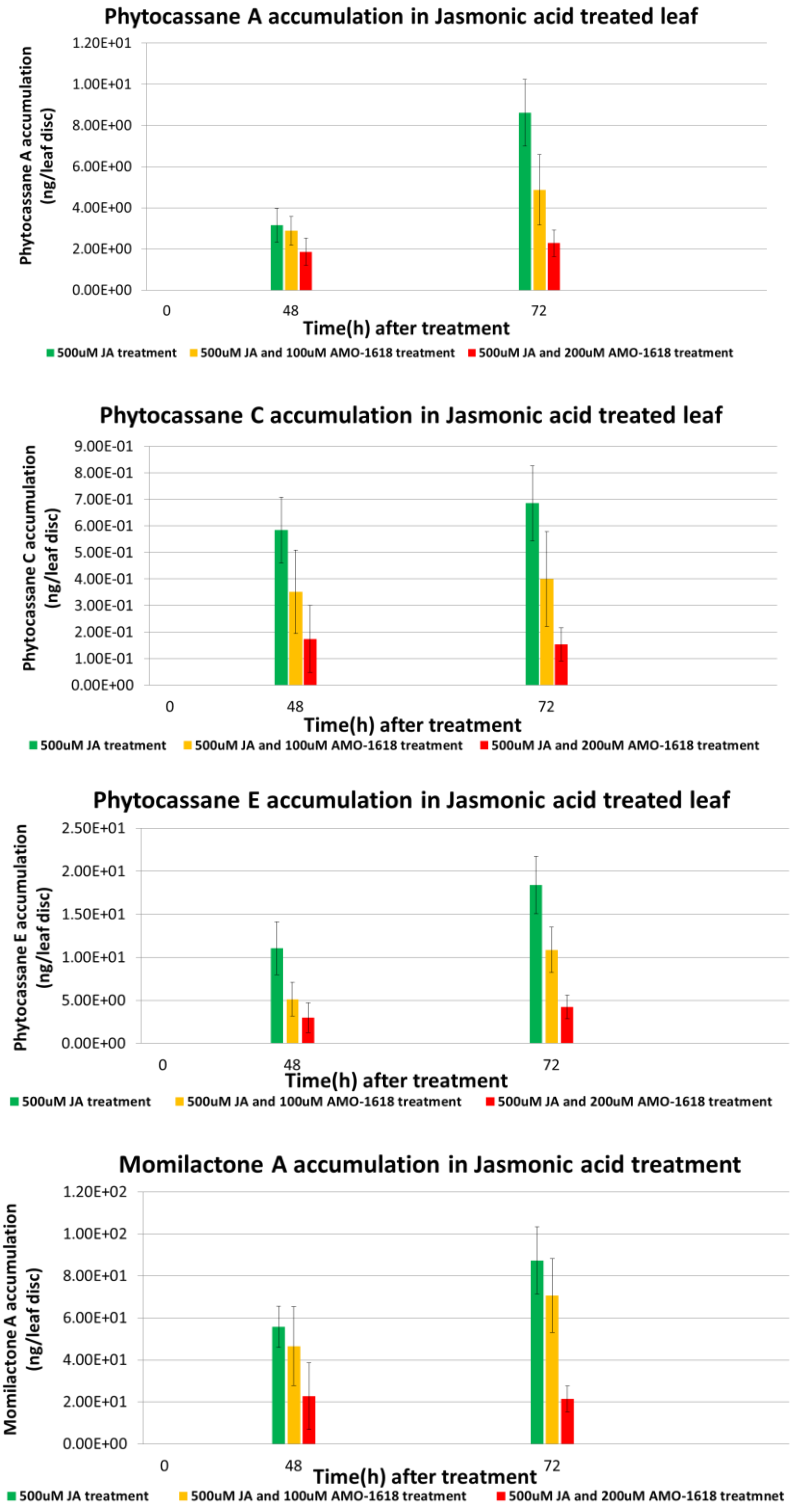

Figure 3-13. The effect of AMO-1618 on phytocassanes and momilactones accumulation level in 6 weeks old leaf disks.

Green column, leaf disks with 500 μM JA treatment; **Yellow column,** 100 μM AMO-1618 was applied to leaf disks with 500 μM JA treatment; **Red column,** 200 μM AMO-1618 was applied to leaf disks with 500 μM JA treatment

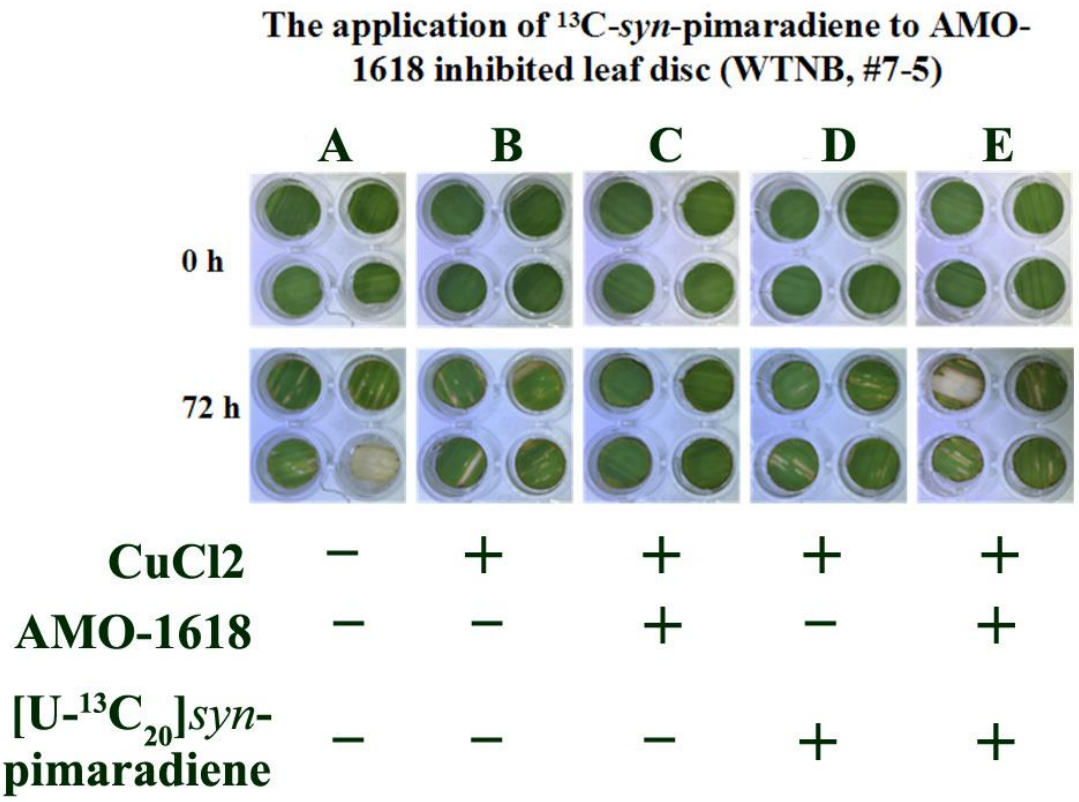

Figure 3-14. The application of [U-$^{13}C_{20}$] *syn*-pimaradiene to AMO-1618 treated leaf disks.

A, Each leaf disk was painted with 1 µl of *n*-hexane on water soaked cheesecloths; **B,** Each leaf disk was painted with 1 µl of *n*-hexane on 500 µM $CuCl_2$ soaked cheesecloths; **C,** Each leaf disk was painted with 1 µl of *n*-hexane on 500 µM $CuCl_2$ and 200 µM AMO-1618 soaked cheesecloths; **D,** Each leaf disk was painted with 1 µg of [U-$^{13}C_{20}$] *syn*-pimaradiene on 500 µM $CuCl_2$ soaked cheesecloths; **E,** Each leaf disk was painted with 1 µg of [U-$^{13}C_{20}$] *syn*-pimaradiene on 500 µM $CuCl_2$ and 200 µM AMO-1618 soaked cheesecloths. All leaf disks were collected at 72 h. 5 µl of each extract was subjected on LC-ESI-MS/MS. n=4.

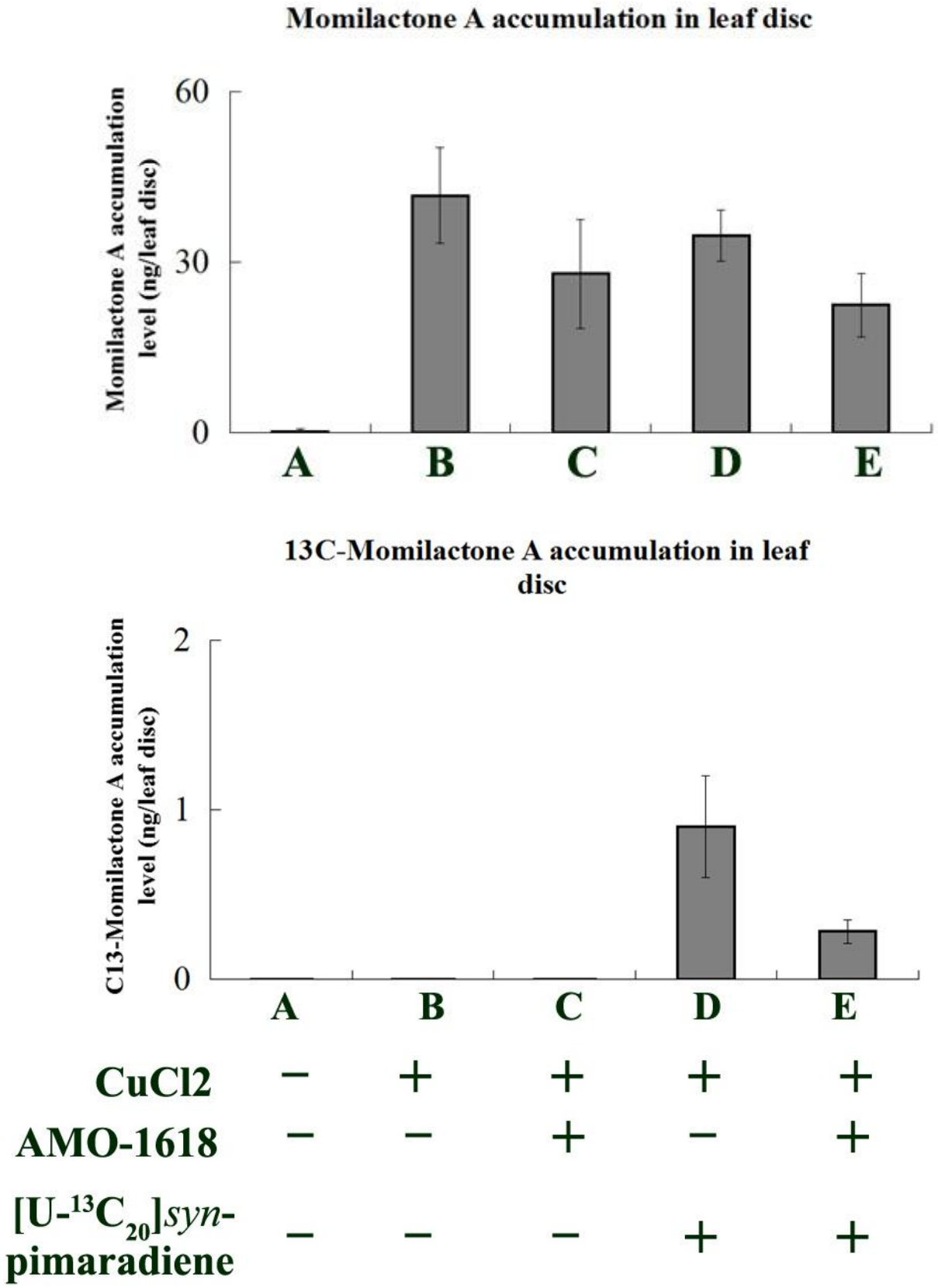

Figure 3-15. Momilactone A or [U-$^{13}C_{20}$] momilactone A biosynthesis in leaf disks under different conditions.

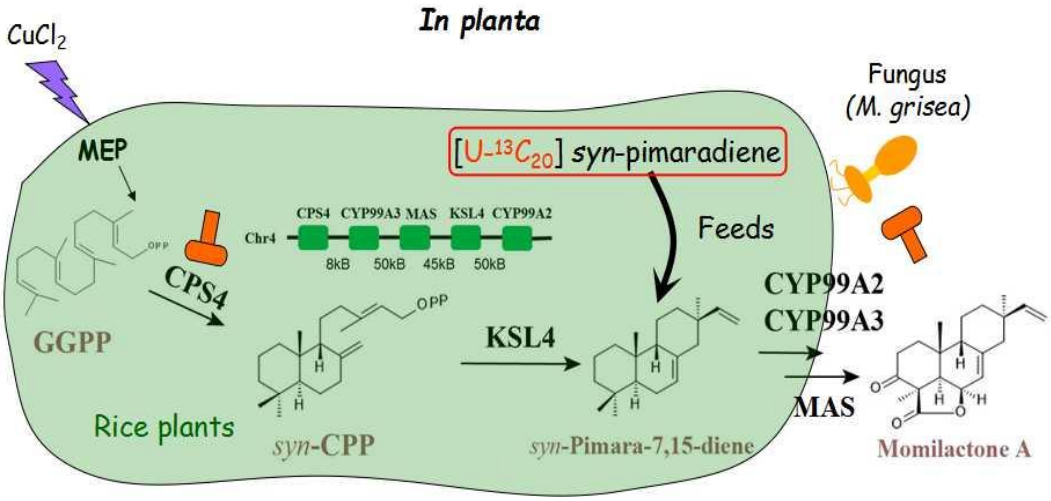

Figure 3-16. A schematic diagram of [U-$^{13}C_{20}$] *syn*-pimara-7,15-diene feeding in *CPS4* Tos-17 mutant rice plants .

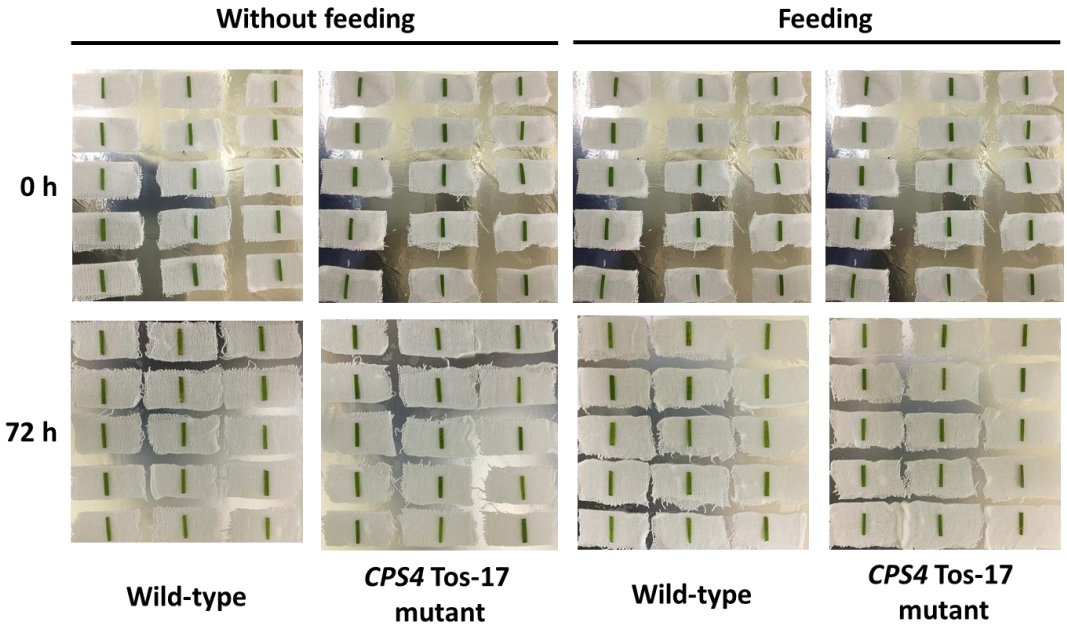

Figure 3-17. The application of [U-$^{13}C_{20}$] *syn*-pimaradiene to 3 weeks old wild-type or *CPS4* Tos-17 mutant leaf piecess.

Without feeding, 1 µl of 99.5% ethanol was applied to each leaf piece in 500 µM $CuCl_2$ soaked cheeseclothes; **Feeding,** 1 µg of [U-$^{13}C_{20}$] *syn*-pimaradiene was applied to one leaf piece in 500 µM $CuCl_2$ soaked cheeseclothes. Length of leaf piece was about 1 cm. 5 leaf pieces were extracted together. n=3. 5 µl of each extract was subjected to LC-ESI-MS/MS.

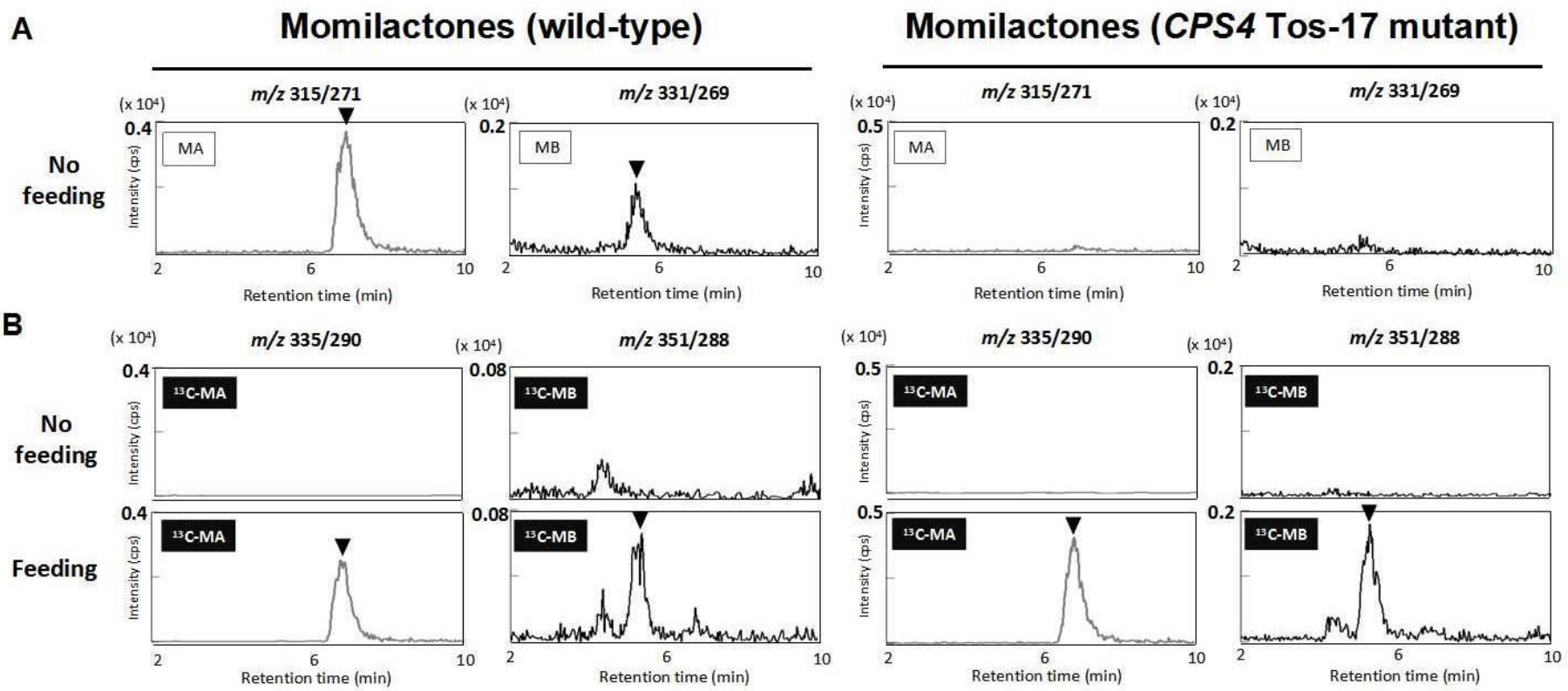

Figure 3-18. Momilactone (A and B) or [U-$^{13}C_{20}$] momilactone (A and B) accumulation level in 3 weeks old wild-type and *CPS4* Tos-17 mutant leaf pieces.

A, unlabeled momilactone (A and B) accumulation level in wild-type and *CPS4* Tos-17 mutant without feeding; **B,** unlabeled momilactone (A and B) and [U-$^{13}C_{20}$] momilactone (A and B) accumulated amount from one gram leaf tissue in both of no feeding and feeding group; C**,** The ratio of [U-$^{13}C_{20}$] momilactone (A and B) to unlabeled momilactone (A and B) in both of wild-type and *CPS4* Tos-17 mutant. n=3. *m/z* 315/271, momilactone A; *m/z* 331/269, momilactone B; *m/z* 335/290, [U-$^{13}C_{20}$]momilactone A; *m/z* 351/288, [U-$^{13}C_{20}$] momilactone B; 5 µl of each extract was subjected to LC-ESI-MS/MS.

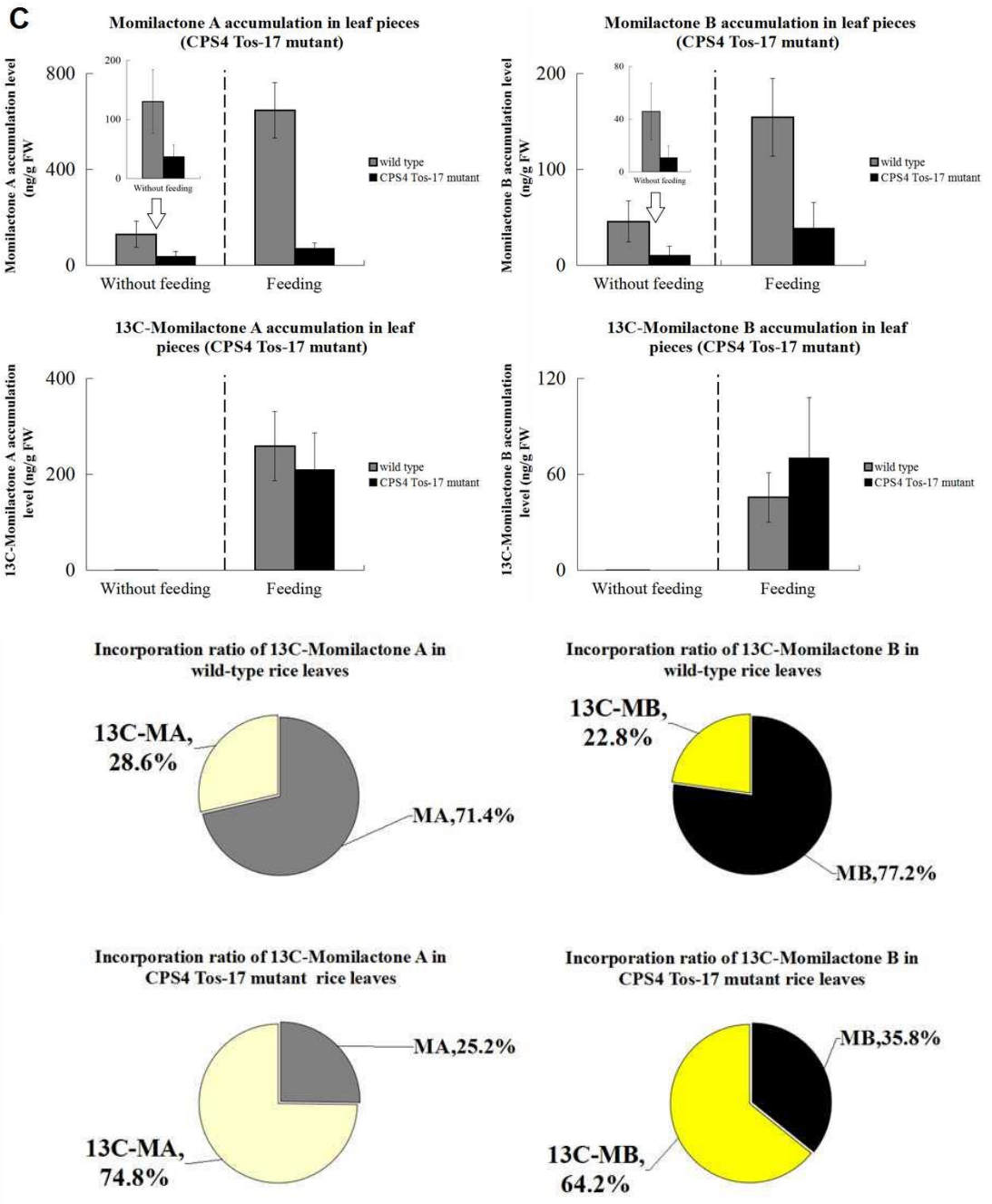

Figure 3-18. Continued

Reference

[1] **Batista Silva W, Daloso DM, Fernie AR, Nunes-Nesi A, Araújo WL.** Can stable isotope mass spectrometry replace radiolabelled approaches in metabolic studies. *Plant Sci*. 2016, 249:59-69

[2] **Sugai Y, Miyazaki S, Mukai S, Yumoto I, Natsume M and Kawaide H.** Enzymatic total synthesis of gibberellin A_4 from acetate. *Biosci Biotechnol Biochem.* 2011a, 75(1): 128-135

[3] **Rademacher W.** GROWTH RETARDANTS: Effects on Gibberellin Biosynthesis and Other Metabolic Pathways. *Annu Rev Plant Physiol Plant Mol Biol*. 2000, 51:501-531.

[4] **Sachs RM, Lang A, Bretz CF and Roach J.** Shoot histogenesis: subapical meristematic activity in a caulescent plant and the action of gibberellic acid and Amo-1618. *American Journal of Botany*. 1960, 260-266

[5] **Kende H, Ninnemann H, Lang A.** Inhibition of gibberellic acid biosynthesis in *Fusarium moniliforme* by AMO-1618 and CCC. *Naturwissenschaften*. 1963, 50: 599-600

[6] **Nojiri H, Sugimori M, Yamane H, Nishimura Y, Yamada A, Shibuya N, Kodama O, Murofushi N, Omori T.** Involvement of Jasmonic Acid in Elicitor-Induced Phytoalexin Production in Suspension-Cultured Rice Cells. *Plant Physiol*. 1996, 110(2): 387‑392.

[7] **Shimizu T, Jikumaru Y, Okada A, Okada K, Koga J, Umemura K, Minami E, Shibuya N, Hasegawa M, Kodama O. Nojiri H and Yamane H.** Effects of a bile acid elicitor, cholic acid, on the biosynthesis of diterpenoid phytoalexins in suspension-cultured rice cells. *Phytochemistry.* 2008, 69: 973-981

[8] **Ingram TJ and Reid JB.** Internode Length in Pisum: Gene na May Block Gibberellin Synthesis between *ent*-7alpha-Hydroxykaurenoic Acid and Gibberellin A_{12}-Aldehyde. *Plant Physiol.* 1987, 83(4): 1048-53

[9] **Cho EM, Okada A, Kenmoku H, Otomo K, Toyomasu T, Mitsuhashi W, Sassa T, Yajima A, Yabuta G, Mori K, Oikawa H, Toshima H, Shibuya N, Nojiri H, Omori T, Nishiyama M and Yamane H.** Molecular cloning and characterization of a cDNA encoding *en*t-cassa-12,15-diene synthase, a putative diterpenoid phytoalexin biosynthetic enzyme, from suspension-cultured rice cells treated with a chitin elicitor. *Plant Journal.* 2004, 37: 1-8

[10] **Jennings JC, Banks JA, Coolbaugh RC.** Subtractive hybridization between cDNAs from untreated and AMO-1618-treated cultures of Gibberella fujikuroi. *Plant Cell Physiol.* 1996, 37(6):847-54.

[11] **Dennis DT, Upper CD, West CA.** An enzymic site of inhibition of gibberellin biosynthesis by Amo 1618 and other plant growth retardants. *Plant Physiol*. 1965, 40(5):948-52.

[12] **Rademacher W.** GROWTH RETARDANTS: Effects on Gibberellin Biosynthesis and Other Metabolic Pathways. Annu Rev Plant Physiol Plant Mol Biol. 2000, 51:501-531.

[13] **Okada K, Kawaide H, Miyamoto K, Miyazaki S, Kainuma R, Kimura H, Fujiwara, K, Natsume M, Nojiri H, Nakajima M, Yamane H, Hatano Y, Nozaki H and Hayashi K.** HpDTC1, a Stress-Inducible Bifunctional Diterpene Cyclase Involved in Momilactone Biosynthesis, Functions in Chemical Defence in the Moss Hypnum plumaeforme. *Sci Rep*. 2016, 6:25316

[14] **Toyomasu T, Usui M, Sugawara C, Otomo K, Hirose Y, Miyao A, Hirochika H, Okada K, Shimizu T, Koga J, Hasegawa M, Chuba M, Kawana Y, Kuroda M, Minami E, Mitsuhashi W, Yamane H.** Reverse-genetic approach to verify physiological roles of rice phytoalexins:

characterization of a knockdown mutant of OsCPS4 phytoalexin biosynthetic gene in rice. *Physiol Plant*. 2014, 150(1):55-62.

CHAPTER 4

INVESTIGATION OF DITERPENE INTERMEDIATES IN THE BIOSYNTHETIC MUTANTS OF CYTOCHROME P450 MONOOXYGENASES FOR DITERPENOID PHYTOALEXINS

4-1. Introduction

In chapter 3, it has been clarified that [U-$^{13}C_{20}$] phytocassanes and [U-$^{13}C_{20}$] momilactones can be biotransformed from [U-$^{13}C_{20}$] *ent*-cassa-12,15-diene and [U-$^{13}C_{20}$] *syn*-pimara-7,15-diene, respectively, in wild-type rice plants or other plants.

In this chapter, further aiming to investigate the intermediates on the route of phytocassanes and momilactones biosynthetic pathways in rice plants, a biosynthetic mutant or RNAi lines defective in the expressions of cytochrome P450 monooxygenases responsible for diterpenoid phytoalexins production were used for discovery of target intermediates.

Swaminathan *et al*. (2009) has confirmed CYP76M7 as a cytochrome P450 monooxygenase that catalyze the C11α-hydroxylation of *ent*-cassa-12,15-diene *in vitro*.[1] Thereafter, CYP76M8 was found responsible for the hydroxylation of a wide range of diterpenes, *ent*-cassa-12,15-diene (C11α), *syn*-pimara-7,15-diene (C6β), *ent*-pimaradiene (C7β), *ent*-kaurene (C9α), *ent*-sandaracopimaradiene (C9α) and *ent*-isokaurene (C7α).[2] This suggested that CYP76M7 or CYP76M8 may be the hypothetical enzymes on the pathway to phytocassanes or momilactones. However, their true substrates and roles *in vivo* are still ambiguous. Genetic approach using *CYP76M7/M8* double knock-down lines done by our laboratory indicated that accumulation of phytocassanes was strongly repressed relative to those of control.[2] Interestingly, *CYP76M7/M8* RNAi rice plants exhibited decrease in momilactones level in addition to phytocassanes depletion [unpublished data, Fig. 4-1]. On the other hand, C3α-hydroxy-C11-keto-*ent*-cassa-12,15-diene (1-deoxyphytocassane C) was assumed to be a hypothetical substrate for CYP71Z7 (Fig.1-3).[3] Such assumption was verified by the analysis of *CYP71Z7* T-DNA mutant (*O. sativa* L.cv. Dongjin) in our group, indicating significant accumulation of 1-deoxyphytocassane C in the mutant (Unpublished data; Fig.4-21).

Therefore, in this chapter, a feeding approach with stable isotope (e.g., ^{13}C) will be utilized to trace as-yet-unknown precursors of phytocassanes and momilactones by using *CYP76M7/M8* RNAi lines, *CYP71Z7* T-DNA mutant and wild-type rice plant.

4-2. Materials and Methods

4-2-1. General materials and methods

Wild-type, *CYP76M7/M8* RNAi lines and *CYP71Z7* T-DNA mutants seeds (*O. sativa* L. cv. Nipponbare and *O. sativa* L. cv. Dongjin) were sterilized by 70% alcohol and 5% HClO solution following dehusking. Seeds were further washed by MilliQ water in clean bench for 5 times at least. Thereafter, sterile seeds were planted in 0.5% agar and grown in a controlled green house. The condition as follows: temperature, 28℃; day length 24 hours;. 6-day old rice plants were enwrapped in cheesecloths, which were soaked in 500 μM $CuCl_2$ in advance. Furthermore, fresh rice leaf pieces and leaf disks on 8 months old or 6 days old rice seedlings were also used as research materials. ^{13}C labeled substrates were applied to fresh leaves for unknown intermediates investigation. Following 72 h [U-$^{13}C_{20}$] *ent*-cassa-12,15-diene incubation, all leaf blades or leaf disks were extracted with 100% methanol for 48 h. The extract was detected on LC-ESI-MS/MS and GC-MS.

4-2-2. Investigation of phytoalexins accumulation on different region in *CYP76M7/M8* RNAi lines leaves.

Fresh leaves from 8 months old *CYP76M7/M8* RNAi lines and wild type rice plants were cut into leaf disk (6 mm diameters). In excision of *CYP76M7/M8* RNAi rice leaves, 3 regions were selected: [LM]Lesion mimic (#4-1), [NC-1]Without lesion mimic (#4-1) and [NC-2]Without lesion mimic (other leaf, #4-1). The leaf disks [WT] were cut from wild-type rice leaves (Fig. 4-1). All leaf disks were treated with 500 μM $CuCl_2$ or water in a multi well plate. After 72 h incubation, each leaf disk was extracted with 500 μl of 100% methanol in enclosed glass tube for 48 h. Subsequently, extracts were analyzed on LC-MS/MS. 5 μl of each extract was subjected.

4-2-3. Application of [U-$^{13}C_{20}$] *ent*-cassa-12,15-diene to *CYP76M7/M8* RNAi lines and wild-type rice plants (*O. sativa* L. cv. Nipponbare)

In the feeding group, 9 μg of [U-$^{13}C_{20}$] *ent*-cassadiene (1 μg/μl in 99.5% ethanol) was fed to leaves of one rice plant (*O. sativa* L. cv. Nipponbare) at 6-day old (Fig. 4-3). Cotton gauze have been. The whole rice plants were enwrapped in this cotton gauze, which had been soaked with 500 μM $CuCl_2$ solution for induction of phytoalexin biosynthesis and incubated in an enclosed 38 mm-diameter glass tube. Following 72 h incubation, the whole shoot was weighted and cut into fragments. All fragments were extracted with 1 ml of 100% methanol for 48 h in 4℃. The extracts were evaporated on a centrifugal vacuum. Residual moisture was removed from enriched extracts using dehydrated Na_2SO_4. The rest of sample was centrifuged on 12,000xg for 5 min. The pellet was removed and supernatant (100 μl) was analyzed on LC-MS/MS and GC-MS. In the group without feeding, leaves from one rice plant were treated with 9 μl of 99.5% ethanol and 500 μM $CuCl_2$ solution.

4-2-4. Application of [U-$^{13}C_{20}$] *ent*-cassa-12,15-diene to *CYP71Z7* T-DNA mutant and wild-type rice plants (*O. sativa* L. cv. Dongjin)

This feeding experiment was performed on 6-week old wild-type and *CYP71Z7* T-DNA mutant leaf disk (*O. sativa* L. cv. Dongjin). In multi well plate, each leaf disk was put on a glob of cheesecloths, which has been soaked in 150 μl of $CuCl_2$ solution. In the feeding group, 1 μg of [U-$^{13}C_{20}$] *ent*-cassadiene (1 μg/μl in 99.5% ethanol) was applied to each leaf disc (Fig. 4-20). In the group without feeding, 1 μl of 99.5% ethanol was applied to one leaf disc. N=24/group. One group was divided into 3 parts, one of which includes 8 leaf disks. 8 leaf disks was collected and extracted with 1 ml of 100% methanol for 48 h. Extracts purification was same to that of previous.

4-2-5. Application of [U-$^{13}C_{20}$] *syn*-pimara-7,15-diene to *CYP76M7/M8* RNAi lines and wild-type rice plants (*O. sativa* L. cv. Nipponbare)

[U-$^{13}C_{20}$] *syn*-pimaradiene feeding experiment in wild-type rice plants and *CYP76M7/M8* RNAi lines (*O. sativa* L. cv. Nipponbare) were also performed. Fresh leaf disks (6 mm diameter) from 8 months old rice plants were used as material. 1 μg of [U-$^{13}C_{20}$] *syn*-pimaradiene (1 μg/μl in 99.5% ethanol) was applied to each fresh leaf disk in multi well plate with 0.5 mM $CuCl_2$ solution soaked cheesecloths. In no feeding group, 1 μl of 99.5% ethanol was painted on each leaf disk (Fig. 4-39). Following 72 h incubation, each group (24 leaf disks) was collected and extracted with 8 ml of 100% methanol for 48 h. The extracts were enriched, filtered and water removed. 5 μl of purified extract was subjected to LC-ESI-MS/MS and 1 μl of each extract was applied to GC-MS.

4-2-6. Analysis of phytoalexins and [U-$^{13}C_{20}$] phytoalexins on HPLC-ESI-MS/MS

The wild type or mutant rice plants with [U-$^{13}C_{20}$] *ent*-cassa-12,15-diene or [U-$^{13}C_{20}$] *syn-pimara-7,15*-diene feeding were extracted with 100% methanol for 48 h in 4℃, of which extracts had been filtrated through cotton gauze inserted in a glass pipet (Asahi Glass Co., LTD, USA) or 0.45μm PVDF membrane. The filtrated methanol extracts were concentrated to 100 μl *in vacuo*. Of 5 μl each extract was subjected to PEGASIL ODS SP100 C_{18} Column (Length 150 mm, diameter 2.1 mm, Senshu Scientific Co., Ltd, Japan) on HPLC-ESI-MS/MS. Acetonitrile/H_2O/Acetic Acid (70/29.9/0.1) were used as flow phase for the quantification of phytocassanes and momilactones from standard and methanol extracts, which were bumped to ESI-MS/MS by HP1100 Series Binary Pump at 0.2 ml/min of flow rate and monitored by a tandem mass spectrometer (API3000, Applied Biosystems, Instrument, Forster City, USA). The condition of ESI-MS/MS was described as previously.[5]

4-2-7. Analysis of intermediates or ^{13}C-intermediates on GC-MS

The extracts from wild type, *CYP76M7/M8* RNAi lines and *CYP71Z7* T-DNA mutant were analyzed by Agilent 6890 N GC-5973 N MSD mass selective detector system (70 eV of ionization voltage) coupled with a capillary column Inert Cap 5MS/Sil (0.25 mm of diameter, 15 m of length, 0.25 μm of film thickness; GL Sciences Inc. Japan). The carrier helium flow rate was controlled at 1 ml/min. Each

sample was autoinjected into column at 70℃. After 1 min hold at 70℃, the oven temperature was increased by 10℃/min to 280℃ with 5 min hold.

4-3. Results

4-3-1. Accumulation level of phytoalexins in different region of *CYP76M7/M8* RNAi lines leaves.

It has been confirmed that phytocassanes and momilactones accumulation were strongly repressed in *CYP76M7/M8* RNAi rice leaves even with 500 μM $CuCl_2$ treatment. Besides, it has also been found that brown spots (lesion mimics) appear after 3 months in the most of leaves from this mutant. When examined phytoalexin accumulation in leaves with lesion mimics, ability to produce phytoalexins was recovered to the level seen in wild-type plant. Therefore, because of this non-uniform RNAi effect, the phytoalexins accumulation in different regions (with or without emerged lesion mimic symptom) of *CYP76M7/M8* RNAi rice leaves was investigated first. LC-ESI-MS/MS analysis indicated phytocassane (A-E) and momilactone (A and B) accumulation level was drastically reduced in the region (NC-1 and NC-2) without lesion mimic relative to those of wild-type (WT) (Fig. 4-2). Unexpectedly, phytocassane (B, C and E) and momilactone (A and B) can be accumulated in the area containing lesion mimic regardless of with or without $CuCl_2$ treatment. Stable accumulation of sakuranetin further consolidated the data showing depletion of inductive production of phytocassanes and momilactones in different regions (Fig. 4-2). Taken together, it can be discreetly concluded that effect of *CYP76M7/M8* RNAi is only active around the region without lesion mimic in rice leaves. Based on this result, selected leaves or seedlings without lesion mimic were subjected to the isotope labeling experiment as materials.

4-3-2. [U-$^{13}C_{20}$] *ent*-cassa-12,15-diene feeding experiment on *CYP76M7/M8* RNAi lines and wild-type rice seedlings (*O. sativa* L. cv. Nipponbare)

Following the region selection in *CYP76M7/M8* RNAi lines, [U-$^{13}C_{20}$] *ent*-cassa-12,15-diene was applied to *CYP76M7/M8* RNAi lines and wild-type rice seedlings successively. LC-ESI-MS/MS results indicated that phytocassane B, C and E were strongly accumulated in wild-type rice plants, but repressed in *CYP76M7/M8* RNAi lines (Fig. 4-4; Fig. 4-5). Additionally, [U-$^{13}C_{20}$] phytocassane C was biosynthesized successfully in wild-type rice seedling, but blocked in *CYP76M7M8* RNAi lines (Fig. 4-4; Fig. 4-5). It was again clarified that CYP76M7/M8 is a dominant enzyme for phytocassane (B, C and E) biosynthesis based on the feeding experiment. From these results in LC-ESI-MS/MS analysis, the intermediates or ^{13}C-intermediates accumulation in *CYP76M7M8* RNAi lines were further investigated by GC-MS. As a result, it was detected an enhanced peak 2 (compound-I) and peak 3 (compound II) in *CYP76M7/M8* RNAi line fed with [U-$^{13}C_{20}$] *ent*-cassa-12,15-diene (shown as peak 1) compared to that in wild type in GC-MS chromatograms (Fig. 4-6).

Mass fragmentation pattern of these peaks were shown in Fig. 4-7. Closer investigation of mass fragmentations indicated that small fragment ions from peak 2 (compound I) and peak 3 (compound II) have similar pattern to that of unlabeled *ent*-cassa-12,15-diene (Fig. 4-8, Fig 4-14). This strongly suggested that compound I and compound II are most likely to be the compounds derived from non-labeled *ent*-cassa-12,15-diene. This result was further validated from selected ion monitoring (SIM) analysis with mass fragmentations distinctive to *ent*-cassa-12,15-diene, such as *m/z* 55, 69, 79, 91 and 105 as shown in Fig.4-9 and Fig.4-15. When SIM analysis with mass fragmentations distinctive to [U-$^{13}C_{20}$] *ent*-cassa-12,15-diene, such as *m/z* 44, 59, 85, 98 and 128, was conducted, small but significant ^{13}C-labeld compound I or compound II were found to exist in peak 2 or peak3, respectively (Fig. 4-10~Fig. 4-12, Fig. 4-15~Fig. 4-18).

Mass spectra of compound I and compound II were checked from known diterpene compounds in the reported literatures. As a result, the mass spectrum of native compound I was identical to those of reference compound, 3α-hydroxy-*ent*-cassadiene, which has been identified as the product of *in vitro* assay with CYP701A8 using *ent*-cassa-12,15-diene as a substrate (Fig. 4-13).[8] The mass spectrum of native compound II was almost identical to those of 3α-hydroxy-*ent*-cassadien-2-one, which has been reported to be produced *in vitro* assay by CYP71Z7 (Fig. 4-19) with *ent*-cassa-12,15-diene as a substrate.[7]

Since no accumulated signals were detected in wild-type, it was consolidated that the existence signal of ^{13}C-compounds in *CYP76M7/M8* RNAi lines are presumably 3α-hydroxy-*ent*-cassadiene and 3α-hydroxy-*ent*-cassadien-2-one (Fig. 4-12; Fig 4-18).

These results suggest that there are two successive intermediates leading to phytocassanes; from *ent*-cassa-12,15-diene to 3α-hydroxy-*ent*-cassadiene (compound I) and 3α-hydroxy-*ent*-cassadien-2-one (compound II), and possible committed enzymes catalyzing each steps can be proposed (Fig. 4-20).

4-3-3. [U-$^{13}C_{20}$] *ent*-cassa-12,15-diene feeding experiment on *CYP71Z7* T-DNA mutant and wild-type rice plants (*O. sativa* L. cv. Dongjin)

It was confirmed that non-labeled phytocassane A, B, C, D and E were accumulated in wild-type leaf disks, but accumulation of phytocassane A, B and D were strongly repressed in *CYP71Z7* T-DNA mutant (Fig. 4-22A; Fig. 4-23). In the feeding experiment, ^{13}C-labeled phytocassane B, C and E were accumulated in wild-type, whereas accumulation of only ^{13}C-phytocassane C and E, but not phytocassane B were found to be drastically increased in *CYP71Z7* T-DNA mutant relative to those of wild-type (Fig. 4-22B; Fig. 4-23). These results provided evidence that CYP71Z7 is responsible for the biosynthesis of phytocassane A, B and D, which are C2-oxygenated type phytocassanes from *ent*-cassa-12,15-diene *in planta*.

In order to clarify the derivatives or ^{13}C-derivatives from *ent*-cassa-12,15-diene or [U-$^{13}C_{20}$] *ent*-cassa12,15-diene in *CYP71Z7* T-DNA mutant in which production of phytocassane A, B and D were inhibited, GC-MS was used for the analysis of unknown intermediates. GC-MS chromatograms from wild-type and *CYP71Z7* T-DNA mutant showed that there were enhanced peak 1(compound-III) and peak 2

(compound IV) in *CYP71Z7* T-DNA mutant fed with [U-$^{13}C_{20}$] *ent*-cassa-12,15-diene compared to that in wild type (Fig. 4-24).

After comparison to authentic 2-deoxyphytocassane A and 1-deoxyphytocassane C mass spectra, GC-MS results suggested that compound III revealed similar spectrum to that of 2-deoxyphytocassane A and only can be detected in peak 1 from *CYP71Z7* T-DNA mutant (Fig. 4-24; Fig. 4-25).

To further clarify this compound III in peak 1, selected ion monitoring (SIM) from unlabeled *ent*-cassa-12,15-diene confirmed compound III is a derivative from *ent*-cassa-12,15-diene (Fig. 4-27). This inference was further verified by ^{13}C-compound III signals detection in *CYP71Z7* T-DNA mutant. In addition, it was difficult to be detected the signals of ^{13}C-compound III in wild-type (Fig. 4-28; Fig. 4-29; Fig. 4-30). These line of evidence strongly suggested that compound III at 17:42 (peak 1) is most likely to be 2-deoxyphytocassane A, and its *in planta* biosynthesis from *ent*-cassa-12,15-diene seems to be evident.

On the other hand, selected ion monitoring from authentic 1-deoxyphytocassane C suggested 1-deoxyphytocassane C was exactly accumulated in peak 2 as the compound IV, and no signals in wild-type was detected (Fig. 4-24; Fig. 4-32). Thus compound IV, which is accumulated in *CYP71Z7* T-DNA mutant, can be confirmed as 1-deoxyphytocassane C. This compound IV was further monitored by selected ion, *m/z* 74, 128, 160, 173 and 201, distinctive fragmentation spectra obtained from [U-$^{13}C_{20}$] *ent*-cassa-12,15-diene. As a result, detected ^{13}C-signal was not strong but clearly be seen in the peak 2 in both wild-type and *CYP71Z7* T-DNA mutant, suggesting that part of compound IV is presumably a derivative of [U-$^{13}C_{20}$] *ent*-cassa-12,15-diene (Fig. 4-34; Fig. 4-35; Fig. 4-36).

Taken together, compound III in peak 1 was confirmed as 2-deoxyphytocassane A and compound IV in peak 2 was confirmed as 1-deoxyphytocassane C.

Hence, it is speculated that compound IV (1-deoxyphytocassane C) is located between compound I (3α-hydroxy-*ent*-cassadiene) and compound III (2-deoxyphytocassane A). On the basis of the findings, a hypothetical pathway of phytocassanes biosynthesis was proposed as shown in Fig. 4-37.

4-3-4. [U-$^{13}C_{20}$] *syn*-pimara-7,15-diene feeding experiment on *CYP76M7/M8* RNAi lines and wild-type rice plants (*O. sativa* L. cv. Nipponbare)

Following [U-$^{13}C_{20}$] *ent*-cassa-12,15-diene feeding experiment, our data also demonstrated momilactones biosynthesis was also strongly repressed in *CYP76M7/M8* RNAi rice leaf disks without lesion mimic (Fig. 4-2). Thus, intermediates on the pathway from *syn*-pimara-12,15-diene to momilactones were investigated. To achieve this end, [U-$^{13}C_{20}$] *syn*-pimara-7,15-diene feeding experiment was performed by application of [U-$^{13}C_{20}$] *syn*-pimara-7,15-diene to *CYP76M7/M8* RNAi plant and wild-type leaf disks (*O. sativa* L. cv. Dongjin). Results from LC-MS/MS analysis revealed that both of momilactone A and [U-$^{13}C_{20}$] momilactone A were strongly repressed in *CYP76M7/M8* RNAi lines relative to those of wild-type, consistent with those of the feeding of [U-$^{13}C_{20}$] *ent*-cassa-12,15-diene (Fig. 4-39).

On the other hand, the extracts were also detected on GC-MS, of which results suggested a new diterpene compound was generated from [U-$^{13}C_{20}$] *syn*-pimara-7,15-diene (Fig. 4-40 Peak 2). The mass spectrum further indicated unknown compound V owned similar molecular ion to those of [U-$^{13}C_{20}$] *syn*-pimara-7,15-diene, but its retention time was quite different from substrate, [U-$^{13}C_{20}$] *syn*-pimara-7,15-diene (Fig. 4-40 Peak 1 and Peak 2). This result suggested the unknown compound V is a related isotopomer of *syn*-pimara-7,15-diene. Furthermore, the amount of unknown compound V can be strongly accumulated in wild-type, but not in the *CYP76M7/M8* RNAi (Fig. 4-40). This suggests that this unknown compound V would be possible product of CYP76M7/M8 and it could be a dead end product in wild-type rice plants due to the apparent accumulation.

4-4. Discussion

Established feasible feeding methods described in former chapter, to be a platform to feed compounds dissolved in an organic solvent to rice plants, were employed to investigate unknown intermediates on the route of phytocassanes and momilactones biosynthesis. Up to date, *ent*-cassa12,15-diene and *syn*-pimara-7,15-diene has been proposed as an intermediate on the pathway to phytocassanes and momilactones *in vitro*.[1,6,7] On the basis of *in vitro* and *in vivo* analysis, CYP76M7/M8 and CYP71Z7 have been shown at first to be responsible for the phytocassanes biosynthesis.[1,7] However, CYP76M8 has been found to catalyze hydroxylation with a wide range of substrates, including *syn*-pimara-7,15-diene, which is the precursor for momilactones biosynthesis.[2] Thus it became one of the focus points to investigate possible pathways or intermediates in *CYP76M7/M8* double knock-down lines and *CYP71Z7* T-DNA mutant when fed with [U-$^{13}C_{20}$] *ent*-cassa12,15-diene and [U-$^{13}C_{20}$] *syn*-pimara-7,15-diene in the feeding approach.

According to the results from LC-MS/MS and GC-MS, all phytocassanes and [U-$^{13}C_{20}$] phytocassanes biosynthesis were strongly inhibited in *CYP76M7M8* RNAi lines (Fig. 4-4; Fig. 4-5). 3α-hydroxy-*ent*-cassadiene and 3α-hydroxy-*ent*-cassadien-2-one have been confirmed as two intermediates on the route of phytocassanes in rice plants (Fig. 4-11; Fig. 4-13; Fig. 4-17; Fig. 4-19; Fig. 4-20). Data in this study supported C3α-hydroxylation of *ent*-cassa-12,15-diene seemed to be first reaction happened *in planta* from *ent*-cassa-12,15-diene. According to *in vitro* assay, CYP701A8 may be responsible for this conversion in rice plants (Fig. 4-13). [8] Furthermore, Kitaoka *et al*. has confirmed that CYP71Z7 can catalyze for conversion from *ent*-cassa-12,15-diene to 3α-hydroxy-*ent*-cassadien-2-one *in vitro* (Fig. 4-19).[7] However, they mentioned in their paper that efficiency of this reaction was very low and CYP71Z7 poorly recognized *ent*-cassa-12,15-diene as a substrate[7]. Thus, it is speculated that *ent*-cassa-12,15-diene is not a true substrate of CYP71Z7 *in planta.* Notably, 3α-hydroxy-*ent*-cassadien-2-one was detected as a native compound II in *CYP76M7M8* RNAi lines under [U-$^{13}C_{20}$] *ent*-cassa-12,15-diene feeding (Fig. 4-15; Fig. 4-17; Fig. 4-18). If *ent*-cassa-12,15-diene is not the true substrate of CYP71Z7, one promising hypothesis should be that 3α-hydroxy-*ent*-cassadiene

(compound I) is the true substrate of CYP71Z7 producing 3α-hydroxy-*ent*-cassadien-2-one (compound II) in rice plant. To confirm this inference, it is needed more critical evidence from *in vitro* assay, such as the reaction of 3α-hydroxy-*ent*-cassadiene with CYP71Z7. Together, it can be speculated that, in rice plant, C2α-hydroxylation of *ent*-cassa-12-15-diene is the process that happens after the C3α-hydroxidation, and 3α-hydroxy-*ent*-cassadiene further oxidized into 1-deoxyphytocassane C and 2-deoxyphytocassane A. The end products structure of phytocassanes suggested that 3α-hydroxy-*ent*-cassadien-2-one could be the precursor of phytocassane D (Fig. 4-37).

Following [U-$^{13}C_{20}$] *ent*-cassadiene feeding experiment in *CYP76M7/M8* RNAi lines, *CYP71Z7* T-DNA mutant feeding experiment was also performed (Fig. 4-21). The results have indicated that function of the CYP71Z7 is located on the biosynthetic route to phytocassane (A, B and D). In *CYP71Z7* T-DNA mutant, phytocassane (C and E) or [U-$^{13}C_{20}$] phytocassane (C and E) were accumulated in a higher level than those of wild-type (Fig. 4-22; Fig. 4-23). It is plausible that C2-hydroxylation is necessary for the biosynthesis of phytocassane (A, B and D), and C3-hydroxylation is required for the production of all types of phytocassanes.[2, 7] Therefore, the role of CYP71Z7 was clarified on the pathway to phytocassane (A, B and D) by the feeding approach as well.

Furthermore, on the process of feeding experiment, possible intermediates of phytocassanes, 1-deoxyphytocassane C and 2-deoxyphytocassane A, were found to be accumulated in *CYP71Z7* T-DNA mutant (Fig.4-25; Fig.4-27; Fig. 4-31; Fig. 4-33.). Hence, it is anticipated that [U-$^{13}C_{20}$] 1-deoxyphytocassane C and [U-$^{13}C_{20}$] 2-deoxyphytocassane A can also be detected on GC-MS as the intermediates. By using SIM from [U-$^{13}C_{20}$] *ent*-cassa-12,15-diene, [U-$^{13}C_{20}$] 2-deoxyphytocassane A can be traced in peak 2 from *CYP71Z7* T-DNA mutant, and no signals in wild-type (Fig. 4-29; Fig. 4-30). This made us convince [U-$^{13}C_{20}$] 2-deoxyphytocassane A was generated and accumulated in *CYP71Z7* T-DNA mutant. The conversion assay *in vitro* should be performed to confirm this enzyme-substrate recognition. We may clarify possible products from 2-deoxyphytocassane A. Furthermore, low level of [U-$^{13}C_{20}$] 1-deoxyphytocassane C can be monitored and detected in both of *CYP71Z7* T-DNA mutant and wild-type (Fig. 4-35; Fig. 4-36). This suggested [U-$^{13}C_{20}$] 1-deoxyphytocassane C can be biosynthesized, but difficult to be accumulated in *CYP71Z7* T-DNA mutant or wild-type. It can be speculated that 1-deoxyphytocassane C locates between 3α-hydroxy-*ent*-cassadiene and 2-deoxyphytocassane A. It might not be the bottleneck compound for further phytocassanes conversion, but it must be the intermediate on the pathway to phytocassanes. Thus the hypothetical pathway of phytocassanes biosynthesis was proposed (Fig. 4-37). Some unknown enzymes remain ambiguous and need to be further investigated.

In an alternative elucidation of the biosynthetic pathway of phytoalexins, the promising intermediate of momilacotones, [U-$^{13}C_{20}$] *syn*-pimaradiene, was subjected to feeding in the phytocassane defective *CYP76M7/M8* RNAi line. In chapter 3, we have clarified [U-$^{13}C_{20}$] *syn*-pimara-7,15-diene can be converted to [U-$^{13}C_{20}$] momilactones in leaf disks. Thus, in this chapter, if the decrease in momilactones

level in *CYP76M7/M8* RNAi would be caused by insufficient biosynthetic flow from *syn*-pimaradiene in the CYP76M7/M8 was verified (Fig. 4-1; Fig. 4-2). LC-MS/MS result showed that accumulations of [U-$^{13}C_{20}$] momilacones decreased in the RNAi line compared to that in wild-type, consistent with the accumulation levels of endogenously produced momilactones.

Unexpectedly, GC-MS result showed a fully ^{13}C-labeled compound V (peak 2), which is observed in both of wild type and *CYP76M7/M8* RNAi lines, but obviously predominant in wild-type (Fig. 4-40). Small fragment ion pattern of Peak 2 and its precursor ion (M^+, 292) indicated that this unknown compound-V should be an isotopomer of [U-$^{13}C_{20}$] *syn*-pimara-7,15-diene (Fig. 4-40). According to previous report, CYP76M8 have strong kinetic affinity to *syn*-pimara-7,15-diene and is responsible for the C6β-hydroxylation of *syn*-pimara-7,15-diene.[7] . These evidences suggested that *syn*-pimara-7,15-diene or its derivatives were catalyzed *in planta* as one of the substrates of CYP76M8 in the biosynthetic pathway of diterpenoid phytoalexin. Since compound V is only accumulated in wild-type plant and disappeared in *CYP76M7/M8* RNAi lines, this compound is thought to be a product catalyzed by *CYP76M7/M8*. It has been reported that CYP76M7 carries out the C2α-hydroxylation of *ent*-cassa-12,15-diene.[1] Therefore, *syn*-pimara-7,15-diene would not be the *in planta* substrate of CYP76M7. Further deep observation will be required to disclose where compound V is placed in the pathway from *syn*-pimara-7,15-diene.

4-5. Brief Summary

Taken together, in this chapter, accumulations of unknown metabolites were found by using a combined analysis of LC-MS/MS and GC-MS. Some unknown compounds (I to V) were detected and clarified in *CYP76M7/M8* double knock down lines and *CYP71Z7* T-DNA mutant under [U-$^{13}C_{20}$] *ent*-cassa-12,15-diene and [U-$^{13}C_{20}$] *syn*-pimara-7,15-diene feeding. The feeding method established in this thesis provided a new insight and potential in discovery of intermediates of ditepenoid phytoalexins in rice plants

4-6. Figures

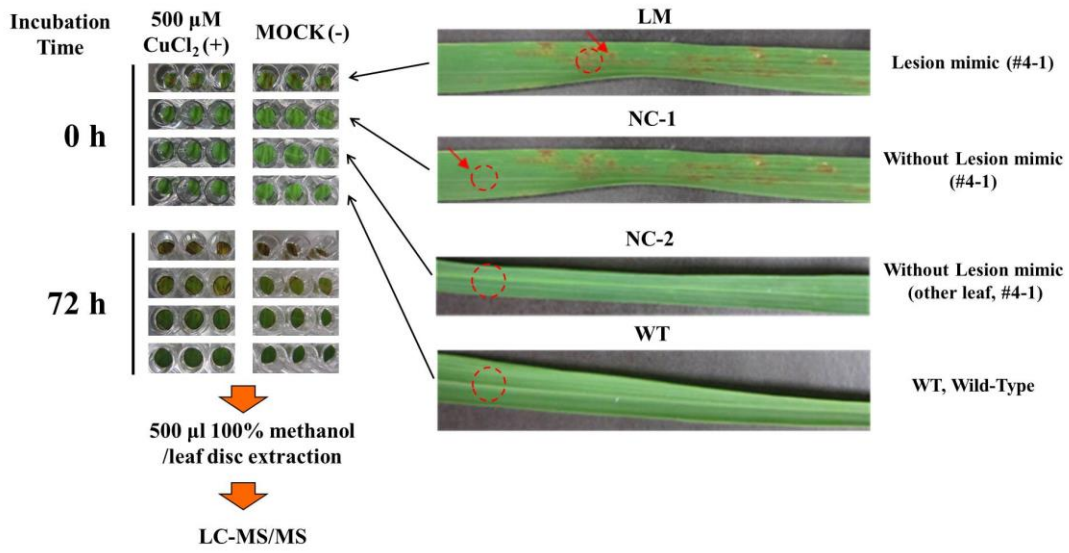

Figure 4-1. The phenotype of *CYP76M7/M8* RNAi lines (#4-1) and wild-type leaves (*O. sativa* L. cv. Nipponbare)

LM, The region on leaf with lesion mimic; **NC-1,** The region on leaf without lesion mimic; **NC-2,** Other leaves without lesion mimic; **WT,** wild-type leaves; (LM, NC-1, NC-2 from the same rice plant); All leaf disks were treated with 500 µM $CuCl_2$ solution.

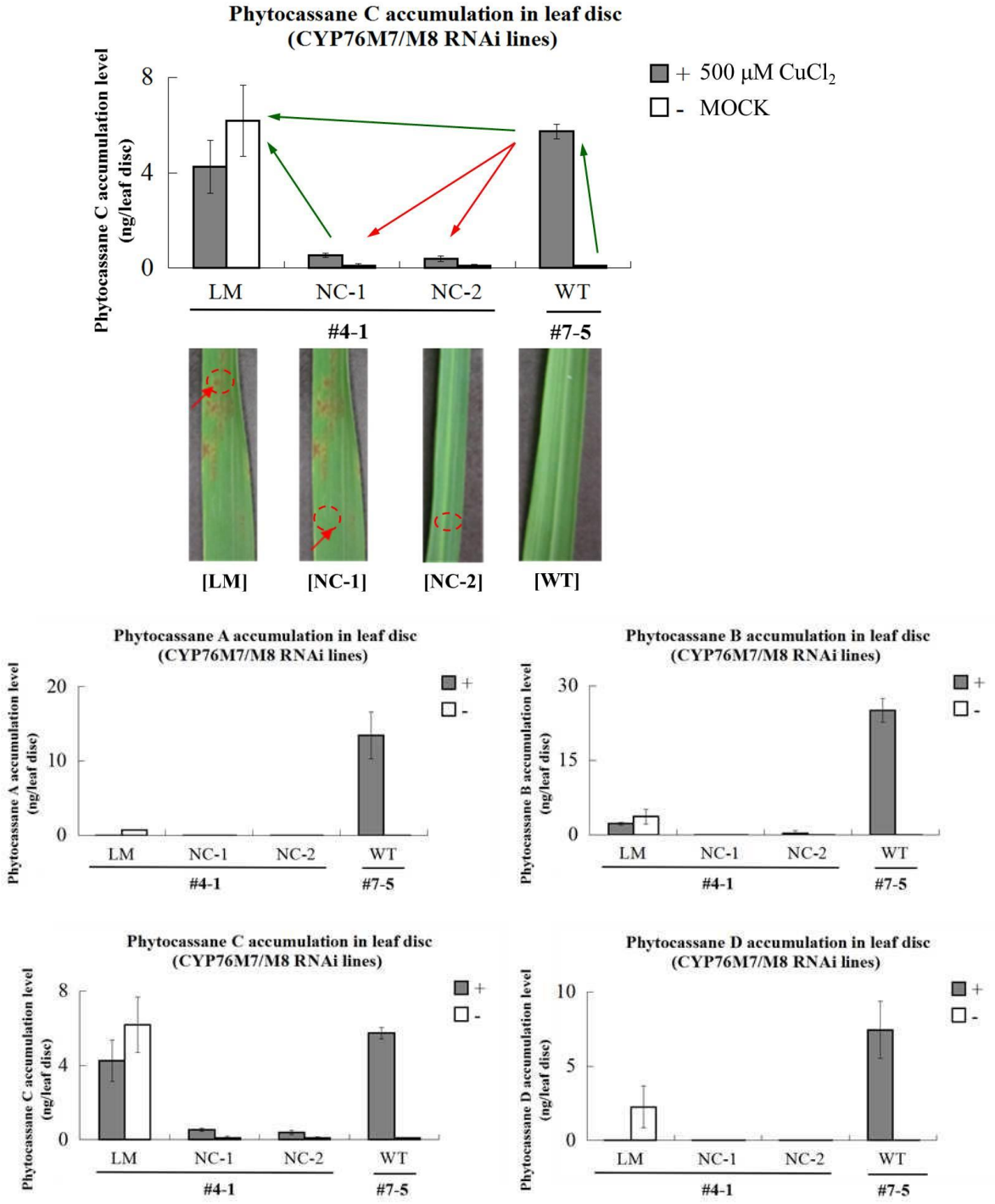

Figure 4-2. Phytoalexins accumulation level in different region of *CYP76M7/M8* RNAi lines and wild-type rice leaves (*O. sativa* L. cv. Nipponbare)

LM, The region on leaf with lesion mimic; **NC-1,** The region on leaf without lesion mimic; **NC-2,** Leaf disks without lesion mimic; **WT,** wild-type leaf disks; **+,** 500 μM $CuCl_2$ treatment; **-,** H_2O; **Red arrow** indicate the decrease of phytocassanes and momilactones accumulation level in the region without lesion mimic on *CYP76M7/M8* RNAi lines; **Green arrow** indicate the increase of phytocassanes and momilactones accumulation level in the region with lesion mimic on *CYP76M7/M8* RNAi lines. 5 μl of each extract was subjected to LC-ESI-MS/MS

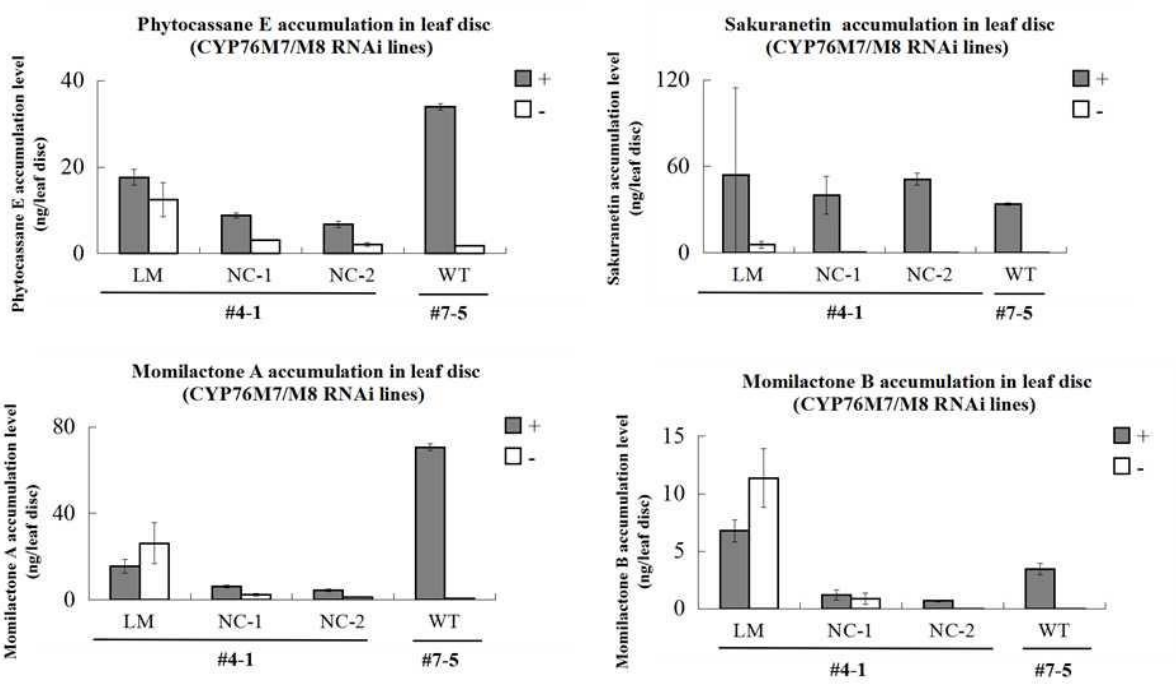

Figure 4-2. Continued

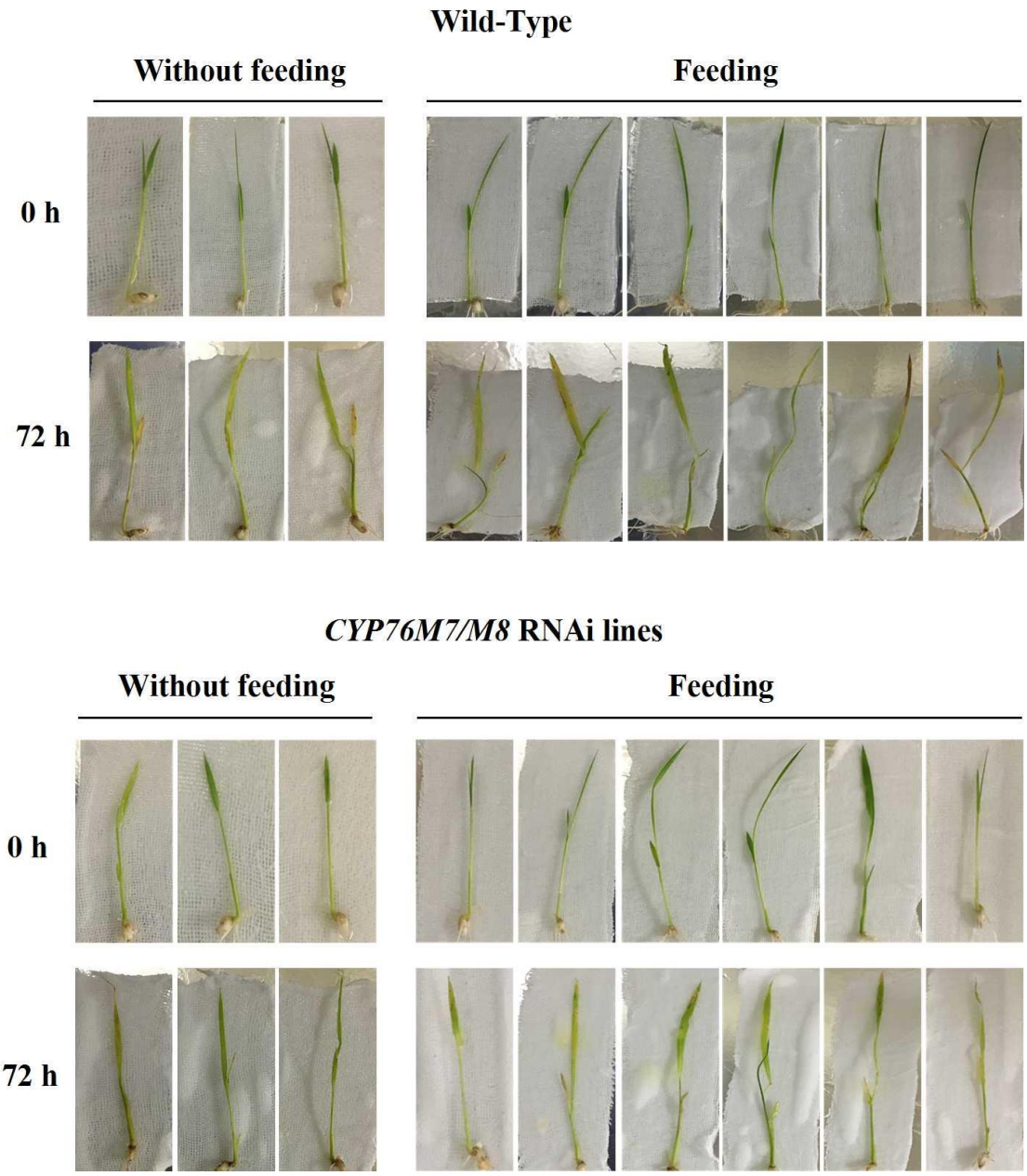

Figure 4-3. The application of [U-$^{13}C_{20}$] *ent*-cassa-12,15-diene to 6-day old *CYP76M7/M8* RNAi and wild-type rice seedlings (*O. sativa* L. cv. Nipponbare)
Without feeding, each rice plant was treated with 9 µl of 100% ethanol, n=3; **Feeding,** 9 µg of [U-$^{13}C_{20}$] *ent*-cassa-12,15-diene was applied to each rice plant, n=6;

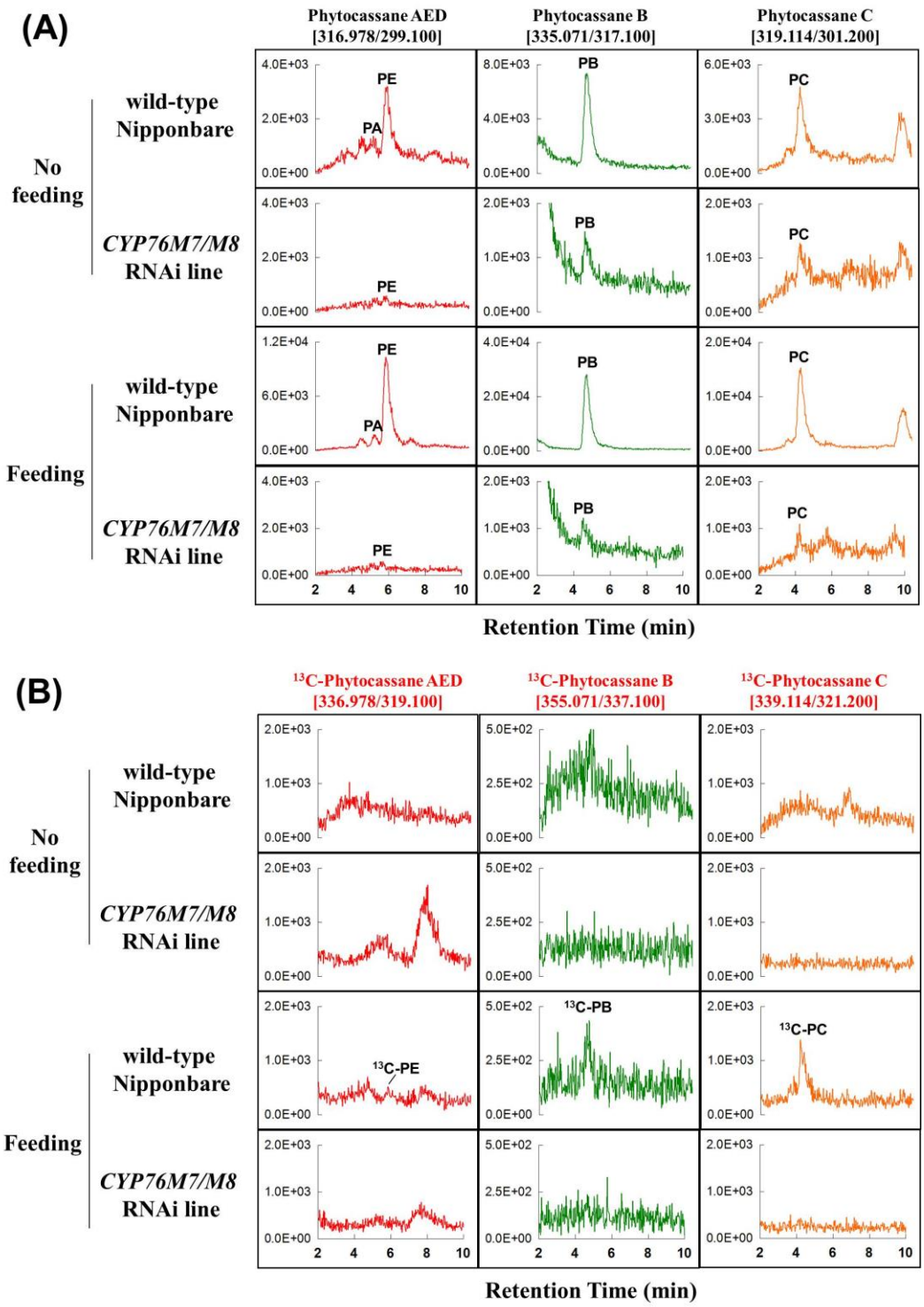

Figure 4-4. Phytocassanes and [U-$^{13}C_{20}$]phytocassanes accumulation level in 6-day old rice shoot (*O. sativa* L. cv. Nipponbare) with 9 µg of [U-$^{13}C_{20}$] *ent*-cassa-12,15-diene feeding and 500 µM $CuCl_2$ elicitation in cheesecloths.

A, Unlabeled phytocassane (A-E) analysis on LC-ESI-MS/MS. **PA,** Phytocassane A; **PB,** Phytocassane B; **PC,** Phytocassane C; **PE,** Phytocassane E. **B,** [U-$^{13}C_{20}$] phytocassane (A-E) analysis on LC-ESI-MS/MS. **^{13}C-PB**, [U-$^{13}C_{20}$] phytocassanes B; **^{13}C-PC**, [U-$^{13}C_{20}$] phytocassane C, **^{13}C-PE,** [U-$^{13}C_{20}$] phytocassane E. 5 µl of each extract was analyzed.

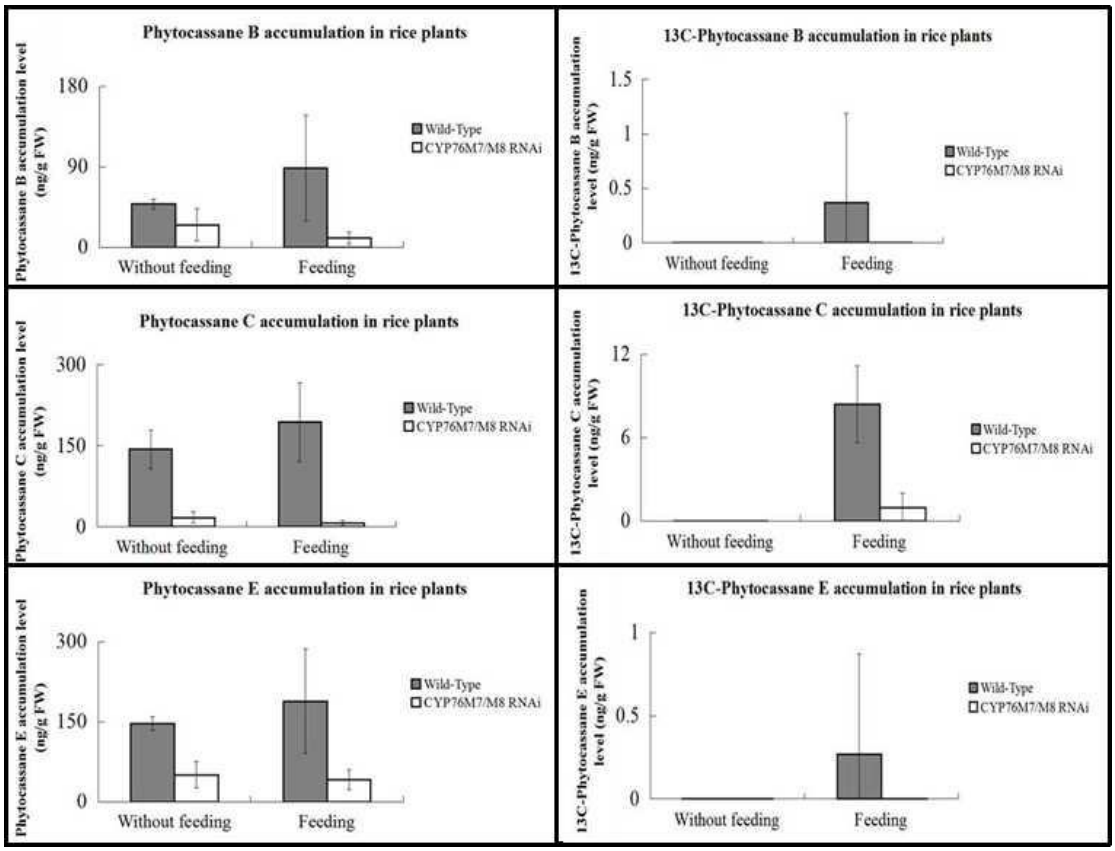

Figure 4-5. Phytocassane (B, C and E) and [U-$^{13}C_{20}$] phytocassane (B, C and E) accumulation level in *CYP76M7/M8* RNAi rice plants (*O. sativa* L. cv. Nipponbare)

Left pane, unlabeled phytocassane (B, C and E) accumulation level in wild-type and *CYP76M7/M8* RNAi lines**; Right pane,** [U-$^{13}C_{20}$] phytocassane (B, C and E) accumulation level in wild-type and *CYP76M7/M8* RNAi lines. Without feeding, n=3; Feeding, n=6.

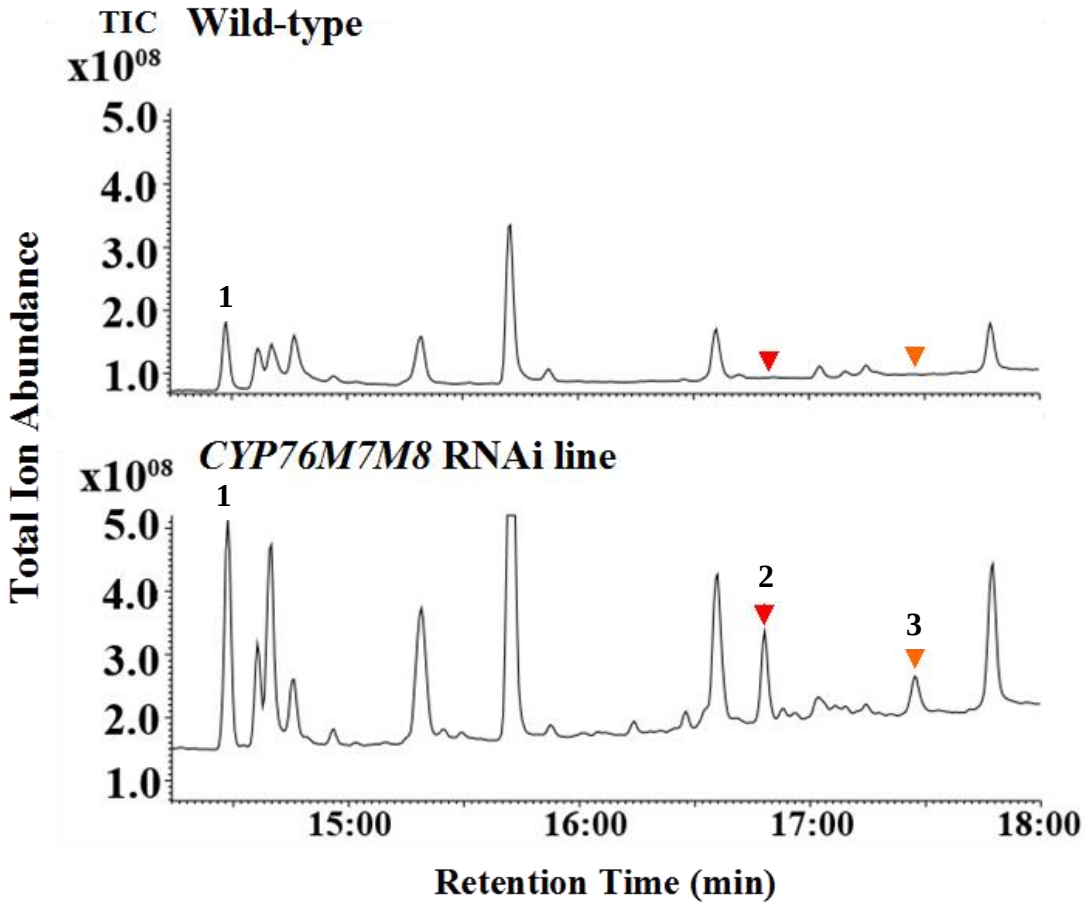

Figure 4-6. GC-MS chromatogram of extract from wild-type and *CYP76M7M8* RNAi lines.

1, [U-$^{13}C_{20}$] *ent*-cassa-12,15-diene detection at retention time, 14:29; **2,** peak 2 detection at retention time, 16:48; **3,** peak 3 detection at retention time, 17:28

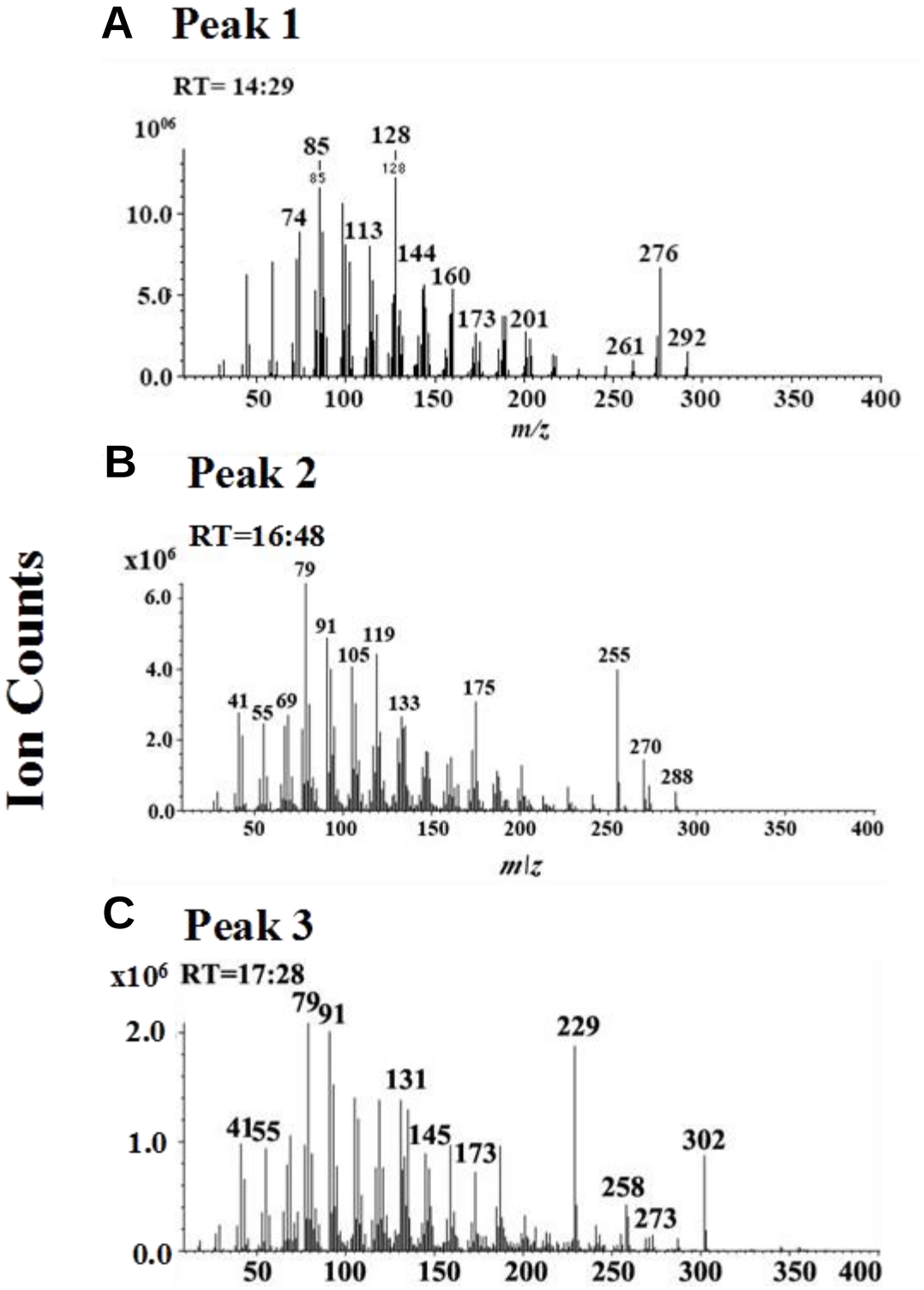

Figure 4-7. Mass spectra for peak 1, peak 2 and peak 3.

A, mass spectra for peak 1 (Substrate, [U-$^{13}C_{20}$] *ent*-cassa-12,15-diene); **B,** mass spectra for peak 2 (unknown compound I); **C,** mass spectra for peak 3 (unknown compound II)

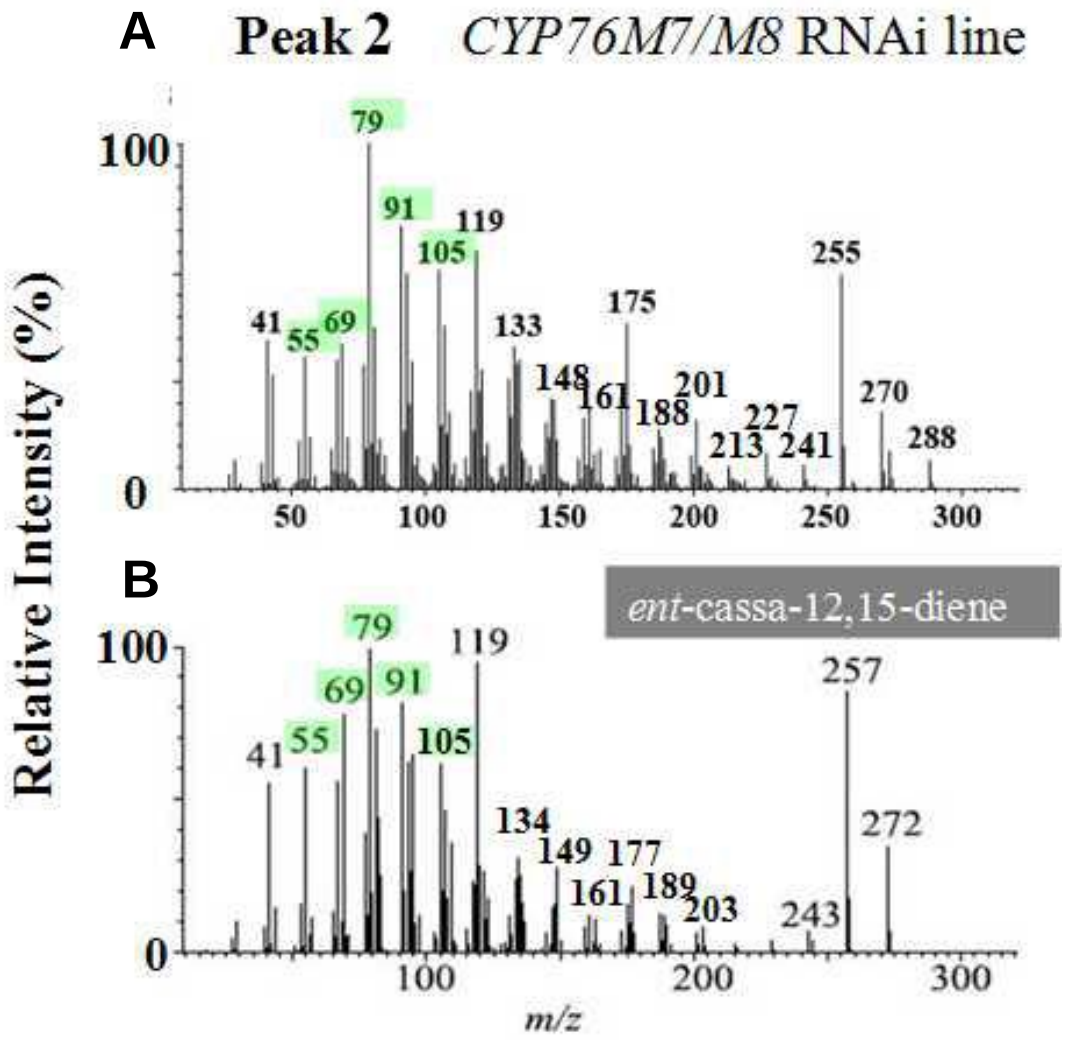

Figure 4-8. Mass spectra for peak 2 and unlabeled *ent*-cassa-12,15-diene.
A, mass spectra for peak 2; B, mass spectra for unlabeled *ent*-cassa-12,15-diene; **Green area,** selected ion from unlabeled *ent*-cassa-12,15-diene

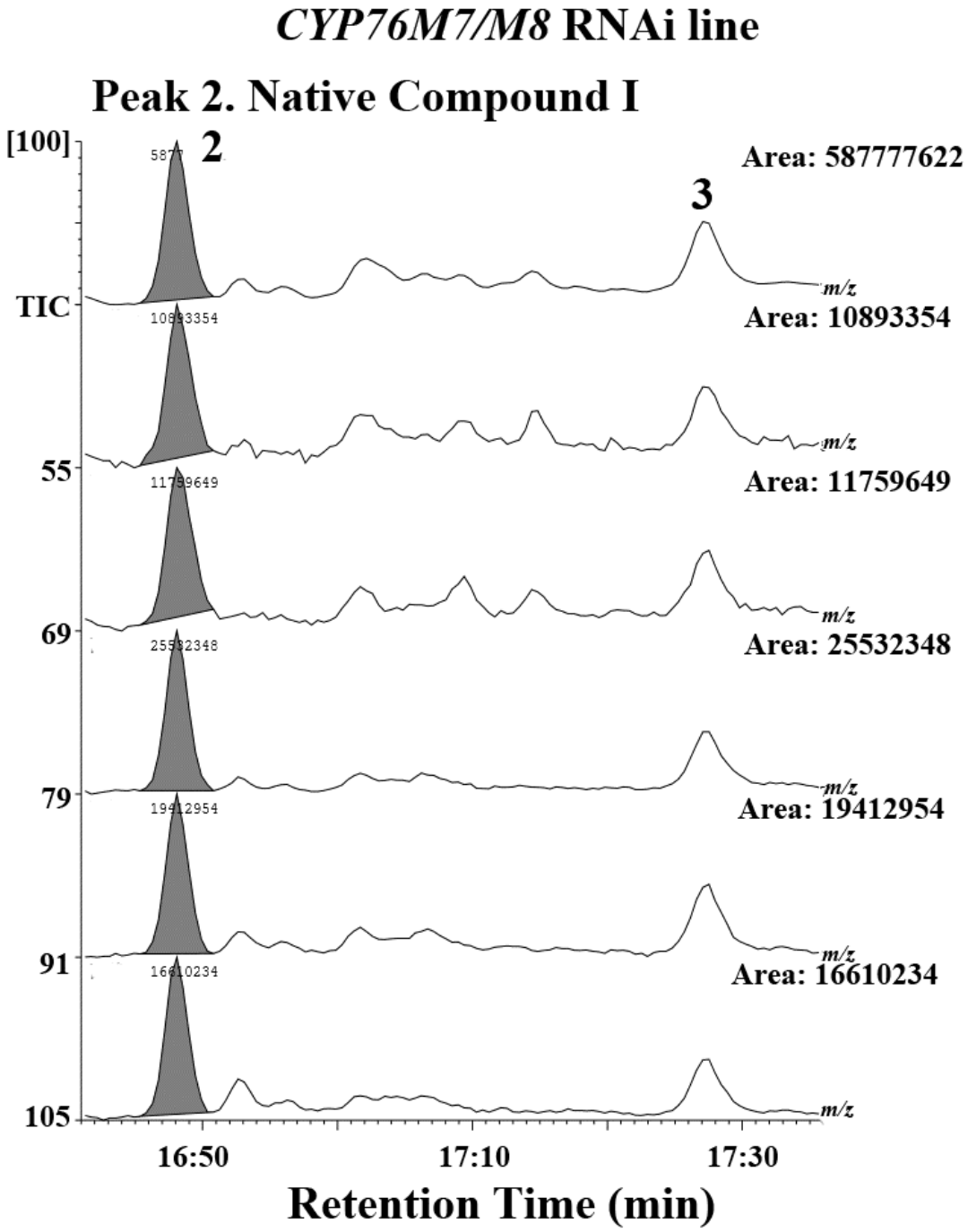

Figure 4-9. Selected ion from unlabeled *ent*-cassa-12,15-diene for monitoring native compound I in peak 2.

Compound I was monitored by selected ion, 55, 69, 79, 91 and 105, from unlabeled *ent*-cassa-12,15-diene.

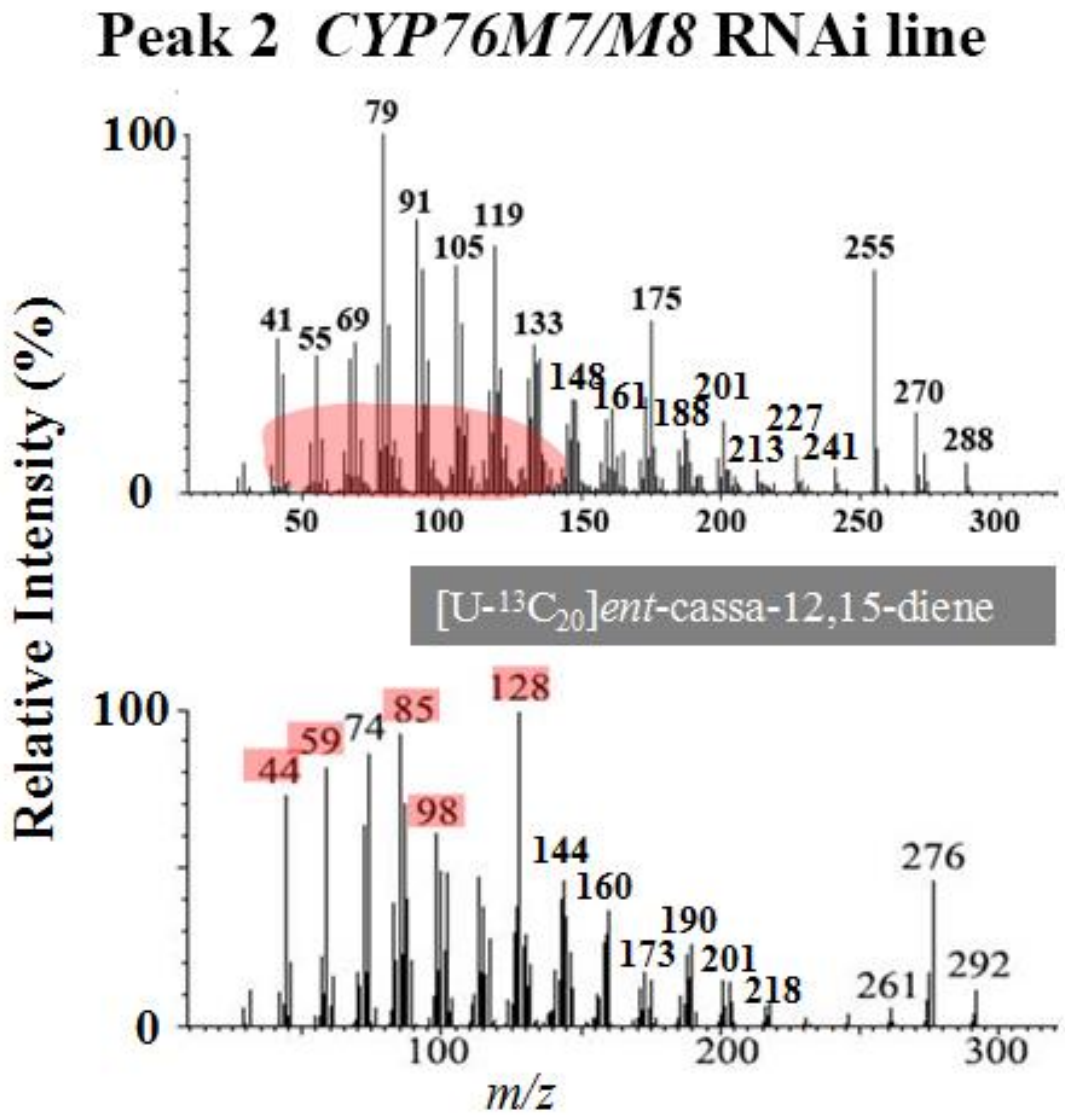

Figure 4-10. Mass spectra for peak 2 and [U-$^{13}C_{20}$] *ent*-cassa-12,15-diene
Red area, selected ion from [U-$^{13}C_{20}$] *ent*-cassa-12,15-diene for monitoring ^{13}C-compound I

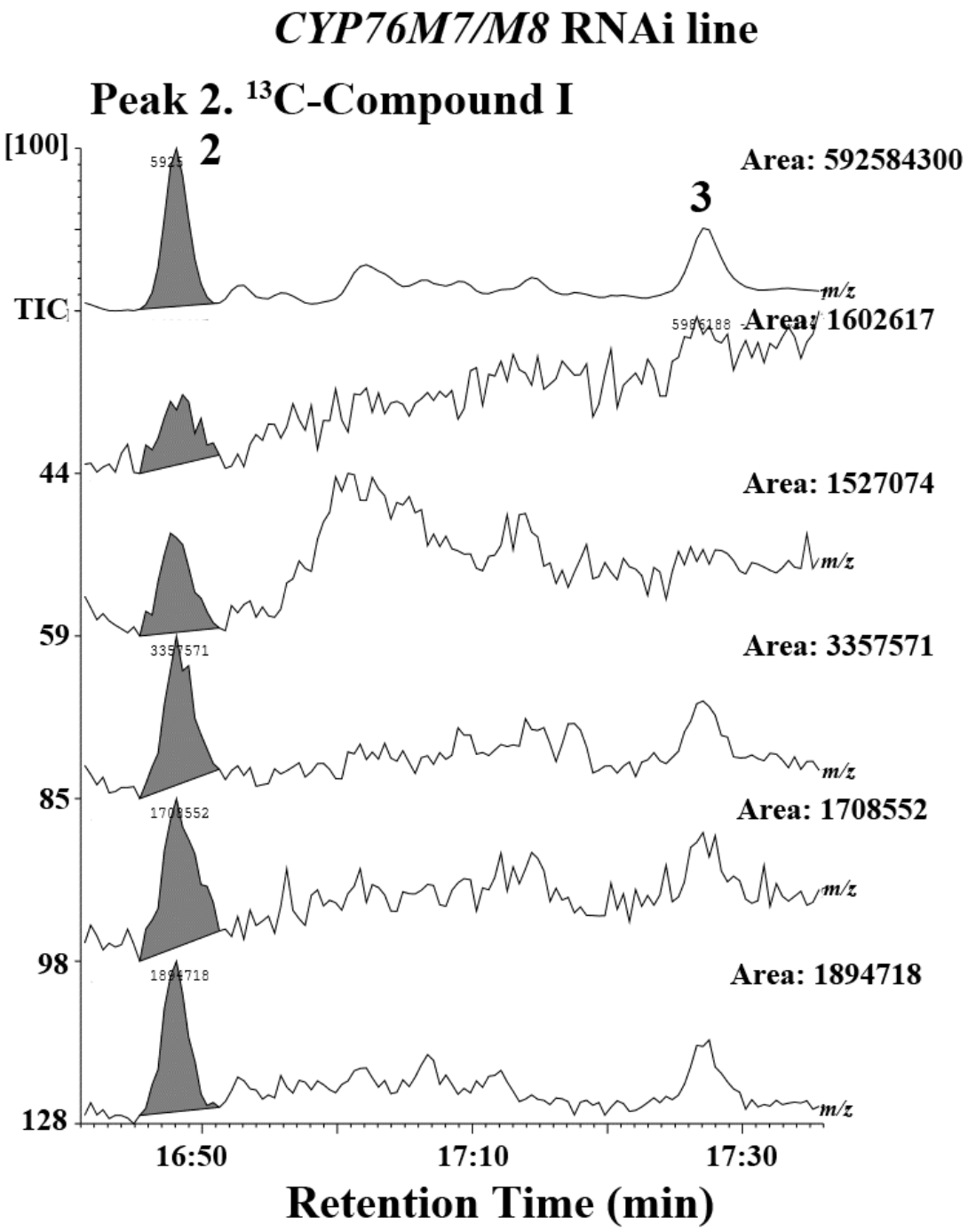

Figure 4-11. GC-MS selected ion monitoring for tracing ^{13}C-compound I in Peak 2 from *CYP76M7M8* RNAi lines.

^{13}C-compound I was monitored by selected ion, 44, 59, 85, 98 and 128, from [U-$^{13}C_{20}$] *ent*-cassa-12,15-diene.

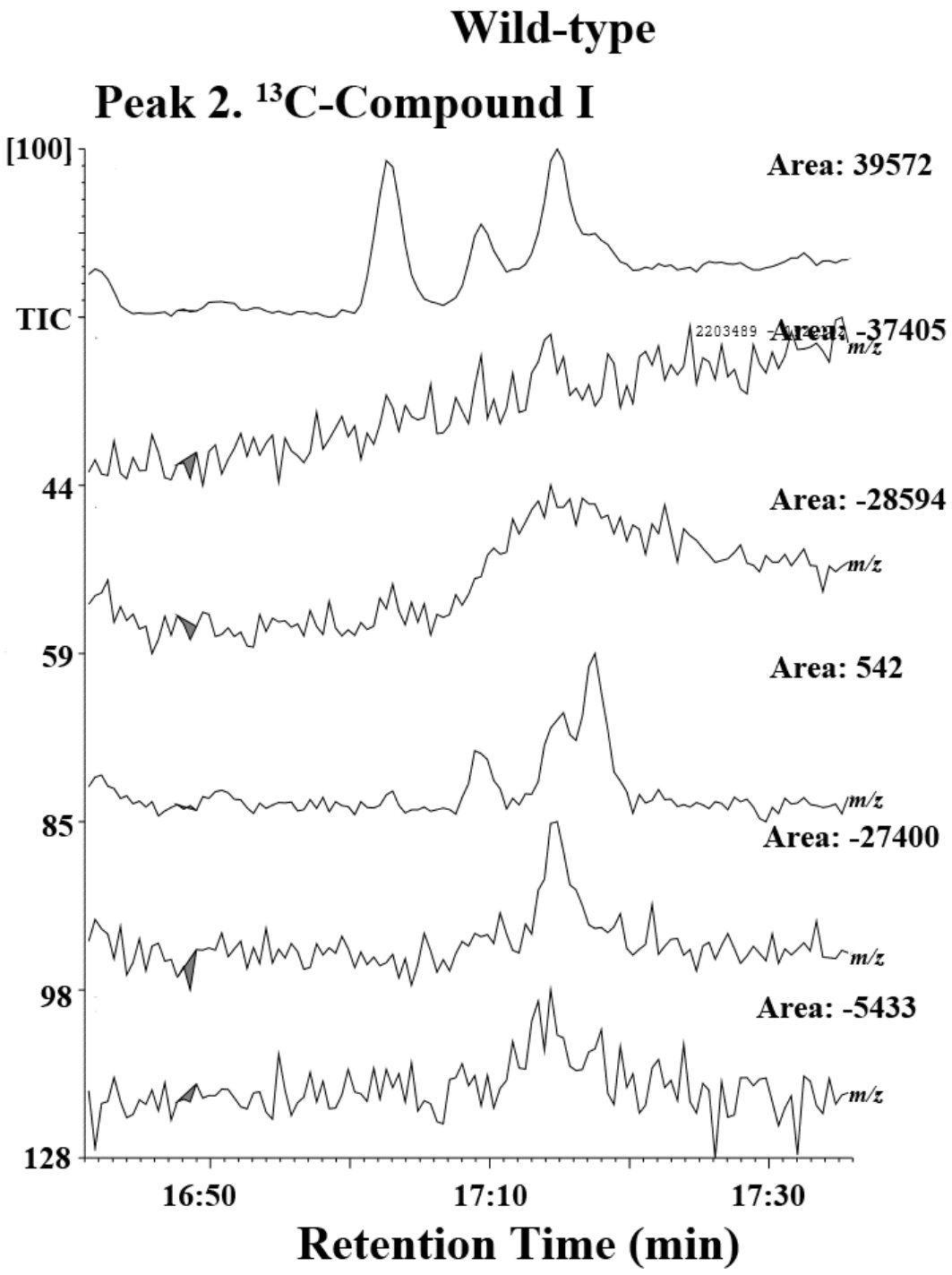

Figure 4-12. GC-MS selected ion monitoring for tracing ^{13}C-compound I in wild-type.

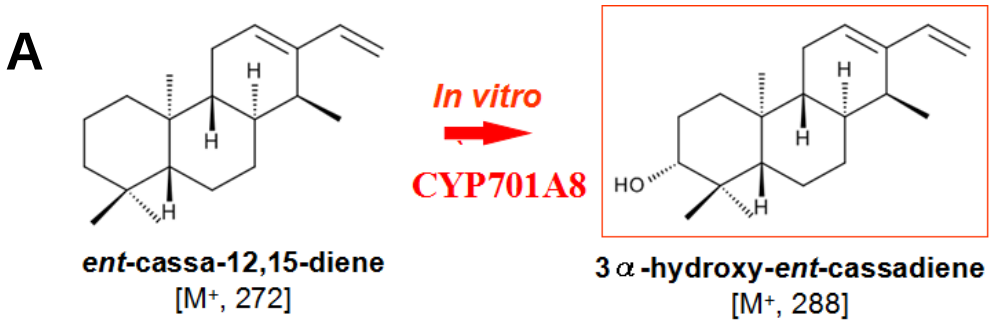

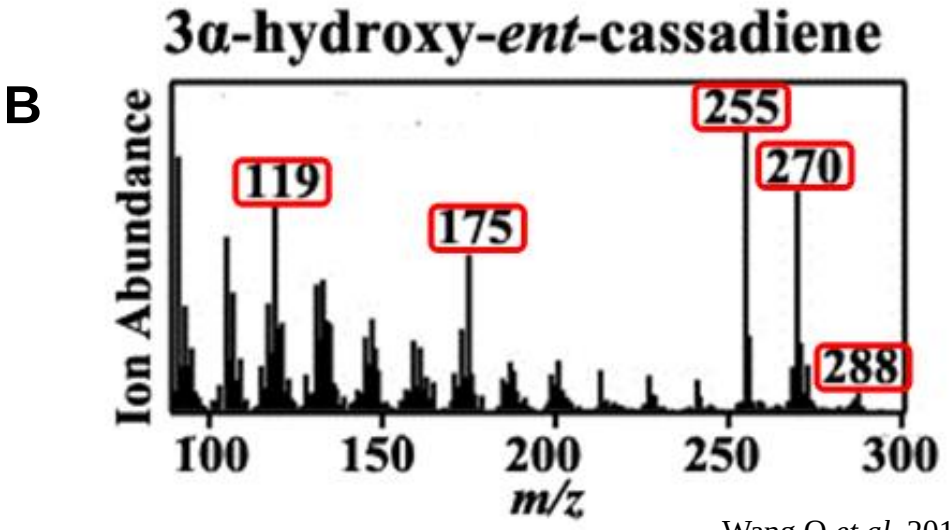

Wang Q *et al*. 2012

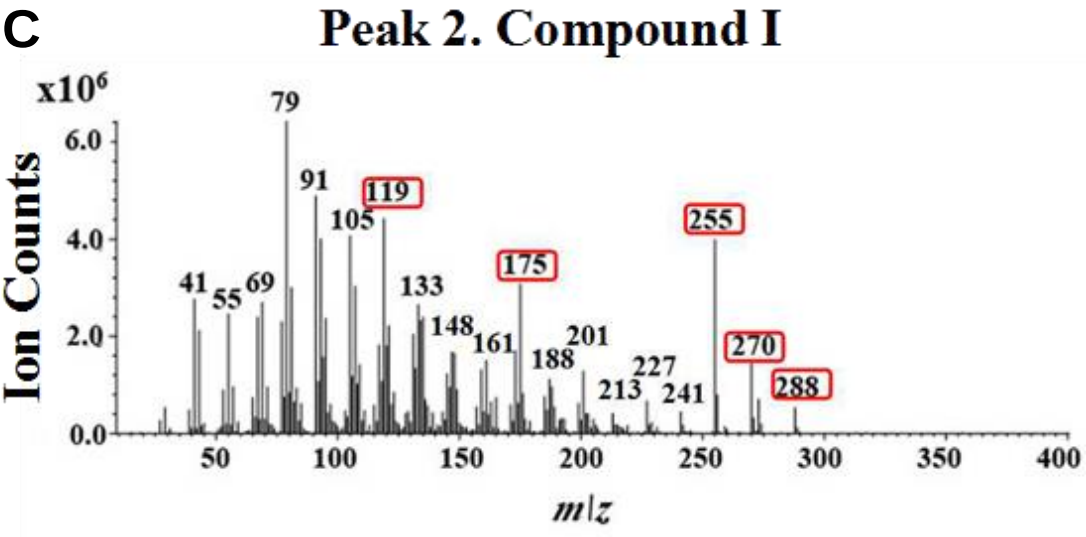

Figure 4-13. The comparison of mass spectra between unknown compound I and a reference compound, 3α-hydroxy-*ent*-cassadiene.

A, 3α-hydroxy-*ent*-cassadiene was produced from *ent*-cassa-12,15-diene *in vitro* assay. CYP701A8 responsible for this reaction.[8] **B,** mass spectra from reference compound, 3α-hydroxy-*ent*-cassadiene. [8] **C,** inquired compound I from *CYP76M7M8* RNAi line. **Red frame,** identical mass spectra between reference compound and inquired compound I

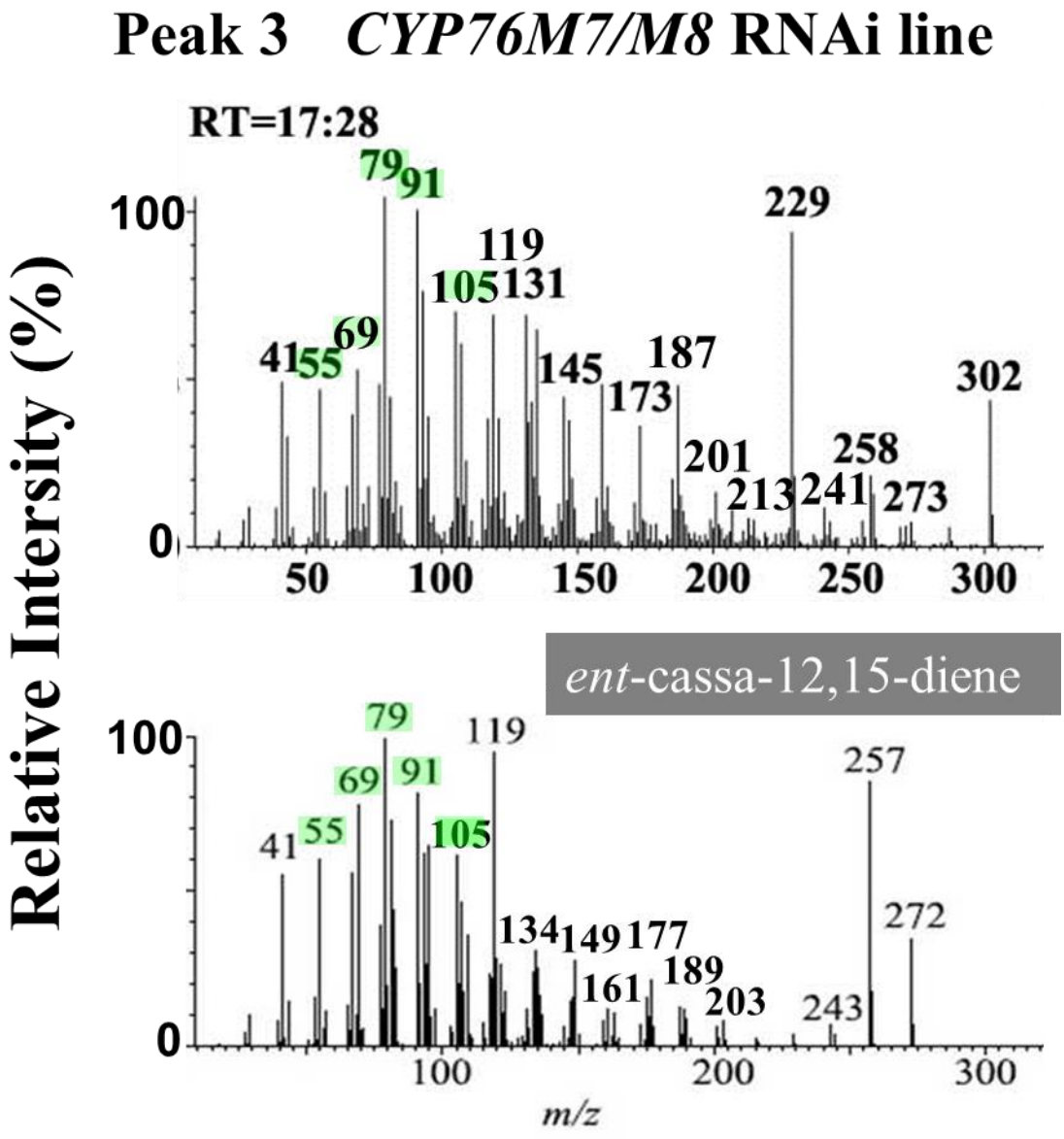

Figure 4-14. Mass spectra for peak 3 and unlabeled *ent*-cassa-12,15-diene.
A, mass spectra for peak 3; B, mass spectra for unlabeled *ent*-cassa-12,15-diene; **Green area,** selected ion from unlabeled *ent*-cassa-12,15-diene

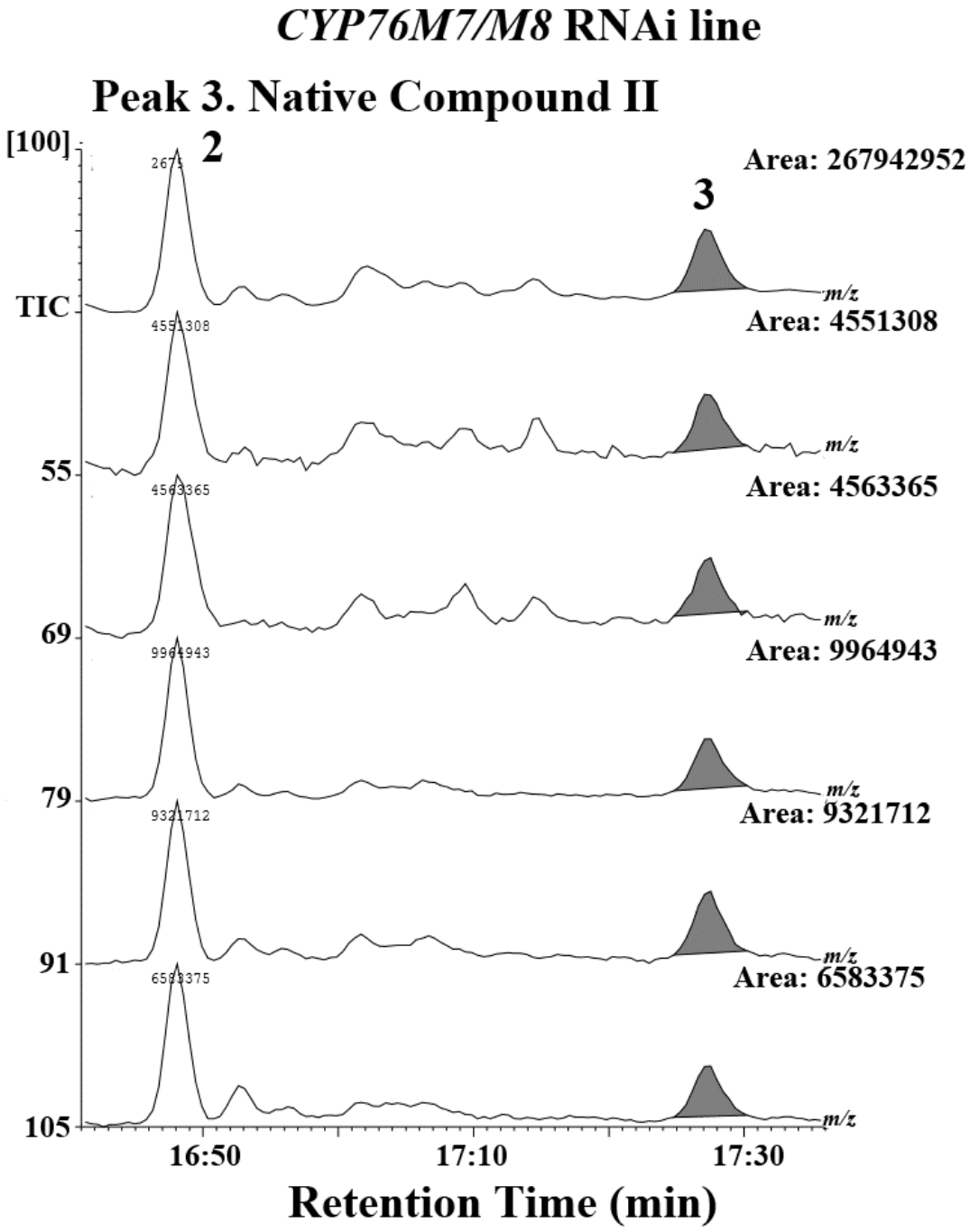

Figure 4-15. Selected ion from unlabeled *ent*-cassa-12,15-diene for monitoring native compound II in peak 3.

Native Compound II was monitored by selected ion, 55, 69, 79, 91 and 105, from unlabeled *ent*-cassa-12,15-diene.

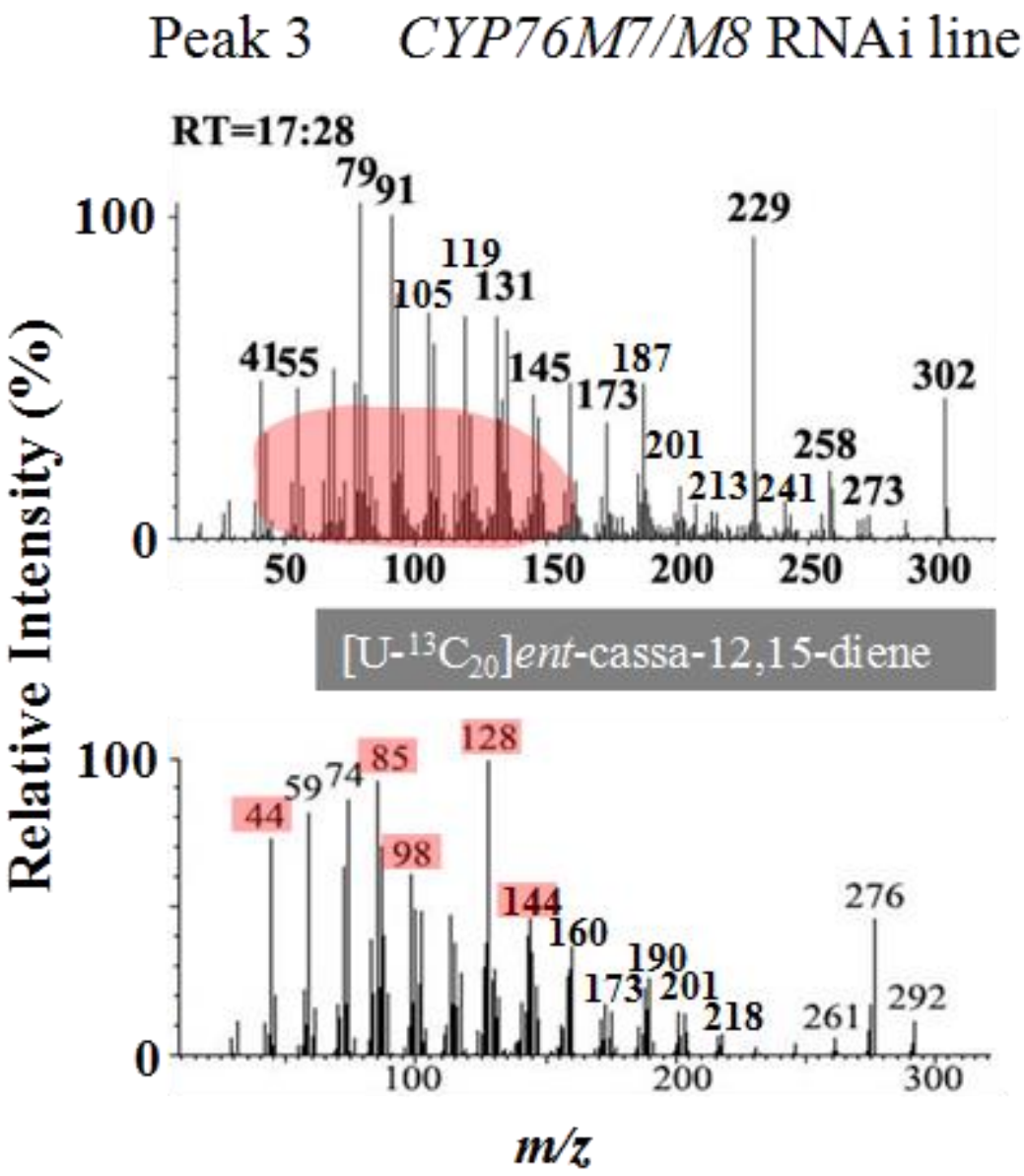

Figure 4-16. Mass spectra for peak 3 and [U-$^{13}C_{20}$] *ent*-cassa-12,15-diene
Red area, selected ion from [U-$^{13}C_{20}$] *ent*-cassa-12,15-diene for monitoring ^{13}C-compound II in peak 3.

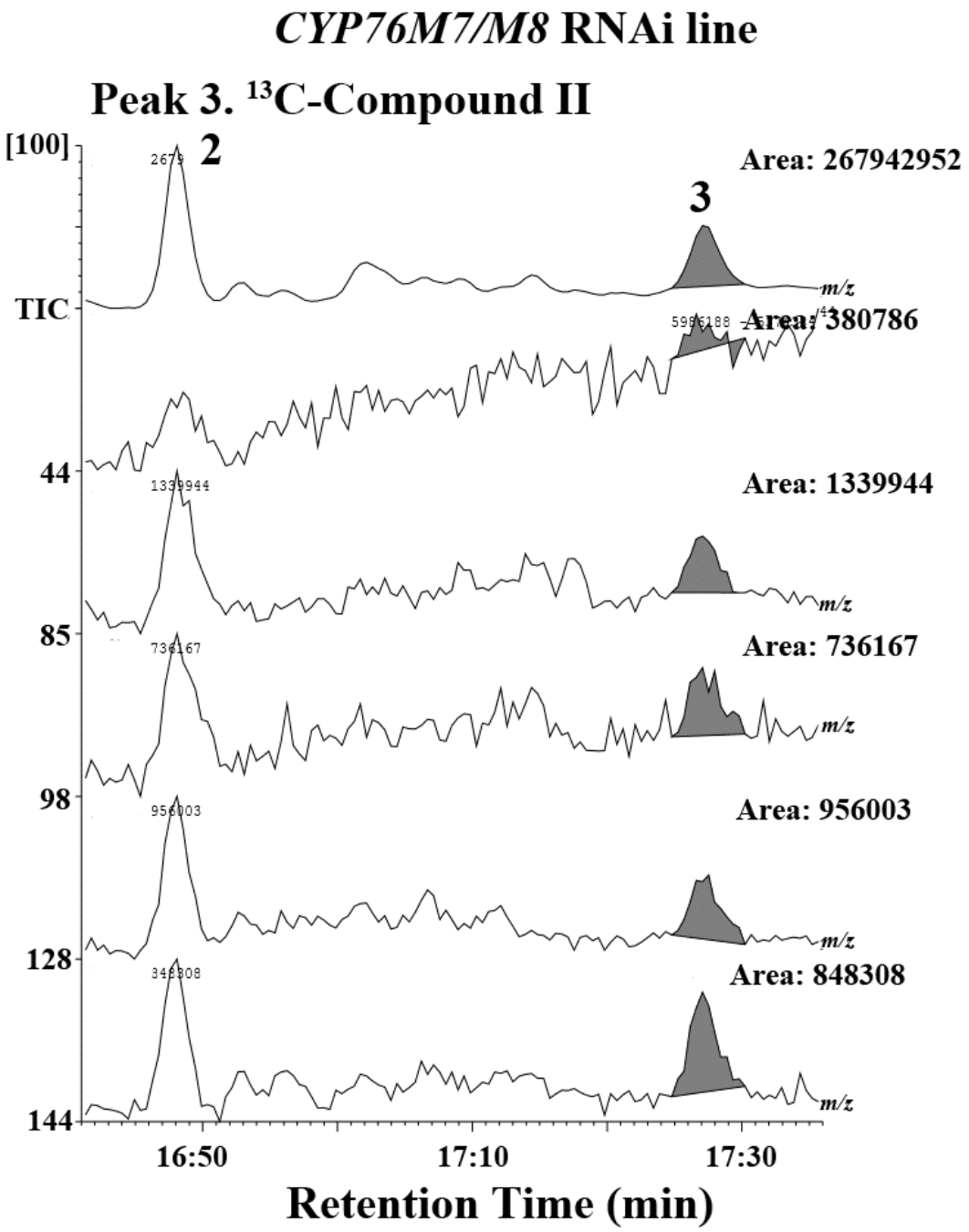

Figure 4-17. GC-MS selected ion monitoring for tracing ^{13}C-compound II in Peak 3 from *CYP76M7M8* RNAi lines.

^{13}C-compound II was monitored by selected ion, 44, 85, 98, 128 and 144 from [U-$^{13}C_{20}$] *ent*-cassa-12,15-diene.

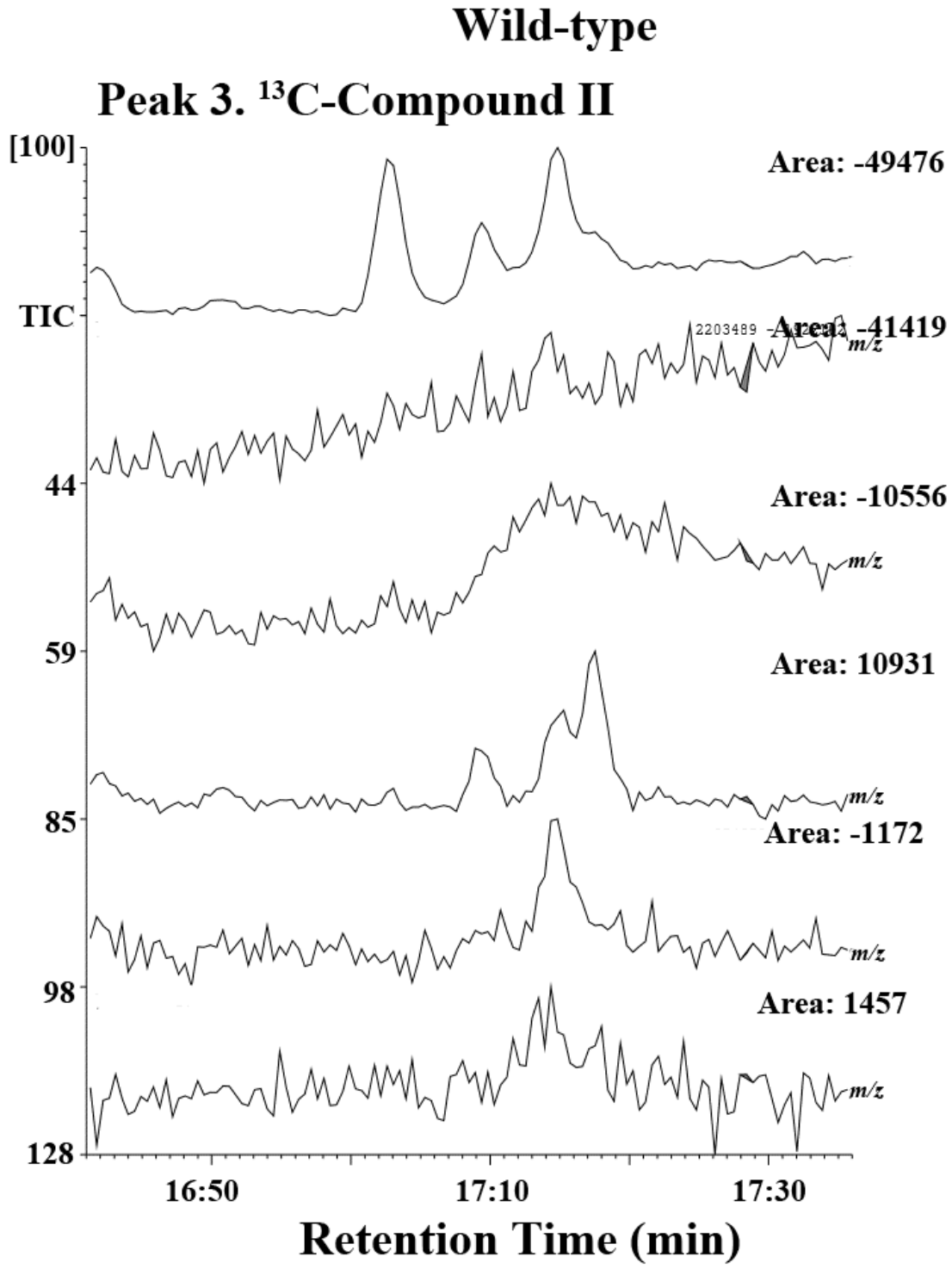

Figure 4-18. GC-MS selected ion monitoring for tracing ^{13}C-compound I in wild-type.

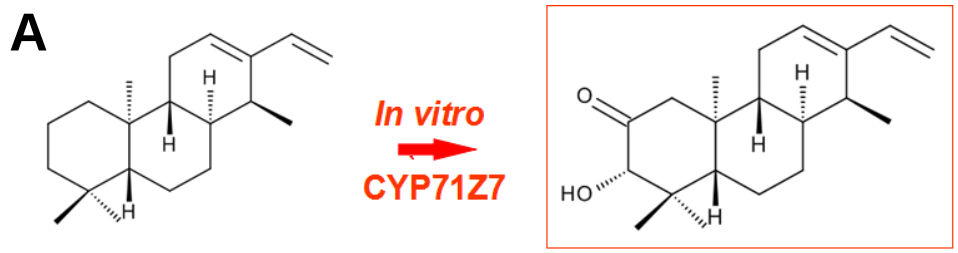

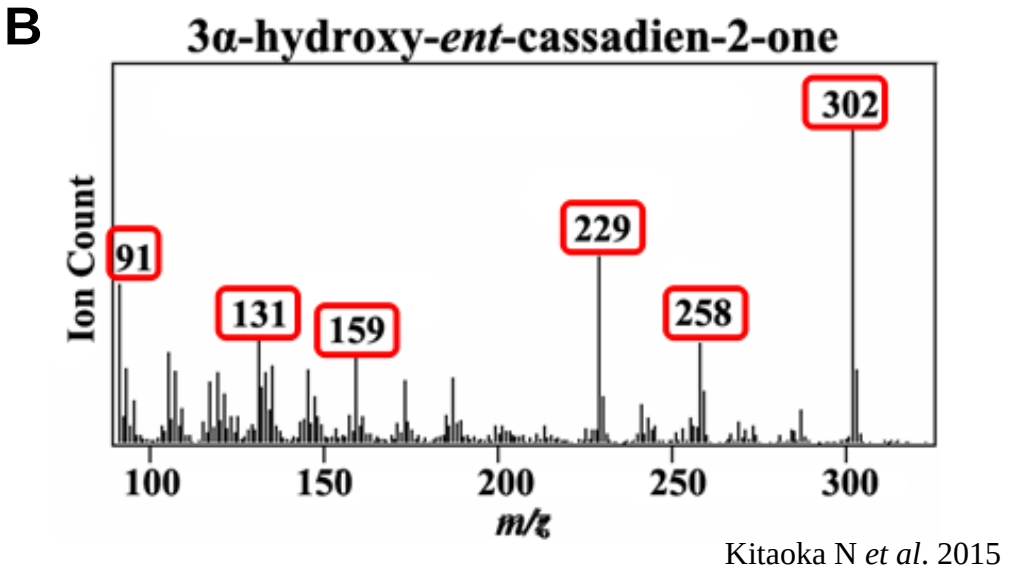

Kitaoka N *et al*. 2015

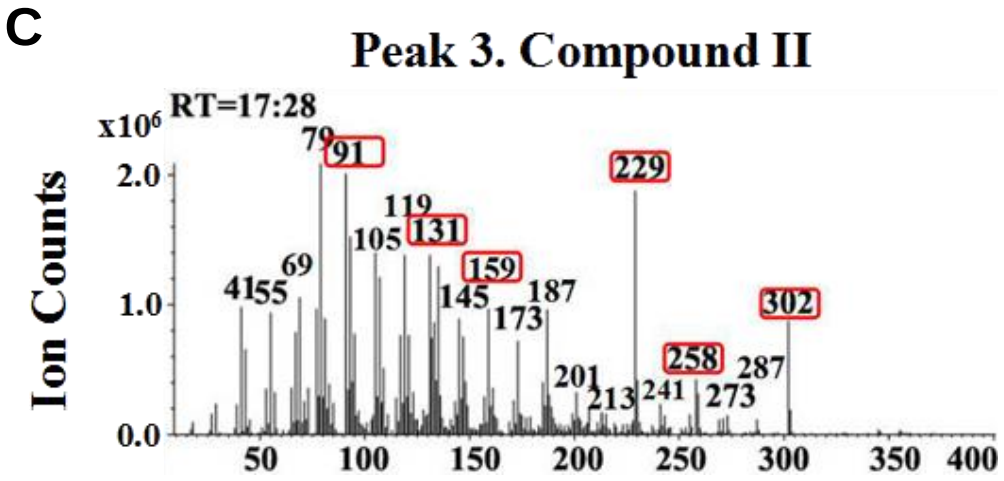

Figure 4-19. The comparison of mass spectra between unknown compound II and a reference compound, 3α-hydroxy-*ent*-cassadien-2-one.

A, 3α-hydroxy-*ent*-cassadien-2-one was generated from *ent*-cassa-12,15-diene *in vitro* assay. CYP71Z7 responsible for this reaction.[7] **B,** mass spectra from reference compound, 3α-hydroxy-*ent*-cassadien-2-one. [7] **C,** inquired compound II from *CYP76M7M8* RNAi line. **Red frame,** identical mass spectra between reference compound and inquired compound II

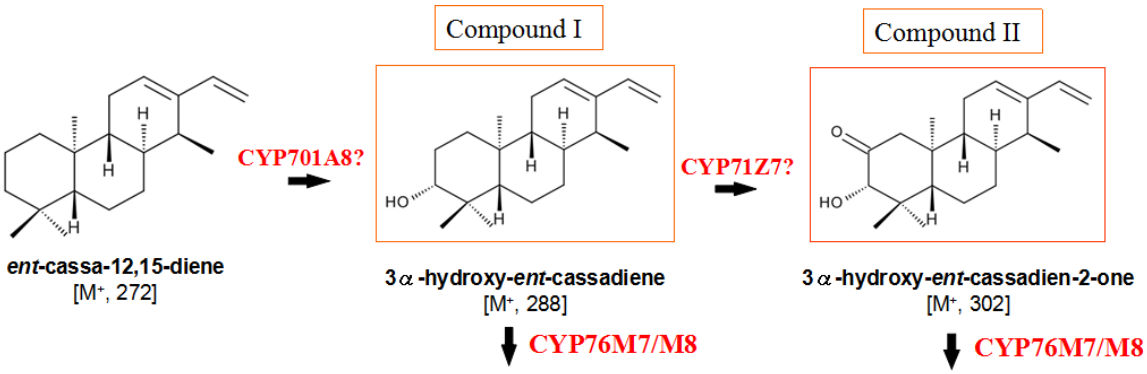

Figure 4-20. Proposed two intermediates derived from *ent*-cassa-12,15-diene in phytocassanes biosynthesis

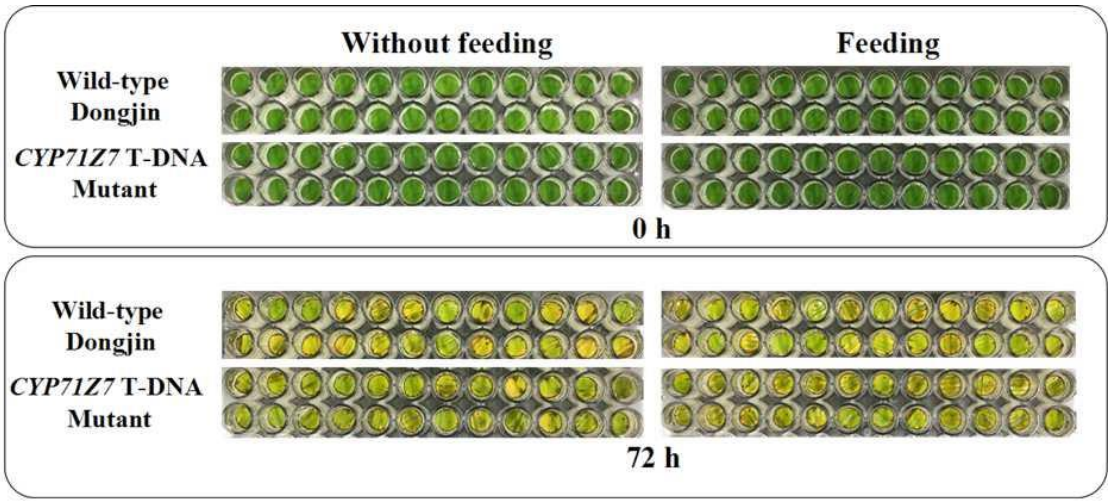

Without feeding: 1 μl 100% Ethanol/leaf disc
Feeding: 1 μg ^{13}C-*ent*-cassadiene/leaf disc

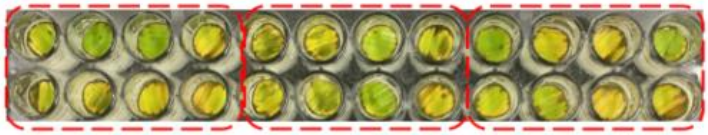

8 leaf disc were extracted with
4 ml 100% methanol for 48 h

(8 leaf disc/group)

Samples were concentrated
on centrifugal vacuum

Water was removed
by dehydrated Na_2SO_4

Centrifuged with 12,000xg
Final volume: 80 μl

LC-MSMS

Figure 4-21. [U-$^{13}C_{20}$] *ent*-cassa-12,15-diene application and phytoalexins extraction method from wild-type and *CYP71Z7* T-DNA mutant leaf disks.

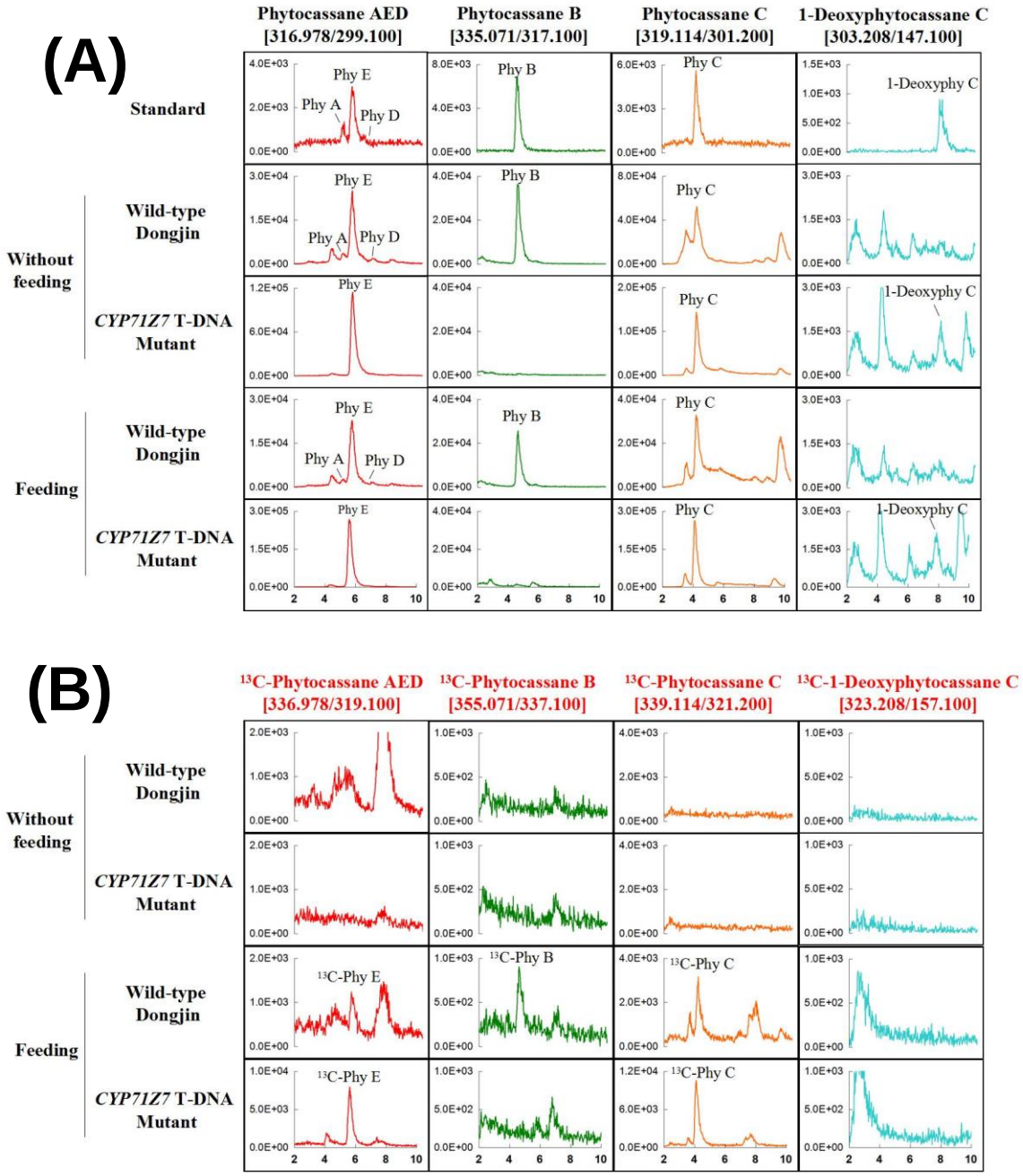

Figure 4-22. LC-ESI-MS/MS analysis of extract obtained from leaf disks (*O. sativa* L. cv. Dongjin) with or without [U-$^{13}C_{20}$] *ent*-cassa-12,15-diene feeding .

A, Native phytocassane (A-E) from wild-type and *CYP71Z7* T-DNA mutant extract; **B,** **[**U-$^{13}C_{20}$] phytocassane (A-E) detection in the extract from wild-type and *CYP71Z7* T-DNA mutant. Phy A, phytocassane A; Phy B, phytocassane B; Phy C, phytocassane C; Phy D, phytocassane D; Phy E, phytocassane E; ^{13}C-Phy B, [U-$^{13}C_{20}$] phytocassane B; ^{13}C-Phy C, [U-$^{13}C_{20}$] phytocassane C; ^{13}C-Phy D, [U-$^{13}C_{20}$]phytocassane D; ^{13}C-Phy E, [U-$^{13}C_{20}$] phytocassane E. 5 µl of each extract was subjected to LC-ESI-MS/MS.

Native phytocassanes ^{13}C labeled phytocassanes

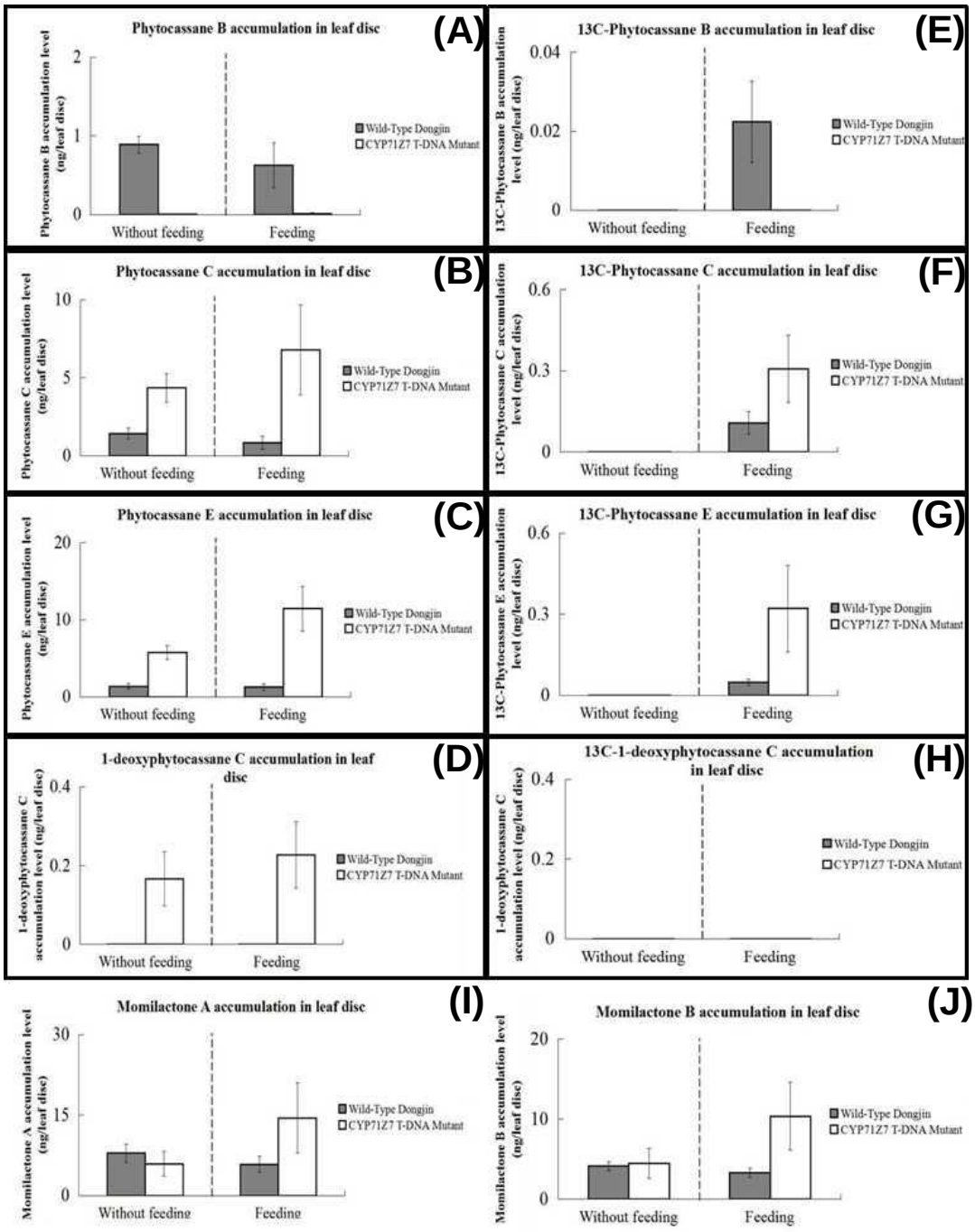

Figure 4-23. Phytocassanes, [U-$^{13}C_{20}$] phytocassanes and momilactones accumulation level in *CYP71Z7* T-DNA mutant and wild-type leaf disks (*O. sativa* L. cv. Dongjin) with or without [U-$^{13}C_{20}$] *ent*-cassa-12,15-diene feeding

A-C, unlabeled phytocassane (B-E) accumulation level in *CYP71Z7* T-DNA mutant and wild-type rice plants; **D,** A putative intermediate, 1-deoxyphytocassane C, accumulation level in wild type and *CYP71Z7* T-DNA mutant; **E-G,** [U-$^{13}C_{20}$] phytocassane (B-E) accumulation level in wild-type and *CYP71Z7* T-DNA mutant; **H,** [U-$^{13}C_{20}$] 1-deoxyphytocassane C accumulation level in wild type and *CYP71Z7* T-DNA mutant; **I and J,** native momilactone (A and B) accumulation level in wild-type and *CYP71Z7* T-DNA mutant. n=3.

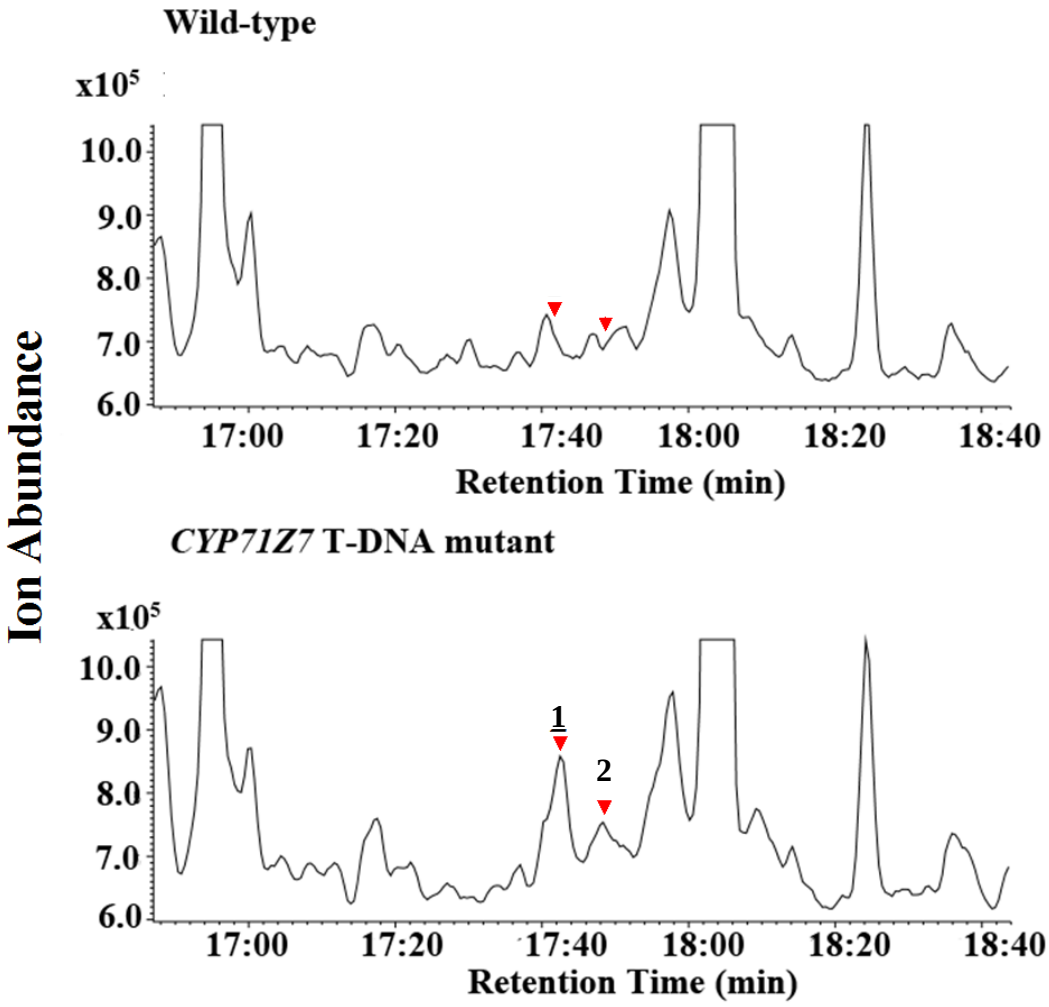

Figure 4-24 GC-MS chromatogram of extract from wild-type and *CYP71Z7* T-DNA mutant.

1, peak 1 from *CYP71Z7* T-DNA mutant was detected at retention time, 17:42; **2,** peak 2 from *CYP71Z7* T-DNA mutant was detected at retention time, 17:48.

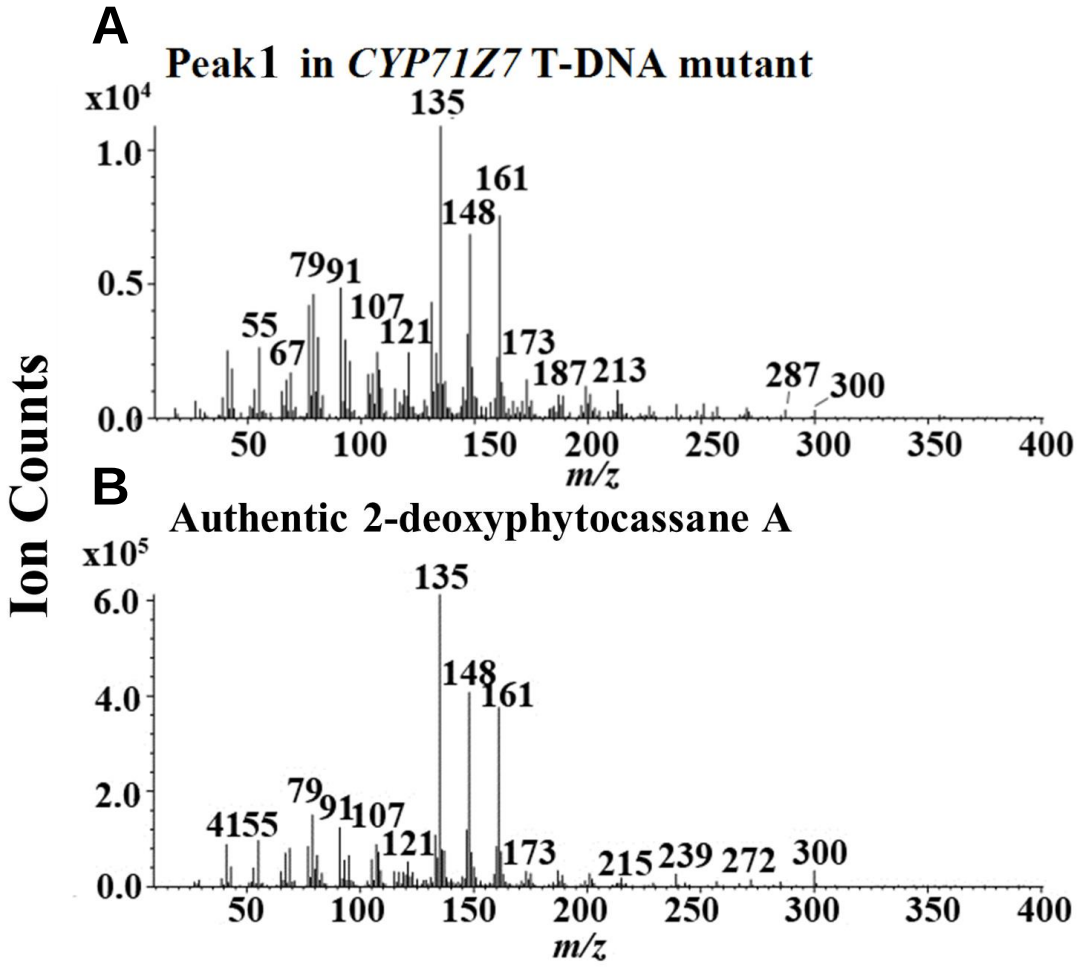

Figure 4-25. Mass spectra for peak 1 from wild-type and *CYP71Z7* T-DNA mutant.

A, mass spectra for peak 1 from *CYP71Z7* T-DNA mutant; **B,** mass spectra for authentic 2-deoxyphytocassane A

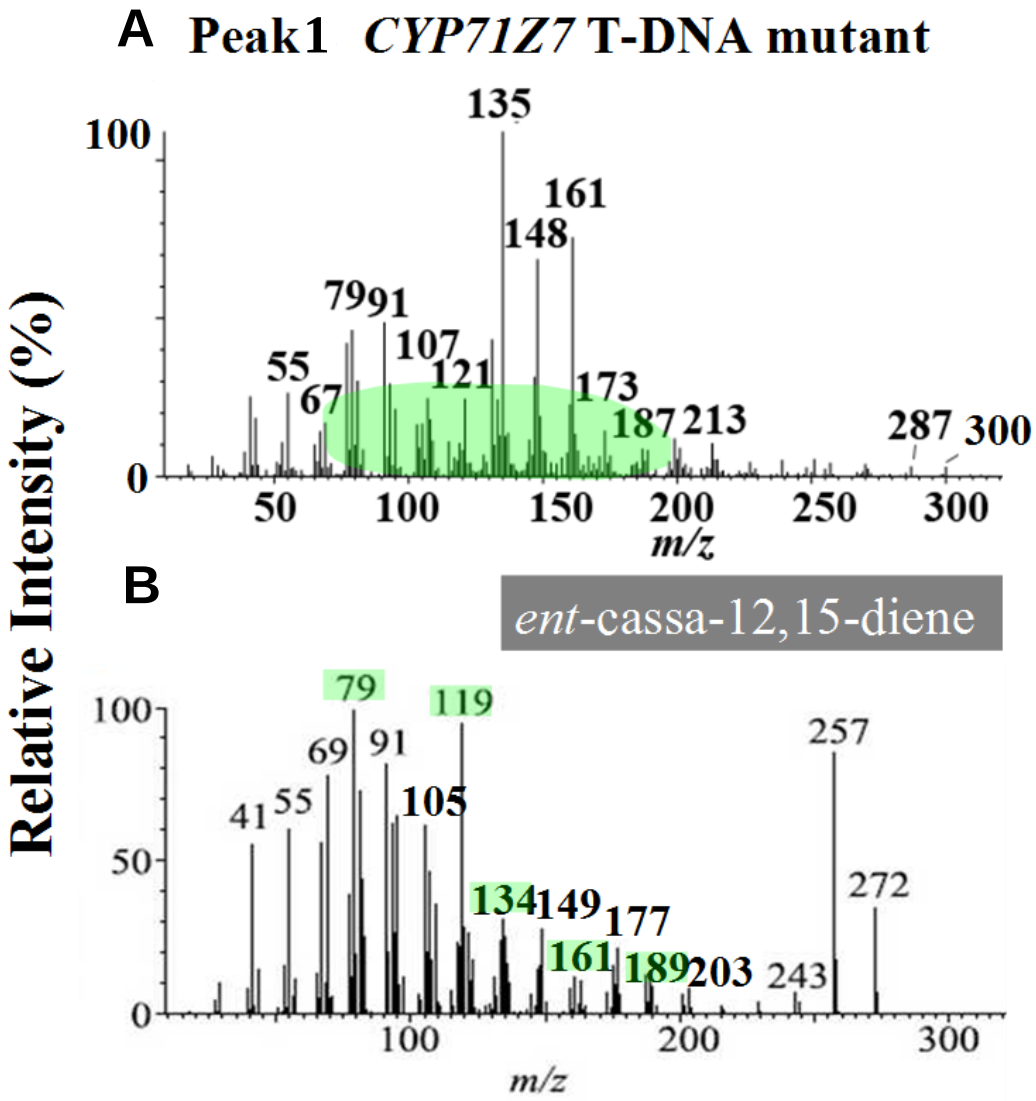

Figure 4-26. Mass spectra for peak 1 from *CYP71Z7* T-DNA mutant and unlabeled *ent*-cassa-12,15-diene.

A, mass spectra for peak 1 from *CYP71Z7* T-DNA mutant; **B,** mass spectra for unlabeled *ent*-cassa-12,15-diene; **Green area,** selected ion from unlabeled *ent*-cassa-12,15-diene for monitoring native compound III in peak 1

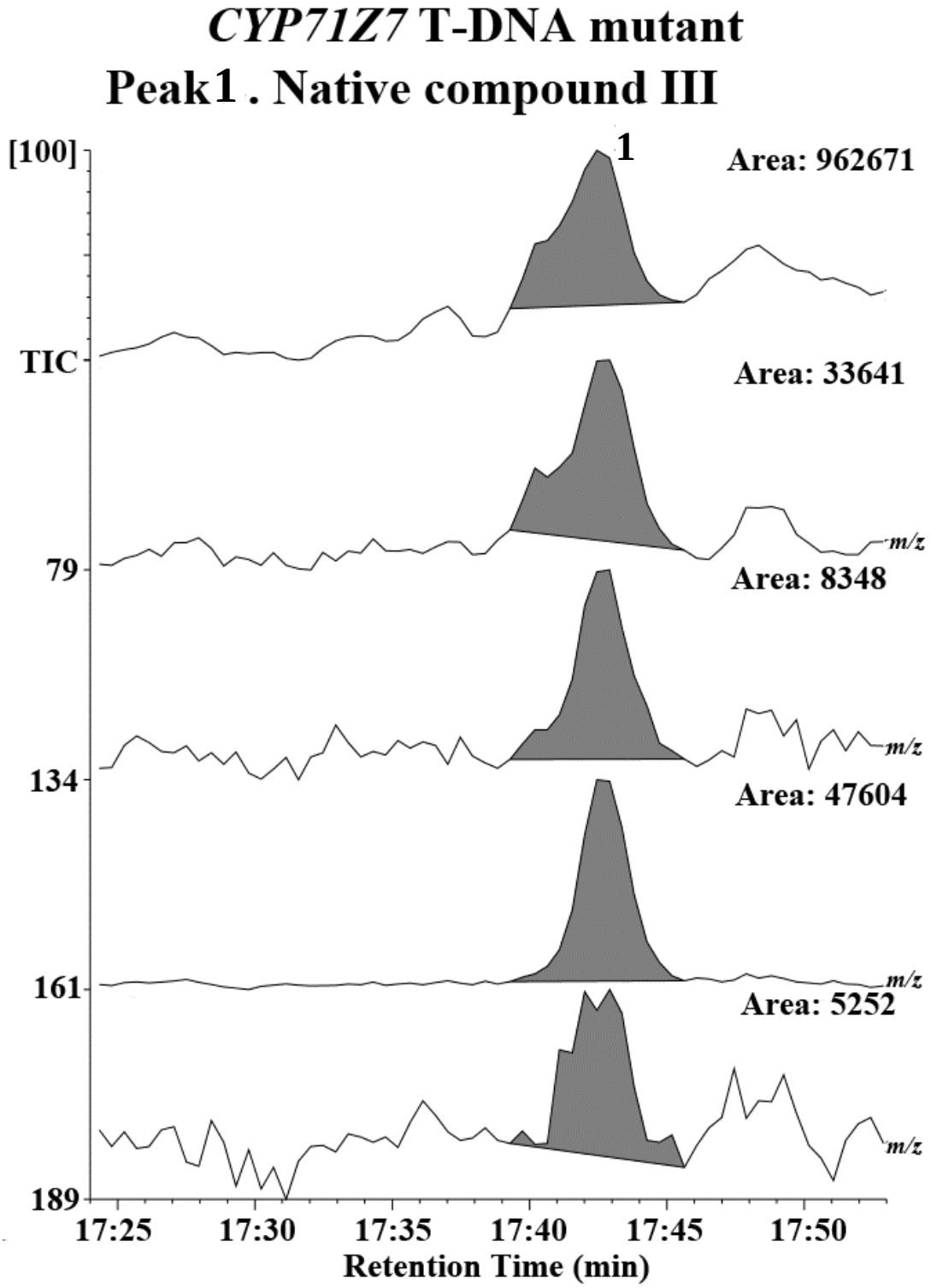

Figure 4-27. Selected ion from unlabeled *ent*-cassa-12,15-diene for monitoring native compound III in peak 1.

Native compound III was monitored by selected ion, 79, 134, 161 and 189, from unlabeled *ent*-cassa-12,15-diene.

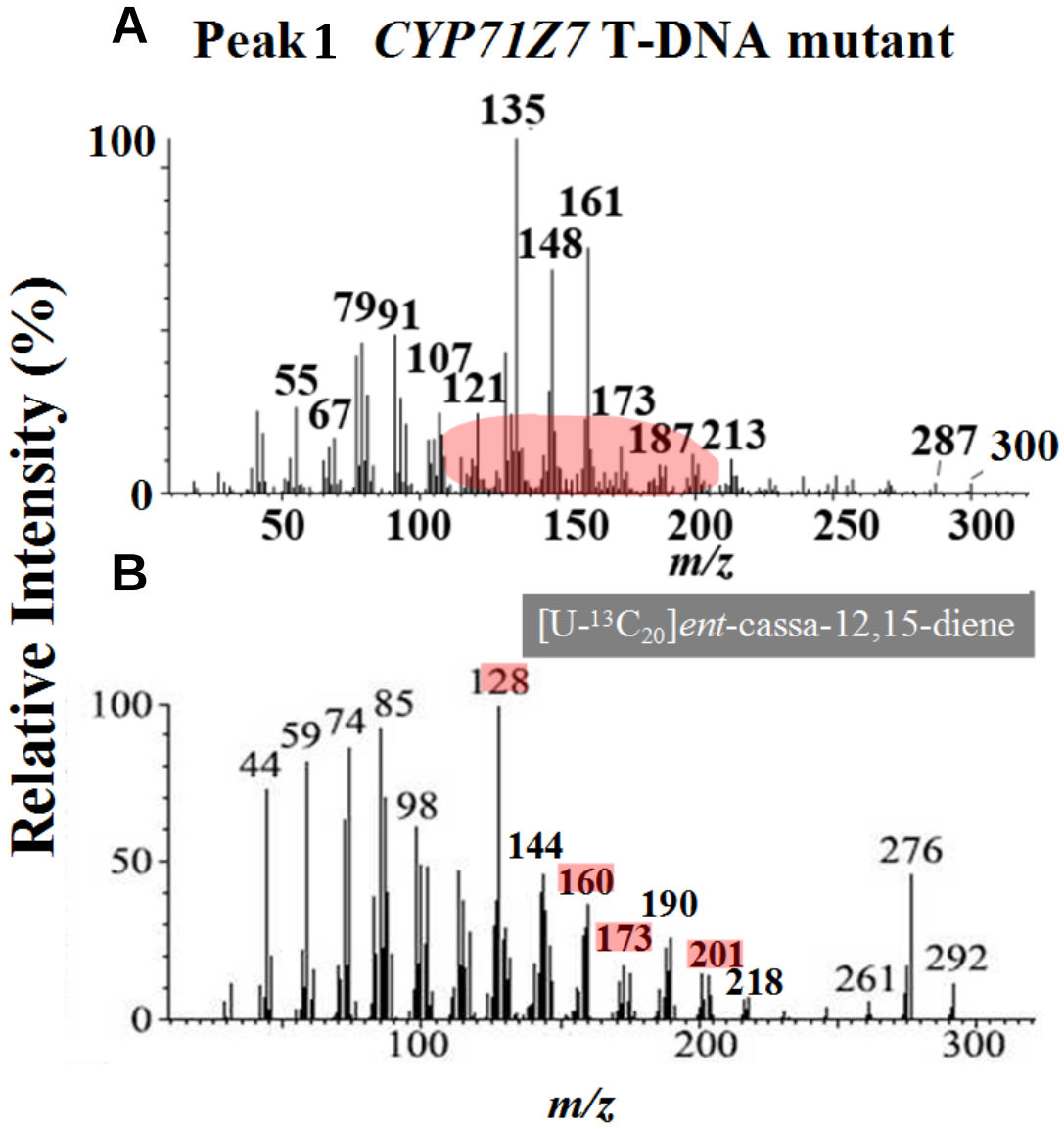

Figure 4-28. Mass spectra for peak 1 and [U-$^{13}C_{20}$] *ent*-cassa-12,15-diene
Red area, selected ion from [U-$^{13}C_{20}$] *ent*-cassa-12,15-diene for monitoring ^{13}C-compound III in peak 1.

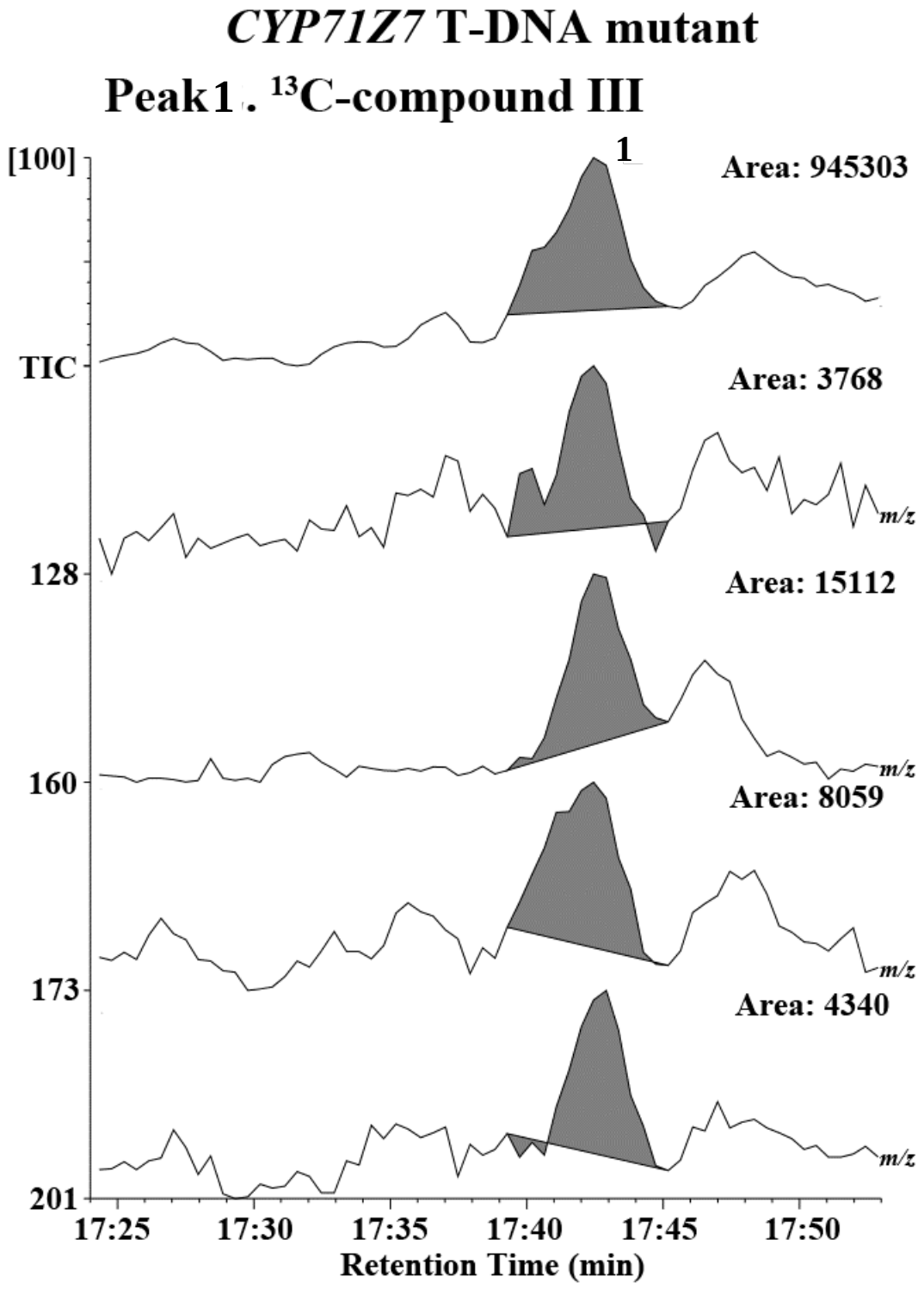

Figure 4-29. Selected ion from [U-$^{13}C_{20}$] *ent*-cassa-12,15-diene for monitoring native compound III in peak 1 from *CYP71Z7* T-DNA mutant.

^{13}C-compound III was monitored by selected ion, 128, 160, 173 and 201, from [U-$^{13}C_{20}$] *ent*-cassa-12,15-diene.

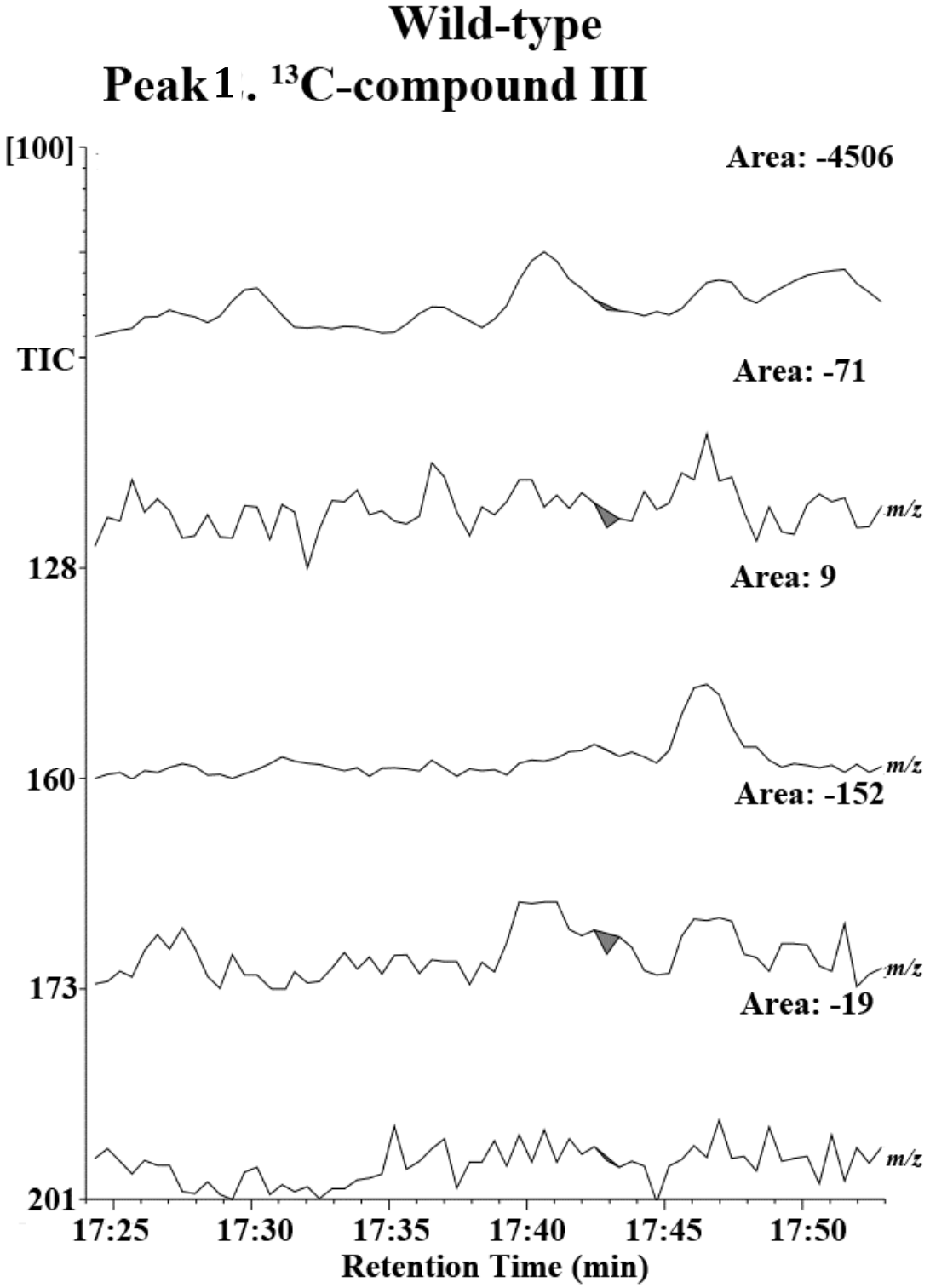

Figure 4-30. Selected ion from [U-$^{13}C_{20}$] *ent*-cassa-12,15-diene for monitoring native compound III in peak 1 from wild-type.

^{13}C-compound III was monitored by selected ion, 128, 160, 173 and 201, from [U-$^{13}C_{20}$] *ent*-cassa-12,15-diene.

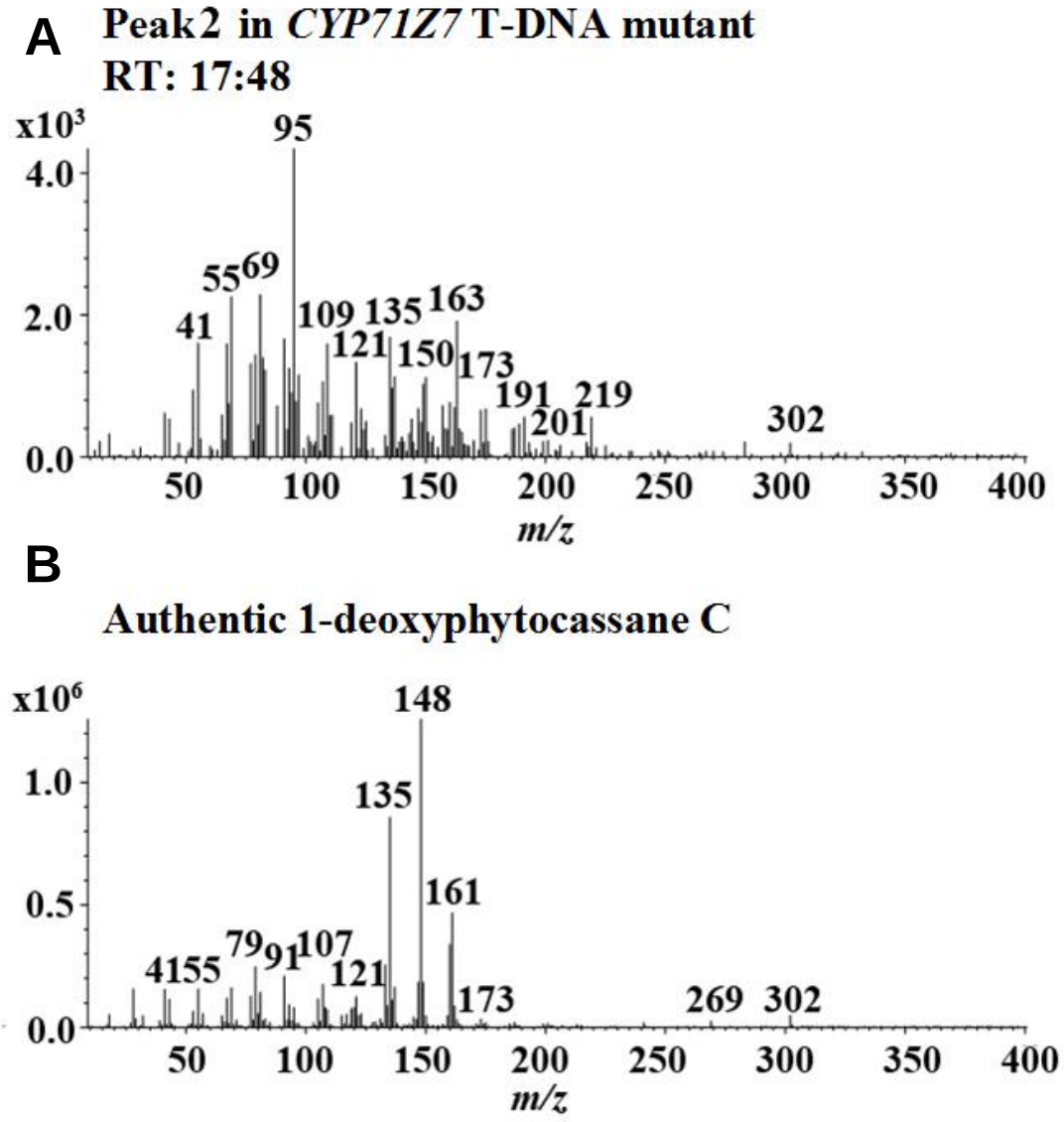

Figure 4-31. Mass spectra for peak 2 and authentic 1-deoxyphytocassane C

A, mass spectra for peak 2 from *CYP71Z7* T-DNA mutant; **B,** mass spectra for authentic 1-deoxyphytocassane C

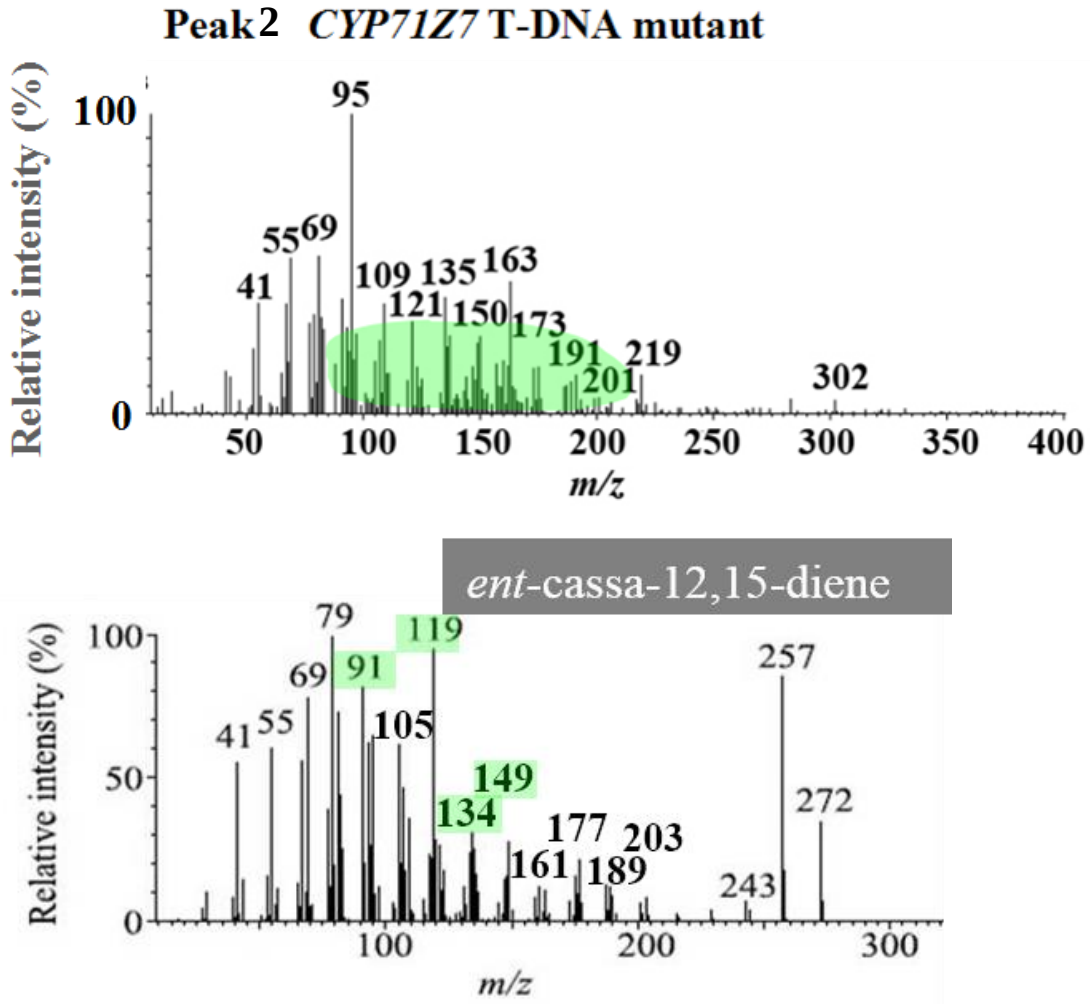

Figure 4-32. Mass spectra for peak 2 and unlabeled *ent*-cassa-12,15-diene
A, mass spectra for peak 2 from *CYP71Z7* T-DNA mutant; **B,** mass spectra for unlabeled *ent*-cassa-12,15-diene; **Green area,** selected ion from unlabeled *ent*-cassa-12,15-diene for monitoring n^{ative} compound IV in *CYP71Z7* T-DNA mutant.

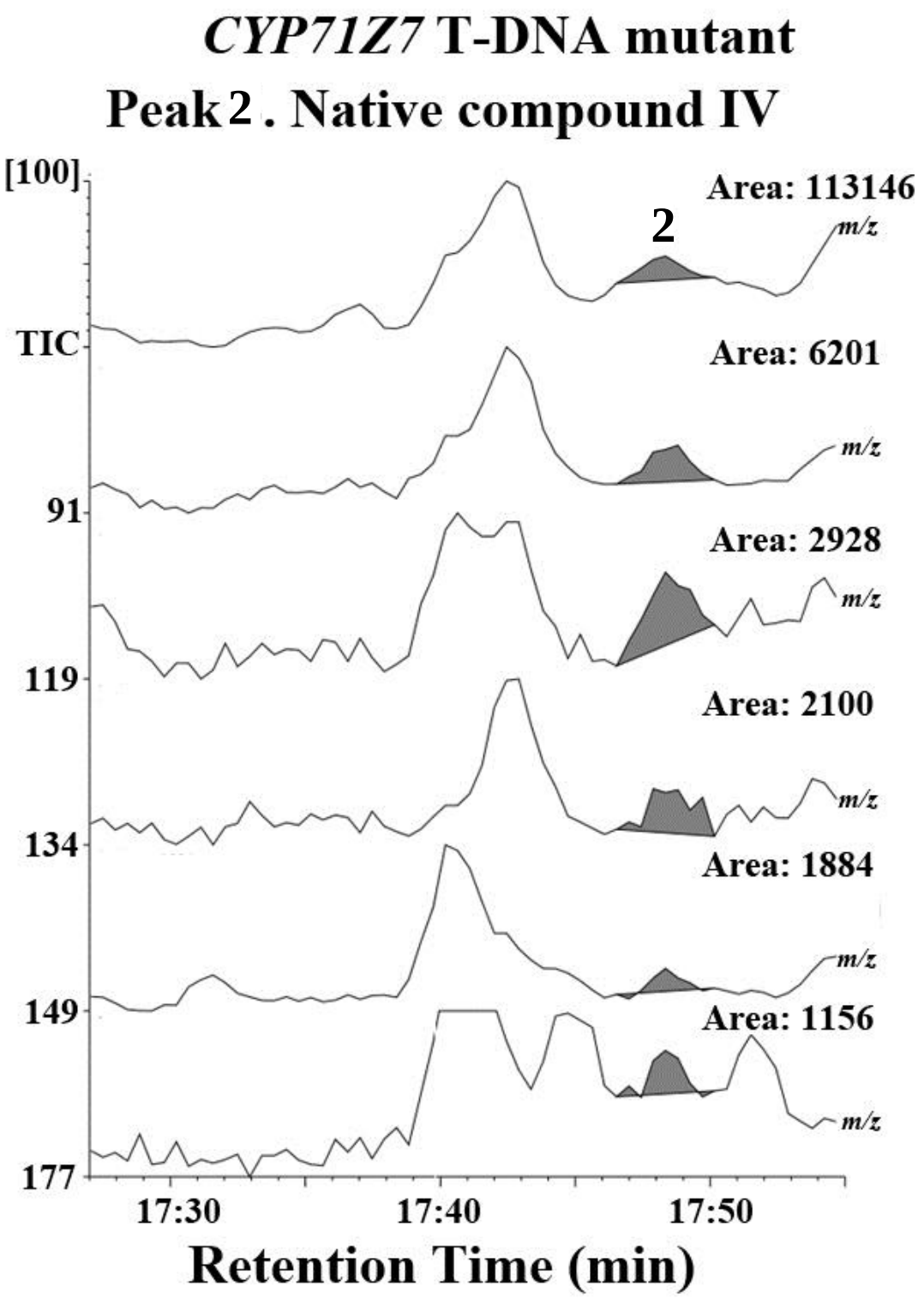

Figure 4-33. Selected ion from unlabeled *ent*-cassa-12,15-diene for monitoring native compound IV in peak 2 from *CYP71Z7* T-DNA mutant.

Native compound IV was monitored by selected ion, 91, 119, 134, 149 and 177, from unlabeled *ent*-cassa-12,15-diene.

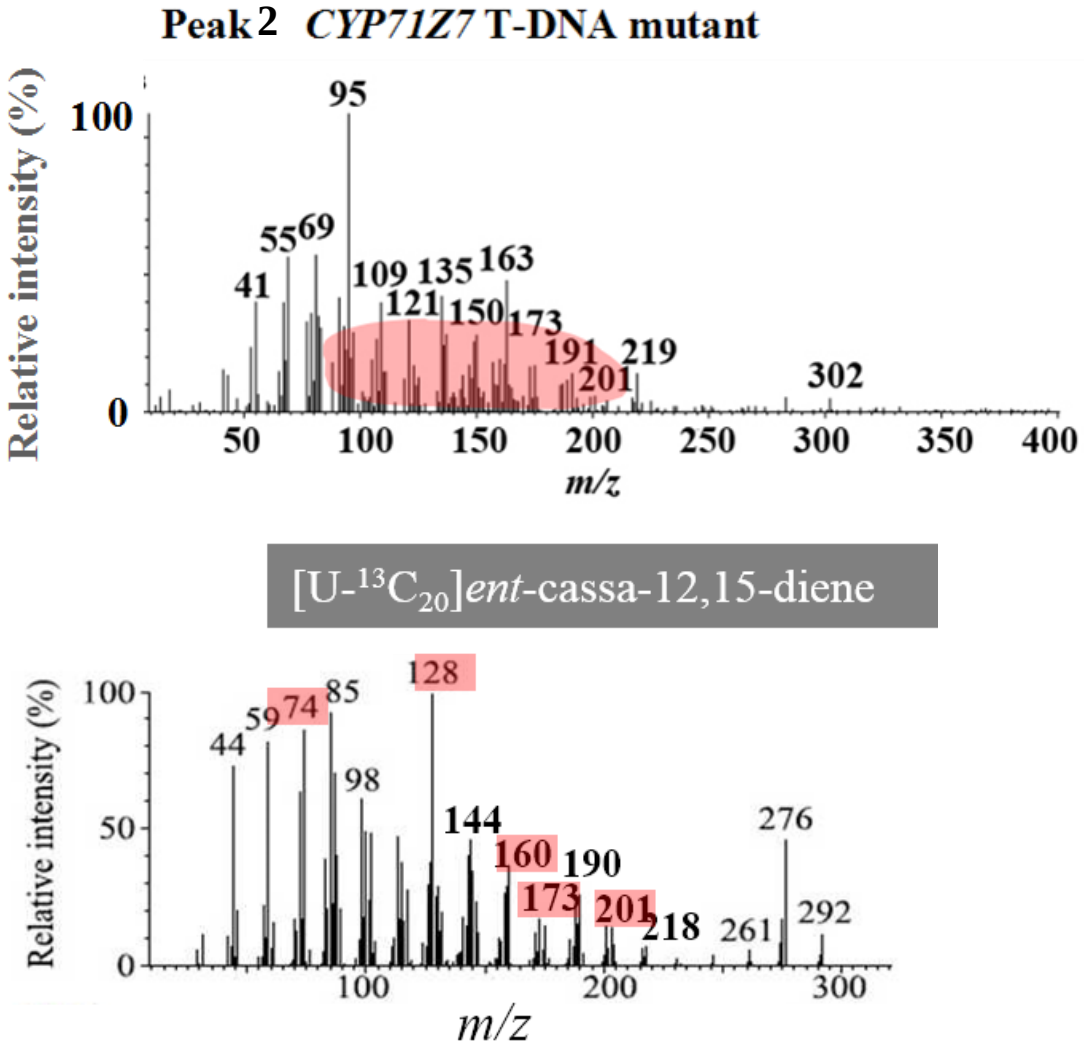

Figure 4-34. Mass spectra for peak 2 and [U-$^{13}C_{20}$] *ent*-cassa-12,15-diene

Red area, selected ion from [U-$^{13}C_{20}$] *ent*-cassa-12,15-diene for monitoring ^{13}C- compound IV in *CYP71Z7* T-DNA mutant.

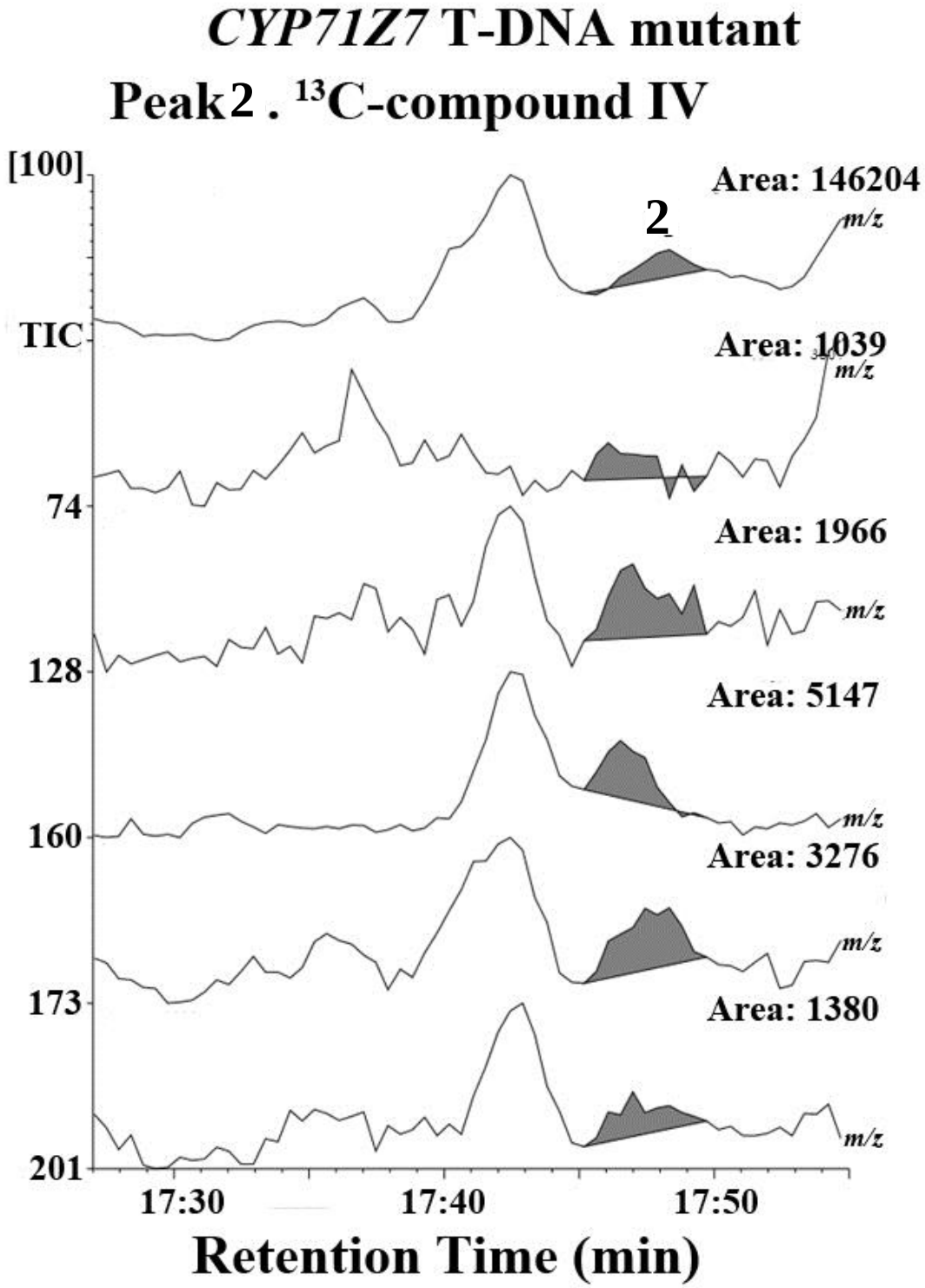

Figure 4-35. Selected ion from [U-$^{13}C_{20}$] *ent*-cassa-12,15-diene for monitoring ^{13}C-compound IV in peak 2 from *CYP71Z7* T-DNA mutant.

^{13}C-compound IV was monitored by selected ion, 74, 128, 134, 149 and 177, from [U-$^{13}C_{20}$] *ent*-cassa-12,15-diene.

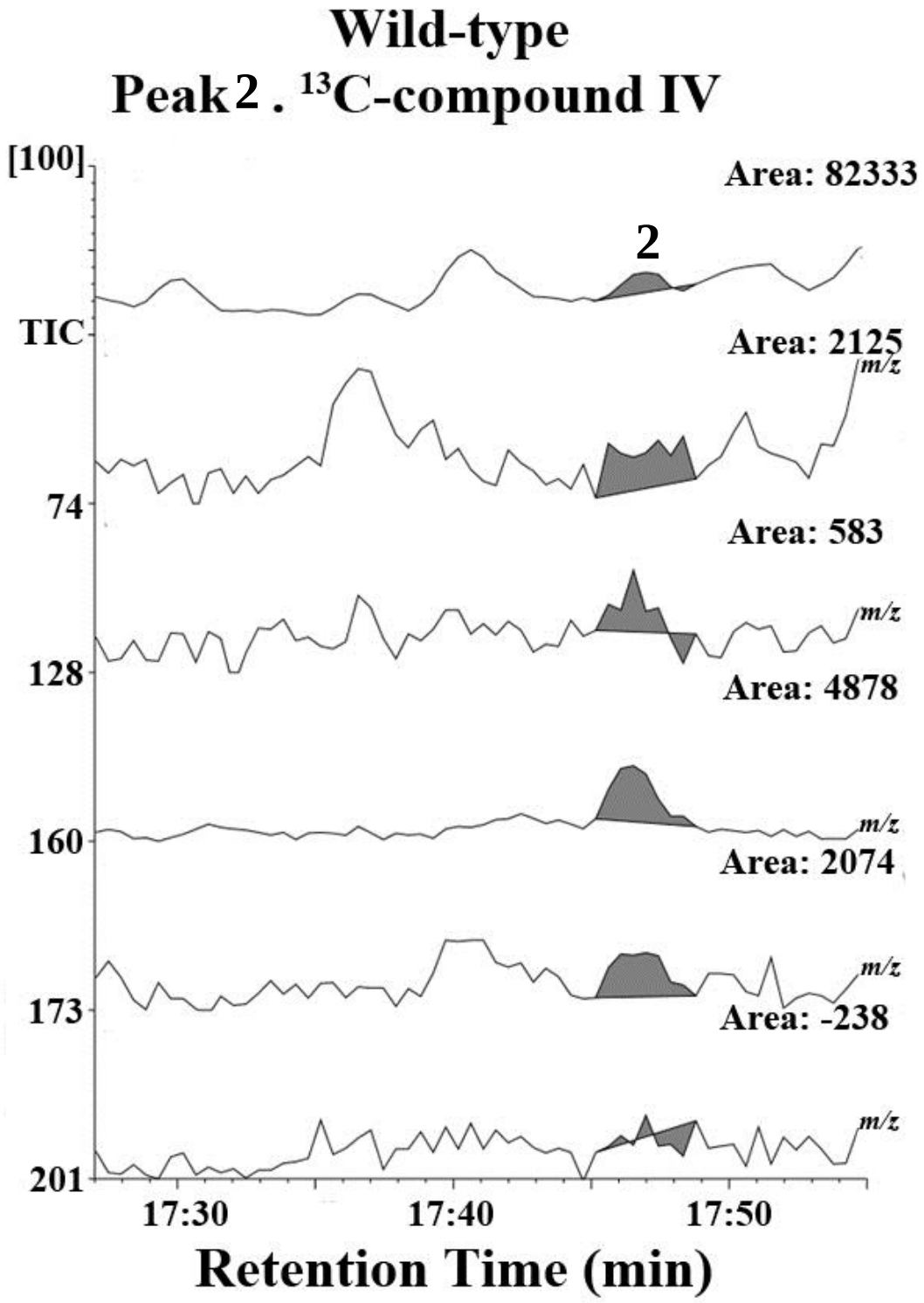

Figure 4-36. Selected ion from [U-$^{13}C_{20}$] *ent*-cassa-12,15-diene for monitoring ^{13}C-compound IV in peak 2 from wild-type.

^{13}C-compound IV was monitored by selected ion, 74, 128, 134, 149 and 177, from [U-$^{13}C_{20}$] *ent*-cassa-12,15-diene.

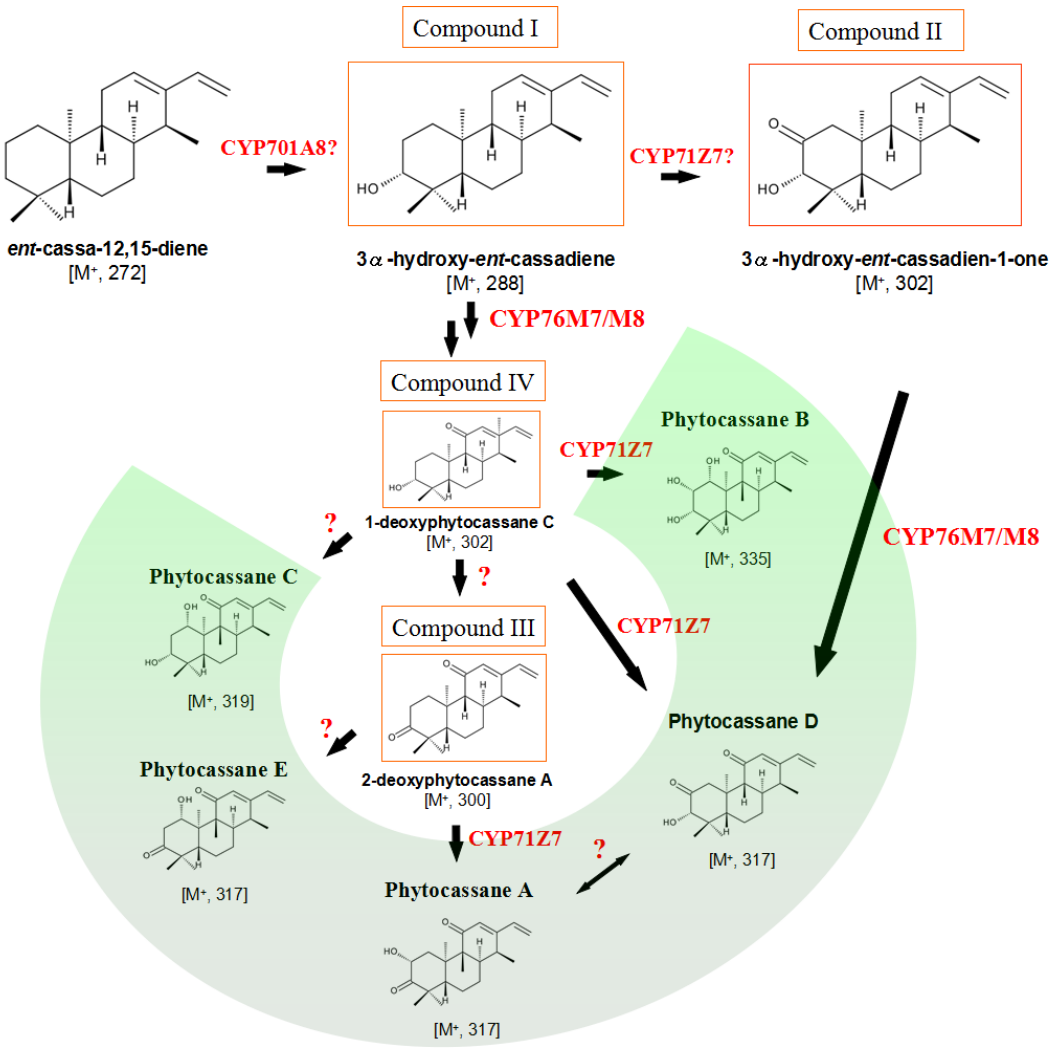

Figure 4-37. Hypothetical pathway of phytocassanes biosynthesis.

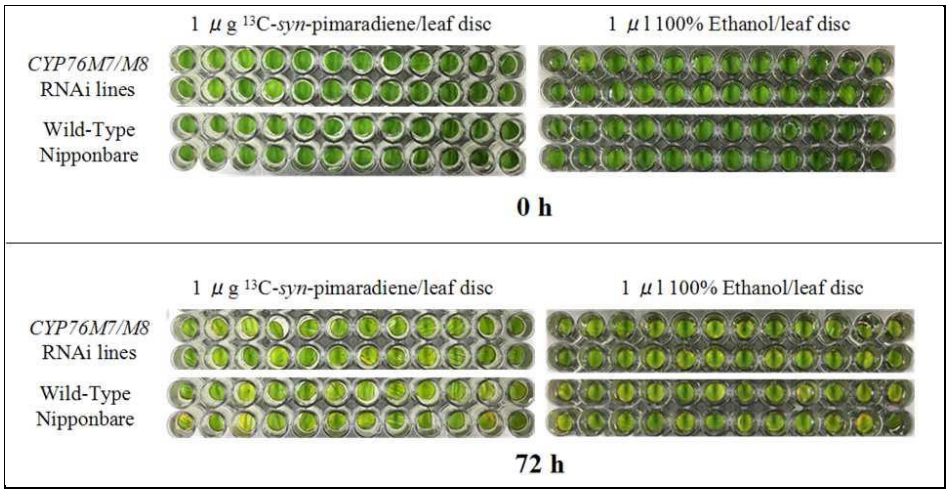

Figure 4-38. [U-$^{13}C_{20}$] *syn*-pimara-7,15-diene application on *CYP76M7/M8* RNAi lines with 500 μM $CuCl_2$ treatment in cheesecloths.

Left pane, leaf disks were incubated with [U-$^{13}C_{20}$] *syn*-pimara-7,15-diene (1 μg/leaf disk); **Right pane,** leaf disks were incubated with 99.5% ethanol (1 μl/leaf disk); Incubation time, 72 h.

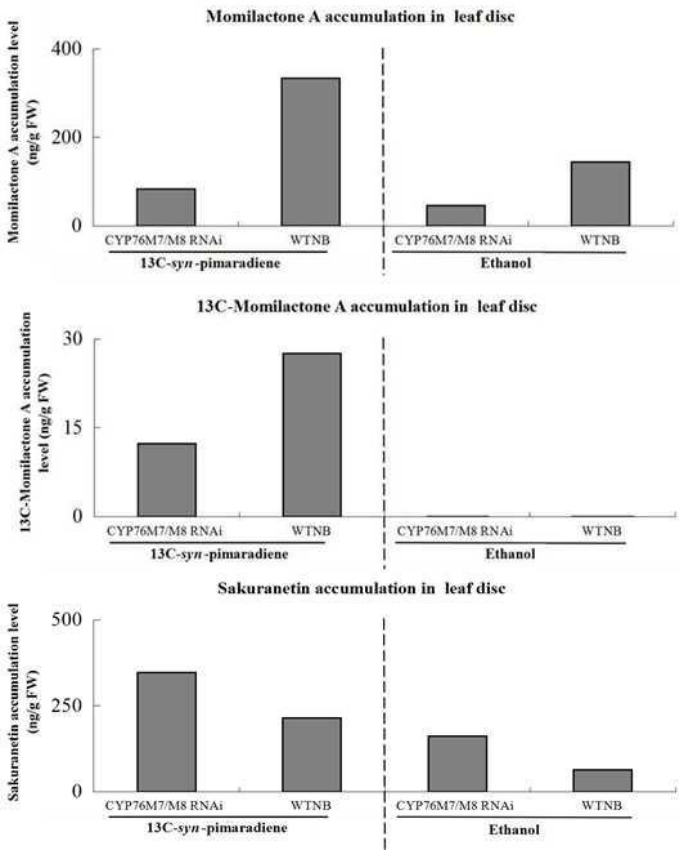

Figure 4-39. Momilactone A and [U-$^{13}C_{20}$] momilactone A accumulation level in *CYP76M7/M8 RNAi* lines and wild-type rice plants (*O. sativa* L. cv. Nipponbare) with [U-$^{13}C_{20}$] *syn*-pimara-7,15-diene feeding.

13C-*syn*-pimaradiene, each leaf disk was fed with 1 μg of [U-$^{13}C_{20}$] *syn*-pimara-7,15-diene; **Ethanol,** each leaf disk was treated with 1 μl of 99.5% ethanol. 5 μl of each extract was subjected to LC-ESI-MS/MS.

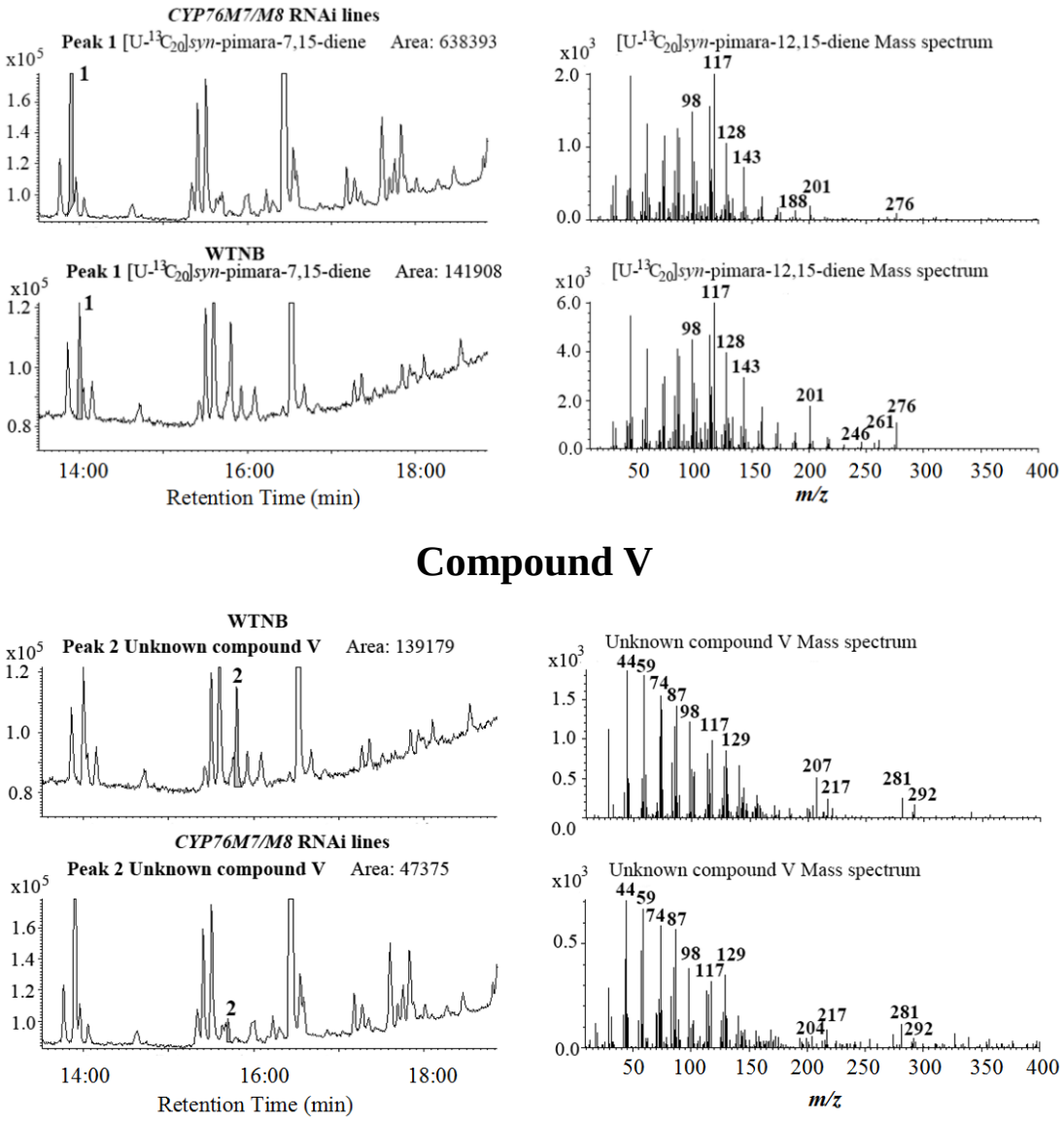

Figure 4-40. GC-MS analysis of wild-type and *CYP76M7/M8* RNAi lines extract obtained from incubation of [U-$^{13}C_{20}$] *syn*-pimara-7,15-diene with leaf disks

1, substrate, applied [U-$^{13}C_{20}$] *syn*-pimara-7,15-diene to wild-type (WTNB) and *CYP76M7/M8* RNAi line; right pane is mass spectra of [U-$^{13}C_{20}$] *syn*-pimara-7,15-diene; **2,** an unknown compound V chromatogram in both of wild-type and *CYP76M7M8* RNAi line; right pane is mass spectra of compound V.

Reference

[1] **Swaminathan S, Morrone D, Wang Q, Fulton DB, Peters RJ.** CYP76M7 is an *ent*-cassadiene C11alpha-hydroxylase defining a second multifunctional diterpenoid biosynthetic gene cluster in rice. *Plant Cell.* 2009, 21(10):3315-3325.

[2] **Wang Q, Hillwig ML, Okada K, Yamazaki K, Wu Y, Swaminathan S, Yamane H, Peters RJ.** Characterization of CYP76M5-8 indicates metabolic plasticity within a plant biosynthetic gene cluster. *J Biol Chem.* 2012, 287(9):6159-6168.

[3] **Yisheng Wu, Matthew L. Hillwig, Qiang Wang, Reuben J. Peters.** Parsing a multifunctional biosynthetic gene cluster from rice: Biochemical characterization of CYP71Z6 & 7. *FEBS Lett.* 2011, 585(21): 3446‑3451.

[4] **Miyamoto K, Fujita M, Shenton MR, Akashi S, Sugawara C, Sakai A, Horie K, Hasegawa M, Kawaide H, Mitsuhashi W, Nojiri H, Yamane H, Kurata N, Okada K, Toyomasu T.** Evolutionary trajectory of phytoalexin biosynthetic gene clusters in rice. *Plant J.* 2016, 87(3): 293-304.

[5] **Shimizu T, Jikumaru Y, Okada A, Okada K, Koga J, Umemura K, Minami E, Shibuya N, Hasegawa M, Kodama O. Nojiri H and Yamane H.** Effects of a bile acid elicitor, cholic acid, on the biosynthesis of diterpenoid phytoalexins in suspension-cultured rice cells. *Phytochemistry.* 2008, 69: 973-981

[6] **Qiang Wang, Matthew L. Hillwig, Reuben J. Peters.** CYP99A3: Functional identification of a diterpene oxidase from the momilactone biosynthetic gene cluster in rice. *Plant J.* 2011, 65(1): 87‑95.

[7] **Naoki Kitaoka, Yisheng Wu, Meimei Xu, Reuben J. Peters.** Optimization of recombinant expression enables discovery of novel cytochrome P450 activity in rice diterpenoid biosynthesis. *Appl Microbiol Biotechnol.* 2015,99(18): 7549‑7558

[8] **Wang Q, Hillwig ML, Wu Y, Peters RJ.** CYP701A8: a rice *ent*-kaurene oxidase paralog diverted to more specialized diterpenoid metabolism. *Plant Physiol.* 2012, 158(3): 1418-25.

.

CHAPTER 5

THE APPLICATION OF ^{13}C-LABELED DITERPENE HYDROCARBONS TO OTHER PLANTS

5-1. Introduction

In 1973, Kato *et al*. first identified momilactone A and momilactone B from rice. Momilactone A and B can also be produced in rice husk and have strongly inhibition effect on other plants growth as an allelopathic compounds. [1,2] Except for rice, moss *H. plumaeforme*, is known as the only plant producing momilactones.[3,4] Since momilactone A and B was identified from *H. plumaeforme* in 2007, Nozaki *et al*. further confirmed extract from *H. plumaeforme* showed allelopathic activity on various plants growth, such as *Arabidopsis*, Tobacco, *P. patense, J. subulata.*[3] Purified fractions from this extract was validated as momilactone A and B, and momilactone B exhibits higher inhibitory effect. [3] In 2016, our group confirmed momilactone B can be strongly accumulated in *H. plumaeforme* under different elicitor treatments, such as $CuCl_2$, 12-oxo phytodienoic acid (OPDA).[5] Furthermore, the extract from $CuCl_2$ treated *H. plumaeforme* exhibited inhibition effect on pathogenic fungus, *B. cinerea*.[5] However, similar to that in rice plant, the pathway from *syn*-pimara-7,15-diene to momilactones were still ambiguous in *H. plumaeforme.* On the other hand, since Tateoka recorded *L. perrieri* in 1963, few papers have been reported regarding this plant.[6] In 2016, our group focused on secondary metabolites of *L. perrieri* and demonstrated that it can not produce momilactones and phytocassane A, B and D, but do produce phytocassanes C and E, possibly due to lack of related genes on the genome responsible for the biosynthesis. Consequently, it is imperative for us to make clear the route of phytocassanes and momilactones in these non-model plant species.

By using already established feeding platform, in this chapter, we also try to feed substrate, [U-$^{13}C_{20}$] *syn*-pimara-7,15-diene to *H. plumaeforme* and [U-$^{13}C_{20}$] *ent*-cassa-12,15-diene to *L. perrieri.* These substrates estimated to be incorporated into [U-$^{13}C_{20}$] momilactones or [U-$^{13}C_{20}$] phytocassanes *in vivo,* respectively.

5-2. Materials and Methods

5-2-1. Application of [U-$^{13}C_{20}$] *syn*-pimara-7,15-diene to moss (*H. plumaeforme*)

Moss (*H. plumaeforme*) was utilized as material for [U-$^{13}C_{20}$] *syn*-pimara-7,15-diene feeding experiment, which was performed on a multi well plate on cotton gauze soaked with 150 μl of $CuCl_2$ solution. Approximately 30 mg/well gametophores were collected and treated with 1 μg of [U-$^{13}C_{20}$] *syn*-pimara-7,15-diene (1 μg /μl in 100% ethanol). In the group without feeding, 1 μl

of 100% ethanol was applied to gametophores in each well. Moss gametophores from 8 wells were collected for each sample and extracted with 6 ml of 100% methanol for 48 h in 4℃(Fig. 5-1). The extracts were enriched, filtered and centrifuged. Residual moisture was removed from supernatant by dehydrated Na_2SO_4. The remaining extracts were analyzed on LC-ESI-MS/MS.

5-2-2. Application of [U-$^{13}C_{20}$] *ent*-cassa-12,15-diene to wild rice (*Leersia perrieri*)

In the feeding group, 9 μg of [U-$^{13}C_{20}$] *ent*-cassa-12,15-diene dissolved in 9 μl of 99.5% ethanol was applied to fresh *L. perrieri* leaves (intact plant) on cotton gauze soaked with 0.5 mM $CuCl_2$ solution. In the group without feeding, *L. perrieri* leaves were treated with 9 μl of 99.5% ethanol (Fig. 5-3). The whole plant with cotton gauze was incubated in an enclosed glass tube (38 mm diameter) for 72 h. Afterward, each shoot was extracted with 0.5 ml of 100% methanol for 48 h in 4℃. The extracts were enriched, filtered, centrifuged and dehydrated. The purified extracts were analyzed on LC-ESI-MS/MS.

5-3. Results

5-3-1. [U-$^{13}C_{20}$] *syn*-pimara-7,15-diene feeding experiment in *H. plumaeforme*

Incorporation of [U-$^{13}C_{20}$] *syn*-pimara-7,15-diene into [U-$^{13}C_{20}$] momilactone A and [U-$^{13}C_{20}$] momilactone B in the moss *H. plumaeforme*, which is recently reported by Okada et al., (2016) as momilactone producers other than *Oryza* species[5] was also analyzed. *H. plumaeforme* can produce both momilactone A and momilactone B, but latter one is the major accumulated substance with greater allelopathy activity to surrounding plants. As shown in Fig. 5-2, feeding of [U-$^{13}C_{20}$] *syn*-pimara-7,15-diene obviously exhibited accumulations of [U-$^{13}C_{20}$] momilactone B (16 ng from 1 g gametophore) and [U-$^{13}C_{20}$] momilactone A (with lesser amount, 2 ng from 1 g gametophore) in gametophore of *H. plumaeforme* by LC-MS/MS analysis, indicating that *H. plumaeforme* actually has the biosynthetic pathway of momilactones derived from *syn*-pimaradiene, whereas the only starting point enzyme gene *HpDTC1* encoding a *syn*-pimaradiene synthase in *H. plumaeforme* has been identified so far.[5]

5-3-2. [U-$^{13}C_{20}$] *ent*-cassa-12,15-diene feeding experiment in wild species (*Leersia perrieri*)

When [U-$^{13}C_{20}$] *ent*-cassa-12,15-diene was fed to leaf blades of *L. perrieri* under the treatment with $CuCl_2$ for 72 h (Fig. 5-3), ^{13}C-labeled both phytocassane C and phytocassane E were detected on LC-ESI-MS/MS analysis together with non-labeled these two phytocassanes (Fig. 5-4). This result suggests that the biosynthetic pathway of phytocassanes derived from *ent*-cassadiene is definitely maintained in *L. perrieri* as in the case of *O. sativa*.

5-4. Discussion

In this study, we successfully traced out the ^{13}C-signal in *H. plumaeforme* (a momilactones producing moss). In the application to the moss *H. plumaeforme*, ^{13}C-labeled *syn*-pimaradiene was successfully incorporated into momilactones (Fig. 5-2). In the report by Okada et al (2016), a bifunctional *syn*-pimaradiene synthase *HpDTC1* gene has been identified on the basis of RNA-seq analysis. Since *syn*-pimaradiene accumulation in the moss treated by $CuCl_2$ was not observed whereas the accumulation was clearly detected in the case of rice leaves elicited by UV irradiation, a metabolic flow via *syn*-pimaradiene in *H. plumaeforme* might be rather faster compared to that in rice. Besides, subsequent biosynthetic pathway consisting of P450 monooxygenases in the moss seems to be somehow different from the pathway in rice.

In the application to *L. perrieri*, a nearest outgroup of *Oryza* species, ^{13}C-labeled *ent*-cassa-12,15-diene was also successfully incorporated into both phytocassane C and phytocassane E (Fig. 5-4). These two distinctive phytocassanes are C2-non-oxydated type phytocassanes, meaning that *L. perrieri* does not have enzymatic activity for hydroxylation of C2 position of phytocassanes. Miyamoto et al (2016) reported that there is no *CYP71Z* type P450 genes in the *L. perrieri* genome. Since CYP71Z6/Z7 is involved in the hydroxylation of C2 position of phytocassane, the result from feeding experiment is well consistent with this evidence.

In future, native intermediate or ^{13}C-intermediates will also be investigated in related genes knock-out mutants in *H. plumaeforme* or *L. perrieri*, if become technicaly available.

5-5. Brief Summary

I have confirmed established feeding method was applied to other plants successfully. The momilactones or phytocassanes accumulation level in *H. plumaeforme* or *L. perrieri* has been clarified. This system can also provide a platform for intermediates investigation in various plants mutant. Thus extensive application of this technique is expected in future.

5-6. Figures

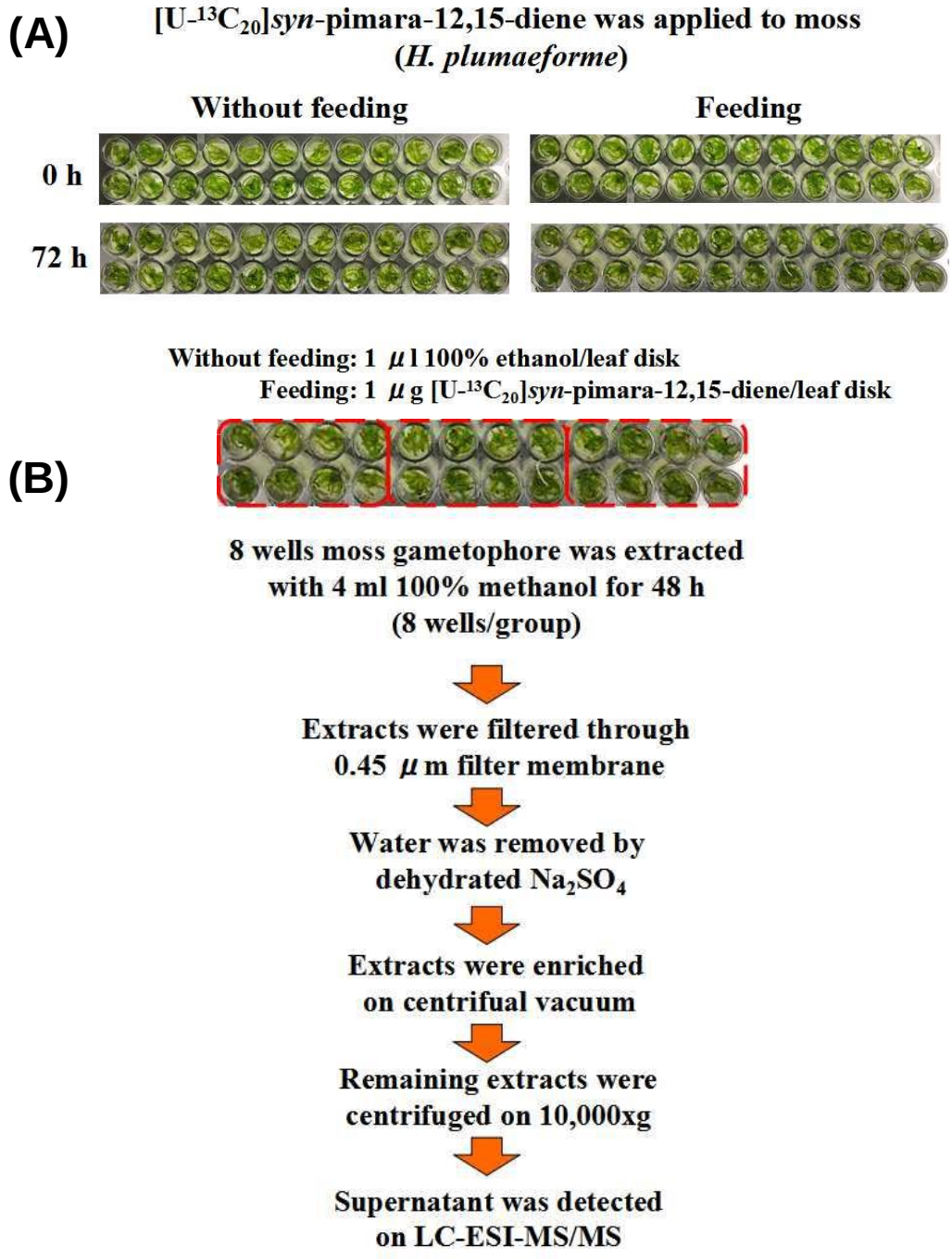

Figure 5-1. The application of [U-$^{13}C_{20}$] *syn*-pimaradiene to one month old moss gametophore (*H. plumaeforme*).

A, Without feeding, 1 µl of 100% ethanol was applied to one well moss gametophore in 500 µM $CuCl_2$ soaked cheesecloths; Feeding, 1 µg of [U-$^{13}C_{20}$] *syn*-pimaradiene was also applied to one well moss gametophore in 500 µM $CuCl_2$ soaked cheesecloths; **B,** a schematic diagram for momilactones or [U-$^{13}C_{20}$] momilactones extraction from moss gametophore. 8 wells moss gametophore for one extract. n=3. 1 µl of each extract was subjected to UPLC-ESI-MS/MS.

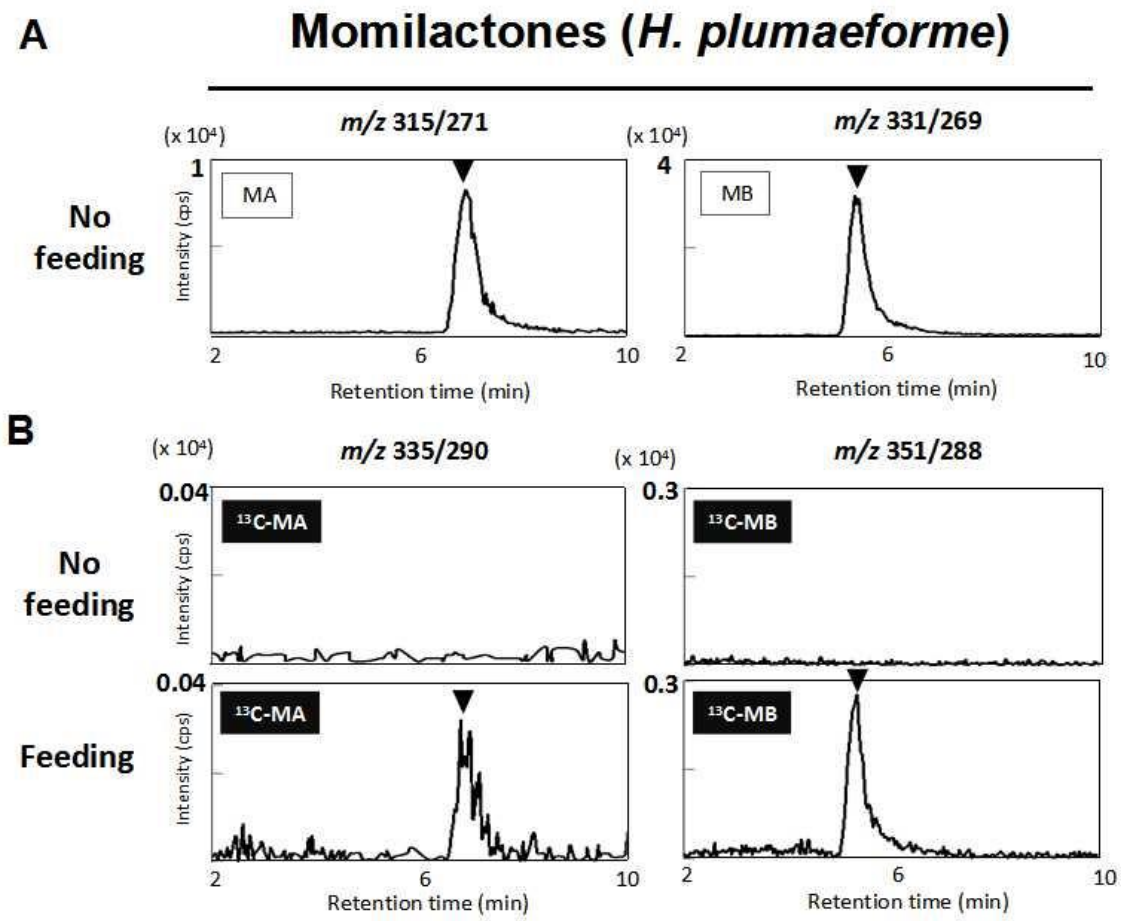

Figure 5-2. The application of [U-$^{13}C_{20}$] *syn*-pimaradiene to one month old moss gametophore (*H. plumaeforme*).

A, unlabeled momilactone (A and B) accumulation level in moss without feeding; B, unlabeled momilactone (A and B) and [U-$^{13}C_{20}$] momilactone (A and B) accumulated amount from one gram gametophores tissue in both of no feeding and feeding group; C**,** The ratio of [U-$^{13}C_{20}$] momilactone (A and B) to unlabeled momilactone (A and B) in *H. plumaeforme*. n=3. 5 µl of each extract was subjected to LC-ESI-MS/MS.

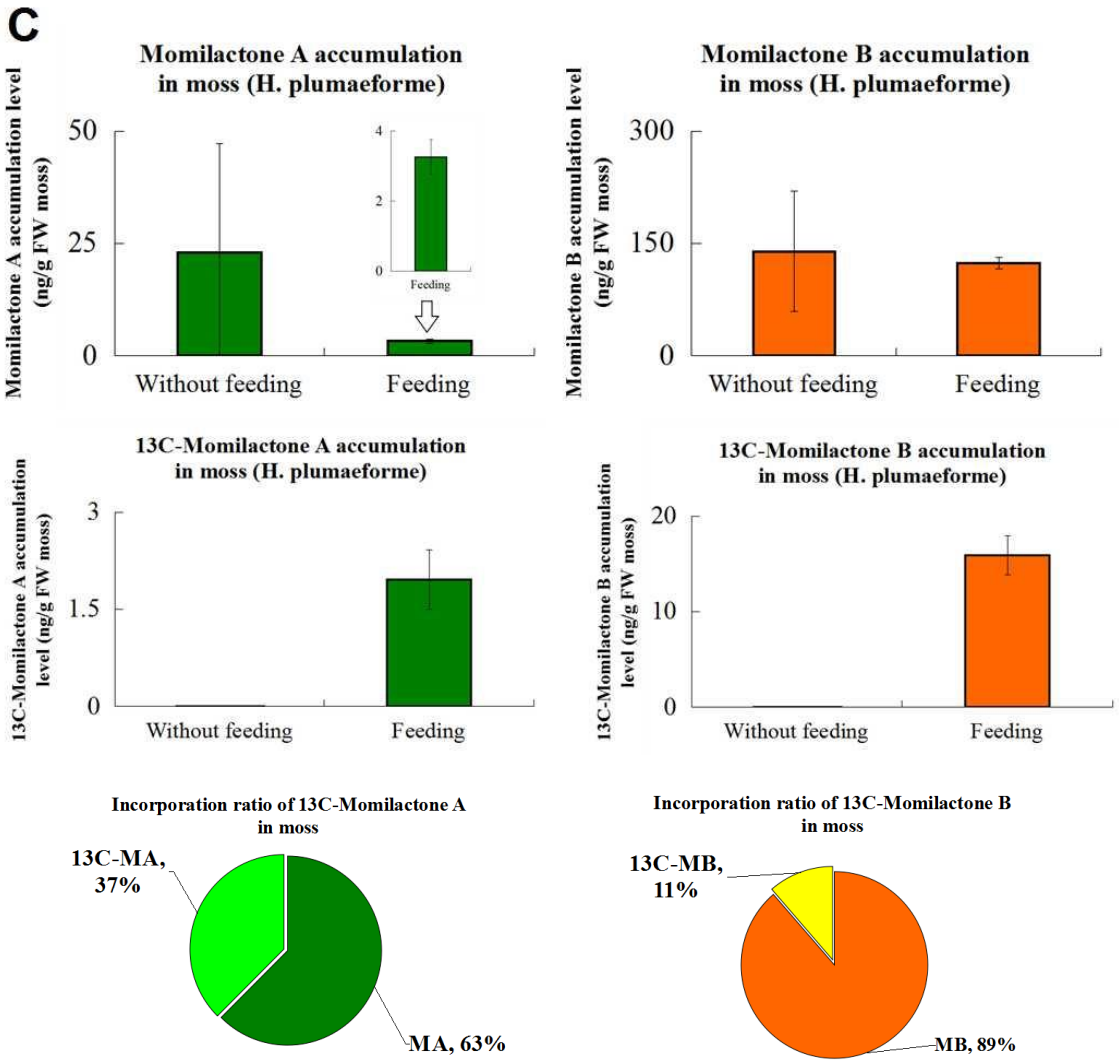

Figure 5-2. Continued

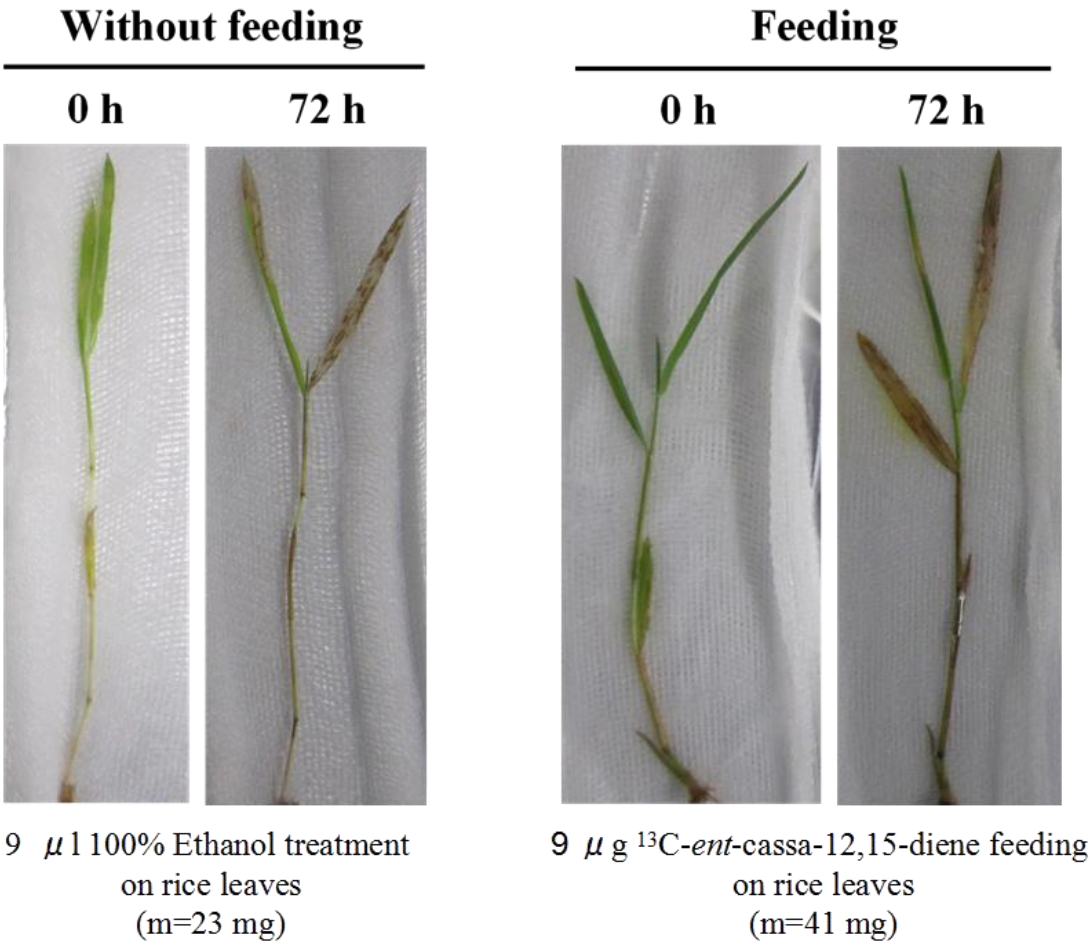

Figure 5-3. [U-$^{13}C_{20}$] *ent*-cassadiene application on wild species (*Leersia perrieri*) with 500 μM $CuCl_2$ treatment in cheesecloths.

Without feeding, expanded leaf was treated with 9 μl of 99.5% Ethanol in 500 μM $CuCl_2$ soaked cheesecloths; **Feeding,** expanded leaf was treated with 9 μg of [U-$^{13}C_{20}$] *ent*-cassadiene (1 μg/μl in 99.5% ethanol) in 500 μM $CuCl_2$ soaked cheesecloths. Incubation time was 72 h.

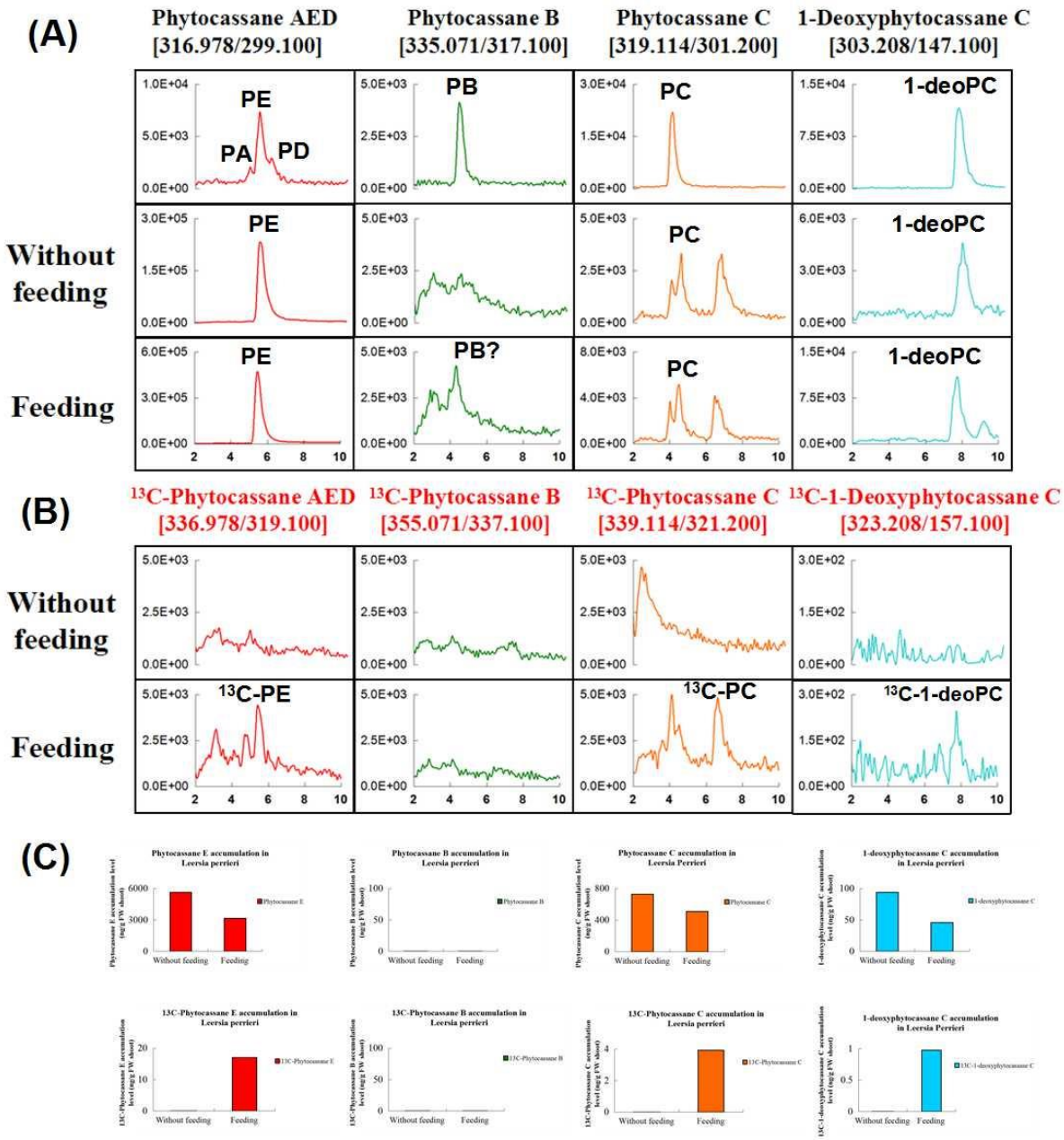

Figure 5-4. LC-ESI-MS/MS analysis of [U-$^{13}C_{20}$] phytocassanes in wild species (*Leersia perrieri*)

A, [U-$^{13}C_{20}$] *ent*-cassa-12,15-diene dissolved in 99.5% ethanol feeding experiment on fresh plants (*L. perrieri*). **B,** Phytocassanes and [U-$^{13}C_{20}$] phytocassanes accumulation level converted from [U-$^{13}C_{20}$] *ent*-cassa-12,15-diene on LC-ESI-MS/MS. **C,** Yield of momilactone (A, B) and [U-$^{13}C_{20}$] momilactone (A, B) in one gram leaf tissue.. **PA,** Phytocassane A; **PB,** Phytocassane B; **PC,** Phytocassane C; **PD,** Phytocassane D; **PE,** Phytocassane E; **1-deoPC,** 1-Deoxyphytocassane C; **^{13}C-PB**, [U-$^{13}C_{20}$]Phytocassane B; **^{13}C-PC**, [U-$^{13}C_{20}$] phytocassane C, **^{13}C-PE,** [U-$^{13}C_{20}$] phytocassane E; **^{13}C-1-deoPC,** [U-$^{13}C_{20}$] 1-Deoxyphytocassane C. Each 5 µl of extract was analyzed on LC-ESI-MS/MS

Reference

[1] **Kato T, Kabuto C, Sasaki N, Tsunagawa M, Aizawa H, Fujita K, Kato Y, Kitahara Y and Takahashi N.** Momilactones, growth inhibitors from rice, *Oryza sativa* L. *Tetrahedron Lett.* 1973, 14: 3861-3864

[2] **Kato T, Tsunakawa M, Sasaki N, Aizawa H, Fujita K. Kitahara Y and Takahashi N.** Growth and germination inhibitors in rice husks. *Phytochemistry*. 1977, 16: 45-48

[3] **Nozaki H, Hayashi K, Nishimura N, Kawaide H, Matsuo A, Takaoka D.** Momilactone A and B as allelochemicals from moss Hypnum plumaeforme: first occurrence in bryophytes. *Biosci Biotechnol Biochem.* 2007, 71(12):3127-30.

[4] **Nozaki H, Hamazaki K, Nishimura N, Udaka H, Takashima N and Takaoka D.** Studies on the constituents of Thuidium kanedae SAK. *Proceeding in the 15th International Botanical Congress*, 1993, 370

[5] **Okada K, Kawaide H, Miyamoto K, Miyazaki S, Kainuma R, Kimura H, Fujiwara K, Natsume M, Nojiri H, Nakajima M, Yamane H, Hatano Y, Nozaki H, Hayashi K.** HpDTC1, a Stress-Inducible Bifunctional Diterpene Cyclase Involved in Momilactone Biosynthesis, Functions in Chemical Defence in the Moss Hypnum plumaeforme. *Sci Rep.* 2016, 6:25316

[6] **Tateoka T.** Taxonomic studies of oryza. III. Key to the species and their enumeration. *Bot. Mag.* 1963. 76, 165-173

CHAPTER 6

CONCLUSIVE REMARK AND FUTURE PROSPECT

The biosynthetic pathways of diterpene phytoalexins in rice have been intensively studied for many years. To further understand and completely unlock the biosynthetic route, key intermediates in the pathway were traced in this study. To this end, enzymatically synthesized ^{13}C-labeled *ent*-cassadiene and *syn*-pimaradiene were applied to plants, successfully achieved *in planta* proof of the biosynthetic pathway of phytocassanes and momilactones in rice.

A start point substrate ^{13}C-MVA, which is also supplied by conversion in enzyme cocktail reaction, was converted into *ent*-cassadiene or *syn*-pimaradiene via geranylgeranyl diphosphate (GGDP) with the aid of a series of recombinant enzymes for the production of isopentenyl diphospate and dimethylallyl diphosphate (both building blocks of terpenoids), GGDP synthase, and diterpene cyclases involved in the production of *ent*-cassadiene (OsCPS2 and OsKSL7) and *syn*-pimaradiene (HpDTC1). It would also be effective to have more labeled compound of ^{13}C-GGDP, directly used in the conversion to ^{13}C-diterpene hydrocarbons. For this purpose it can be used the fermentative method with ^{13}C-glucose in an actinomycete, which has strong ability to produce GGDP from glucose via MVA pathway reported by Meguro A *et al* (2015).[1] By coupling of the fermentative GGDP production and expression of the diterpene cyclases in the actinomycete would provide efficient amount of ^{13}C-labeled phytocassanes and momilactones.

Using the prepared ^{13}C-labeled diterpene hydrocarbons, we clearly showed ^{13}C labeling into end product of the pathway in our feeding experiment (Fig. 6-1; Fig. 6-2). However, efficiency of the incorporation of ^{13}C-diterpene hydrocarbons into the diterpene phytoalexins was high enough to be detected but somehow limited. Efforts to enhance the incorporation of ^{13}C-diterpene hydrocarbons by blocking of metabolic pathways leading to natural abundance of cassadiene and pimaradiene using AMO-1618, a potential chemical inhibitor for diterpene cyclase was made in this study. Actually, AMO-1618 treatment to leaf disks exhibits obvious inhibition of inductive production of diterpene phytoalexins. At the same time, this treatment, however, affected incorporation of ^{13}C-diterpene hydrocarbons; AMO-1618 treated samples consequently revealed less accumulation of ^{13}C-momilactones and phytocassanes. Hence, there might be unknown side effects for incorporation of ^{13}C-diterpene on AMO-1618 treatment. In addition, enhanced production of diterpenoid phytoalexins in rice root treated with AMO-1618 was collaterally found in the course of experiments. Currently, the reason why the AMO-1618 inhibitory effect links to the enhanced accumulation of diterpenoid phytoalexins is unclear, it would be possible to occur cross regulation of the metabolic flow between root and shoot or the biosynthetic pathways among diterpenoids by the action of AMO-1618.

An alternative way to enhance the ^{13}C incorporation in plants would be using genetically modified plants, which are defective in the production of *syn*-pimaradiene or *ent*-cassadiene. The application of [U-$^{13}C_{20}$] *syn*-pimara-7,15-diene to a

knockdown mutant of *OsCPS4* and wild-type provided the evidence that [U-$^{13}C_{20}$] momilactones can be biosynthesized in both of *OsCPS4 Tos-17* mutant and wild-type rice plants successfully. However, the accumulation level of [U-$^{13}C_{20}$] momilactones in *OsCPS4 Tos-17* mutant was similar to those of wild-type. On another aspects, ratio of natural abundant and ^{13}C-labeled diterpenoid phytoalexins were clearly different; that is high existence of ^{13}C-compound was evident in the *OsCPS4* T-DNA mutant compared to that of wild-type plant. Therefore, such approach with genetically modified plant would be promising ways to detect more intensive ^{13}C-signal from diterpenoid intermediate of interest.

In addition to the proof of biosynthetic route leading to diterpene phytoalexins from *ent*-cassadiene and *syn*-pimaradiene in rice, this feeding system successfully traced out the ^{13}C-signal in *L. perrieri* (a phytocassanes producer) and *H. plumaeforme* (a momilactones producing moss) (Fig. 6-3). It has previously been reported that *L. perrieri* could produce non-C2-hydroxylated type phytocassane C and phytocassane E, but not C2-hydroxylated types of phytocassane A, phytocassane B, and phytocassane D, suggesting that position C2-hydroxylation does not occur in *L. perrieri*. In the labeling experiments also revealed that phytocassane C and phytocassane E were the only ^{13}C-labeled phytocassanes detected, further supporting the existing of distinctive biosynthetic pathway for phytocassanes in *L. perrieri* (Fig. 6-2; Fig. 6-3). In the application to the moss *H. plumaeforme*, ^{13}C-labeled *syn*-pimaradiene was also successfully incorporated into momilactones produced in *H. plumaeforme* (Fig. 6-3). In previous report, a bifunctional *syn*-pimaradiene synthase *HpDTC1* gene has been identified on the basis of RNA-seq analysis. Since *syn*-pimaradiene accumulation in the moss treated by $CuCl_2$ was not observed whereas the accumulation was clearly detected in the case of rice leaves elicited by UV irradiation, a metabolic flow via *syn*-pimaradiene in *H. plumaeforme* might be rather faster compared to that in rice. Besides, subsequent biosynthetic pathway consisting of P450 monooxygenases in the moss seems to be somehow different from the pathway in rice; CYP99A2 and A3 or CYP71Z7 and CYP76M7, M8 are shown to be responsible for the either momilactones or phytocassanes production in rice, however, similar homologs with high homology were not found in the RNA-seq data. Seeking of ^{13}C-labeled intermediates, which is converted from ^{13}C-pimaradiene, might be possible approach that will be able to find a biosynthetic pathway committed by as yet unknown P450 enzymes distinctive in the moss. Further applications could also be possible to focus on the degradation of diterpenoid phytoalexins in natural environment, which might occur in rhizosphere around the plants producing such bioactive diterpenoid phytoalexins, by using biotransformed ^{13}C-labeled compounds.

Regarding the application of this feeding system on the biosynthetic mutants responsible for the diterpenoid phytoalexins production, some unknown compounds were able to find to be ^{13}C-labeled substances, which are likely to be intermediates of diterpenoid phytoalexins. However, in some cases, none of ^{13}C labeled products could be detected from [U-$^{13}C_{20}$] *ent*-cassa12,15-diene in *CYP76M7/M8* RNAi lines, though an unlabeled unknown compound was detected. In another case, it is also indicated that possible candidate of cold phytocassane intermediates, 2-deoxyphytocassane A

and 1-deoxyphytocassane C, were accumulated in CYP71Z6/Z7 T-DNA mutant, but these corresponding ^{13}C-labeled substances were hardly detected in the mutant. This might be because low efficiency of incorporation level of ^{13}C-labeled compound and/or dilution by natural abundant compound in the system makes it difficult to detect on the analysis on LC-MSMS. Improvement of ^{13}C-incorporation to target substances will be important clue to overcome this issue, and combination of biosynthetic mutants responsible for upper pathway in the biosynthetic route has to be used in this feeding experiments.

In this study, a feasible method for feeding of ^{13}C-labeled diterpene hydrocarbons, [U-$^{13}C_{20}$] *ent*-cassa-12,15-diene and [U-$^{13}C_{20}$] *syn*-pimara-7,15-diene, which can be systematically synthesized from [U-$^{13}C_6$] MVA in enzymes cocktail was successfully established. Bioconversion of [U-$^{13}C_{20}$] phytocassane (A-E) and [U-$^{13}C_{20}$] momilactone (A and B) in rice plants was achieved for the first time, and indicated genuine biosynthetic routes obviously existed in the plants more than rice, which are known as diterpenoid phytoaexin producers, the moss *H. plumaeforme* and a nearest species of *Oryza* family *L. perrieri*. This labeling method was also confirmed as a powerful tool for intermediates investigation, leading to unlocking of diversification and complexity of diterpenoid phytoalexins produced in plant species.

In *CYP76M7/M8* RNAi lines and *CYP71Z7* T-DNA mutant, 5 intermeidates or end-products were found and most of their reaction steps were also clarified. Phytocassanes biosynthetic pathway was proposed (Fig. 6-4).

In continuing study of much detailed observations into mass spectra from ^{13}C-labeled compounds, *in vitro* substrate-enzymes assay is required for proposed pathway validation.

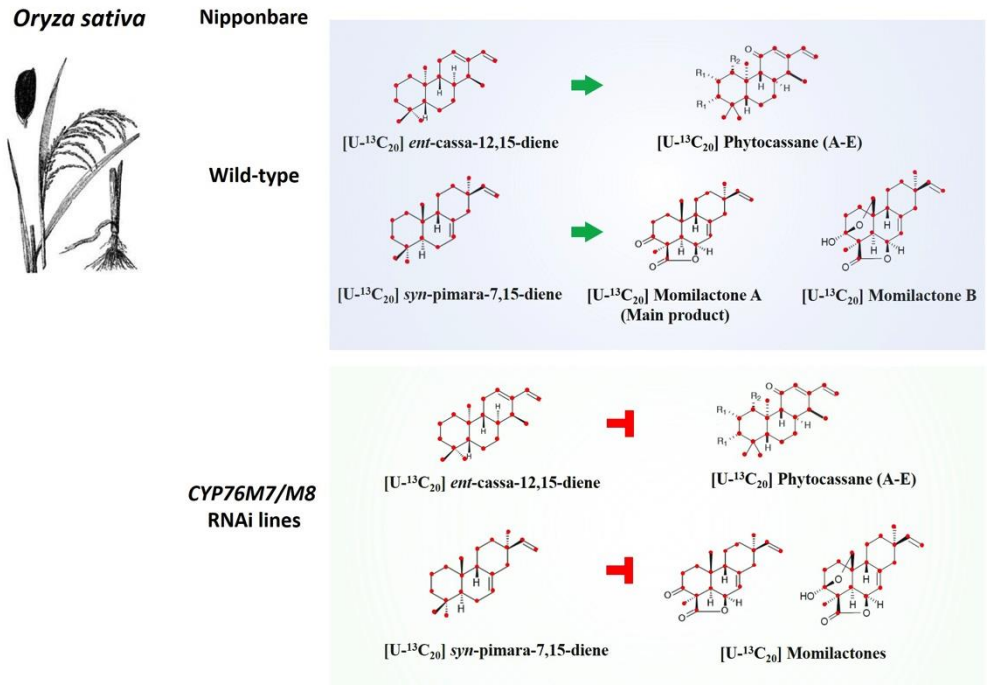

Figure 6-1. The conversion of [U-$^{13}C_{20}$] *ent*-cassa-12,15-diene and [U-$^{13}C_{20}$] *syn*-pimara-7,15-diene in wild-type and *CYP76M7/M8* RNAi rice plants (*O. sativa* L. cv Nipponbare)

Green arrow indicated exogenous labeling substrates can be converted to end products in vivo;
Red pause indicated exogenous labeling substrates conversion was repressed in this plant.

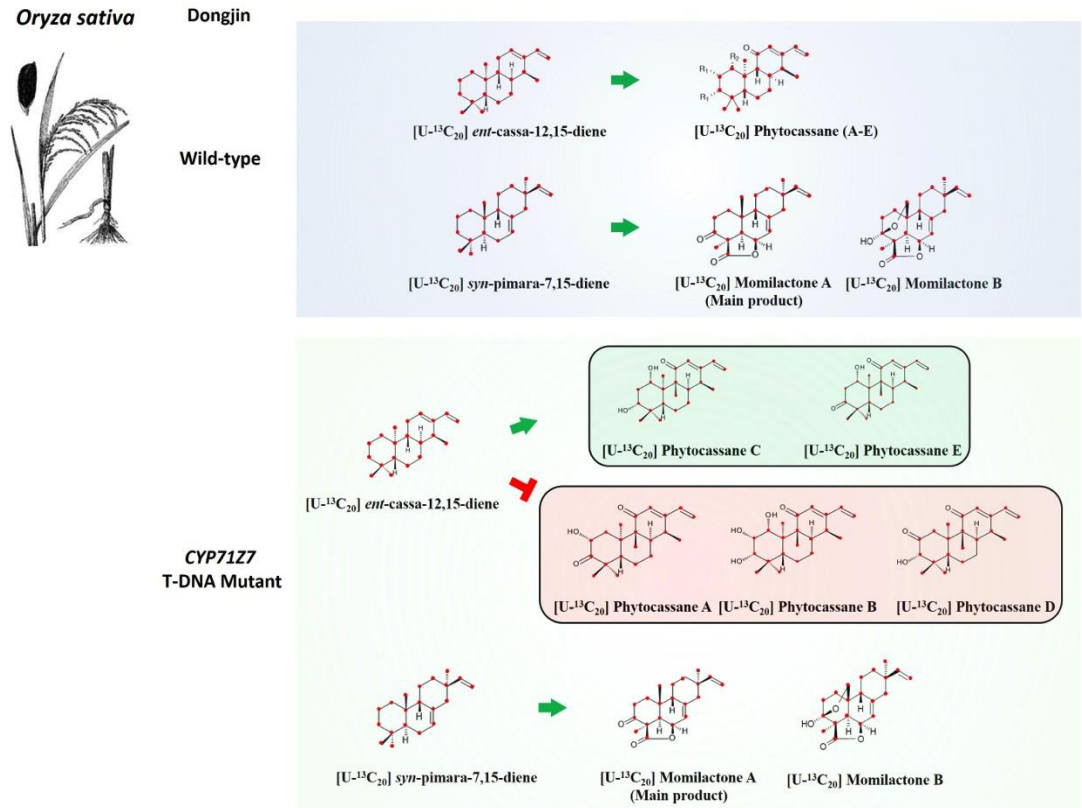

Figure 6-2. The conversion of [U-$^{13}C_{20}$] *ent*-cassa-12,15-diene and [U-$^{13}C_{20}$] *syn*-pimara-7,15-diene in wild-type and *CYP71Z7 T-DNA mutant* (*O. sativa* L. cv Dongjin)

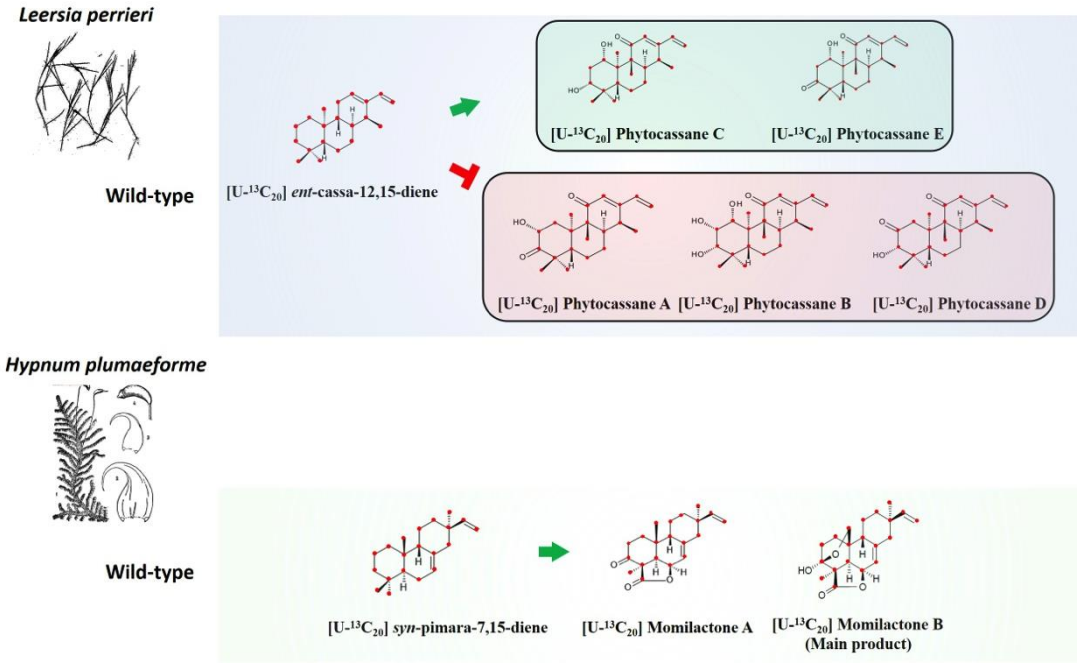

Figure 6-3. The conversion of [U-$^{13}C_{20}$] *ent*-cassa-12,15-diene in wild-type *L. perrieri* and [U-$^{13}C_{20}$] *syn*-pimara-7,15-diene in wild-type *H. plumaeforme*

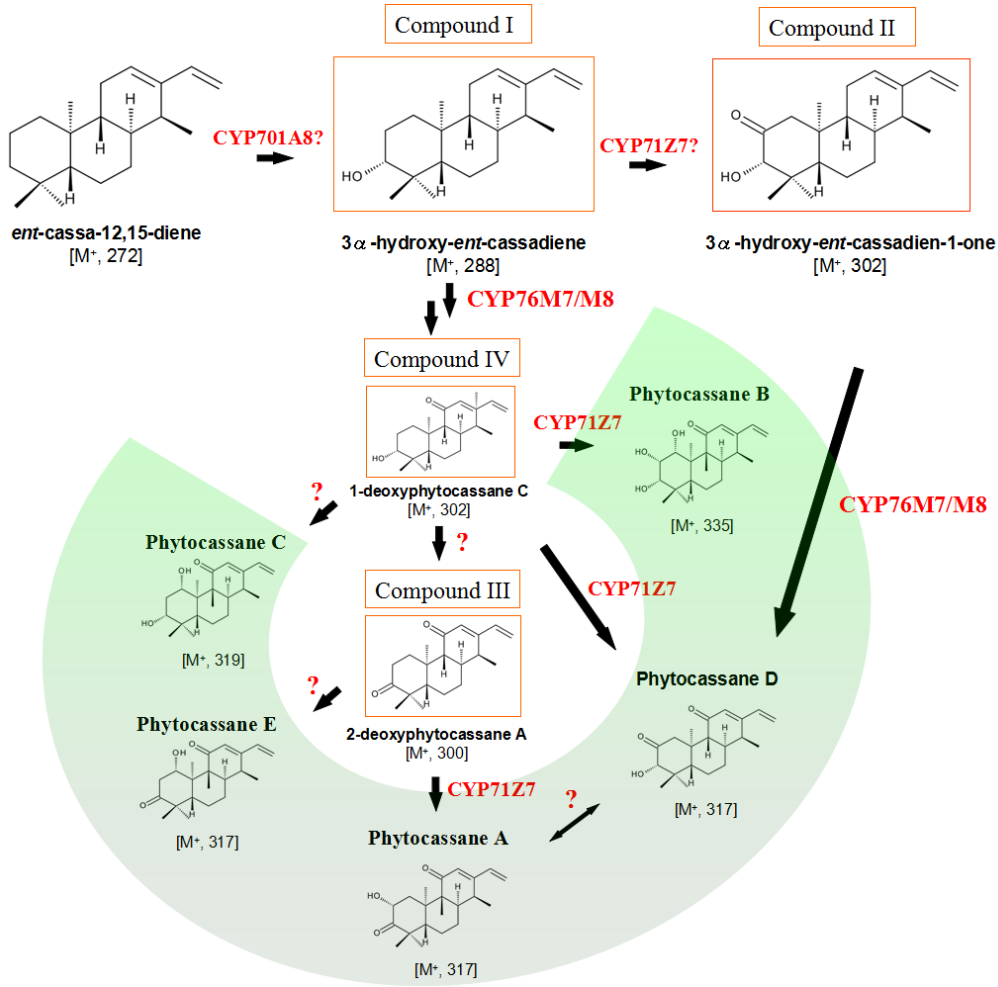

Figure 6-4. Proposed phytocassanes biosynthetic pathway.

Reference

[1] **Meguro A, Motoyoshi Y, Teramoto K, Ueda S, Totsuka Y, Ando Y, Tomita T, Kim SY, Kimura T, Igarashi M, Sawa R, Shinada T, Nishiyama M, Kuzuyama T.** An unusual terpene cyclization mechanism involving a carbon-carbon bond rearrangement. *Angew Chem Int Ed Engl.* 2015. 54(14): 4353-4356

Appendix

Appendix

S-I. Incubation time for $CuCl_2$ treatment

Methods

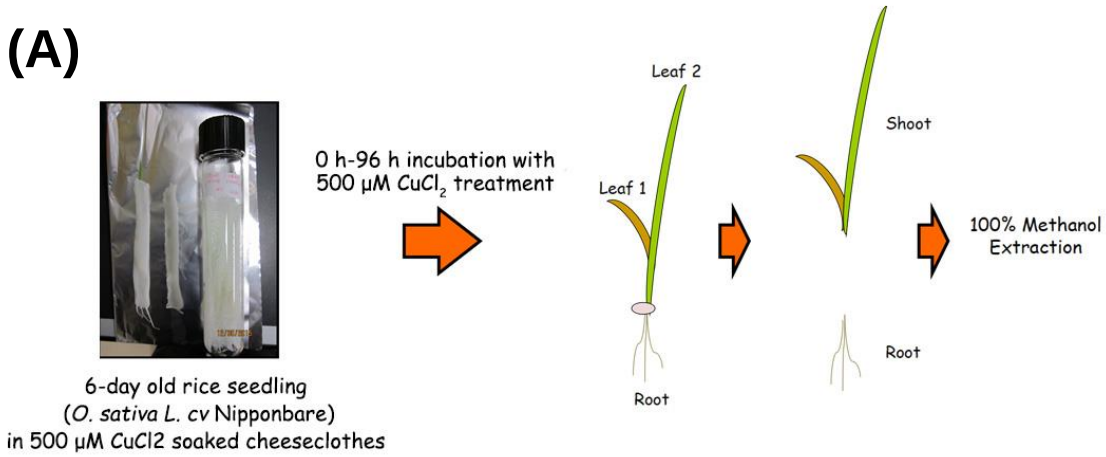

Results

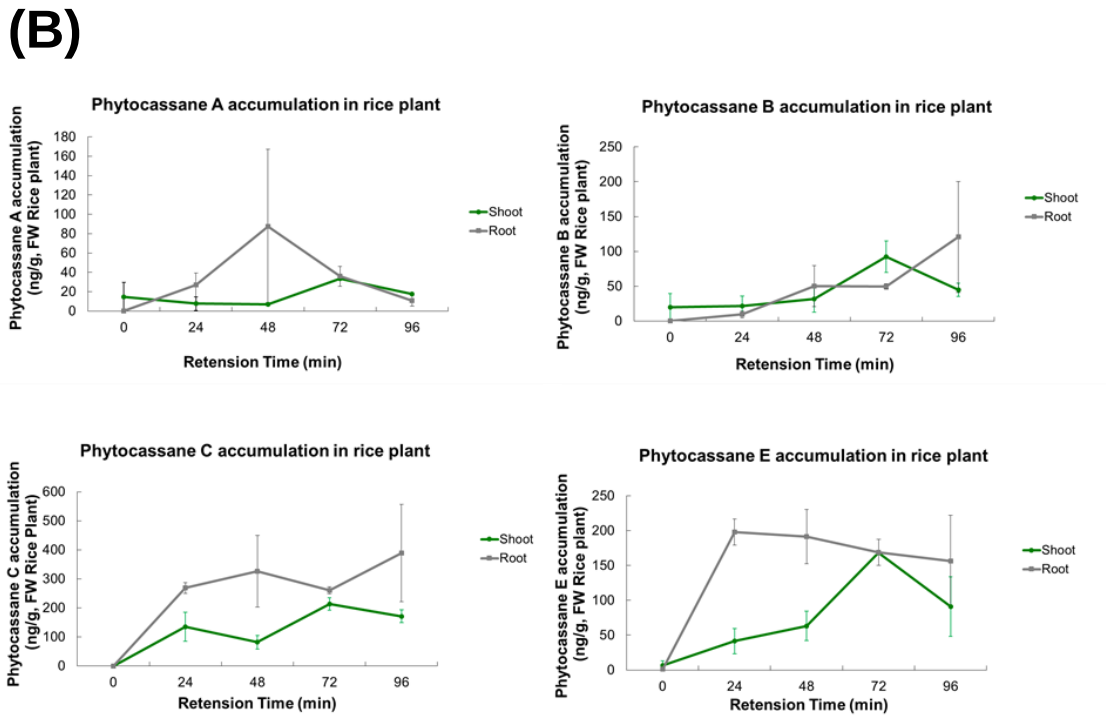

Figure S-1. Phytocassanes accumulation level in time course with 500 µM $CuCl_2$ treatment in cheesecloths

A, Method for 500 µM $CuCl_2$ treatment on 6-day old rice seedling in cheesecloths based on time course (0 h-96 h); **B,** The variation of phytocassane (A, B, C and E) level based on time course in shoots and roots . 5 µl of each extract was subjected to LC-ESI-MS/MS; n=3

S-II. The amount and times for [U-$^{13}C_{20}$] *ent*-cassa-12,15-diene feeding

Method

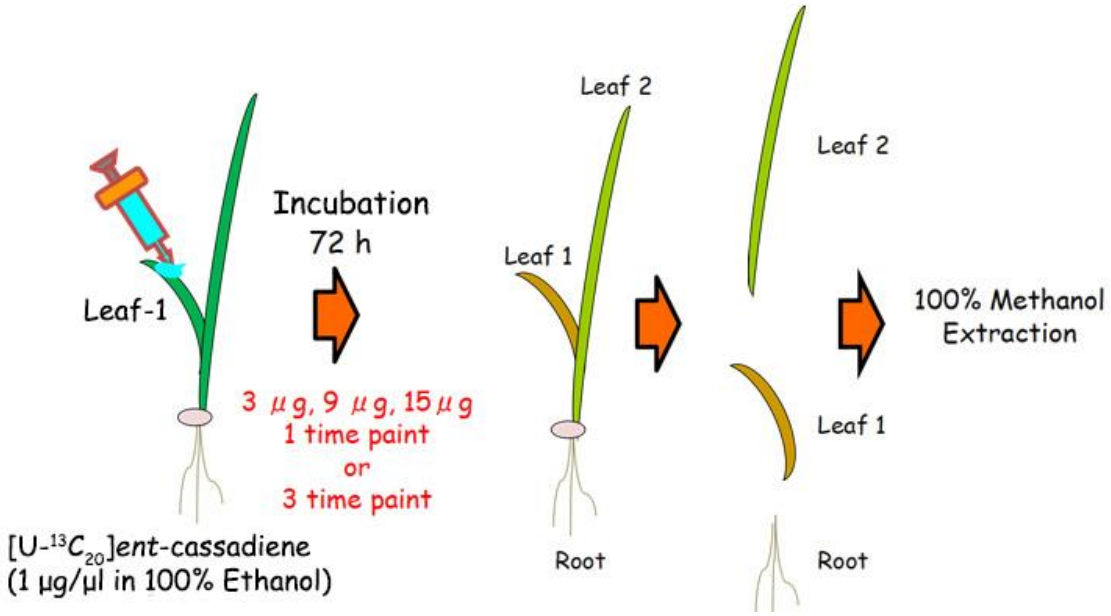

Figure S-2. A schematic diagram of feeding experiment on 6-day old rice seedling (leaf-1) in 500 μM $CuCl_2$ soaked cheesecloths.

1 time paint: 3 μg, 9 μg or 15 μg of [U-$^{13}C_{20}$] *ent*-cassadiene was applied to leaf-1 at 0 h, respectively; **3 times paint:** 1 μg, 3 μg or 5 μg was applied to leaf-1 at 0h respectively. Same feeding amount (1 μg, 3 μg or 5 μg) was further applied to the same position (leaf-1) at 24 h and 48 h, respectively.

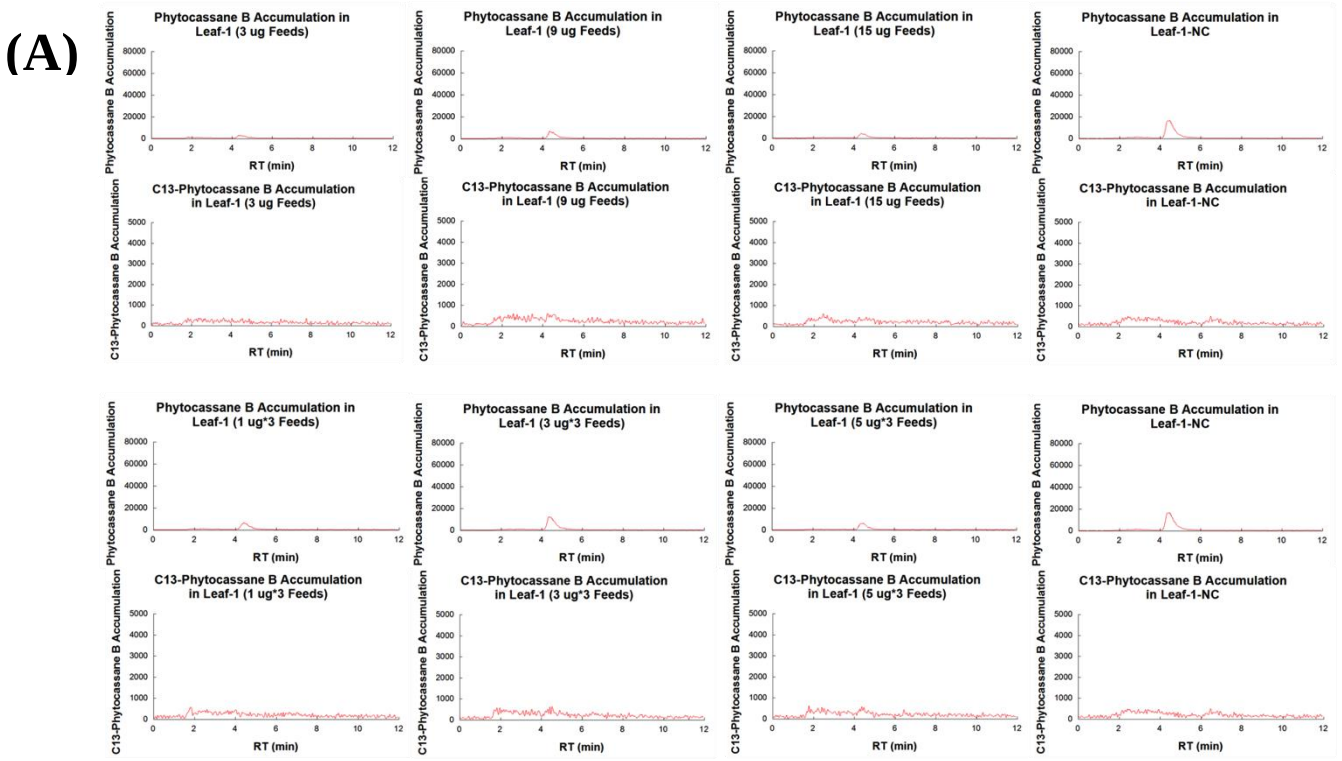

Figure S-3. Optimization of [U-$^{13}C_{20}$] *ent*-cassa-12,15-diene feeding condition in leaf-1 labeling experiment.

[The application of [U-$^{13}C_{20}$] *ent*-cassa-12,15-diene (3 µg, 1 µg*3, 9 µg, 3 µg*3, 15 µg and 5 µg*3) to leaf-1] **A,** Phytocassane B and [U-$^{13}C_{20}$] phytocassane B accumulation level in leaf-1, which is the only position be painted with [U-$^{13}C_{20}$] *ent*-cassa-12,15-diene directly; **B,** Phytocassane B and [U-$^{13}C_{20}$] phytocassane B accumulation level in leaf-2; **C,** Phytocassane B and [U-$^{13}C_{20}$] phytocassane B accumulation level in root; **DEF,** Phytocassane C and [U-$^{13}C_{20}$] phytocassane C accumulation level in leaf-1, leaf-2 and root, respectively; **GHI,** Phytocassane E and [U-$^{13}C_{20}$] phytocassane E accumulation level in leaf-1, leaf-2 and root, respectively; Red arrow indicated a suitable condition for [U-$^{13}C_{20}$] phytocassane (B, C and E) biosynthesis in rice plants; 5 µl of each extract was subjected to LC-ESI-MS/MS; N=1

Phytocassane B and [U-$^{13}C_{20}$] Phytocassane B accumulation in leaf-2

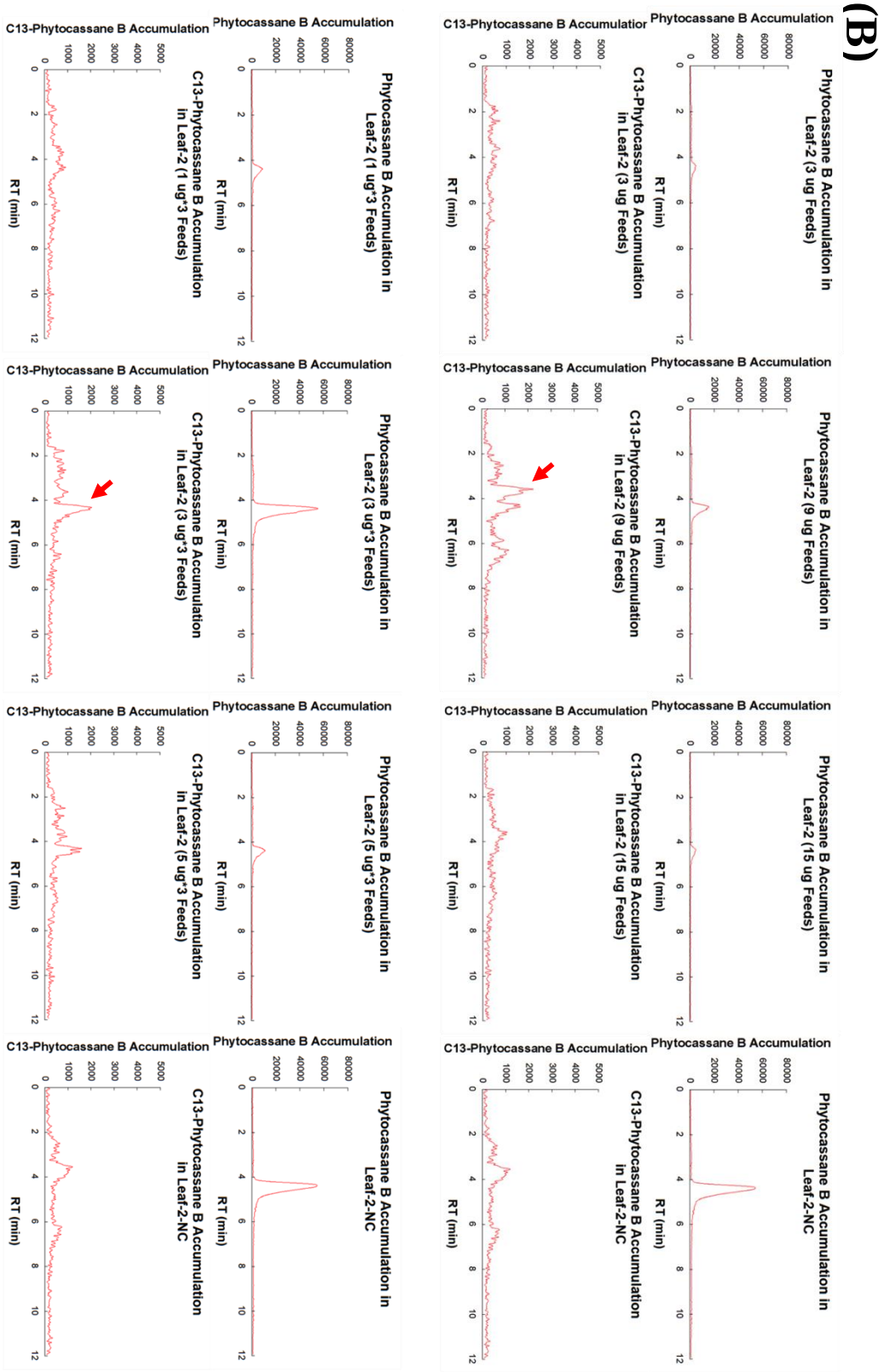

Figure S-3. Continued

phytocassane B and [U-$^{13}C_{20}$] Phytocassane B accumulation in root

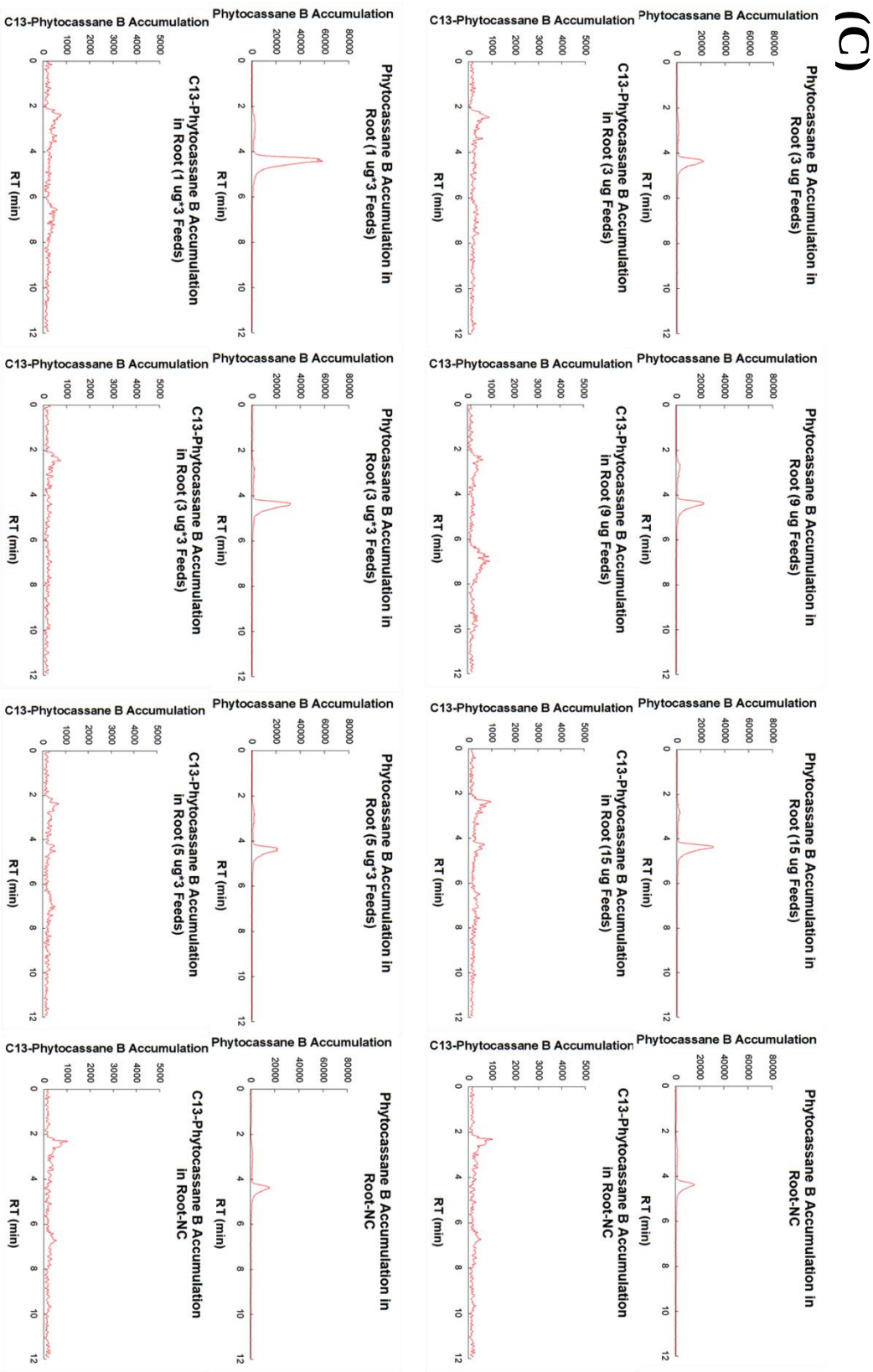

Figure S-3. Continued

Phytocassane C and [U-$^{13}C_{20}$] Phytocassane C accumulation in leaf-1

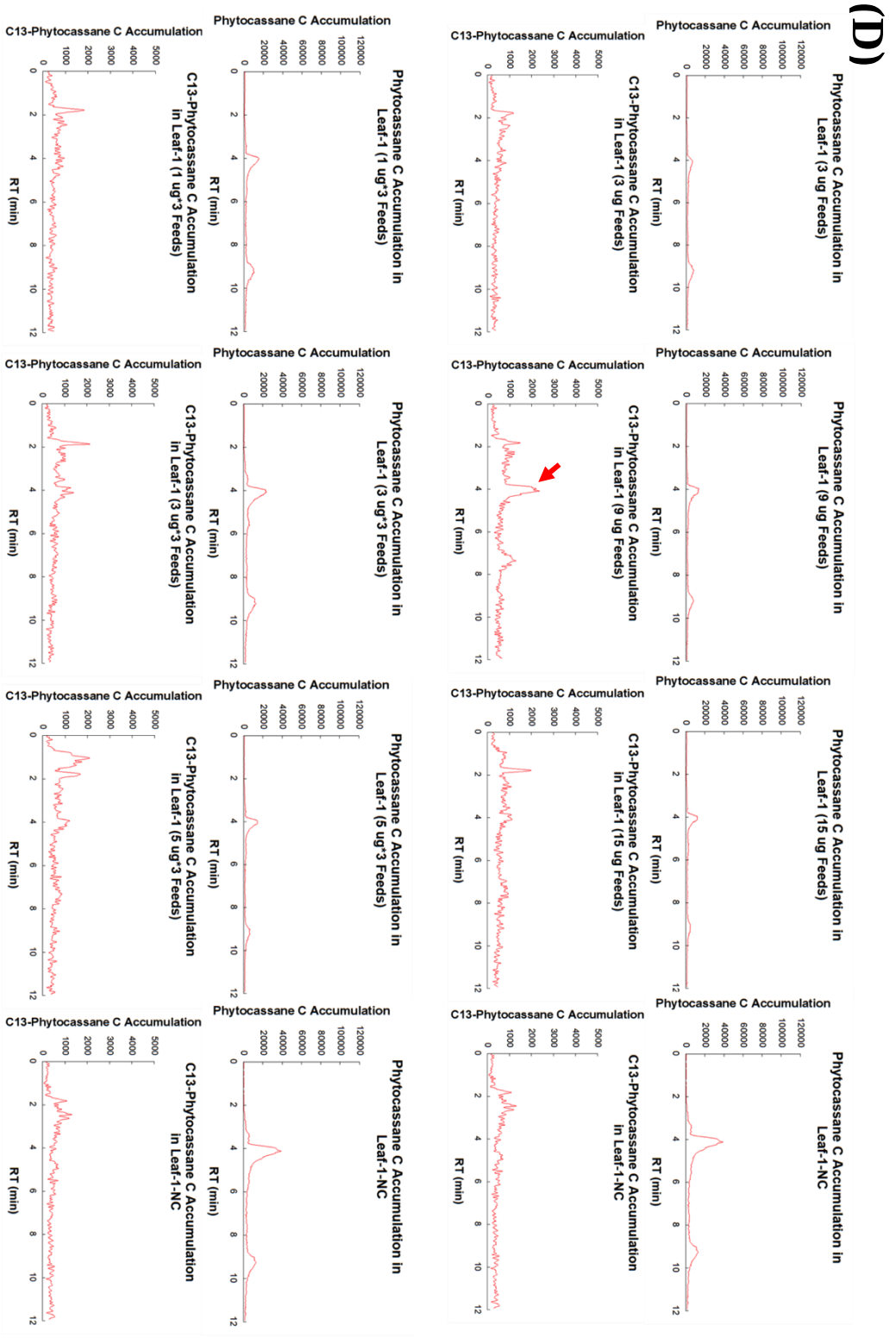

Figure S-3. Continued

Phytocassane C and [U-$^{13}C_{20}$] Phytocassane C accumulation in leaf-2

(E)

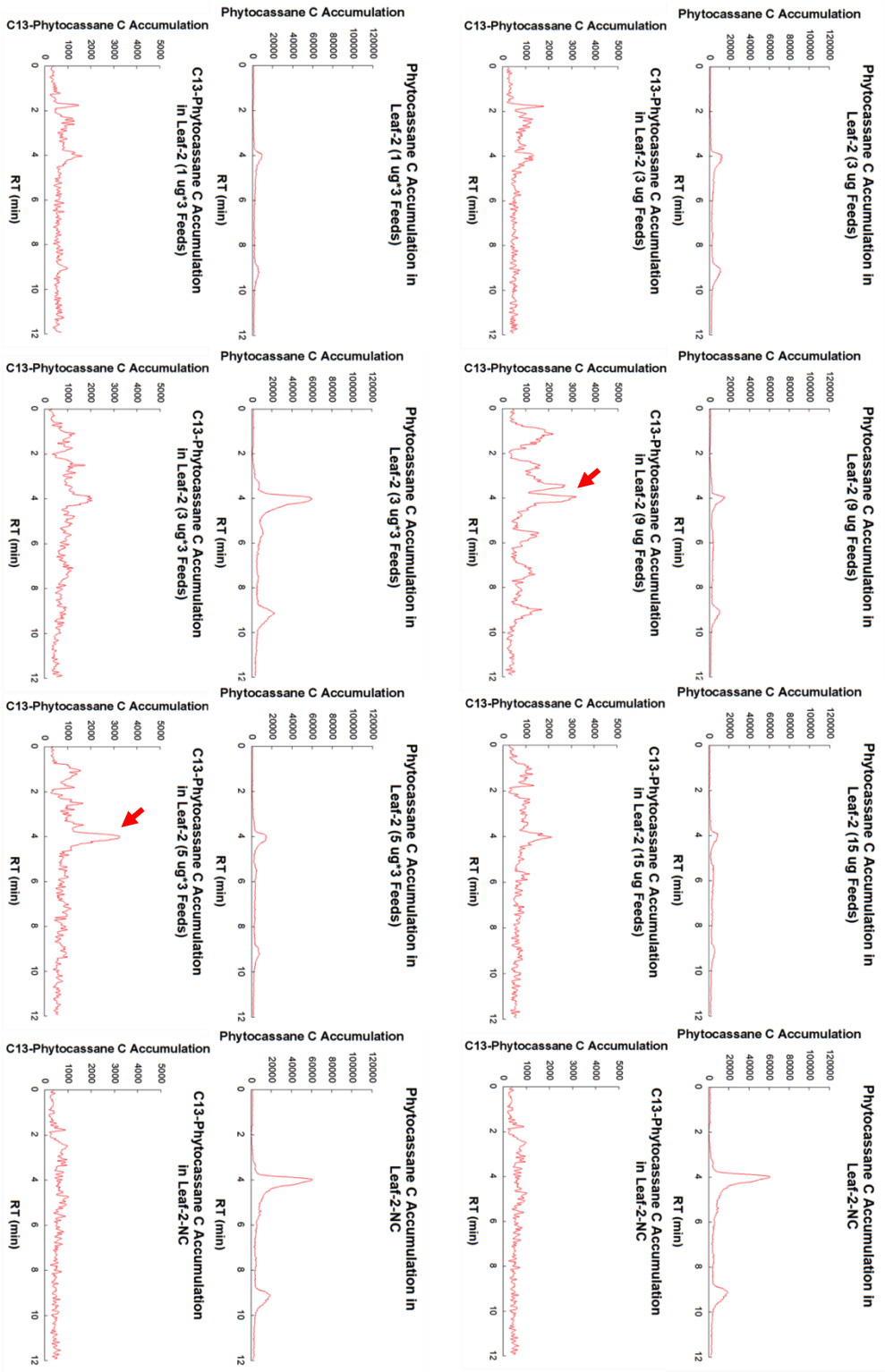

Figure S-3. Continued

Phytocassane C and [U-$^{13}C_{20}$] Phytocassane C accumulation in root

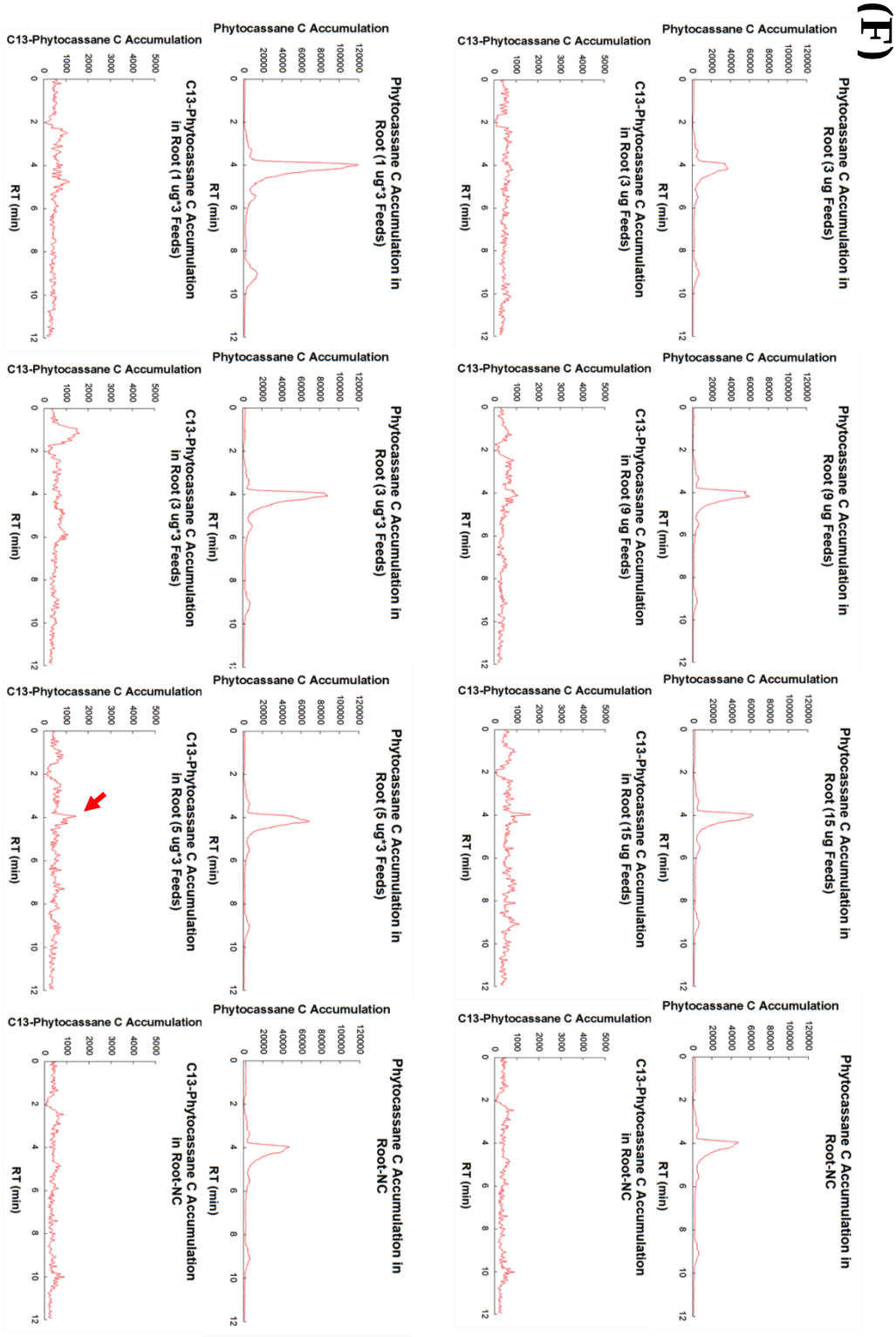

Figure S-3. Continued

Phytocassane E and [U-$^{13}C_{20}$] Phytocassane E accumulation in leaf-1

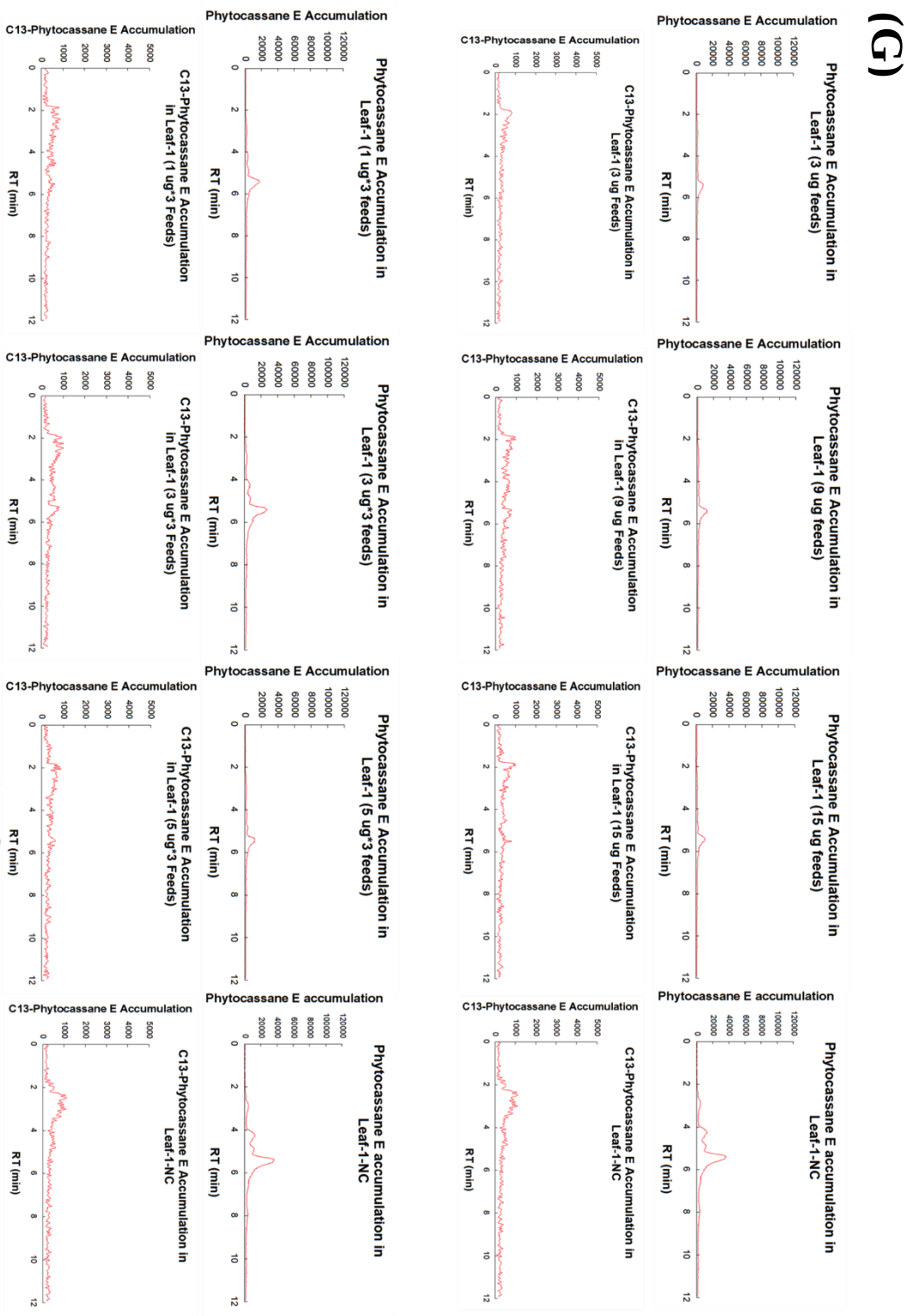

Figure S-3. Continued

Phytocassane E and [U-$^{13}C_{20}$] Phytocassane E accumulation in leaf-2

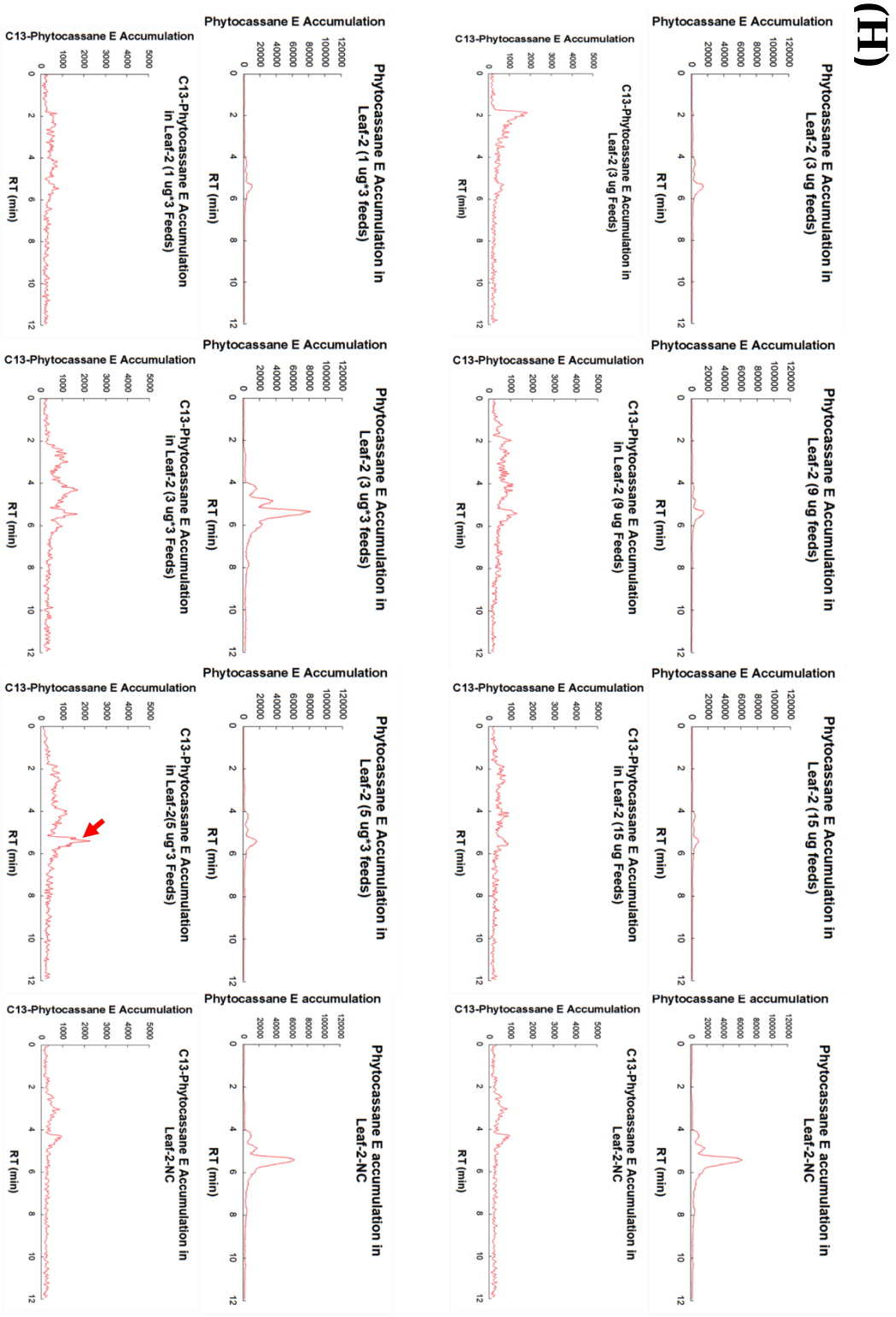

Figure S-3. Continued

Phytocassane E and [U-$^{13}C_{20}$] Phytocassane E accumulation in root

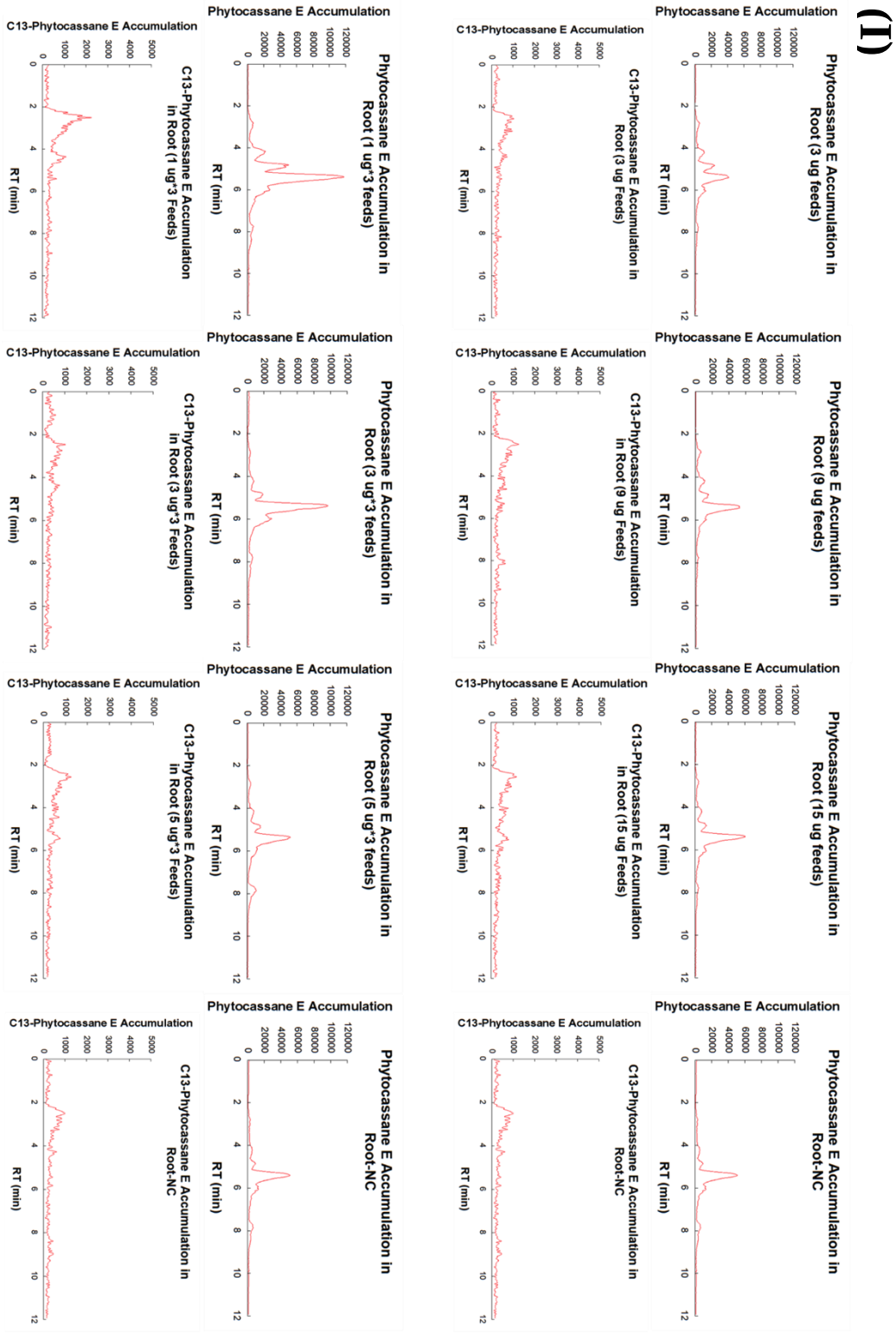

Figure S-3. Continued

S-III. Incubation time for 9 µg of [U-$^{13}C_{20}$] *ent*-cassa-12,15-diene labeling

Methods

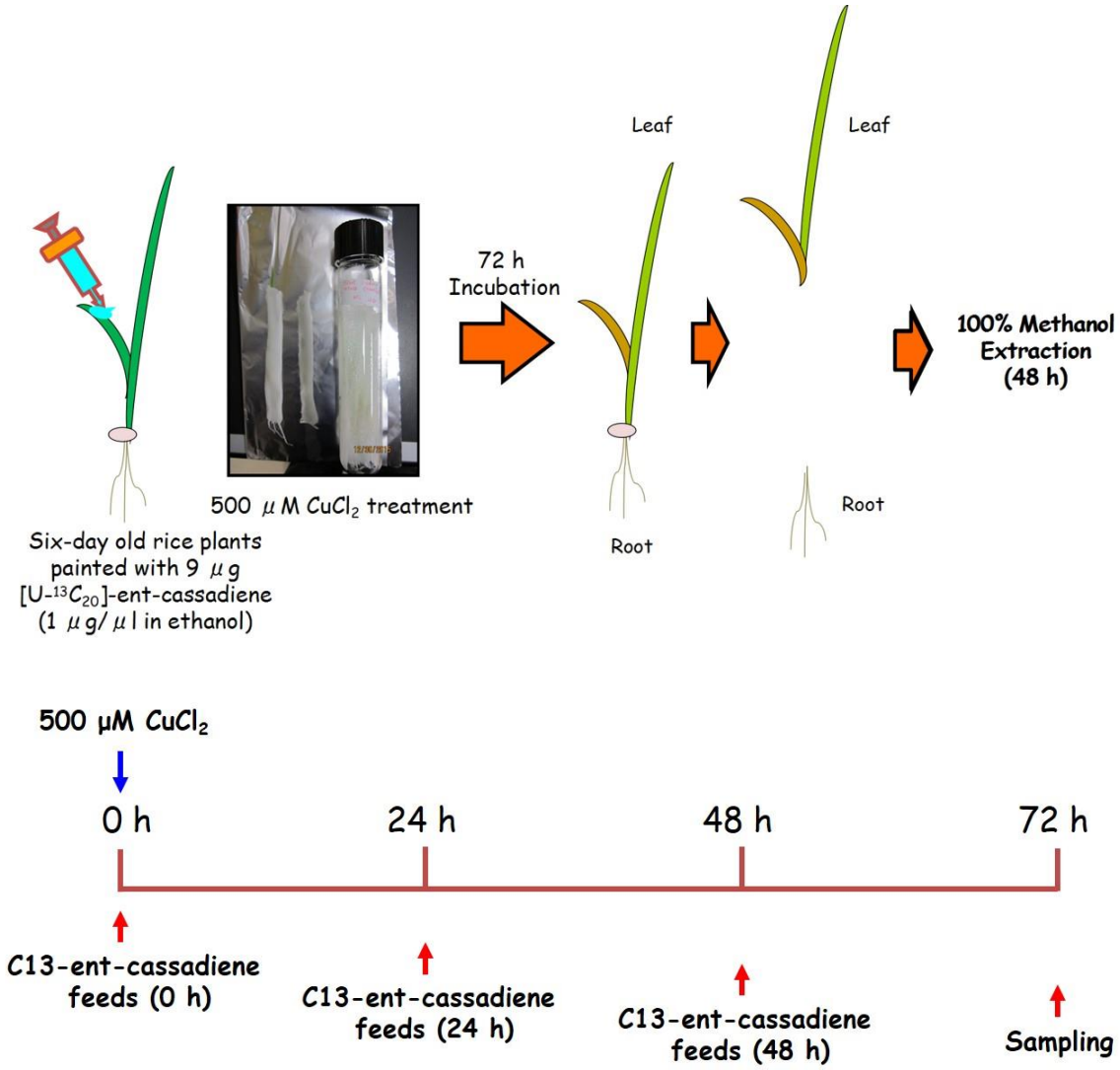

Figure S-4. Optimization of [U-$^{13}C_{20}$] *ent*-cassadiene feeding condition (time course) in leaf-1 for [U-$^{13}C_{20}$] phytocassanes accumulation.

Results

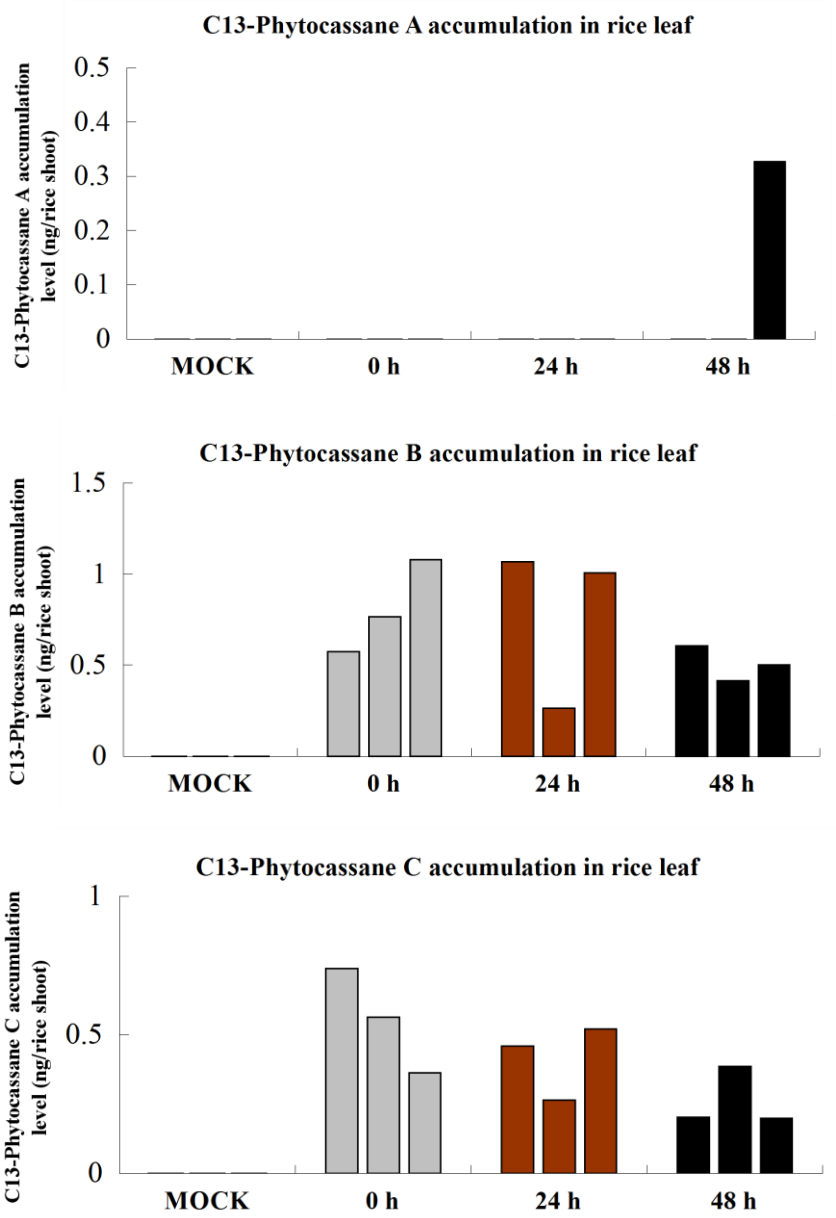

Figure S-5. [U-$^{13}C_{20}$] phytocassanes accumulation level with [U-$^{13}C_{20}$] *ent*-cassadiene feeding based on time course.

MOCK, 9 µl of 99.5% ethanol was incubated with leaf-1 for 72 h; **0h,** 9 µg of [U-$^{13}C_{20}$] *ent*-cassa-12,15-diene was painted to three rice plants (leaf-1) at 0 h; **24 h,** 9 µg of [U-$^{13}C_{20}$] *ent*-cassa-12,15-diene was painted to three rice plants (leaf-1) at 24 h with 500 µM CuCl2 elicitation; **48h,** 9 µg of [U-$^{13}C_{20}$] *ent*-cassa-12,15-diene was painted to three rice plants (leaf-1) at 48 h with 500 µM CuCl2 elicitation. Rice plants were incubated in 500 µM CuCl2 soaked cheesecloths for 72 h. 5 µl of each sample was subjected to LC-ESI-MS/MS. n=3

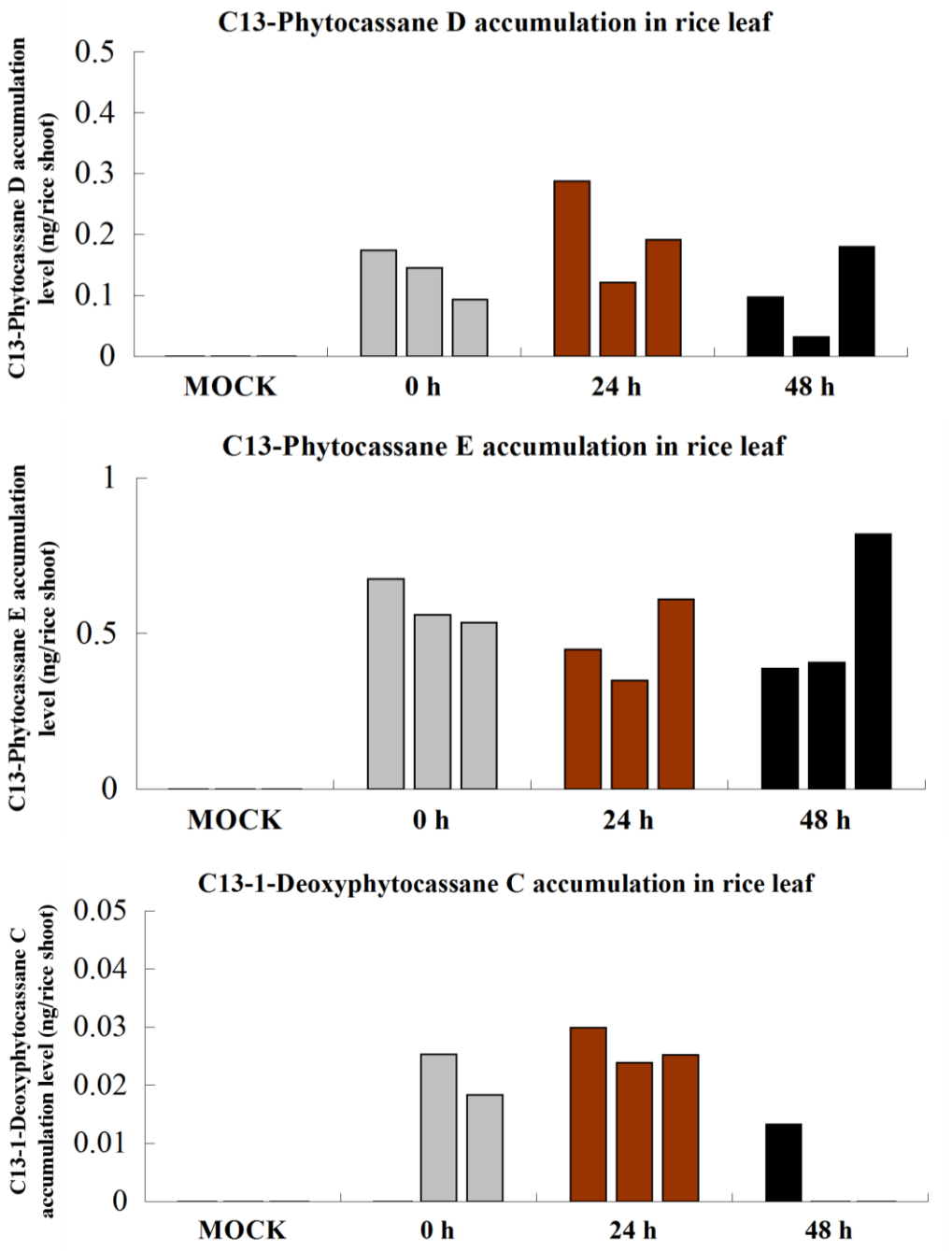

Figure S-5. Continued

S-IV. Organic solvent selection for feeding experiment in leaf disk

Methods

[U-$^{13}C_{20}$] *syn*-pimara-7,15-diene was performed on rice leaves. In the application of 1 μg of [U-$^{13}C_{20}$] *syn*-pimara-7,15-diene to rice leaf disk, three solvent, ethanol (99.5%), methanol (100%) and *n*-hexane (100%), were used for feeding experiment (Fig. S-6). LC-MS/MS results from each extract confirmed [U-$^{13}C_{20}$] momilactone A and B can be converted from [U-$^{13}C_{20}$] *syn*-pimara-7,15-diene in leaf disc (Fig. S-7). Furthermore, ethanol (99.5%) was demonstrated as the best organic solvent for [U-$^{13}C_{20}$] *syn*-pimara-7,15-diene feeding on rice leaves (Fig. S-7).

Results

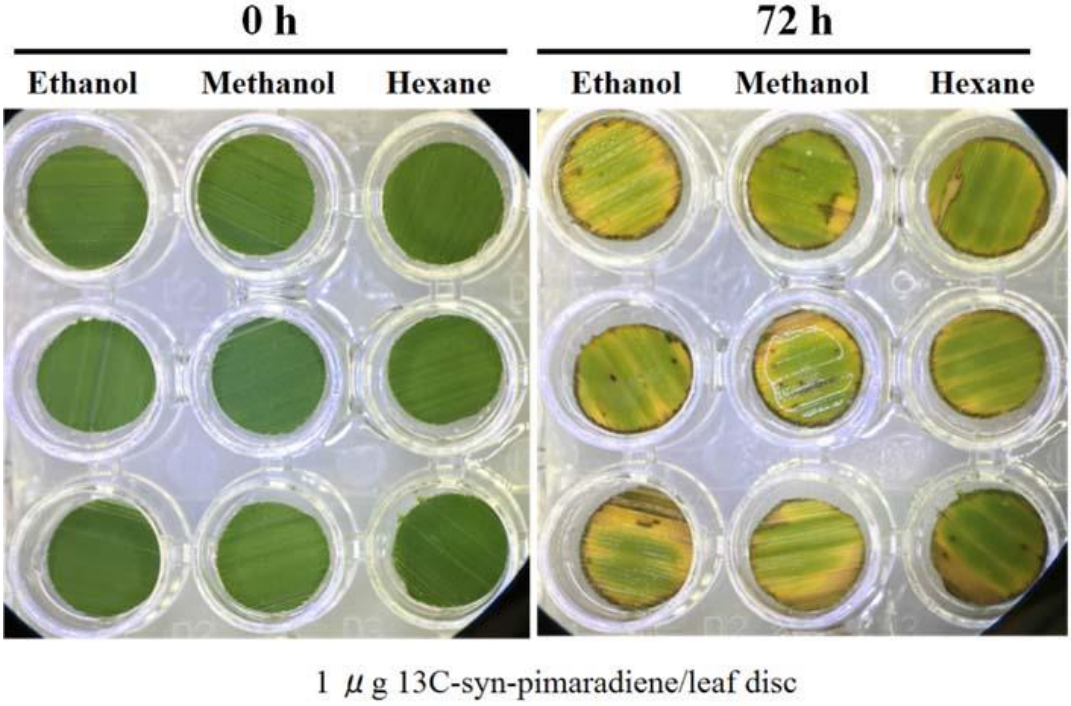

Figure S-6. [U-$^{13}C_{20}$] *syn*-pimara-7,15-diene dissolved in different organic solvent was applied to wild-type leaf disks (*O. sativa* L.cv. Nipponbare)

Left pane, Ethanol (99.5%), methanol (100%) or n-hexane (100%) dissolved [U-$^{13}C_{20}$] *syn*-pimara-7,15-diene (1 μg/μl) painting on leaf disk at 0 h, respectively. **Right pane,** leaf disks with [U-$^{13}C_{20}$] *syn*-pimara-7,15-diene feeding after 72 h incubation. All leaf disks were treated with 500 μM $CuCl_2$ soaked cheesecloths.

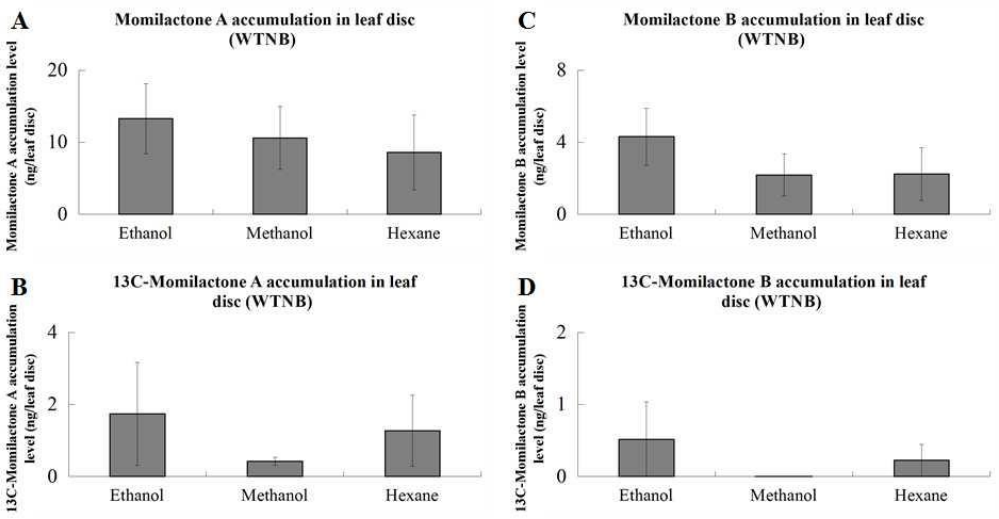

Figure S-7. Momilactones and [U-$^{13}C_{20}$] momilactones accumulation level in leaf disks with different organic solvent dissolved [U-$^{13}C_{20}$] *syn*-pimara-7,15-diene feeding.

A, Momilactone A accumulation level in wild-type leaf disk; **B,** [U-$^{13}C_{20}$] momilactone A accumulation level in wild-type leaf disk; **C,** Momilactone B accumulation level in wild-type leaf disk; **D,** [U-$^{13}C_{20}$] momilactone B accumulation level in wild-type leaf disk. Each 5 μl of extract was analyzed on LC-ESI-MS/MS

S-V. The effect of AMO-1618 on phytocassanes and momilactones accumulation in rice callus

Materials and Methods

Cell Culture

N6 Medium (1 liter)

20x CHU (N6) Basal Salt Mixture (Sigma) 50 ml containing components (KNO_3 2830 mg, $(NH_4)SO_4$ 463 mg, $CaCl_2{\cdot}2H_2O$ 125.3 mg, $MgSO_4{\cdot}7H_2O$ 90.37 mg, K_3PO_4 400 mg, $FeSO_4{\cdot}7H_2O$ 27.85, Na_2-EDTA 37.25 mg, $MnSO_4{\cdot}H_2O$ 3.3 mg, $ZnSO_4{\cdot}7H_2O$ 1.5 mg, KI 0.8 mg). 1000x Murashige and Skoog Vitamin Mixture (Sigma) 1 ml (H_3BO_3 1.6 mg, Nicotinic acid 0.5 mg, Thiamine-HCl 0.1 mg, Pyridoxine-HCl 0.5 mg, Myo-Inositol 100 mg, Glycine 2 mg). Sucrose 30000 mg. 2,4-D (3 mg/ml) 1 mg. Medium pH was adjusted to 5.8 with KOH. 3 g agar was added to N6 medium for making 1 liter solid N6D medium,. [6]

To investigate the effect of AMO-1618 on callus, rice seeds (*O. sativa* L. cv. Nipponbare) were also sterilized by 70% alcohol and 5% HClO solution following dehusking. Seeds were further washed by MilliQ water in clean bench for 5 times at least. Thereafter, sterile seeds were planted in prepared solid N6D medium. Then it was cultured in dark. After 8 days incubation, new produced callus were transferred to a fresh N6D solid medium plate. Following another 2 weeks incubation, callus were further cultured in 30 ml of N6 medium and shake on a rotor (120 rpm) in 25℃ dark. This rice cells were harvested every 2 weeks and collected on a 20-mesh filter by a 10

ml of glass pipet. All aggregated rice cells were separated through this 20-mesh filter. In each of collection, 2 ml of aliquot of resulting callus were transferred to 30 ml of fresh N6 medium and further cultured on shaker.[6]

The application of AMO-1618 on wild-type rice callus (O. sativa L. cv. Nipponbare)

A stock solution of chitin oligosaccharide and AMO-1618 were added to rice cells at 7th day following the transfer to 30 ml of fresh N6 medium. The final concentration of chitin oligosaccharide and AMO-1618 reached to 1.24 μM and 200 μM, respectively (Fig. S-8). The callus with different treatment was incubated on a rotary shaker at 120 rpm and 25℃ in the dark. 50 μl of medium was collected at 0 h, 12 h, 24 h, 36 h, 48 h, 60 h, 72 h, 96 h after different treatment. 3 parallel repetition was set at each time point. The resulting medium after incubation was extracted with 65 μl of ethyl acetate for 3 times. About 150 μl of ethyl acetate extract was evaporated to dryness by centrifugal vacuum. The residual was dissolved in 200 μl of phytoalexins extraction solvent (79% EtOH, 13.99% H_2O, 7% MeCN, 0.01% AcOH) (Fig. S-8). 5 μl of resultant extract was subjected to LC-MS/MS.

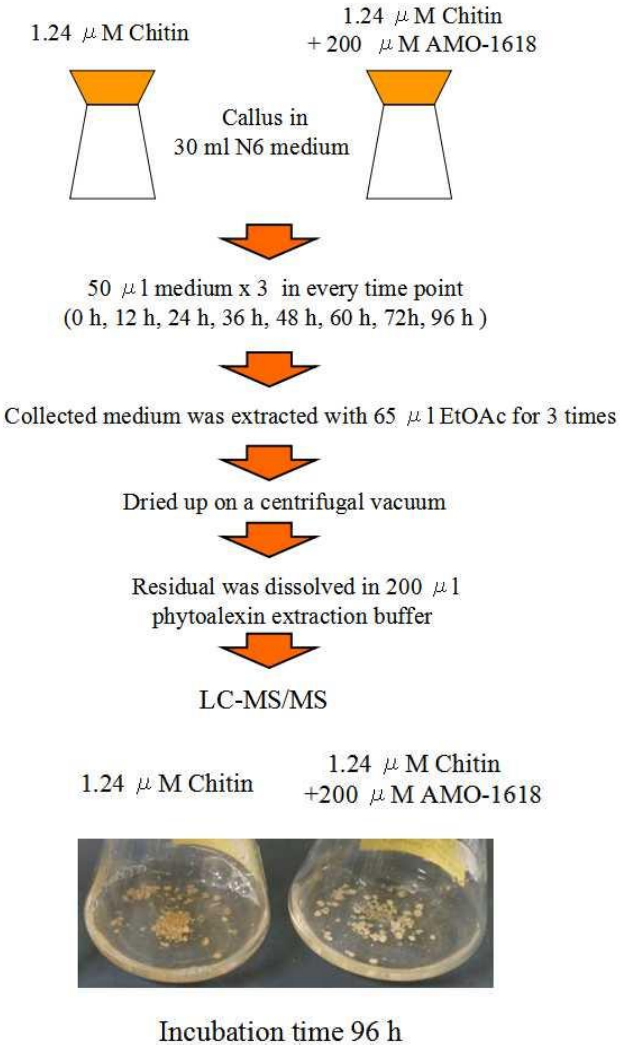

Figure S-8. The method for extraction from chitin oligosaccharides and AMO-1618 treated rice callus.

Results

The effect of AMO-1618 on phytoalexins accumulation in rice callus (O. sativa L. cv. *Nipponbare)*

In wild-type rice cells (*Oryza sativa* L. cv. Nipponbare), our results suggested phytocassanes and momilactones were strongly elicited with 1.24 μM chitin oligosaccharides after 24 h incubation (Fig. S-9). LC-ESI-MS/MS analysis further indicated that phytocassane (C, E) and momilactone B were the main products in rice cells under 1.24 μM chitin oligosaccharides elicitation (Fig. S-9). Simultaneously, another group of rice cells were treated with 1.24 μM chitin and 200 μM AMO-1618. Resulting results showed that both of phytocassanes and momilactones accumulation were strongly inhibited by 200 μM AMO-1618 relative to those of without AMO-1618 treatment. Some papers have reported that AMO-1618 act as a CPP synthase inhibitor in both of higher plants and fungus *Gibberella fujikuroi*.[12-14] It also have a weak inhibition effect on *ent*-kaurene synthase activity.[14] Token together, we concluded AMO-1618 may strongly inhibit CPS 2 and CPS 4 activity and further block the pathway from GGDP to phytocassanes and momilactones in rice cells.

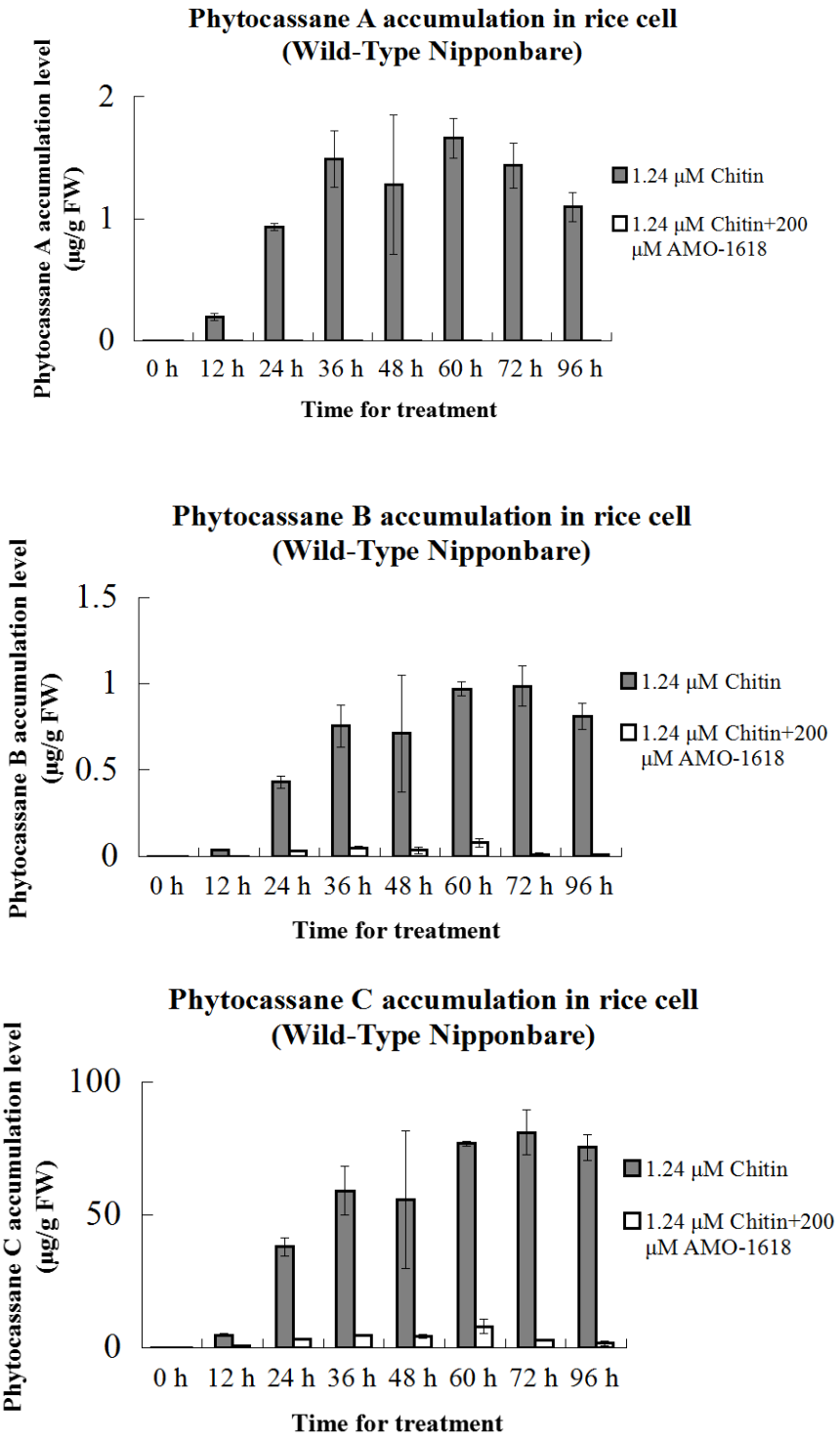

Figure S-9. The effect of AMO-1618 on phytocassanes and momilactones biosynthesis in rice callus.

1.24 μM chitin, 1.24 μM chitin oligosaccharides were applied to fresh rice cells, of which medium were collected on time course; **1.24 μM chitin+200 μM AMO-1618,** 1.24 μM chitin oligosaccharides and 200 μM AMO-1618 were used to treat fresh rice cells, of which cultured medium was collected from 0h to 96 h. All extracts from collected medium were analyzed on LC-ESI-MS/MS. 5 μl of each extract was subjected to LC-ESI-MS/MS. Three repetition was set at each time point.

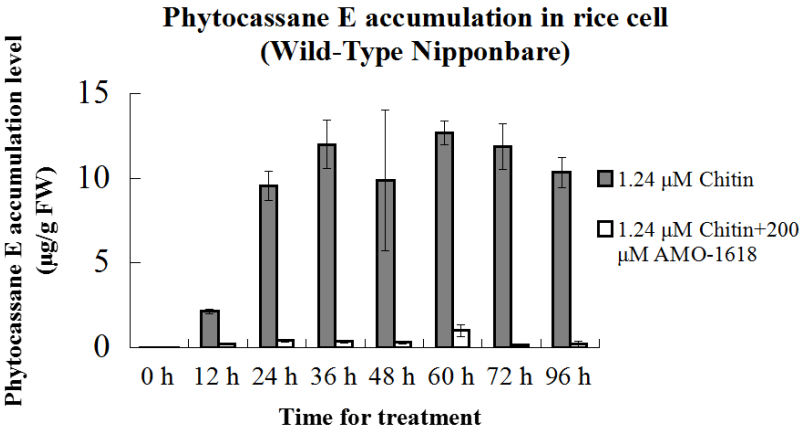

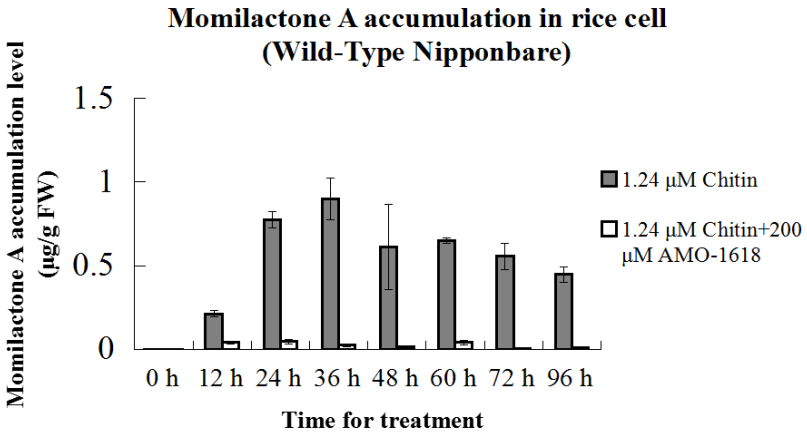

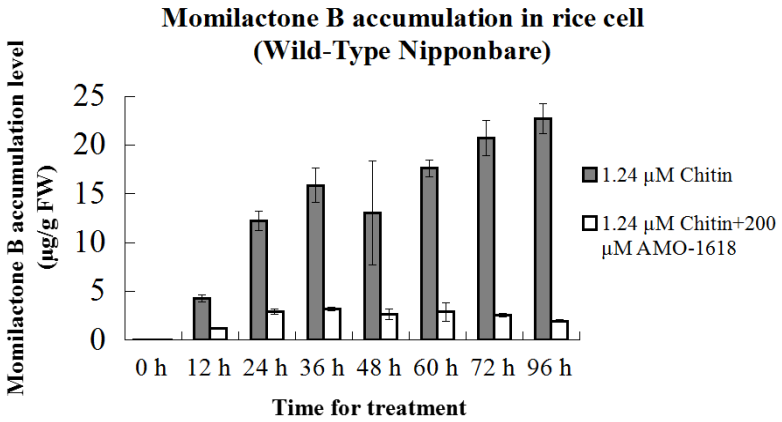

Figure S-9. Continued

S-VI. The effect of AMO-1618 on phytocassanes and momilactones accumulation in rice roots

Results

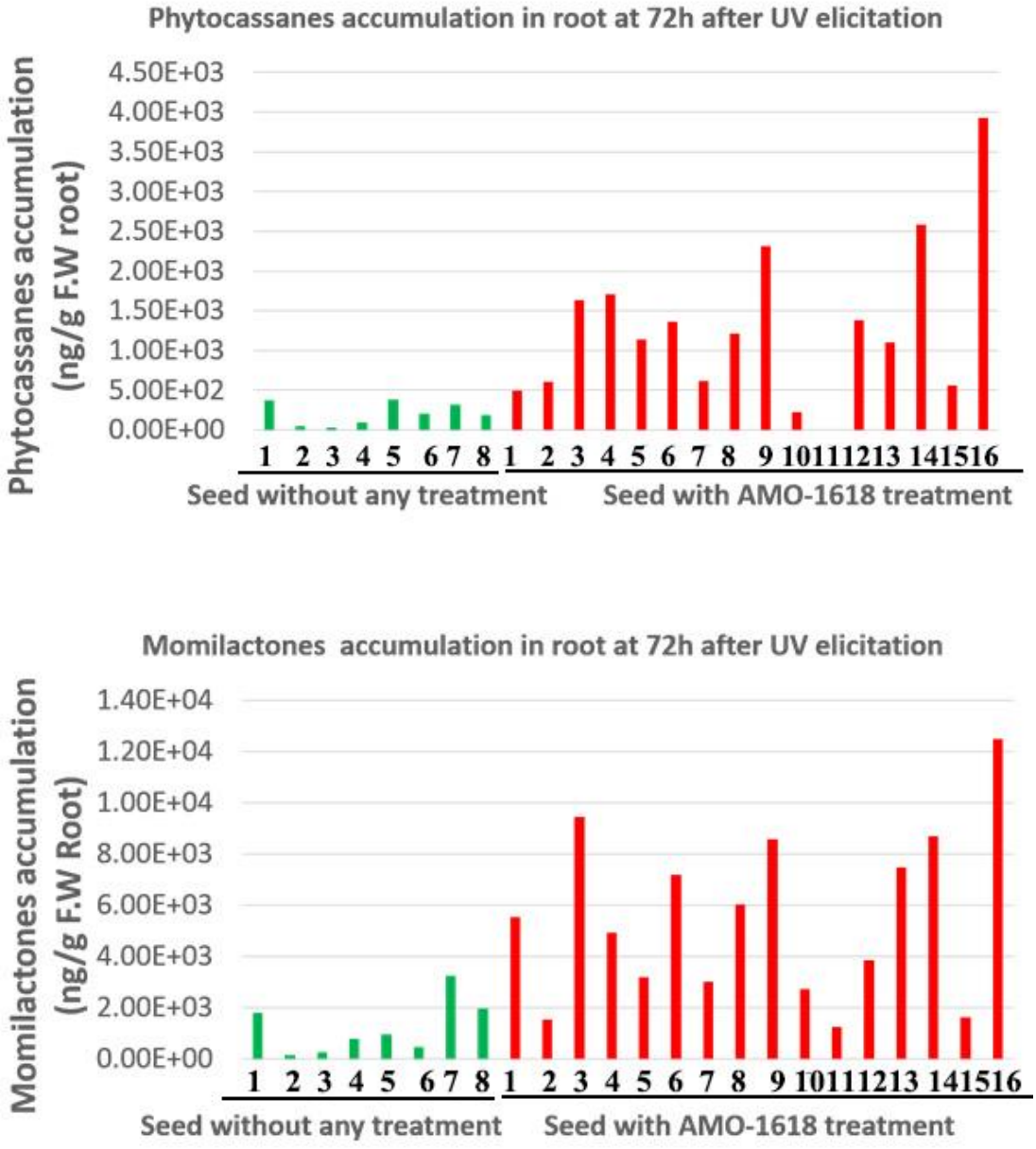

Figure S-10. The effect of AMO-1618 on phytocassanes and momilactones accumulation level in rice roots under UV-irradiation

ACKNOWLEDGEMENT

First and foremost I offer my sincerest gratitude to my major professor Dr. H. Nojiri and associate professor Dr. K. Okada of Biothechnology Research Center, the University of Tokyo. Without their creative advice and supportive input, the breakthrough in labeling experiment could not have been successfully achieved. Professor Dr. H. Nojiri gave me great suggestion in every presentation. The research can not be moved on in short time without his unique viewpoint. Associate professor Dr. K. Okada has supported and supervised me thoughout my thesis with his patience and knowledge whilst allowing me the space to work in my own idea. I attribute the level of my doctoral degree to his encouragement and effort and without him this thesis, too, would not have been completed or written.

I would also wish to thank Prof. Dr. H. Kawaide of Graduate School of Agriculture, Tokyo University of Agriculture and Technology. Prof. Dr. H. Kawaide provided technical assistance and supplied fully ^{13}C labeled substrate for feeding experiment. I extremely thank his lab for NMR analysis of fully ^{13}C labeled *ent*-cassa-12,15-diene and *syn*-pimara-7,15-diene. This doctoral thesis could not be completed without Prof. Dr. H. Kawaide's support.

I would also like to thank assistant professor Dr. C. Suzuki-Minakuchi of Biothechnology Research Center, the University of Tokyo. Dr. C. Suzuki-Minakuchi helped me to improve my logic in presentation. She always encouraged me and gave me her suggestion in every aspect.

Other past and present group members that I have had the pleasure to work with or alongside of are grad students Mr. J Matsuzawa, Mr. T Kotake, Mr. R Tsutsumi, Mr. S. Ogawa, Mr. D. Shibuya, Mr. A. Moteki, Mr. D. Alan; Post doc Dr. C. Joydeep. I deeply thank them for their help and encouragement in either research or daily life.

I would also deeply thankful to all the members of Biothechnology Research Center, the University of Tokyo. I thank them for their great help and patient communication in Japanese.

Lastly, I would like to thank my family for all their love and encouragement. For my parents Mr. YE MUSHUI and Mrs. CHEN ZHIMEI who raised me with a love of science and supported me in all my pursuits. And most of all for my loving, supportive, encouraging, and patient wife Mrs. HE MINYUAN whose faithful support during the final stages of this Ph.D. is so appreciated. Love all of you. Thank you

YE ZHONGFENG
The University of Tokyo
December 2016